

**URANIUM RECOVERY FROM EFFLUENTS
GENERATED IN URANIUM PROCESSING
PLANT USING NOVEL SORBENT**

By

SANTOSH KUMAR SATPATI

ENGG 01200904020, Dt. 01-09-2009

Bhabha Atomic Research Centre, Mumbai, India

A thesis submitted to the

Board of Studies in Engineering Sciences

In partial fulfilment of requirements

for the Degree of

DOCTOR OF PHILOSOPHY

Of

HOMI BHABHA NATIONAL INSTITUTE, MUMBAI



March, 2016



Homi Bhabha National Institute

Recommendations of the Viva Voce Committee

As members of the Viva Voce Committee, we certify that we have read the dissertation prepared by **Santosh Kumar Satpati** entitled ” **Uranium Recovery from Effluents generated in Uranium Processing Plant using Novel Sorbent**” and recommend that it may be accepted as fulfilling the thesis requirement for the award of **Degree of Doctor of Philosophy**.

Chairperson - **Prof. S. B. Roy**

Date:

Guide & Convener - **Prof. P.K.Tewari**

Date:

Co-Guide - **Prof. S.B. Roy**

Date:

Examiner – **Prof. Madhu Vinjamur**

Date:

Member 1 - **Dr. D. Srivastava**

Date:

Member 2- **Dr. S. Mukhopadhyay**

Date:

Member 3 - **Dr. R. Kapoor**

Date:

Technical Advisor: **Dr. Sangita Pal**

Date:

Final approval and acceptance of this thesis is contingent upon the candidate’s submission of the final copies of the thesis to HBNI.

I/We hereby certify that I/we have read this thesis prepared under my/our direction and recommend that it may be accepted as fulfilling the thesis requirement.

Date:

Place:

Co-guide

Guide

Prof. S.B. Roy

Prof. P.K. Tewari

STATEMENT BY AUTHOR

This dissertation has been submitted in partial fulfilment of requirements for an advanced degree at Homi Bhabha National Institute (HBNI) and is deposited in the Library to be made available to borrowers under rules of the HBNI.

Brief quotations from this dissertation are allowable without special permission, provided that accurate acknowledgement of source is made. Requests for permission for extended quotation from or reproduction of this manuscript in whole or in part may be granted by the Competent Authority of HBNI when in his or her judgment the proposed use of the material is in the interests of scholarship. In all other instances, however, permission must be obtained from the author.

Santosh Kumar Satpati

संतोष कुमार सतपती

DECLARATION

I, hereby declare that the investigation presented in the thesis has been carried out by me. The work is original and has not been submitted earlier as a whole or in part for a degree / diploma at this or any other Institution / University.

Santosh Kumar Satpati

Statement under section 0.771

The work reported in this thesis was planned, carried out and interpreted by me. I was helped by Prof. P.K. Tewari through valuable discussions. Part of the work reported in this thesis has been published as listed below.

List of Publications

Journals

1. Recovery and pre-concentration of uranium from secondary effluent using novel resin: Sangita Pal, **S. K. Satpati**, K.N. Hareendran, Sanjukta A. Kumar, K.L. Thakor, S.B. Roy and P.K. Tewari; Int. J. Nuclear Desalination, 2010, 4 (1), 28 – 36 .
2. Studies on uranium recovery from inlet stream of Effluent Treatment Plant by novel “In-House” sorbent; Sangita Pal, Suchismita Mishra, **S. K. Satpati**, G.G. Pandit, P.K. Tewari and V.D. Puranik; J. Radioanal Nucl Chem., 2011, 290(1), 67 – 73 .
3. Removal of uranium(VI) from dilute aqueous solutions using novel sequestering sorbent poly-acryl hydroxamic acid, **Santosh Kumar Satpati**, Sangita Pal, Saswati B. Roy, P.K. Tewari, J. of Environmental Chemical Engg., 2014, 2, 1343 – 1351.
4. Extraction of uranium from nuclear industrial effluent using polyacrylhydroxamic acid sorbent, **S. K. Satpati**, S. Pal, D. Goswami, P.K. Tewari and S.B. Roy: Int. J. Environ. Sci. Technol., 2015, 12(1), 255-262.
5. Separation and recovery of uranium from wastewater using sorbent functionalized with hydroxamic acid, **S. K. Satpati**, S. Biswas, S. Pal, S. B. Roy, P. K. Tewari, Sep. Sci. Technol., 2015, 50(3), 387 – 394.

Conferences

1. Study for Recovery of Uranium from waste effluent by nitrogen based Sorbent: **Satpati SK**, Pal Sangita, Hareendran KN, Thalor KL, Roy SB and Tewari PK; CHEMCON-2009, TS-1277, Abstract page 55, 27-30 December, 2009, Visakhapatnam, AP.
2. “Pre-concentration of Uranium from Nuclear Waste Effluent by Fractional Elution Study Using “IN-HOUSE” Resin”, **S. K. Satpati**, Sangita Pal, Sanjukta Kumar, K. Hareendran, K.L.Thalor, S.B.Roy, P.K.Tewari, InDACON 2010, Chennai
3. Performance and Efficiency of “In-House” Resin for the Treatment of Nuclear Plant Effluents: **SK Satpati**, Sangita Pal, KN Hareendran, SB Roy and PK Tewari; 2nd International Conference on Asian Nuclear Prospects (ANUP- 2010), WM-5, 10-13 October 2010, Mamallapuram, T.N.

Santosh Kumar Satpati

DEDICATED TO MY PARENTS

ACKNOWLEDGEMENTS

My deepest gratitude is to my research Guide, Prof. P. K. Tewari, Distinguished Scientist, Former Associate Director, Chemical Engineering Group, Bhabha Atomic Research Centre whose advice, support and patience have been fundamental for the completion of this thesis. I am grateful and indebted to him for having taught me how to do research and for accepting me as student.

I want to express my gratitude to my Co-Guide Prof. S. B. Roy, Outstanding Scientist, Associate Director, Chemical Engineering Group & Head, Uranium Extraction Division, Bhabha Atomic Research Centre for her constant help, her continuing enthusiasm, and for her trust in my abilities, that motivated me to do this research.

I am especially thankful to Dr. Sangita Pal (Technical Advisor), DD/BARC, Dr. D.K. Maity (Technical Advisor), Associate Dean, HBNI, Dr. S. Mukhopadhyay, ChED/BARC for their constant and enormous help and encouragement. Chairman/Chairperson and members of the doctoral committee are gratefully acknowledged for their critical review and suggestion during progress review and pre-synopsis viva-voce.

I would like to thank all my colleagues at UED who have supported me during the last five-six years and who have contributed, directly or indirectly, to the success of this programme.

Finally, I want to thank my family members and friends who have supported and helped me to overcome setbacks and to stay focused on my work, without which all this work would not have been possible.

Santosh Kumar Satpati

CONTENTS

		Page No.
SYNOPSIS		16
LIST OF FIGURES		28
LIST OF TABLES		34
CHAPTER 1: INTRODUCTION		35
1.1	Nuclear power programme	36
1.2	Nuclear Fuel Cycle	37
1.3	Uranium	38
1.3.1	Natural occurrence of uranium	40
1.3.2	Uranium metal preparation	41
1.3.3	Toxicity of uranium	42
1.3.4	Uranium bearing wastewater	43
1.4	Uranium separation techniques	44
1.4.1	Membrane filtration technique	45
1.4.1.1	Nanofiltration technique	45
1.4.1.2	Ultra-filtration technique	46
1.4.1.3	Reverse osmosis technique	46
1.4.2	Chemical precipitation technique	47
1.4.2.1	Reductive precipitation of uranium(VI)	47
1.4.2.2	Bio-precipitation of uranium	47
1.4.3	Extraction technique	48
1.5	Solid Phase Extraction (SPE)	50
1.5.1	Minerals and inorganic oxides	52
1.5.2	Carbonaceous materials	53

1.5.3	Biosorbent	56
1.5.3	Polymers/copolymers	58
1.6	Promising chelating sorbent for uranium extraction	62
1.7	Uranium sorption mechanism by molecular modelling	64
1.7.1	Need of computational chemistry	64
1.7.2	Molecular modelling methodology	65
1.7.3	Uranium complex analysis	67
1.8	Problem definition and scope of work	70
CHAPTER 2: SORBENT AND WASTEWATER		73
2.1	Introduction	74
2.1.1	Novelty of the sorbent	75
2.1.2	Uranium processing plant effluent (wastewater)	76
2.2	Sorbent synthesis and physical characterisation	77
2.2.1	Materials	77
2.2.2	Synthesis of sorbent	78
2.3	Physical characterisation of sorbent	80
2.3.1	Mesh size distribution of sorbent	81
2.3.2	Effect of mesh size on density and swelling of sorbent	81
2.3.3	Effect of competitive ions and its concentration on sorbent swelling with mesh size variation	83
2.3.4	Swelling of sorbent in different medium	85
2.3.5	Solubility of sorbent in different media	86
CHAPTER 3: INSTRUMENTAL CHARACTERIZATION		87
3.1	Introduction	88
3.2	Instrument used for characterisation	89
3.3	Results and discussion	89

3.3.1	Brunauer–Emmett–Teller (BET) analysis	89
3.3.2	Optical microscopic view	91
3.3.3	Scanning electron microscope (SEM) & energy dispersive X-ray spectroscopy (EDS) analysis	92
3.3.4	Differential Scanning Calorimetry (DSC), Thermogravimetric (TG) & differential Thermogravimetric (dTG) analysis	93
3.3.5	Fourier transforms infrared (FTIR) study	95
3.3.6	Characterization of sorbent using Raman Spectroscopy	97
3.3.7	Uranium sorbed PHOA characterisation by EDXRF	99
CHAPTER 4: BATCH EXPERIMENT: SORPTION		100
4.1	Introduction	101
4.2	Materials and Methods	102
4.2.1	Sorbent	102
4.2.2	Uranium solution	102
4.2.3	Uranium and other metal ion determination	102
4.2.4	Reagents	103
4.2.5	Apparatus	103
4.2.6	Sorption / uptake evaluation method	103
4.2.7	Sorption isotherm models	104
4.2.7.1	Langmuir isotherm model	104
4.2.7.2	Freundlich isotherm model	105
4.2.7.3	Other isotherm models	106
4.2.8	Kinetic models	107
4.2.8.1	Sorption mechanism analysis	107
4.2.8.2	Pseudo first order kinetic model	109
4.2.8.3	Pseudo-second order kinetic model	110
4.2.8.4	Elovich model	110

4.2.8.5	Intra-particle diffusion	111
4.2.9	Thermodynamic properties	112
4.3	Experimental procedure for sorption parameters	113
4.4	Results and discussion	114
4.4.1	Sorbent performance with plant effluent	114
4.4.2	Effect of sorbent size on uranium uptake	115
4.4.3	Effect of sorbent quantity on uranium uptake	115
4.4.4	Effect of solution pH on uranium uptake	116
4.4.5	Effect of agitation on uranium uptake	119
4.4.6	Uranium sorption in presence of competitive ions (cations and anion)	120
4.4.6.1	Combined effect of competitive ions on sorption of uranium	120
4.4.6.2	Effect of individual Ca^{2+} , Mg^{2+} , Mn^{2+} , Cu^{2+} , Fe^{3+} and NO_3^- ion on sorption of uranium	121
4.4.7	Sorption isotherm	124
4.4.7.1	Langmuir isotherm	124
4.4.7.2	Freundlich isotherm	126
4.4.7.3	Other isotherms	127
4.4.8	Sorption kinetic study	128
4.4.8.1	Sorption mechanism analysis and kinetic	128
4.4.8.2	Pseudo first order kinetic	133
4.4.8.3	Pseudo-second order kinetic	134
4.4.8.4	Intra-particle diffusion	136
4.4.9	Uranium uptake with temperature variation	137
4.4.10	Reusability of sorbent	140
4.5	Conclusion	141
CHAPTER 5: BATCH EXPERIMENT: ELUTION		142

5.1	Introduction	143
5.2	Materials and methods	144
5.2.1	Sorbent	144
5.2.2	Elute solution preparation	144
5.2.3	Metal ion determination	144
5.2.4	Reagents	144
5.2.5	Apparatus	145
5.2.6	Desorption / recovery evaluation method	145
5.3	Experimental procedure for sorption parameters	145
5.4	Results and discussion	146
5.4.1	Selection of effective eluent	146
5.4.2	Effect of concentration of eluent on recovery	147
5.4.3	Effect of agitation on uranium recovery	149
5.4.4	Recovery of uranium from plant effluent	150
5.4.5	Kinetic study of uranium desorption process	150
5.4.6	Effect of temperature on uranium desorption process	152
5.4.7	Effect of presence of competitive ions on the uranium elution process	152
5.4.8	Recycle of the PHOA sorbent	157
5.5	Conclusion	158
CHAPTER 6: COLUMN EXPERIMENT: SORPTION AND ELUTION		159
6.1	Introduction	160
6.2	Materials and methods	161
6.2.1	Sorbent	161
6.2.2	Uranium solution	161
6.2.3	Uranium and other metal ion determination	161

6.2.4	Reagents	162
6.2.5	Apparatus	162
6.3	Column model evaluation	162
6.3.1	Column model	162
6.3.2	Kinetic models	163
6.3.2.1	Yoon–Nelson model	164
6.3.2.2	The Thomas model	164
6.3.2.3	Adam-Bohart model	165
6.3.2.4	Bed Depth Service Time (BDST)	165
6.3.2.5	Mass transfer coefficient	166
6.4	Experimental procedure for column parameters	167
6.5	Results and discussion	168
6.5.1	Column performance – sorption and elution	168
6.5.2	Column performance at various operating conditions	169
6.5.2.1	Effect of inlet U(VI) concentration	169
6.5.2.2	Effect of U(VI) solution flow rate	170
6.5.2.3	Effect of sorbent bed height	171
6.5.2.4	Effect of column diameter	172
6.5.3	Breakthrough curve modelling	174
6.5.3.1	Application of Thomas model	174
6.5.3.2	Application of the Adams–Bohart model	175
6.5.3.3	Bed Depth Service Time (BDST)	176
6.5.3.4	Effect of kinetic constant on breakthrough	177
6.5.4	Evaluation of mass transfer coefficient	178
6.5.5	Elution performance of column	178
6.5.5.1	Effect of wastewater flow rate	178

6.5.5.2	Effect of PHOA bed depth	179
6.5.5.3	Effect of elution column diameter	180
6.6	Conclusion	181
CHAPTER 7: MOLECULAR MODELLING FOR URANIUM SORPTION ONTO PHOA		182
7.1	Introduction	183
7.2	Materials and methods	184
7.3	Computational Methods	184
7.4	Results and discussion	185
7.4.1	Computational studies of complexes	185
7.4.1.1	Uranyl ion with two monomer functional groups from different sorbent chain	185
7.4.1.2	Uranyl ion with two monomer functional groups from different sorbent chain and water	186
7.4.1.3	Two uranyl ion with four functional group and water	188
7.4.2	Validation of the modelling results	191
CONCLUSION AND RECOMMENDATION		192
REFERENCES		193



Ph. D. PROGRAM

1. Name of Student **Santosh Kumar Satpati**
2. Name of the Constituent Institution **Bhabha Atomic Research Centre Trombay, Mumbai – 400085**
3. Enrollment NO. **ENGG 01200904020**
4. Title of Ph.D. Thesis **Uranium Recovery from Effluents generated in Uranium Processing Plant using Novel Sorbent**
5. Board Of Studies **Engineering Sciences (Chemical Engineering), HBNI**

SYNOPSIS

India's fuel situation, with shortage of fossil fuels, is driving the nuclear investment for electricity and 25% nuclear contribution is the ambition for 2050, when 1094 GWe of base-load capacity is expected to be required. Uranium is the key material for nuclear energy program and its resources are inadequate with rising demand. Therefore, it is required to explore various other resources of uranium including secondary resources to meet the long term energy sustainability of Indian nuclear program. It is important and necessary to recognize the concern over the environmental and health impacts in parallel to ensure a long term supply of uranium to sustain India's nuclear power program. Adopting innovative and advanced technology for enhancing efficiency of uranium recovery from its available sources is additional challenging task.

Recovery of uranium from industrial effluents has recently become the centre of a wide interest in exploiting undeveloped energy sources along with the remediation of wastewater [1]. Today, unconventional resources of uranium are playing more important role and engaging more attention than before. Some of the unconventional sources are exploitable by using unconventional techniques improving techno-economic constraints. Thus the uranium recovery technique or separation methodology should be recognized as having a bright future. Water and soil contamination with uranium ions has become a global environmental problem. Uranium subsists in the environment due to leaching from mine tailings, natural deposits, uranium combustion products, emissions from the nuclear industries, corrosion of uranium and use of uranium-containing phosphate fertilizers. These Nuclear fuel sources cause continuous release of trace uranium ions into the environment and impose radio-toxicity in the environment [2,3].

Uranium is the heaviest naturally abundant actinide element. In spite of radio-toxicity it reflects its unique quality in nuclear energy contribution. Although used in nuclear power segment but safe disposal of related waste effluent and removal of uranium by selective, stable matrix is a new and novel field of harnessing uranium due to its Jekyll and Hyde reputation. Even at low concentrations, because of its persistent and accumulative nature, uranium is toxic and chronic exposure of this heavy metal is known to cause bone degeneration, liver, lung and blood damage [3]. Therefore, separation and recovery of uranium are of great practical significance, not only in reutilization of uranium resources and sustainable development of nuclear energy, but also for protection of human health, and to create eco-friendly environment. Hence, the development of clean-up / remediation technologies for removing uranium from industrial wastewaters are very important and have drawn attention of many researchers [4-7].

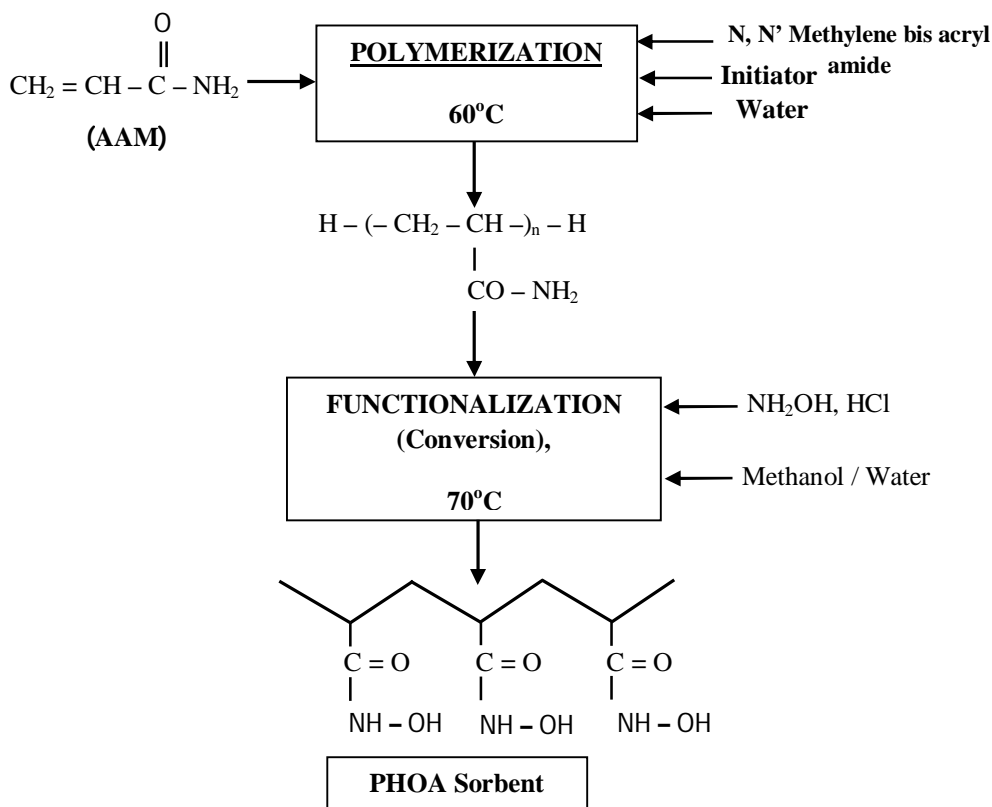
The major problems pertaining to the development of a suitable separation technique for uranium from nuclear waste solution are due to its very low concentration (below 10 mg/L), chemical form in solution (mostly cationic), solution pH and presence of higher concentration of competitive ions in the solution.

The thesis elaborates detailed and systematic studies of selection, synthesis and characterization of novel sorbent, development of treatment methodology of typical nuclear plant effluent for effective separation and recovery of uranium and analysis of uranium complexation with the sorbent along with validation with experimental findings using computational chemistry. The thesis is divided into eight chapters. A brief description of each chapter is given below:

Chapter 1: This chapter deals with chemistry of uranium, hazards associated with uranium, importance of removal of uranium from industrial wastewater, different separation techniques for uranium, different types of solid phase extractants, basic principle of methodology selection for solid phase extractant, role of computational chemistry for uranium sorption mechanism analysis and problem definition. Several works have been carried out on the development of suitable techniques for removal and recovery of uranium from the industrial wastes adopting different processes like foam based separation, ion exchange, solvent extraction, bio-sorption/remediation, chromatographic, electro-deposition, solid phase extraction (SPE) through sorption, membrane separation etc. Amongst all, SPE through sorption process has gained popularity due to its high separation efficiency, reproducibility and simplicity [7-12]. SPE has many additional advantages over other separation techniques such as (i) reduced solvent usage (ii) low disposal costs, (iii) short extraction times, (iv) high efficiency, (v) ecologically-safe, (vi) elimination of some of the glassware, (vii) isolation of analytes from large volumes of sample with minimal or zero evaporation losses (for pre-concentration), (viii) reduced exposure of analysts to organic solvents (ix) more reproducible

results (x) remote operation etc. In this regard, design and development of a suitable sorbent and its thorough performance evaluation is an important task.

Chapter 2: The “In-House” designed and developed sorbent PHOA (poly hydroxamic acid) is a synthesized product starting from monomer acrylamide in water with cross linker N,N’ methylene bis acrylamide to polymerize to polyacrylamide (PAAM) by addition polymerization and followed by chemical conversion using hydroxylamine hydrochloride and NaOH to synthesize three-dimensionally cross-linked hydrophilic macromolecules with hydroxamic acid groups as pendant functional moieties to be used for ionization, electrostatic interaction, chemical bond formation and chelation with uranium containing species in stepwise manner. This chapter deals with novelty of the sorbent used for the study and characterization of plant effluent to be treated. Sorbent synthesis procedure has been briefed. This chapter also describes physical characterization of the sorbent in details for understanding its nature before application.



Synthesis scheme of PHOA

The sorbent contains hydroxamic acid functional group for selectively chelating the soluble U(VI) species present in the plant effluent. The plant effluent is alkaline ($\text{pH} > 7$) in nature having U(VI) concentration <10 mg/L along with calcium, magnesium, and nitrate ions concentration in g/L level and other metal ions (specially transition metals e.g., Fe, Mn, Cu <5 mg/L) as competitive ions.



PAAM

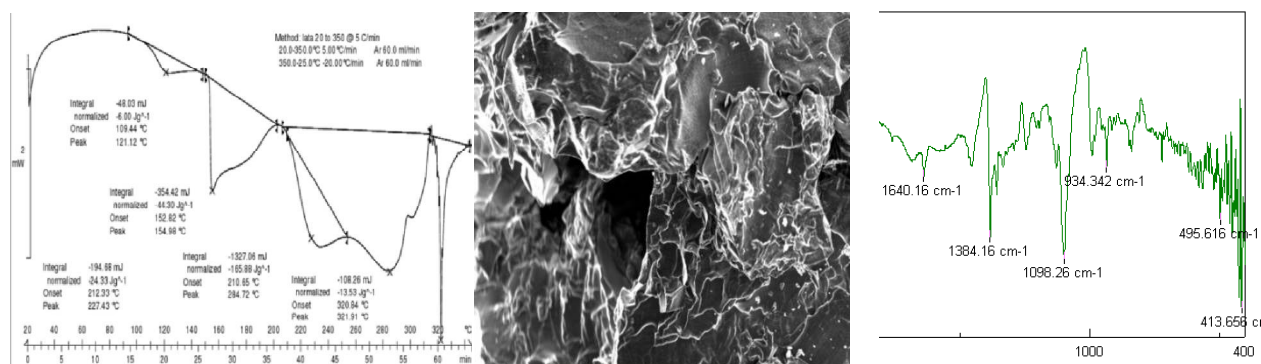
PHOA

Uranium loaded PHOA

The sorbent, PHOA is prepared following eco-friendly procedure and the synthesis process is cheaper and easy to handle.

Chapter 3: This chapter presents results obtained from different instrumental analysis of the virgin PHOA sorbent, uranium loaded sorbent and eluted sorbent. Different instrumental analysis like BET for pore size and specific pore volume measurement, optical microscopic view for appearance of pores; SEM & EDS for morphology and elemental studies; DSC, TG and DTG for thermal stability studies; FTIR and Raman spectra for functional group characterization and EDXRF for elemental characterization are discussed thoroughly. Details of equipment used for the analysis are illustrated. Pore specific volume was found to be $0.0063 \text{ cm}^3/\text{g}$ of sorbent. PHOA has well-defined, interconnected, three dimensional porous structures with pores of mean size $50\mu\text{m}$. The stable chains in PHOA have contributed to support the pore wall to engage and trap uranium (VI). EDS and EDXRF characterization based on elemental analysis of uranium confirmed the uranium(VI) sorption on the sorbent. The PHOA is thermally stable upto about 225°C with its functional group. FTIR and Raman spectra confirm the participation of the functional group for U(VI) sorption and regeneration

of the PHOA after elution. Feed, filtrate and laden PHOA eluted solutions were quantified using ICP-AES.



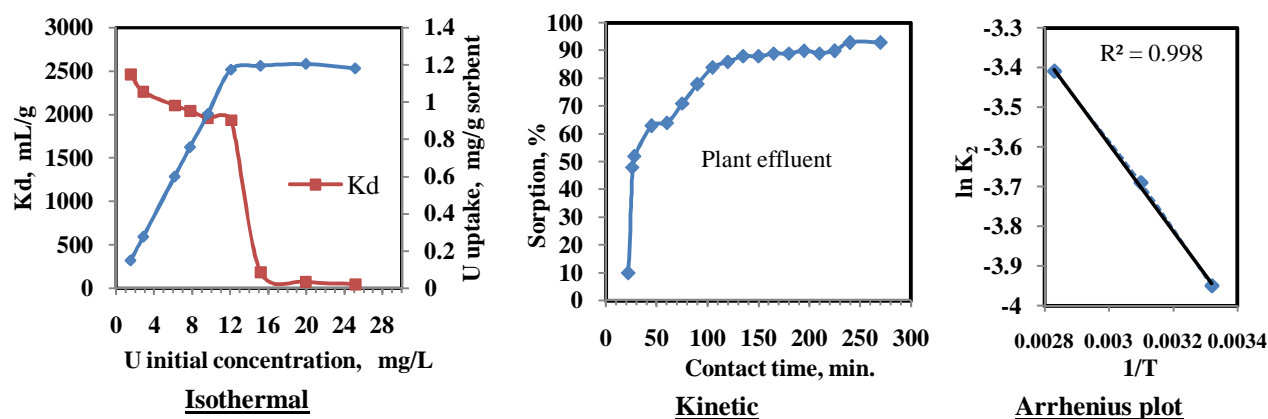
SEM (PHOA)

DSC (Loaded PHOA)

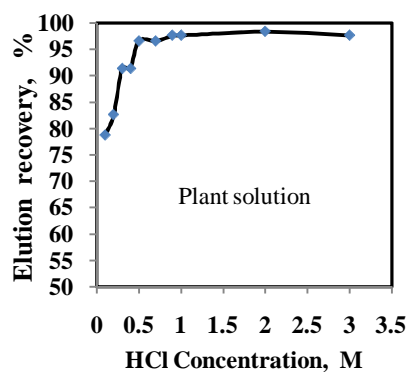
FTIR (Loaded PHOA)

Chapter 4: Batch experimental details of sorption process and basic principles of sorption performance evaluation have been described in this chapter. The methodology of different process parameters and their experimental set up are detailed. Sorption characteristics like uranium uptake in different condition, distribution coefficient, sorption isotherms, sorption kinetics, sorption thermodynamic studies, and sorption mechanism are important for assessing the performance and its applicability. Determination of metal ions and solution condition are mentioned. This chapter also includes the methods of preparation of stock solutions of metal ions, extractant and their properties. Effective uptake was reduced with increase of mesh size because of hindrance of sorbent swelling due to compactness of lower size beads (density increased). The sorption of uranium was increased from 19.8% to 97.5% with an increase in pH of the solution from 5 to 9. Distribution coefficient (K_d) of uranium was substantially higher, about 100 times than that of calcium and magnesium. Percent sorption of uranium was about 93% whereas, for calcium and magnesium it was about 10% and 15% respectively from plant effluent. The effluent contains almost comparable amount of Fe^{3+} in feed with respect to uranium, Fe^{3+} showed almost 100% separation compared to separation of uranium which was in the range of 80-90%. Uptake of uranium onto PHOA is strongly affected by $Fe(III)$, $Cu(II)$ and $Mn(II)$ ions as competitive ions (< 5 mg/L in the

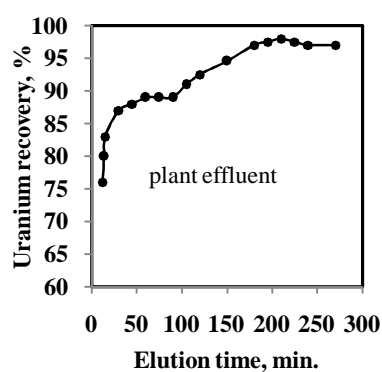
effluent). Isotherm study indicates that U(VI) sorbed on PHOA is a monolayer sorption. Dimensionless equilibrium parameter indicates suitability of the sorbent for U(VI) sorption in the alkaline aqueous solution. The sorption system obeys the pseudo-second order kinetic model. The rate determining step of the sorption reaction of the system depends on both, the textural properties as well as the total content of the PHOA active sites. The sorption is not significantly increases with temperature increase as indicated from experiment as well as thermodynamic parameters evaluated. The sorption process follows a physical sorption (8-40 KJ.mol⁻¹) mechanism with activation energy value 9.137 KJ.mol⁻¹. The sorbent can be reused for U(VI) sorption from plant effluent for 5 times.



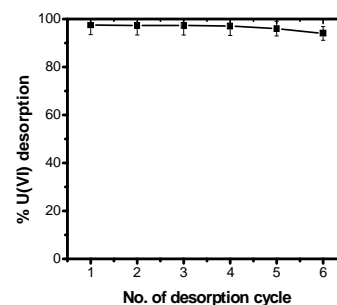
Chapter 5: Sorbent usefulness depends on the probability of valuable recovery from the laden sorbent matrix and reusability of the sorbent thereafter. Recoverability, immobilization factor, elution kinetics are desorption characteristic. This chapter deals with the desorption of U(VI) from loaded PHOA under a wide range of conditions such as variation of eluent, concentration of eluent, presence of competitive ions etc. Kinetic and thermodynamic studies have also been illustrated in the chapter. Percentage recovery of uranium and immobilization factors is evaluated in different conditions. The complexing ability of various anions with UO_2^{2+} ion follow the order $H_2SO_4 > HCl > HNO_3 > \text{Organic acids}$ and hence the efficiencies of elution follow the same order. 1M HCl is chosen as chemical agent /suitable eluent.



Eluent



Kinetics



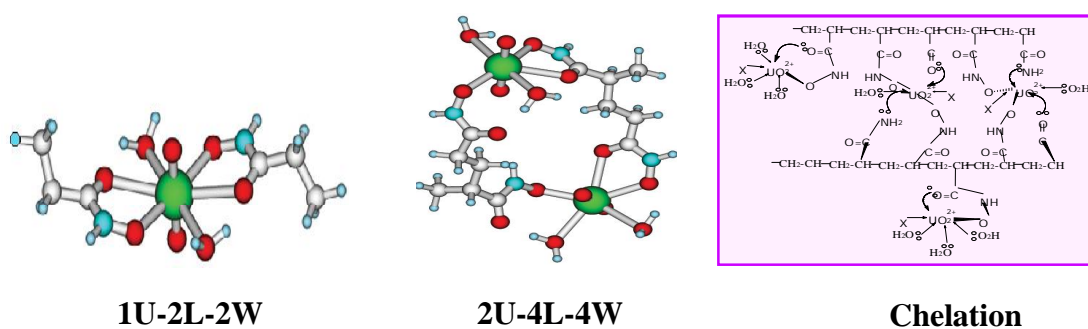
Reusability

About 97% recovery was achieved in the plant effluent with PHOA and recovery of magnesium and calcium was found to be 96.5% and 86.5% respectively. The elution kinetics was found to be faster than the sorption kinetics and presence of competitive ions does not affect the elution kinetic. Uranium elution from the loaded PHOA is found to be independent of temperature. From fractional elution study it is observed that except Fe^{+++} ion all other metal ions get separated from the PHOA at lower HCl concentration and Fe^{+++} ion gets separated in higher concentration i.e. 1M HCl solution.

Chapter 6: In this chapter, column experiments for the sorption of U(VI) onto PHOA from plant effluent and also for the elution of U(VI) from the loaded PHOA has been described. The effect of process variables like i) quantity of sorbent, ii) effluent flow rate, iii) column diameter were studied in details and results have been analyzed. Mass transfer coefficient correlations and breakthrough analysis models have been described. Evaluated mass transfer coefficient was found to be 0.008 – 0.009 cm/s which is comparable with other promising sorbent. Bed depth service times (BDST) have been evaluated for different conditions using Bohart and Adams model. Theoretical breakthroughs were predicted with the variation of rate constant value (pseudo second order kinetic basis).

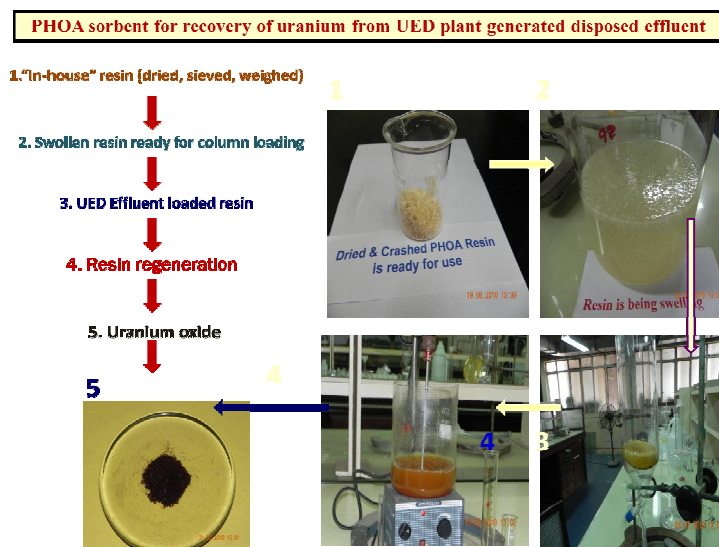
Chapter 7: It is important to understand the uranium coordination chemistry related to metal-ligand bonding for specifically developed effective sorbent. The thermodynamic stabilities of

some important aqueous uranium complexes and hydroxides need to be confirmed. In this context, an outline using molecular modelling is needed to address understanding the hydration of UO_2^{2+} in probable planar equatorial coordination geometry in sorbed condition [13]. Possible geometries need to evaluate under the prevailing conditions and relative stabilities of possible binding motifs [14-15]. The theoretical model result has to be supported by the instrumental measurement as well as experimental analysis. This chapter deals with the molecular modelling of the sorption process to understand stable structure of the chelating complex of PHOA and U(VI). The study also aims to discuss the possible structural consequences observed when the hydroxamate anion binds UO_2^{2+} applying molecular modelling using DFT method. Theoretical aspect of computational chemistry, method of evaluation and model structure analysis are included in the chapter. Modelling results are also compared with experimental findings and instrumental characterisations. Spatial orientation optimization for different complexes with varying number of water molecule has been carried out applying non-local correlated hybrid density functional named as B3LYP. The complex structures are taken for optimization locating the minimum energy structure using quasi-Newton-Raphson based algorithm and calculations are performed applying the GAMESS suit of *ab initio* programs. Stability analysis was carried out of complex-geometry in different combinations of U-L-W and the results were compared with findings of FTIR, DSC and experimental studies.



In summary, the important highlights of this thesis are as follows:

1. Uranium can be removed from the effluents of uranium processing plant by sorption process with novel selective sorbent such as PHOA.
2. Sorbent with high surface area [$\sim 55 \text{ m}^2/\text{g}$ (BET)], layer structure (SEM), hydroxamate functional groups (FT-IR), thermal stability (DSC) characteristics promote and encourage the use of PHOA to recover uranium from wastewater having uranium $< 10 \text{ mg/L}$.
3. High distribution co-efficient and selectivity values of uranium for removal and low immobilisation factor for recovery were indicative measures for successful process development.
4. Column study with plant effluent in higher scale indicates possibility of recovery of uranium and reuse of recovered valuables further.
5. Modelling and the experimental results are in well agreement with the derived facts as proved by the instrumental analysis and matrix diagnosis.
6. The experimental study and plant study is in well agreement and is also indicative of the fact that **Uranium recovery from effluents generated in Uranium processing plant using Novel Sorbent, PHOA is viable and technologically implementable.**



References:

- [1] J.D. Van Horn, H. Huang, Uranium (VI) bio-coordination Chemistry from biochemical solution and protein structural data, *Coord. Chem. Rev.* 250 (7-8) (2006) 765-775.
- [2] W. Zou, L. Zhao, R. Han, Removal of uranium (VI) by fixed bed ion-exchange columns using natural zeolite coated with manganese oxide, *Sep. Sci. Engg.* 17 (4) (2009) 585-590.
- [3] C. Gok, Sule. Aytas, Biosorption of uranium (VI) from aqueous solution using selenium alginate beads, *J. Hazard. Mater.* 168 (2009) 369-375.
- [4] K. Mirjalili, M. Roshani, Resin-in-pulp method for uranium recovery from leached pulp of low grade uranium ore, *Hydrometallurgy.* 85 (2007) 103-109.
- [5] D. James, G. Venkateswaran, T. Prasad Rao, Removal of uranium from mining industry feed simulant solutions using trapped amidoxime functionality within a mesoporous imprinted polymer material, *Micropor. Mesopor. Mater.* 119 (2009) 165-170.
- [6] K. Akhtar, A.M. Khalid, M.W. Akhtar, M.A. Ghauri, Removal and recovery of uranium from aqueous solutions by Ca-alginate immobilized *Trichoderma harzianum*, *Bioresour. Technol.* 100 (2009) 4551-4558.
- [7] J.M. Duran-Blanco, B.E. Lopez-Munoz, M.T. Olguin, Influence of pH on U(VI) adsorption using a thermally-treated Mg-Al hydrotalcite and a natural zeolite in a batch system, *J. Sep. Sci. Technol.* 48 (2013) 797-804.
- [8] F.A. Aydin, M. Soylak, Solid phase extraction and preconcentration of uranium (VI) and thorium (IV) on Dilute XAD761 prior to their inductively coupled plasma mass spectrometric determination, *Talanta.* 72(1) (2007) 187-192.
- [9] M. Sprynskyy, I. Kovalchuk, B. Buszewski, The separation of uranium ions by natural and modified diatomite from aqueous solution, *J. Hazard. Mater.* 181 (2010) 700-707.

- [10] M.S. Hosseini, A. Hosseini-Bandegharai, Comparison of sorption behaviour of Th(IV) and U(VI) on modified impregnated resin containing quinzarin with that conventional prepared impregnated resin, *J. Hazard. Mater.* 190 (2011) 755-765.
- [11] H. Sepehrian, M. Samadfam, Z. Asadi, Studies on the recovery of uranium from nuclear industrial effluent using nanoporous silica adsorbent, *Int. J. Environ. Sci. Technol.* 9 (2012) 629-636.
- [12] H. Wang, L. Ma, K. Cao, J. Geng, J. Liu, Q. Song, S. Yang, S. Li, Selective solid-phase extraction of uranium by salicylideneimine-functionalized hydrothermal carbon, *J. Hazard. Mater.* 229-230 (2012) 321-330.
- [13] R. Kannappan, S. Tanase, , D.M. Tooke, A.L. Spek, I. Mutikainen, U. Turpeinen, J. Reedijk, Separation of actinides and lanthanides: crystal and molecular structures of N,N'-bis(3,5-dit-butylsalicylidene)-4,5-dimethyl-1,2-phenylenediamine and its uranium complex. *Polyhedron.* 23 (2004) 2285–2291.
- [14] K. E. Gutowski, D.A. Dixon, *J. Phys. Chem. A*, 110 (2006) 8840-8856.
- [15] B. Siboulet, C.J. Marsden, P. Vitorge, *New J. Chem.* 32 (2008) 2080-2094.

LIST OF FIGURES

		Page No.
Figure 1.1	Nuclear energy generation 2010	36
Figure 1.2	Various steps of a typical nuclear fuel cycle	38
Figure 1.3	Hydrolysis of uranium(VI) as a function of pH	39
Figure 1.4	Adsorption as a surface phenomenon	51
Figure 1.5	Geometrical models for the hydration of UO_2^{2+}	69
Figure 2.1	Process flow sheet of uranium production plant	77
Figure 2.2	Preparation scheme of PHOA	80
Figure 2.3	Mesh size distribution of sorbent	81
Figure 2.4	Volume of sorbent in dry and fully swelled in DW (room temperature)	82
Figure 2.5	Effect of Na^+ and Mg^{++} concentration on swelling of sorbent (1g sorbent, RT, time 3h)	83
Figure 2.6	Effect of Ca^{++} concentration on swelling of sorbent (1g sorbent, RT, time 3h)	84
Figure 2.7	Swelling of PHOA (as prepared) with time in different medium	85
Figure 3.1	Isotherm profile of PHOA sorbent in BET	90
Figure 3.2	Microscopic view of PHOA and loaded PHOA	91
Figure 3.3	Morphology view of PHOA before and after uranium sorption and after uranium elution	92
Figure 3.4	EDS analysis of PHOA before and after uranium sorption and after uranium elution	93
Figure 3.5	DSC thermo-grams of the uranium loaded PHOA sorbent	94
Figure 3.6	TG and dTG thermo-grams of the PHOA, (a) before, (b) after uranium sorption and (c) after uranium elution	94
Figure 3.7	FTIR spectra of (A) PHOA, (B) loaded PHOA and (C) eluted PHOA	96

Figure 3.8	Raman spectra of (a) fresh sorbent and (b) uranium loaded sorbent	97
Figure 3.9	EDXRF spectra of PHOA sorbed with uranium	99
Figure 3.10	EDXRF of (a) reference and (b) uranium loaded PHOA sorbent	99
Figure 4.1	Uranium uptake with mesh size variation (effluent pH 8.1, RT, time 24h, sorbent 0.5g)	115
Figure 4.2	Variation of K_d and uranium uptake vs. Sorbent dosage (synthetic solution U: 9.37 mg/L, V: 50 mL, pH: 9, t: 240 min, T: 301K)	116
Figure 4.3 a)	Effect of pH on K_d of U(VI) ions on the PHOA beads (U: 8.87 mg/L, m:0.5 g, V: 50 mL, t: 24 h, T: 301K)	117
Figure 4.3 b)	Effect of pH on K_d of U(VI) ions on the PHOA beads (plant effluent, m:0.5 g, V: 50 mL, t: 24 h, T: 301K)	117
Figure 4.4	Probable (envisaged) structure of hydrated complex: $[UO_2(R)_2(H_2O)_2]$	118
Figure 4.5	Effect of agitation of solution-sorbent mixture on sorption of uranium on PHOA sorbent beads (U: 8.87 mg/L, m: 0.5 g, V: 50 mL, pH: 9, T: 301K)	119
Figure 4.6	Combine effect of competitive ions on uranium sorption on the PHOA (U: 9.37 mg/L, Mg^{+2} : 4.86 g/L, Ca^{+2} : 600 mg/L, Mn^{+2} : 5.5 mg/L, Fe^{+3} : 5.6 mg/L Cu^{+2} : 6.4 mg/L, NO_3^- : 87 g/L, pH: 9, m: 0.5 g, V: 50 mL, t: 240 min, T: 301K)	121
Figure 4.7	Effect of individual competitive ion on uranium sorption in PHOA	123
Figure 4.8	Variation in K_d , uptake and % sorption on PHOA beads as a function of initial uranium concentration (m: 0.5 g, V: 50 mL, pH: 9, t: 24 h, T: 301K)	124
Figure 4.9	Langmuir sorption isotherm of uranium ion on PHOA beads	125
Figure 4.10	Freundlich sorption isotherm of uranium ion on PHOA beads	127
Figure 4.11	Temkin sorption isotherm of uranium ion on PHOA beads	127
Figure 4.12	Dubinin–Radushkevich sorption isotherm of uranium ion on PHOA beads	128

Figure 4.13	Plot for prediction of monolayer sorption of U(VI) with respect to contact time (PHOA:0.5g, U(VI):9.11 mg/L, pH:9, Temperature: 301K)	129
Figure 4.14	Plot for prediction of multilayer sorption of U(VI) with respect to contact time (PHOA:0.5g, U(VI):9.11 mg/L, pH:9, Temperature: 301K)	129
Figure 4.15	Effect of U(VI) concentration on the sorption of PHOA at pH value 9, the PHOA concentration of 9.11 g/L, residence time 24h and temperature 301K	130
Figure 4.16	Effect of PHOA concentration on the adsorption of U(VI) at U(VI) concentration of 9.11 mg/L, pH value of 9, residence time 24h and temperature 301K	130
Figure 4.17	Effect of pH on the sorption of U(VI) (PHOA:10 g/L, U(VI):9.11 mg/L, Temperature: 301K, Residence time: 24h)	131
Figure 4.18	Swelling effect of PHOA in NaOH solution at temperature 301K	132
Figure 4.19	Kinetics of uranium sorption onto PHOA (PHOA: 0.5g, synthetic U(VI): 9.11 mg/L, T: 301K, pH: ~9)	133
Figure 4.20	Pseudo-first order plot for sorption of U(VI) (PHOA:0.5g, U(VI):9.11 mg/L, pH:9, Temperature: 301K)	134
Figure 4.21	Pseudo-second order plot for sorption of U(VI) (PHOA:0.5g, U(VI):9.11 mg/L, pH:9, Temperature: 301K)	135
Figure 4.22	Boyd plot for U(VI) sorption onto PHOA (PHOA:0.5g, U(VI):9.11 mg/L, pH:9, Temperature: 301K)	136
Figure 4.23	Intra-particle diffusion model plot for sorption of U(VI) (PHOA:0.5g, U(VI):9.03 mg/L, pH:9, Temperature: 301K)	137
Figure 4.24	Influence of temperature on the thermodynamic properties of uranium sorption process on PHOA beads (U: 9.37 mg/L, m: 0.5 g, V: 50 mL, pH: 9.1, t: 240 min)	138
Figure 4.25	Influence of temperature on kinetic property of uranium sorption process on PHOA beads (U: 9.37 mg/L, m: 0.5 g, V: 50 mL, pH: 9.1, t: 240 min)	139
Figure 4.26	The Arrhenius plot for U(VI) sorption on PHOA	140
Figure 4.27	Stability of PHOA with respect to sorption of uranium	141

Figure 5.1	Desorption performance of uranium from loaded PHOA with various eluent	147
Figure 5.2	Elution performance of uranium from loaded PHOA with different HCl concentration (synthetic solution, U: 9.11 mg/L)	148
Figure 5.3	Elution performance of uranium from loaded PHOA with different HCl concentration (Plant effluent)	148
Figure 5.4	Elution performance of uranium from loaded PHOA with variation of agitation, a) loaded sorbent with synthetic uranium solution, b) loaded sorbent with plant effluent	149
Figure 5.5	Elution performance with time (1M HCl, RT) with a) synthetic U solution and b) plant effluent	151
Figure 5.6	Elution performance with temperature	152
Figure 5.7	Metals ions loaded PHOA: a) Cu^{++} , b) NO_3^- , c) Fe^{+++} , d) Ca^{++} , e) Mg^{++} and f) Mn^{++}	153
Figure 5.8	Eluted PHOA: a) Cu^{++} , b) NO_3^- , c) Fe^{+++} , d) Ca^{++} , e) Mg^{++} , f) Mn^{++}	153
Figure 5.9	Effect of presence of competitive on elution performance a)-c): Ca^{++} , d)-f): Mg^{++} , g)-i): Mn^{++} , j)-l): Cu^{++} , m)-o): Fe^{+++} , p)-r): NO_3^-	155
Figure 5.10	Reusability of PHOA with respect to desorption of uranium	157
Figure 6.1	Experimental set up for column study	167
Figure 6.2	Breakthrough of sorption and elution in 1" ID column using plant effluent, PHOA: 5g, flow rate: 2 mL/min, U: 9.81 mg/L	168
Figure 6.3	Effects of inlet uranium concentrations on sorption breakthrough	169
Figure 6.4	Sorption breakthroughs for different flow rates of effluent solution	170
Figure 6.5	Sorption breakthroughs for different masses of sorbent, PHOA loaded in a column (bed height)	172
Figure 6.6	Effects of 2.5" ID column diameter on sorption breakthrough	173
Figure 6.7	Effects of 3.5" ID column diameter on sorption breakthrough	173

Figure 6.8	Thomas model plot for column 2" ID with different bed height	174
Figure 6.9	Thomas model plot for column 2.5" ID with different bed height	175
Figure 6.10	Adam-Bohart model plot for column 2" ID with different bed height	176
Figure 6.11	Adam-Bohart model plot for column 2.5" ID with different bed height	176
Figure 6.12	Bed depth service time of column at different bed height: $C_0=9.81$ mg/L and flow rate = 15 mL/min	177
Figure 6.13	Effect of variation of k_a at fixed capacity: $C_0=9.81$ mg/L, flow rate = 15 mL/min	177
Figure 6.14	Estimation of mass transfer coefficient for sorption of U(VI) on PHOA at pH 9	178
Figure 6.15	Effect of flow rate on elution breakthrough: 1M HCl	179
Figure 6.16	Effect of PHOA bed depth on elution breakthrough in 2" column: 1M HCl	179
Figure 6.17	Effect of PHOA bed depth on elution breakthrough in 2.5" column: 1M HCl	180
Figure 6.18	Effect of PHOA bed depth on elution breakthrough in 3.5" column: 1M HCl	181
Figure 7.1	Multi scale molecular modelling scheme	184
Figure 7.2	Optimised structure of complex containing two functional groups (from different sorbent chain) and one uranyl ion in gas phase, without water, anti position	186
Figure 7.3	Optimised structure of complex containing two functional groups (from different sorbent chain) and one uranyl ion in gas phase, without water, syn position	186
Figure 7.4	Optimised structure of complex containing two functional groups (from different sorbent chain) and one uranyl ion in gas phase with one water, anti position	187

Figure 7.5	Optimised structure of complex containing two functional groups (from different sorbent chain) and one uranyl ion in gas phase and liquid phase with one water, syn position	187
Figure 7.6	Optimised structure of complex containing two functional groups (from different sorbent chain) and one uranyl ion in liquid phase with two waters, anti position	188
Figure 7.7	Optimised structure of complex containing two functional groups (from different sorbent chain) and one uranyl ion in liquid phase with two waters, syn position	188
Figure 7.8	Optimised structure of complex containing four functional groups and two uranyl ions (a) without water, (b) with one water	189
Figure 7.9	Optimised structure of complex containing four functional groups and two uranyl ions with two waters	189
Figure 7.10	Optimised structure of complex containing four functional groups and two uranyl ions with three waters	190
Figure 7.11	Optimised structure of complex containing four functional groups and two uranyl ions with four waters	190

LIST OF TABLES

Table 1.1	Comparison of efficiency of fuel resources in energy production	37
Table 1.2	Comparative evaluation of various metal ions removal techniques	51
Table 1.3	Solid phase extractants for uranium separation	60
Table 1.4	Major Sorbents reported for the uranium recovery from seawater / dilute solutions	63
Table 2.1	Composition of plant wastewater	77
Table 2.2	C, N, H, O analysis of novel sorbent, POHA; 5% POHA	80
Table 2.3	Solubility of sorbent, PHOA in different solvents	86
Table 3.1	BET results of the PHOA sorbent	90
Table 3.2	Raman spectral data of fresh sorbent and uranium loaded sorbent	98
Table 4.1	Sorption characteristics of uranium, magnesium and calcium using plant effluent in batch experiment	114
Table 4.2	Isotherm parameters of sorption of uranium ion on PHOA sorbent beads	126
Table 4.3	Kinetic parameters for U(VI) sorption into PHOA at 301 K	134
Table 4.4	Thermodynamic parameters of sorption of uranium ion on PHOA sorbent beads	139
Table 5.1	Elution characteristics of uranium, magnesium and calcium in plant effluent in batch experiment	150
Table 6.1	Thomas model parameters for 2" ID and 2.5" ID column with different bed	174

CHAPTER – 1

INTRODUCTION

1. Introduction

1.1 Nuclear power programme

India's primary energy consumption is going to be more than doubled between 1990 and 2012. There is an acute demand for more and more reliable power supply in India. About 20 billion kWh power was generated using nuclear fuel which is 3.7% of India's total electricity generation in 2011 [1]. In India, the nuclear investment for electricity is being promoted due to shortage of fossil fuels and about 25% nuclear contribution in total energy is the ambition by 2050 when 1094 GWh of base-load capacity is expected to be required [2]. Hence, Department of Atomic Energy, India has initiated the generation of sustainable nuclear power program in three steps to meet India's energy demand [3].

Nuclear power has to play an important role to meet the world energy demand with the diminishing sources of fossil fuels and it contributes about 13.5% of world's electricity demand (Figure 1.1) [4]. There is no other energy source which gives large amount of power using a small amount of fuel and space (Table 1.1). In India, Natural uranium reserve is about 1, 72,000 tonnes of U_3O_8 [5]. Therefore, it is required to explore various other resources of uranium including secondary resources to meet sustainable Indian nuclear programme [3,6].

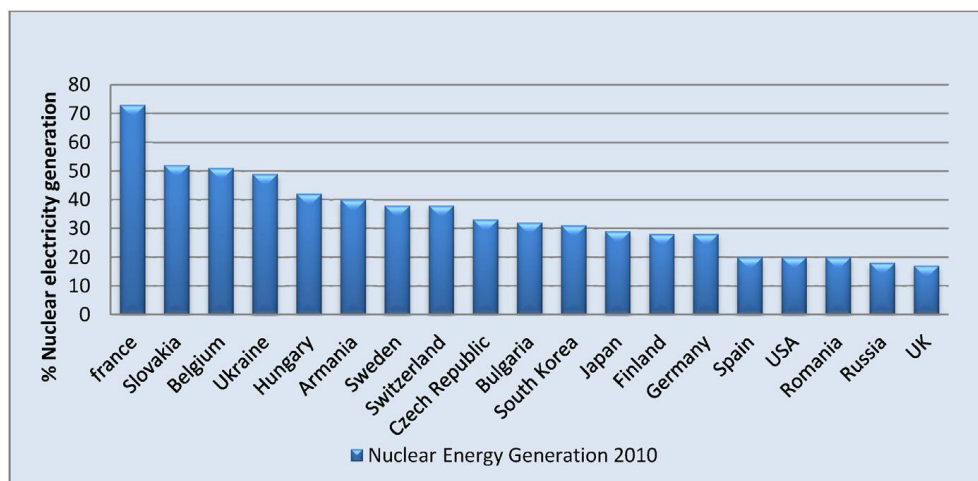


Figure 1.1: Nuclear energy generation 2010

Table 1.1: Comparison of efficiency of fuel resources in energy production

To generate 12,000 KWh (units) we approximately need	
Oil	1 ton
Coal	1.5 ton
Natural gas	1.11 x 10³ cuM
Uranium	0.06 Kg

It is also important and necessary to recognize the concern over the health and environmental impacts of uranium in parallel to ensure a long term supply of uranium to sustain any country's nuclear power program. It is necessary to adopt innovative and advanced technology for enhancing efficiency of uranium recovery from its sources. Responsibility of uranium material processing facilities cannot be denied to meet high level environmental standards and legislations being set in nuclear business. As a result of the developments that have taken place world wise in the areas of uranium recovery from unconventional sources or from its lean solution, the philosophy and the concept of the processing of the plant effluent have changed from the traditional methodology. Today, unconventional resources of uranium are playing more important role and engaging more attention than before [6]. Some of the unconventional sources are exploitable by using unconventional techniques improving techno-economic constraints. Thus the uranium recovery technique or separation methodology should be recognized as having a bright future considering both, the recovery and the environmental effects.

1.2 Nuclear Fuel Cycle

It refers to the steps by which fissionable (for example ^{233}U , ^{235}U , ^{239}Pu) and fertile (for example, ^{238}U , ^{232}Th) materials are prepared for use in, and recycled or discarded after

discharge from, the nuclear reactor. These steps include mining and milling of uranium or thorium bearing ores to form concentrates. **Figure 1.2** shows the different steps of a typical nuclear fuel cycle.

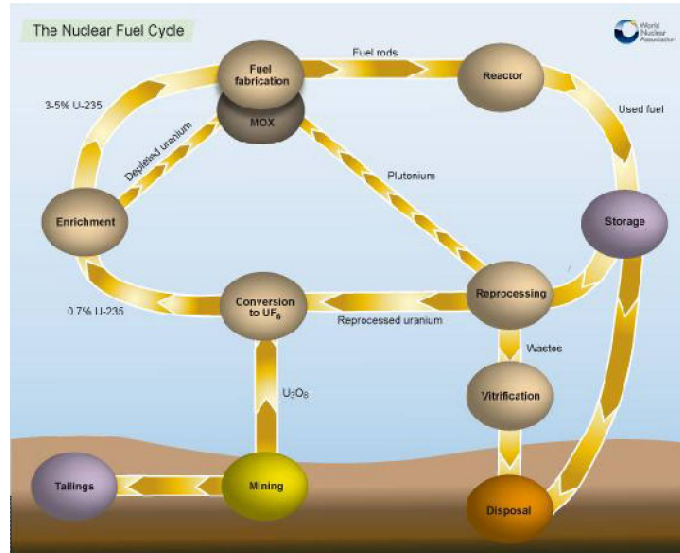


Figure 1.2: Various steps of a typical nuclear fuel cycle

Waste management includes the treatment, storage, and disposal of radioactive wastes from the different parts of the fuel cycle, is comprised of different important processes which are under continuous development.

1.3 Uranium

It is required to understand the chemistry and properties of uranium for developing its separation process. Symbol of uranium is “U”, atomic mass 90, atomic weight 238.03, density 18.9 gm/cc, melting point 1132°C. The element was discovered by Martin Heinrich Klaproth in 1789. In 1841 the element was first isolated in metallic form by EM Peligot. Uranium is a member of actinide family (group – III B). Chemically uranium resembles group VIB elements. Uranium is having 14 isotopes with mass number $227 \leq A \leq 240$ and all are radioactive. Naturally occurring uranium contains 99.28% U²³⁸, 0.72% U²³⁵ and traces of other isotopes. Electronic configuration of gaseous uranium is Rn 5f³ 6d¹ 7s² and uranium is having four oxidation states as U³⁺, U⁴⁺, U⁵⁺ and U⁶⁺ out of which U⁴⁺ and U⁶⁺ states are stable in nature.. In hexavalent state it exists as stable divalent uranyl ion, UO²⁺. Like iron

uranium has strong affinity for oxygen, reacting readily with water to form oxides. No simple ions of oxidation state U^{2+} are known in solution [7]. In the tetravalent state its ionic radius is 0.101 nm with coordination number (CN) 8 and 0.097 nm with CN 6. The hexavalent ionic radius is 0.080 nm with CN 6. The uranyl complex UO_2^+ develops in aqueous solution as: $U^{4+} + 2H_2O = UO_2^{2+} + 4H^+ + 2e^-$. The hexavalent uranium ion lies in between two oxygen ions in a linear dumbbell-shaped structure, 0.34 nm long and 0.14 nm wide, in the uranyl complex which forms preferentially layered structure minerals, with basic formulae: A $(UO_2)(RO_4)^- \cdot X H_2O$ and B $(UO_2)(RO_4)^{2-} \cdot X H_2O$ where, $R=P^{5+}, V^{5+}, As^{5+}$; $A=K^+, Na^+$; $B= Ba^{2+}, Ca^{2+}, Fe^{2+}, Mg^{2+}, Pb^{2+}$. The U^{4+} and UO_2^{2+} ion complexes are readily available with carbonate, chloride, sulphate, nitrate, phosphate, citrate, thiocyanate and organic anions. At low temperature and pH 4.5-7, uraniferous complexes find to be insoluble, but dominant above $150^\circ C$. Uranyl complexes are soluble over a wide range of conditions. Uranyl fluoride complexes are dominant at pH value less than 4 even at $25^\circ C$, uranyl phosphate in pH 4-7.5, uranyl di- and tri-carbonate complexes at pH 7.5 and uranyl hydroxide predominates at above $100^\circ C$. The uranyl ion can be viewed as the end result of extensive hydrolysis the highly charged, hypothetical, U^{6+} cation as in **Equation 1.1**. Hydrolysis of uranium(VI) as a function of pH is reported to be as shown in **Figure 1.3**.

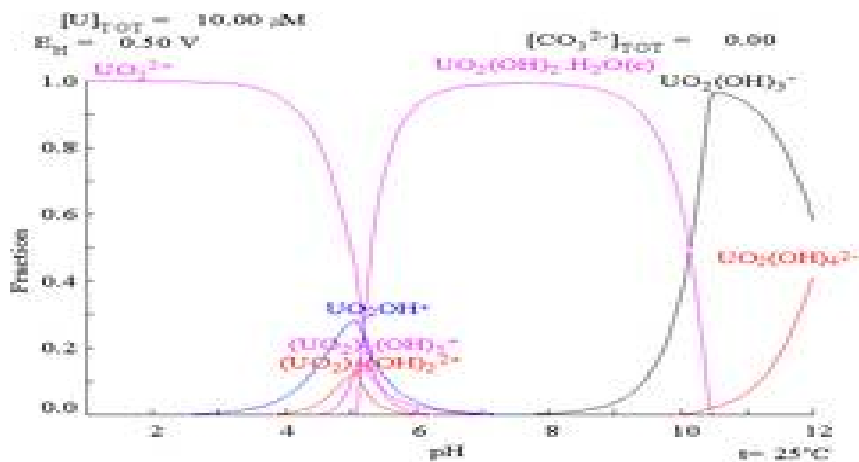
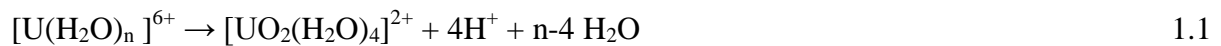


Figure 1.3: Hydrolysis of uranium(VI) as a function of pH [7]

The driving force for this hypothetical reaction is the reduction in charge density on the uranium atom. The number of water molecules attached to the uranyl ion in aqueous solution is mostly five [8]. Further hydrolysis occurs with a further reduction in charge density when one or more equatorial water molecules are replaced by an hydroxide ion. In fact the aqueous uranyl ion is a weak acid [9]. Uranium metal has three distinct crystalline forms: alpha, to 660°C; beta, from 660°C to 770°C; and gamma, from 770°C to melting point. In the past, uranium has found various industrial and laboratory uses like, colouring of glasses, leather & woods, ceramic glazes, as alloying component of steel, determining of sodium in laboratory etc. The use of uranium and its products as a source of radioactive emission is of increasing importance in research and industry.

1.3.1 Natural occurrence of uranium

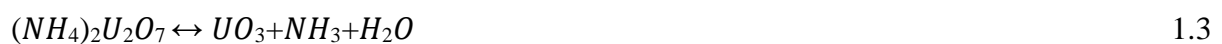
Uranium is believed to be concentrated largely in the Earth's crust, where the average concentration is 4 parts per million (ppm). For comparison, the crust contains 0.1 ppm silver and 0.5 ppm mercury. Basic rocks (basalts) contain less than 1 ppm uranium, whereas acidic rocks (granites) may have 8 ppm or more. Estimates for sedimentary rocks are 2 ppm, and for ocean water is 0.0033 ppm. The total uranium content of the Earth's crust to a depth of 25 km is calculated to be 4.5×10^{17} kg; the oceans may contain 4.5×10^{13} kg of uranium [10]. Several uranium-containing minerals have been identified, but only a few are of commercial interest. Pitchblende, a variety of uraninite found in hydrothermal veins, is the most important mineral of uranium. With the discovery of nuclear fission and the potential of atomic power, the possession of uranium reserves became vitally important. Uranium reserves containing more than 1g U_3O_8 /kg of ore for that part of the world for which statistics are available, are estimated at about 2.2×10^9 kg U_3O_8 , and those of the United States are about 10^9 kg U_3O_8 [11-14]. In addition to the different occurrences, extensive reserves of low- grade ore (0.005 to 0.02% uranium) exist in phosphate deposits

(Florida, Brazil, Soviet Union, and North Africa), in bituminous shales (Soviet Union, Sweden, and Tennessee), and in lignites (the Dakotas) [15].

In India, the major uranium deposit sites are: a) Jaduguda, b) Bhatin, c) Narwapahar, d) Turamdih, e) Mohuldih and f) Bagjata, located in eastern region. In addition to that 14 middle Proterozoic basins have identified since 1990 which are expected to possess geological setting conducive to host this type of deposit. Further, the deposit of Tummalapalle is lower grade (~0.042 % U₃O₈) but reasonably large reserve and it is confined in the host rock of alkali (dolomite and calcite).

1.3.2 Uranium metal preparation

Uranium is a very dense, strongly electropositive, reactive metal; it is ductile and malleable, but a poor conductor of electricity. It is most conveniently prepared by the reduction of a halide (UF₄) with calcium or magnesium in a sealed bomb at 1200-1400°C (2190-2550°F) [16]. The steps involved in preparation of the metal from uranyl nitrate are summarized by reactions **Equation (1.2) - (1.6)**.



Uranium metal exists in three crystalline modifications: (a) uranium (25-668°C or 68-1234°F) is orthorhombic, with four atoms per unit cell, and density of 19.04 g/cm³. Its structure is interpreted as (a) distorted hexagonal lattice containing corrugated sheets of uranium atoms; (b) The beta phase (668-775°C or 1234-1427°F) is a complex tetragonal structure, with 30 atoms per cell, and a density of 18.13 at 720°C (1328°F); and (c) Uranium (775-1132°C or 1427-2070°F) is body-centred cubic, with two atoms per cell, and density of

18.06 g/cm³ at 805°C (1481°F). The beta phase can be stabilized at room temperature by addition of small amounts of chromium, the gamma form with molybdenum. Aluminium, beryllium, bismuth, cadmium, cobalt, gallium, germanium, gold, indium, iron, lead, manganese, mercury, nickel, tin, titanium, zinc, and zirconium can form one or more inter-metallic compounds with uranium [17]. Chromium, magnesium, silver, tantalum, thorium, tungsten, and vanadium, as well as calcium, sodium, and some of the rare-earth metals, form neither compounds nor extensive solid solutions. Many uranium alloys are of great interest in nuclear technology because the pure metal is chemically active and anisotropic and has poor mechanical properties. Uranium depleted of the fissile isotope ²³⁵U has been used in shielded containers for storage and transport of radioactive materials. Nitric acid dissolves the metal, but non-oxidizing acids, such as sulphuric, phosphoric, or hydrofluoric acid, react very slowly. Usually a trace of mercuric nitrate tends to catalyze the dissolution. Uranium metal is inert to alkali metals, but addition of peroxide causes formation of water-soluble peruranates.

1.3.3 Toxicity of uranium

The amount of uranium in the environment has exceeded due to activities of nuclear industry, mineral extraction, uranium combustion, mining processes and use of phosphate fertilizer that contains uranium [18,19]. As per the World Health Organization (WHO) standards, the maximum acceptable concentration of U(VI) in water is 50 mg L⁻¹ [20]. The tolerable daily intake of soluble uranium declared by WHO based on Gilman's studies is 0.6 mg/kg of body weight per day [21]. Daily intake of uranium in food and water varies from approximately 1–5 mg U/d daily in uncontaminated regions and 13–18 mg U/d or more in uranium mining areas [22]. Inhalation of respirable air-borne uranium containing aerosols and anthropogenic foundations are another major source of uranium in the body.

Toxicity of uranium is closely associated with its solubility [23]. Hexavalent uranium compounds are highly water soluble as compared to tetravalent forms [24]. In regions of radioactive contamination of local soil and groundwater, the chemical toxicity of uranium has tremendously aggravated health concerns [25]. Uranium, due to its superior binding affinity to bio molecules, is known to be a mutagen and an ephrotoxin. Exposure to uranium radionuclides formed during decay for a long period is known to develop cancer [26,27]. Samples around the coal-fired power plants in Amritsar district of Punjab were analyzed and the uranium concentration was found up to 15 times higher than the recommended World Health Organization's maximum safe limits. It was observed that a large part of Punjab was affected due to Uranium contamination, which houses 24 million people [28]. New Mexico, on July 16, 1979, witnessed the Church Rock Uranium mill spill [29,30]. Around 1100 tons of solid radioactive mill waste and 93 million 119 US gallons of radioactive tailing solution having pH 1.2 entered the Puerco river, near Navajo, raising the uranium concentration to 7000 times the acceptable limit [31,32]. Navajo, since then, has had significantly higher cancer rates than the country's average, resulting in widespread death of residents as well as cattle.

1.3.4 Uranium bearing wastewater

Water and soil contamination with uranium ions has become a global environmental problem. Uranium subsists in the environment due to leaching from mine tailings, natural deposits, uranium combustion products, emissions from the nuclear industries, corrosion of uranium and use of uranium-containing phosphate fertilizers [33–35]. These sources cause continuous release of trace uranium ions into the environment. Even at low concentrations, because of their persistent and accumulative nature are toxic [36,37]. Chronic exposure to elevated levels of this heavy metal is known to cause the bone degeneration, the liver and the lung and blood damage. On the other hand, limited quantities of uranium minerals in nature and the expected

shortage of uranium in the near future [38] also restrict mining, production, and consumption of this metal. Therefore, separation and recovery of uranium are of great practical significance, not only in reutilization of uranium resources and sustainable development of nuclear energy, but also for protection of both human health and ecological environment. Thus, the development of clean-up / remediation technologies for removing uranium from industrial wastewaters is very important and has drawn attention of many researchers [39–41].

1.4 Uranium separation techniques

Literature reports manifest the remediation technologies that have been studied for the removal and recovery of uranium from industrial effluents and waste water. Toxic metals like uranium can be removed from wastewaters, for the clean-up process, by a number of separation technologies, such as chemical precipitation [42], membrane process [43,44], solvent extraction [45], ion exchange [46], floatation [47], coagulation [48] and sorption process [49–52]. Despite different techniques applied for the remediation of uranium removal from wastewater, it is important to mention that the selection of the most apposite treatment techniques depends on the composition of the wastewater, initial metal concentration, principal investment and operational cost, plant tractability and reliability and environmental impact. Major efficient and facile techniques that are in application in the present scenario for uranium removal have been highlighted and discussed. Membrane filtration, chemical precipitation and extraction techniques are widely used for retrieval of uranium(VI) ion from dilute solutions. Among all, solid phase extraction (SPE) technique has been proven to be superior technique for wastewater treatment in terms of initial cost, flexibility, and simplicity of design, ease of operation and insensitivity to toxic pollutants. SPE being the most successful technique has eliminated high capital investment and operating cost and in addition to this, generation of solid waste which poses proper disposal challenges [53–60].

1.4.1 Membrane filtration technique

Membrane filtration technologies, with various modifications, have seen prodigious application in heavy metal removal for their high efficiency, easy operation and space saving. The widely used membrane processes to remove metals from the wastewater are nanofiltration, ultrafiltration and reverse osmosis.

1.4.1.1 Nanofiltration technique

Nanofiltration (NF) membranes are charged (due to the material or adsorption in aqueous solution) and reject multivalent ions whereas mono-valent ions are only partly rejected. Nanofiltration has an advantage over reverse osmosis, as it can be carried out at lower osmotic pressures, signifying the proportionally lower consumption of energy [61]. Due to high charge on the uranyl ion, NF membranes are able to reject U(VI) from mineral water with a relatively high selectivity, despite a high concentration of competing alkaline and alkaline-earth cations. During membrane filtration, the metal ions in the feed water are convectively driven to the membrane surface due to which a concentrated polarization boundary layer near the membrane is formed. This resulted in reduction in the charge density of the membrane and subsequently, diminishes the electrostatic repulsions between the metal ions in solution and the charge of the membranes, leading to a decrease in the rejection [62]. The rejection of U(VI) with water sample was found to be 40% with G10 (MWC = 2500 Da), and 95% and 99% for DL(MWC = 300 Da) and DK(MWC = 150–300 Da) membranes [63]. The size and charge of solutes influence the extent of rejection by nanofiltration membranes and the mechanism of this rejection is closely related to the type of membrane used [64]. Raff and Wilken [65] found that 81–99% uranium could be rejected simply using NF. The summarized results of all experiments showed that the uranium removal from water at the tested NF membranes was mainly between 90 and 98%. This seems to be effective over a wide range of hydro-chemical settings such as highly acidic water. While varying the

uranium concentration from 10 mg/L to 1 mg/L, no major difference in the removal efficiencies of the membranes was witnessed [66].

1.4.1.2 Ultrafiltration technique

Ultrafiltration (UF) is a type of membrane filtration in which hydrostatic pressure is the driving force for waste rejection. High molecular weight suspended solids and solutes are retained, whereas water and low molecular weight solutes percolate through the membrane. Ultrafiltration is fundamentally similar to microfiltration or nanofiltration except in terms of the size of the molecules it retains. UF membranes are usually polymer coated to improve the rejection efficiency. Based on this, various polymers were tested and the best results were obtained by using polyethylenimine (PEI) [66] with a molecular mass of 60,000 and with branched structure of molecules. This polymer features the ability to form complex compounds with numerous ions of heavy metals. To ensure that the uranium is mostly in ionic form, the experiments were carried out at pH 4. The trans-membrane flux was varied slightly and was at the equal to 20 mg/s at pH 4.0 and a bit lower level of 18 mg/s at pH 5.0 [65]. The retention coefficient was found to be 0.21 (at pH 4.0) and 0.999 at pH 5.0. The system has not been tested and reported in alkaline medium.

1.4.1.3 Reverse osmosis technique

The reverse osmosis (RO) process uses a semi-permeable membrane, allowing the feed to pass through it and rejecting the contaminants. The RO systems concentrate the uranium in the permeate stream. The major drawback of RO is the high power consumption due to the high pressures required and the restoration of the membranes, though, reverse osmosis membranes operable at ultralow pressures have been developed [67,68]. Reverse osmosis involves a diffusive mechanism so that separation efficiency is dependent on pressure, solute concentration, and water flow rate [69]. Membrane filtration technology can remove uranium

ions with high efficiency, but its problems such as high cost, process complexity, membrane fouling and low permeate flux have limited their use in uranium removal.

1.4.2 Chemical precipitation technique

1.4.2.1 Reductive precipitation of uranium(VI)

Zero valent iron (Fe^0) filings were used as reductants, and the adsorbents included iron oxide, peat materials, and a carbon-based sorbent (Cercona Bone-Char). Results indicate that Fe^0 filings are much more effective than the adsorbents in removing uranyl (UO_2^{2+}) from the aqueous solution [70]. Reductive precipitation through iron oxide is more favoured when the surface of the material is not covered by corrosion products (especially around pH 4) [55]. Generated corrosion products have greater affinity for U than the bare iron oxide surface even under anoxic conditions. Selecting iron oxide for remediation of uranium is simplified because reactivity is a unique function of the material dissolution, and not of the specific interaction of the contaminant with the material [55]. Nearly 100% of uranium was removed through reactions with Fe^0 at an initial concentration up to 76 mM (or 18,000 mg) of U/L. Results from the batch adsorption and desorption and from spectroscopic studies indicate that reductive precipitation of U on Fe^0 is the major reaction pathway. Only a small percentage (<4%) of UO_2^{2+} appeared to be adsorbed on the corrosion products of Fe^0 and carbonate solution can easily be desorbed.

1.4.2.2 Bio-precipitation of uranium

Algae are of principal interest for the because of their ability to remove U(VI) and because some algae can live under extreme environmental conditions, frequently in abundance. It was found that the charged surface of bacteria was present with multitude of functional groups that form complexes with uranium(VI) in soil solution, thereby facilitating its removal [71]. In the extreme environments, bacteria may interact efficiently with these inorganic contaminants through different mechanisms such as precipitation [72,73,74], intracellular

accumulation [75] and biosorption at the cell surfaces [76]. The uranium– bacterial interaction experiments were performed when the uranium aqueous speciation is dominated by highly mobile uranyl ions at lower pH values (2.0–4.5) [77].

1.4.3 Extraction technique

Removal, separation, enrichment and recover of trace/heavy and precious metals in aqueous solutions play an important role for the analysis of waste waters, industrial and geological samples, as well as for environmental remediation. Exhaustive works has been carried out on the uranium separation processes, their feasibility and economics. Amongst several separation techniques solvent extraction is recognized as a versatile for laboratory as well as for large scale separation of uranium from different streams [78 - 81]. However, separation and recovery of uranium by conventional solvent extraction has some short coming with respect to third phase formation, crude oil formation as well as solvent loss [82,83]. Moreover, this method cannot be used for effective separation and recovery of metal ions from dilute solutions. Thus the development of more efficient techniques has lead to development of liquid-membrane based separation which holds promise for recovery of uranium ions from dilute resources and has received a considerable attention in separation science and technology [84,85].

Liquid membrane processes are finding increasing application in chemical industry for achieving energy efficient separations from very dilute medium. Liquid membranes possess high selectivity and hence, less staging requirements. In general two types of liquid membranes - bulk / supported liquid membrane (BLM / SLM) and emulsion liquid membrane (ELM) have been reported widely are being extensively studied, for their application in extraction and concentration of dissolved metals from effluents. Several studies on the recovery of uranium from waste solutions using various extractants by supported liquid membranes have been described in literatures [86, 87]. Supported liquid membrane (SLM)

studies have been carried out employing di(2-ethylhexyl) phosphoric acid (D2EHPA) with and without neutral oxodonors (tri-*n*-butyl phosphate (TBP), di-butyl butyl phosphonate (DBBP), tri-*n*-octyl phosphine oxide (TOPO), and Cyanex 923 (a mixture of four trialkyl phosphine oxides viz. R_3PO , $R_2R'PO$, RR'_2PO and R'_3PO where R: *n*-octyl and R': *n*-hexyl chain)) for the recovery of uranium(VI) from phosphoric acid medium [88-90]. Detailed study has been carried out on solvent extraction of uranium from various medium using either Cyanex 272 or a mixture of Cyanex 272 with other extractants [91]. Swant et.al investigated the transport of uranium from nitric acid solution over plutonium, americium and other fission products across flat sheet supported liquid membrane under varying experimental conditions [92]. Few reports are available in literature on permeation of uranium from nitric acid medium using supported liquid membrane in presence of Cyanex 272 as a carrier [92]. The problem of low flux rate due to high diffusion resistances, inefficient operation and exorbitant costs encountered in bulk and supported liquid membranes (SLM / BLM) are overcome in an ELM. In the ELM process, an emulsion of organic membrane phase and aqueous inner phase is dispersed in the continuous aqueous feed phase. This gives a highly selective and ultra thin liquid film generating a large mass transfer area for separation. Liquid Emulsion Membrane technique has been tried by various workers for recovery of uranium, plutonium and lanthanides from dilute secondary solutions. Various carriers have been used for various feed streams. Reefy et al. (1997) [93] used TOPO to selectively recover uranium and thorium from a nitrate solution containing other metal impurities. They obtained 98% recovery of uranium and 92% recovery of thorium using cyclohexene as the diluent, 0.1M sodium citrate as the strip and SPAN 80 as the surfactant. Reefy et al. (1998) [94] also used TOPO for separation of uranium and thorium from chloride medium. TOPO has been used for recovery of uranium from nitrate medium with sodium carbonate as strip by Kulkarni et al. (2002) [95]. Studies on kinetics, swelling, leakage and equilibrium behaviour of LEM

systems have been done with uranium by Kedari (2001) [96]. Their reports include removal of uranium from nuclear waste streams. According to them advantages of LEM over conventional solvent extraction process are its low solvent inventory, low equipment cost and higher mass transfer rate due to larger surface area for extraction. But, main disadvantages are the leakage and swelling problems and difficulties in de-emulsification step for which the technology yet to be brought up to industrial scale with full confidence. Hence, solid phase extraction for separation and removal of uranium ions is the method of choice due to its high separation efficiency, good reproducibility of retention parameters, and simplicity and is a popular method owing to its applicability to both pre-concentration and separation [97,98].

1.5 Solid Phase Extraction (SPE)

SPE has many additional advantages over other separation techniques such as (i) reduced solvent usage (ii) low disposal costs, (iii) short extraction times, (iv) high efficiency, (v) ecologically-safe, (vi) elimination of some of the glassware, (vii) isolation of analytes from large volumes of sample with minimal or zero evaporation losses (for pre-concentration), (viii) reduced exposure of analysts to organic solvents (ix) more reproducible results (x) remote operation etc. In recent years, SPE is the most often used method in trace metal analysis in environment for the separation and/or pre-concentration purposes. A wide range of solid phases is available for column SPE technique which can be easily automated. To give a clear depiction, a comparative evaluation of the aforementioned techniques has been portrayed in **Table 1.2**. The **Table 1.2** lists the advantages and disadvantages of the most widely used techniques. Of all the listed suitable techniques, adsorption was found to be most suitable technique and for which a detailed analysis is required.

SPE is called sorption which defined as a surface phenomenon; sorption is the adhesion of a molecule onto the adsorbent surface (**Figure 1.4**). The process of sorption involves a solid phase (sorbent) and a liquid phase (solvent) containing a dissolved species to be sorbed and

proceeds by rather complex process affected by several mechanisms involving adsorption by physical forces on surface and pores, chemisorptions, ion exchange, complexation, chelation, and entrapment in capillaries [99]. Due to high affinity of the sorbent for the uranium(VI) ion species, the latter is attracted and bound by the sorbent via these mechanisms.

Table 1.2: Comparative evaluation of various metal ions removal techniques

Technique	Advantages	Disadvantages
Adsorption	Reusability Selectivity Ease of operation No sludge produced	High adsorbent cost (e.g. graphene oxide, calixarenes etc.)
Membrane filtration	High efficiency (up to 99%) Low waste produced	High cost Process complexity Low permeate flux
Microbiological methods	Cheap High efficiency Bio-degradable waste	Anaerobic reaction conditions
Phytoremediation	Economical No secondary pollution	Low efficiency Depends on the many environmental conditions
Reductive precipitation	Highly efficient Ease of operation	High cost Complex processes

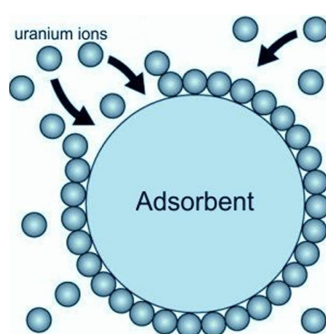


Figure 1.4: Adsorption as a surface phenomenon.

A solid phase extractant, adsorbent consists of two parts: a matrix and functional components. An inert host structure which allows diffusion of hydrated ions i.e. a hydrophilic matrix is an essential part of any sorbent. The selection of the matrix depends on several important criteria of application like regular and reproducible form of its structure, stability in

conditions of application medium, option on the type of exchanger etc. The functional group, which represent the ligands required for metal complexation. The most common coordinating atoms present in the main or side chain are N, O, P and S. It is possible to make chelating sorbent that have a selective adsorption capacity for specific metal ions by fixing the desired ligands groups on the sorbent matrix. Commonly used materials for the matrix can be broadly divided into the following four groups:

- (i) **Minerals and Inorganic oxides:** clay, diatomite, zeolite, alumina, silica, ceramic, tin oxide, iron oxide etc.
- (ii) **Carbonaceous materials:** activated carbon (AC), mesoporous carbon, carbon nanotubes (CNTs), graphite and its derivatives/ grapheme etc.
- (iii) **Biosorbent:** Chitosan, yeast, alga, agro-waste etc.
- (iv) **Polymers/copolymers:** resins, hybrid materials/composites, gels and related materials.

For each type of matrix have advantages and disadvantages based on its application. The detailed study has been carried out on the basis of sorbent matrix category for SPE of uranium metal ions.

1.5.1 Minerals and inorganic oxides

Being a low-cost material mineral type sorbent seems to be one of the most perspective sorbents taking into account its ability of heavy metals removal from wastewater. Adsorption of U(VI) on the natural diatomite from aqueous solutions by diatomite [100] were studied. It is reported that OH groups and oxygen bridges of the diatomite surface act as adsorption sites forming hydrogen bonds with the adsorbate. Analysis on kinetic and equilibrium adsorption of uranium ions from water solution onto the natural diatomite and the diatomite modified by hexa-decyl-tri-methyl-ammonium (HDTMA) has been reported [101]. New solid phase extraction technique was developed based on the pre-concentration of UO_2^{2+} ion in

environmental samples on sodium dodecyl sulphate (SDS) coated alumina prior to the determination by spectrophotometry method [102]. A pre-concentration factor more than 200 was achieved and the average recovery of U(VI) was 99.5%. Various low-cost clay/soil based ceramics have been developed to treat liquid wastes by removing various hazardous metals ions [103-106]. Talc is a layered magnesium silicate mineral with the chemical formula $Mg_3Si_4O_{10}(OH)_2$ [107]. The surface area occupied by the maximum amount of uranium adsorbed (41.6 mg/g) as a monolayer was $58.3 \text{ m}^2/\text{g}$ [108]. In a study, tin oxide has been synthesized with nano structure as an absorbent in order to separate uranium and thorium by homogenous precipitation method in the presence of urea [109]. The application of nano- Fe^0 for the removal of radionuclides, however, remains less widely researched with studies limited to uranium [110-112]. Amidoxime-functionalized silica coated Fe_3O_4 ($Fe_3O_4@SiO_2-AO$) exhibited enhanced sorption capacity for U(VI) in comparison with raw silica coated Fe_3O_4 due to the strong chelation of amidoxime to U(VI). The kinetic process of U(VI) sorption on $Fe_3O_4@SiO_2-AO$ reached equilibrium within 2h [113]. Another latest technology involving yolk-shell microsphere with magnetic Fe_3O_4 cores and hierarchical magnesium silicate shells ($Fe_3O_4@MS$) have been successfully synthesized by combining the versatile sol-gel process and hydrothermal reaction. The maximum adsorption capacity for uranium(VI) was calculated to be 242.5 mg/g at pH 5.5 [114].

1.5.2 Carbonaceous materials

Carbon materials offer an advantage of higher thermal and radiation resistance than organic exchange resins and better chemical stability than familiar inorganic sorbents in strongly acidic solutions in the majority of nuclear wastewaters. Carbonaceous materials, such as activated carbon, carbon nano-tubes and mesoporous carbon are widely used nowadays in applications of metal separation [115]. These carbon based materials generally require the addition of specific functional ligands for selective uranium(VI) ions coordination and the

advancement of their adsorption efficiency [116–118]. Activated carbon is highly priced and is partially lost during the regeneration which restricts its application. Activated carbon one of the most widely used adsorbents in underdeveloped countries [119], activated carbon is chosen for its chemical, thermal and radiation stability and rigid porous structure and mechanical strength [120-121]. It can be considered as the most economic process. Activated carbon is prepared by carbonization at high temperature of 800⁰C or even higher under high energy-consuming conditions [122,123]. The maximum removal of uranium(VI) (>98%) was observed at pH 3.0-0.1 at initial concentration of 100 mg/L and an amount of activated carbon equal to 0.1 g [124]. To enhance the adsorption capacity, benzoylthiourea was chosen as an additive. This chelating component is known to have strong tendencies to form complexes with uranyl ions through the N–CS–NH–CO–Ph chelating ligand [125]. The adsorbent exhibited excellent affinity and selectivity for uranium(VI), even in the solution containing abundant competing ions [101,102]. The removal of uranyl ions by the activated carbon (F400) functionalized with carboxymethylated polyethyleneimine (CMPEI) was also carried out [126].

Hydrothermal carbon (HTC) majorly possesses spherical skeleton with comparatively stable physico-chemical properties, and paralleling with the other carbonaceous materials, it contains more oxygen-containing functional groups and active sites on the surface [127]. HTC can be prepared from various inexpensive and pervasive saccharides or other biomass by using a mild hydrothermal process, avoiding the requisite of using any organic solvents, catalysts or surfactants at moderate temperatures (generally <200⁰C) [128, 129]. An alkaloid, 5-azacytosine (Acy), was chosen as the chelating ligand on solid phase extractant (SPE), because Acy belongs to multi-dentate N-donor ligands that have shown noticeable selectivity towards actinides separation via liquid–liquid extraction techniques [130-132]. The adsorption of U(VI) increased with rise in the temperature from 283 to 333 K.

Due to the large specific surface areas and structural properties, carbon nanotubes (CNTs) have shown their potential to remove micro-contamination and as promising adsorbents in water and wastewater treatment [133]. Solid-phase extraction techniques based on carbon nano tube materials have been used in the removal and recovery of uranium from aqueous solutions [134]. The two categories of Carbon nanotubes CNTs involve single-walled CNTs and multi-walled CNTs. The preparation of carbon nanotubes is via more severe physical and chemical methods such as laser ablation, arc-discharge and chemical vapour deposition which generally involve calcination at extremely high temperatures, thus, high energy consuming [135,136]. The application of carboxymethyl cellulose (CMC) grafted MWCNTs (MWCNT-g-CMC) in the removal of UO_2^{2+} from aqueous solution were also investigated [137]. The results indicate that MWCNT-g-CMC composites have much higher adsorption ability in the removal of UO_2^{2+} than the as-produced MWCNTs. The complex mechanisms by which the metal ions are sorbed onto CNTs appear attributable to electrostatic attraction, precipitation and complexation between the metal ions and the carboxylic functional groups of CNTs. The sorption capacity of CNTs for uranium is well comparable with that of other sorption materials such as silica, iron oxy-hydroxide or titanium dioxide. The costs of CNTs would still need to fall greatly to make them competitive to standard sorbents for uranium recovery.

Graphene, a carbon layer only one atom thick, is composed of sp^2 -bonded carbon atoms. Since the discovery of its electrical properties in 2004, it has enticed deep interest due to its unique two-dimensional (2D) structure and first-rate physicochemical properties, essentially, extreme mechanical strength, ultra-light weight, high electronic and thermal conductivity, and a huge specific surface area (e.g. $2620 \text{ m}^2/\text{g}$ [138]). Graphene oxide (GO) is an oxidized graphene sheet with the basal plane reformed mostly with epoxide and hydroxyl groups in addition to carbonyl and carboxyl groups located presumably at the edges which predominantly responsible uranium sorption [139]. Adsorption of uranium (VI) from aqueous

solution using a graphene oxide-activated carbon felt composite was studied and reported [140]. The only downside is cost of graphene oxide, which is relatively high when compared with other traditional adsorbents. Another latest technology involving graphene oxide nano-sheets has attracted multidisciplinary attention due to their unique physicochemical properties and higher uranium sorption capacity [141].

The development of porous materials namely mesoporous carbon with large surface areas is currently an area of extensive research, particularly with regard to potential applications as environmental remediation [142]. Some researchers modified and functionalized the surface of the OMC/CMK (Oxide modified mesoporous carbon) for separation applications. A significant attempt to anchor an oxime-containing ligand onto CMK-5 to offer an efficient sorbent for selective separation of U(VI) ions from various aqueous solutions was initiated. The functionalized CMK-5 (Oxime-CMK-5) was characterized and its sorption behaviour of U(VI) ions was investigated in detail using batch equilibrium methods under varying operating conditions [143].

1.5.3 Biosorbent

Biosorption is a term that describes the removal of metals ions by the binding to living/ non-living biomass from an aqueous solution. Biosorption can be used to bind and concentrate heavy metals or radionuclides from aqueous solutions. It has been regarded as an innovative technology to remove uranium contaminants from industrial effluents [144]. Studies on uranium biosorption have already been performed using various microorganisms, viz. fungi, yeast, algae and bacteria [145-147]. *Rhodotorula glutinis*, common yeast, was found to be a good sorption material for uranium [148]. The efficiency of *S. cerevisiae* for uranium sorption was also tested in pure uranium solution [149] and wastewater from uranium mill [150]. Biosorption of uranium onto chemically modified yeast cells, *Rhodotorula glutinis*, was reported in order to study the role played by various functional groups in the cell wall

[151]. Magnetic separation is a new separation technique and has recently been found many interesting applications in various areas of bioscience and biotechnology [152]. Adsorption of uranium from aqueous solution onto the magnetically modified yeast cell, *Rhodotorula glutinis*, was investigated in a batch system [153]. Among several biopolymers, alginate has shown potential for uranium binding applications due to the presence of reactive carboxylic groups [154-156]. Alginate–alumina–collagen fiber (AACF) adsorbents were developed at different mixing ratios, and applied to treat synthetic and real mine drainage focusing on the removal of uranium ions in batch and column reactors [157]. The physical crosslinking of alginate in the presence of divalent cations like calcium can be used to achieve a three-dimensional hydrogel. These hydrogels in the bead form provide a large surface area for increasing the binding of metals like uranium [158]. Chitosan (CTS) is a major component of crustacean shells and one of the most abundant biopolymer in nature. The adsorption behaviour of different composites toward uranium(VI) from aqueous media was studied under varying operating conditions of pH, concentration of U(VI), contact time, adsorbent dose and temperature [159]. Agricultural waste materials are considered to be potential option for uranium remediation due to their economic and ecofriendly nature, unique chemical composition, availability in abundance, renewable, low cost and more efficiency. The adsorption of heavy metal ions by low cost renewable organic materials has seen increased use since 1990s [160]. A wide variety of natural/agricultural waste materials such as peanut hulls, sawdust, shells of wheat, shells of lentil, shells of rice, rubber tree leaf, modified meranti sawdust, wheat straw, oil palm leaf powders etc. were used as low cost adsorbents for removal of different metal including uranium. The functional groups present in biomass molecules include acetamido groups, carbonyl, phenolic, structural polysaccharides, amido, amino, sulphhydryl carboxyl groups alcohols and esters. These groups have the affinity for uranium(VI) complexation [161]. To ensure pronounced uranium absorption at room

temperature, the natural rice straw is soaked for 20–30 days in acidic solution (pH 1–2) to facilitate cellulose disintegration [162]. The study on the use of palm shell powder as well as modified and activated palm shell powder was used for the removal of uranium [163].

Compared with the conventional methods, the biosorption process offers several advantages, such as low operating cost, high efficiency in detoxifying very dilute effluents and a minimal volume of disposable sludge. However, in real use, disadvantages like post-separation, clogging, washout, etc. of the biomass appear. Among these disadvantages, the most troublesome is the post-separation of biosorbent from metal solution. Usually, centrifugation and filtration are used, which definitely increase the treatment cost.

1.5.4 Polymers/copolymers

According to the theory of Hard-Soft-Acid-Base (HSAB), heavy metal ions have a strong affinity towards ligands containing S, N and O atoms. Many papers reported a vast number of chelating resins with various functionalities, usually thiol and amine derivatives. Ion exchange resins are successfully employed for uranium recovery from dilute solutions, among these resins, strong base anion exchangers are the most suitable resins for uranium recovery. Batch adsorption experiments are used easily in the laboratory for the treatment of small volume of effluents, but less convenient to use on industrial scale, where large volumes of waste are continuously generated [164]. Strong base anion exchanger Amberlite CG-400 was used for uranium recovery from aqueous solutions (synthetic solution and UCF liquid waste) using a fixed-bed column [165]. The maximum breakthrough capacity of uranium ions were achieved by CG-400 resin at a flow rate of 0.2 mL /min and bed height 9.1 cm (4 g resin). Hydrogels are three-dimensional, hydrophilic, polymeric networks capable to retain large amounts of water, or biological fluids, characterized by a soft and rubbery consistence, being thus similar with living tissues. Hydrogels may be chemically stable or “reversible” (physical gels) stabilized by molecular entanglements, and/or secondary forces including

ionic, H-bonding or hydrophobic interactions, these hydrogels being non-homogeneous [166]. To enhance the mechanical strength and swelling/de-swelling response, multi-component networks as interpenetrating polymer networks (IPNs) have been designed. IPNs are “alloys” of cross-linked polymers, at least one of them being synthesized and/or cross-linked within the immediate presence of the other, without any covalent bonds between them, which cannot be separated unless chemical bonds are broken [167]. Metal complexing membranes have been prepared by semi-IPN technique and their sorption properties for metal ions [168,169] have been investigated. Liu et al. synthesized an IPN ion-imprinting hydrogel (IIH) via cross-linking of blended CS/PVA with ethylene glycol diglycidyl ether using uranyl ion as template [170] and reported encouraging separation results.

Chitosan, a polymer composed of glucosamine, is prepared from chitin by partial deacetylation of its acetamido groups by means of a strong alkaline solution. Owing to its high contents of amino and hydroxyl functional groups, chitosan have been reported to have high tendency for adsorption of uranyl ions [171]. To enhance the resistance of chitosan against acid, alkali and chemicals along with increasing its adsorption capacity and mechanical strength, cross-linking is a crucial step [172]. To accomplish this, epichlorohydrin is employed as an additive which has an advantage of not eliminating the cationic amine function of chitosan [173,174]. The adsorption capacity of uranium(VI) onto cross linked chitosan (CCTS) increases with an increase of contact time and reaches equilibrium within 120 min. [175].

Amidoxime-functionalized silica coated Fe_3O_4 ($\text{Fe}_3\text{O}_4@\text{SiO}_2$ -AO) exhibited enhanced sorption capacity for U(VI) in comparison with raw silica coated Fe_3O_4 due to the strong chelation of amidoxime to U(VI) [176, 177].

Chelating resins exhibit high adsorption capacity and selectivity due to which they have witnessed an increasing use for the removal of metal ions. On account of this, a chelating

resin was prepared by developing poly(amido)amine (PAMAMG3) dendron on the surface of styrene divinylbenzene (SDB). It was found that U(VI) adsorption on PAMAMG3-SDB charted monolayer sorption [178].

The mechanism of retention of metal ion on solid phases depends on the nature of the solid phase and the nature of the species to be retained. The retention process usually involves adsorption of the metal ions at the surface of the sorbent via interactions with various functional groups, and ion exchange, chelation and ion-pair formation processes. It depends on the experimental conditions, such as pH, temperature, presence of competitive ions and target metal ion concentrations. The list of various adsorbents that are used after 1995 for uranium removal along with their adsorption capacities and suitable pH are mentioned in

Table 1.3.

Table 1.3: Solid phase extractants for uranium separation

Adsorbents	Maximum Adsorption Capacity	pH / Acidic
Activated carbon	151.5 mg/g	pH 4
Hydrothermal carbon	408.36 mg/g	pH 4.5
CNT	73 mmol/g	pH 5
Graphene oxide	299 mg/g	pH 4
Cross linked chitosan	49.05 mg/g	pH 3
Talc	41.6 mg/g	
- PAMAM Dendron 5.5	130.25 mg/g	
Alga Sargassum fluitants	562 mg/g	pH 4
Actinomycetes <i>S. levoris</i>	419 mg/g	pH 5.8
Bacteria <i>Arthrobacter nicotianae</i>	615 mg/g	pH 5.8
Fungus <i>M. javanicus</i>	302 mg/g	pH 5.8
Chitosan resin (CCTS-DHBA)	291 mg/g	pH 3

Amidoximated hydrogels	564 mg/g	pH 4
Diatomite HDTMA	158 mg/g	pH 6
Mesoporous silica	153 mg/g	pH 4
MCM-41	125 mg/g	pH 6
Coir pith	232 mg/g	pH 4.5
Humic acids	190 mg/g	pH 2.5
Clinoptilolite PAN	88 mg/g	pH 5.0
Zeolite X	220 mg/g	--
Carboxymethylated polyethyleneimine (CMPEI)-modified mesoporous carbon	250 mg/g	pH 4
Oxidized MWCNTs	45.9 mg/g	pH 5
Carboxymethyl cellulose (CMC)-grafted MWCNTs	112 mg/g	pH 5
Amidoximated magnetite/graphene oxide composites	284 mg/g	pH 5
Iron oxyhydroxide	278 mg/g	pH 6
Compacted bentonite		pH 7
MX-80 bentonite	37.369 mg/g	pH 5.5-6
Na-attapulgite with fuming acid	89 mg/g	pH 4.5
Carboxylate functionalized graft copolymer based On TiO ₂ -desfied cellulose	99 mg/g	--
Cyanex272 impregnated on Amberlite XAD-2	--	--
Tributyl phosphate (TBP) impregnated Styrene-divinylbenzene copolymer	--	5.5 M
Tributyl phosphate (TBP) impregnated Cellulose	--	2 M
Diaryl(dialkylcarbamoylmethyl)-phosphine oxides (CMPO) impregnated Wofait EP 60	--	3 M
Tri-n-octylphosphine oxide (TOPO) impregnated C18-SiO ₂	--	0.5 M

2-Ethylhexyl (N,N-diethylcarbamoylmethyl)phenylphosphinate impregnated Amberlite XAD-75	--	3-5 M
N,N,N',N',-Tetraoctyldiglycolamide (TODGA) impregnated SiO ₂	--	3 M
N,N,N',N',-Tetraoctyldiglycolamide (TODGA) impregnated Amberchrom CG-71	--	3 M
N,N'-Diethyl-N,N'(p-tolyl)-dipicolinamide impregnated Polyacrylonitrile fiber	--	2-6 M
Tridodecylamine (TDA) impregnated Amberlite XAD--	--	6 M
p-Butylcalix[4]arene impregnated silica gel	--	pH 6
Octacarboxymethyl-C-methylcalix-[4]resorcinolarene impregnated Amberlite XAD-4	--	pH 3 (Th) pH 4 (U)
5,7-Dichloro-8-quinolinol impregnated Naphthalene	--	pH 4.5-7.0
Carboxylic acids impregnated Carbon material	--	pH 1-2

1.6 Promising chelating sorbent for uranium extraction

Chelating agents are those compounds containing donor atoms that can combine by coordinate bonding with a single metal ion to form a cyclic structure called as a chelate. The metal acts as a Lewis acid (that is, it tends to acquire enough electrons to reach an inert state), and the ligand acts as a Lewis base (that is, it has electron pairs that can be shared with the metal). Co-ordination, then, is a Lewis acid – Lewis base neutralization process. Complexing sorbents of new types are developed deliberately; possessing a tailor made structure that would bind the element with the monomeric ligand. The ability of the metal ion to form the optimal coordination polyhedron from a set of hetero-atoms offered depends on the basicity of the donor atoms of the functional groups of the ligand and on the conformational mobility of these atoms, the latter being determined by the possibility of bond atom and bond length

distortions in these functional groups. The mechanism by which the selectivity can be designed into ion exchange resins where the concept of ion exchange occurring concurrently with chemical reactions of the metal ion was treated theoretically. Neutralization, hydrolysis and complexation were cited as the reactions which could accompany ion exchange. They fall into four types listed as: i) type I processes – counter-ions released by the ion exchanger reacted with co-ions in solution; ii) type II processes – solution counter-ions react with the immobilized exchange sites on the polymer; iii) type III processes – start with un-dissociated polymeric exchange sites which are then ionized by reaction with solution co-ions; iv) type IV processes – un-dissociated polymeric exchange sites are converted from one un-dissociated form to another by reaction with the solution co-ions. Thus, ability of a ligand to complex with a target metal ion is not only a function of the intrinsic ligand-ion interaction, but also a function of the solution pH and the presence of competing anions.

The removal of desirable metal ions from wastewaters and process effluent stream has led to the development of several types of selective ion exchangers. As for example, development of selective ion exchangers for recovery of natural uranium from process effluent is a challenging task due to the solution pH > 7 and the presence of competing cations. Some of the uranophiles, such as poly (acrylamidoxime), poly (acrylhydroxamic acid) [179], 2-2-dihydroxyazobenzene attached to polymer matrices [180], Calixarene, Macrocyclic hexacarboxylic acid are found to be promising for the recovery of uranium from lean solution. The potential sorbent for uranium recovery from dilute solution has been listed in

Table 1.4.

Table 1.4: Major Sorbents reported for the uranium recovery from seawater / dilute solutions

Chemical form	Suitability
Hydrous titanium oxide (developed before 90's)	Difficulty in large scale application in submerged mode
Macrocyclic hexacarboxylic acid (developed before 90's)	Difficulty in production of polymer-bound hexacarboxylic acid.
Amidoxime (developed	Most extensively studied, suitable for large scale production

before 1995) Amidoxime + Methacrylic acid [181]	in the form of fibers, resin, or grafted fibrous sheet, slow kinetics and limited selectivity. Have advantages of Amidoxime group and show better uranium sorption kinetics.
Calixarene-based uranophiles (developed before 90's)	Highly selective towards uranium, slow sorption kinetics, difficulty in anchoring in polymer matrix, synthetic chemistry involved is not suitable for large scale production.
2,2'-dihydroxy azobenzene and related chemical groups [182]	Involve synthetic chemistry, not evaluated for real application.
Poly(Hydroxamic Acid) Resin (developed before 90's and recently [179])	Have all advantages of hydroxamic acid group for recovery heavy metals including uranium along with iron. Most suitable till now.

1.7 Uranium sorption mechanism by molecular modelling

1.7.1 Need of computational chemistry

Theoretical chemistry is the subfield where mathematical methods are combined with fundamental laws of physics to study processes of chemical relevance. Molecules are traditionally considered as “composed” of atoms or, in a more general sense, as a collection of charged particles, positive nuclei and negative electrons. Given a set of nuclei and electrons, theoretical chemistry can attempt to calculate things such as:

- Which geometrical arrangements of the nuclei correspond to stable molecules?
- What are their relative energies?
- What are their properties (dipole moment, polarizability, NMR coupling constants, etc.)?
- What is the rate at which one stable molecule can transform into another?
- What is the time dependence of molecular structures and properties?
- How do different molecules interact?

Computational chemistry is focused on obtaining results relevant to chemical problems, not directly at developing new theoretical methods. A very large fraction of the computational resources in chemistry and physics is used in solving the so-called many-body problem. Computational methods can, however, produce approximate solutions, which in principle

may be refined to any desired degree of accuracy. In order to describe a system we need four fundamental features such as system description, starting condition, interaction in the system and dynamical equation.

1.7.2 Molecular modelling methodology

The Born–Oppenheimer separation of the electronic and nuclear motions is a cornerstone in computational chemistry. Once the electronic Schrödinger equation is solved for a large number of nuclear geometries, the potential energy surface (PES) is known. The motion of the nuclei on the PES can be solved either classically (Newton) or by quantum (Schrödinger) methods. It should be stressed that nuclei are heavy enough that quantum effects are almost negligible, i.e. they behave to a good approximation as classical particles. Methods aimed for solving the electronic Schrödinger equation are broadly referred to as “electronic structure calculations”. Accurate determination of the electronic wave function is very demanding. The interesting parts of a PES are usually nuclear arrangements that have low energies. Different aspects of solving the electronic Schrödinger equation and various technical points of commonly used methods have been reported [183]. For time independent phenomena, the problem reduces to calculating the energy at a given geometry. Often the interest is the finding stable geometry of stable molecules with different conformations. The target is then reduced to finding energy minima on the potential energy surface.

Describing the electron distribution in detail, there is no substitute for quantum mechanics. Electrons are very light particles and they cannot be described correctly even qualitatively by classical mechanics. We need to solve the time-independent Schrödinger equation, which in shorthand operator form is given in **Equation 1.7**.

$$\mathbf{H}\psi = \mathbf{E}\psi \quad 1.7$$

If solutions are generated without reference to experimental data, the methods are usually called *ab initio* (Latin: “from the beginning”) method. An essential part of solving the

Schrödinger equation is the Born–Oppenheimer approximation, where the coupling between the nuclei and electronic motion is neglected. This allows the electronic part to be solved with the nuclear positions as parameters, and the resulting potential energy surface (PES) forms the basis for solving the nuclear motion. The major computational effort is in solving the electronic Schrödinger equation for a given set of nuclear coordinates [184].

A significant simplification, both conceptually and computationally, can be obtained by introducing independent-particle models, where the motion of one electron is considered to be independent of the dynamics of all other electrons. An independent-particle model means that the interaction between the particles is approximated, either by neglecting all or by taking all interactions into account in an average fashion. Within electronic structure theory, only the latter has an acceptable accuracy, and is called Hartree–Fock (HF) theory. In the HF model, each electron is described by an orbital, and the total wave function is given as a product of orbitals. Since electrons are indistinguishable fermions (particles with a spin of $1/2$), (however the overall wave function must be antisymmetric (change sign upon interchanging any two electrons)), which is conveniently achieved by arranging the orbitals in a Slater determinant. The best set of orbitals is determined by the variational principle, i.e. the HF orbitals give the lowest energy within the restriction of the wave function being a single Slater determinant. The shape of a given molecular orbital describes the probability of finding an electron, where the attraction to all the nuclei and the average repulsion to all the other electrons are included. Since the other electrons are described by their respective orbitals, the HF equations depend on their own solutions, and must therefore be solved iteratively. When the molecular orbitals are expanded in a basis set, the resulting equations can be written as a matrix Eigen value problem. The elements in the Fock matrix correspond to integrals of one and two-electron operators over basis functions, multiplied by density

matrix elements. The HF equations in a basis set can thus be obtained by repeated diagonalisation of a Fock matrix.

HF theory only accounts for the average electron–electron interactions, and consequently neglects the correlation between electrons. Methods that include electron correlation require a multi-determinant wave function, since HF is the best single determinant wave function. Multi-determinant methods are computationally much more involved than the HF model, but can generate results that systematically approach the exact solution of the Schrödinger equation.

Density Functional Theory (DFT) in the Kohn–Sham version can be considered as an improvement on HF theory, where the many-body effect of electron correlation is modelled by a function of the electron density. DFT is, analogously to HF, an independent-particle model, and is comparable to HF computationally, but provides significantly better results. The main disadvantage of DFT is that there is no systematic approach to improving the results towards the exact solution. Spin-dependent effects are relativistic in origin (e.g. spin–orbit interaction), but can be introduced in a postulated fashion in non-relativistic theory, and calculated as corrections (for example by means of perturbation theory) after the electronic Schrödinger equation has been solved.

1.7.3 Uranium complex analysis

The aqueous chemistry of uranium is quite well known and understood. The studies on uranium sorption on sorbent have been carried out along with uranium complex analysis by many researchers [185-187]. The thermodynamic stabilities of some important aqueous uranium complexes and hydroxides need to be confirmed. In this section an outline with few examples using molecular modelling has been addressed. The thermodynamic stabilities of chemical species are given by the G , Gibb's energies of formation reactions or of any well chosen Equilibria at given temperature. Evaluating G is not straightforward use of molecular

modelling, and in most cases the accuracy is not sufficient for reactions in liquid water. Conversely, molecular modelling is often appropriate for obtaining geometries, which is often useful to understand stabilities. Quantum mechanics is needed to understand covalent bonding: UO_2^{2+} is typically a linear covalent molecular ion. Many molecular modelling methods are currently used based on classical or quantum mechanics giving optimized structures or simulating the dynamics of the system. Quantum calculations essentially describe electrons, while classical molecular models usually describe the atoms typically with given charges and eventually polarizabilities, but without explicit description of their electronic origins [188]. For this reason, classical -i.e. no explicitly quantum- molecular modelling is not especially appropriate to simulate the formation of covalent bonds. Furthermore classical models require empirical potentials to account for the essentially quantum interactions [189]: these potentials are nowadays parameterized with quantum calculations, which are used in most molecular modelling methods. Quantum calculations are easier with closed-shell electronic structures, so for this reason it is logical to start the molecular modelling studies of uranium with U(VI). The geometries of the U(VI) species in liquid water and in many other media are well known: they are usually built on the linear UO_2^{2+} uranyl molecular dication. It is also interesting to check that UO_2^{2+} is the most stable isomer in aqueous solutions.

Number of reports are available for quantum calculation results of $\text{UO}_2(\text{H}_2\text{O})_i^{2+}$ species built by adding H_2O molecules one by one to UO_2^{2+} up to the saturation of its first hydration layer in the gas phase in an aim to start modelling the aqueous chemistry of U(VI) or at least its hydration [190, 191]. The maximum coordination number of 4 they observed for hydrated $\text{UO}_2(\text{OH})^+$ in the gas phase is the same as that it proposed from quantum calculations for $\text{UO}_2(\text{OH})^+$ in liquid water [192,193]. Stability of the linear UO_2^{2+} uranyl ion is simply due to its electronic configuration, which is not substantially altered on adding ligands, even when

the bonding with equatorial ligands has some covalent character [190,194]. The two-sphere cluster method was recently developed to study the hydration of UO_2^{2+} [Figure 1.5].

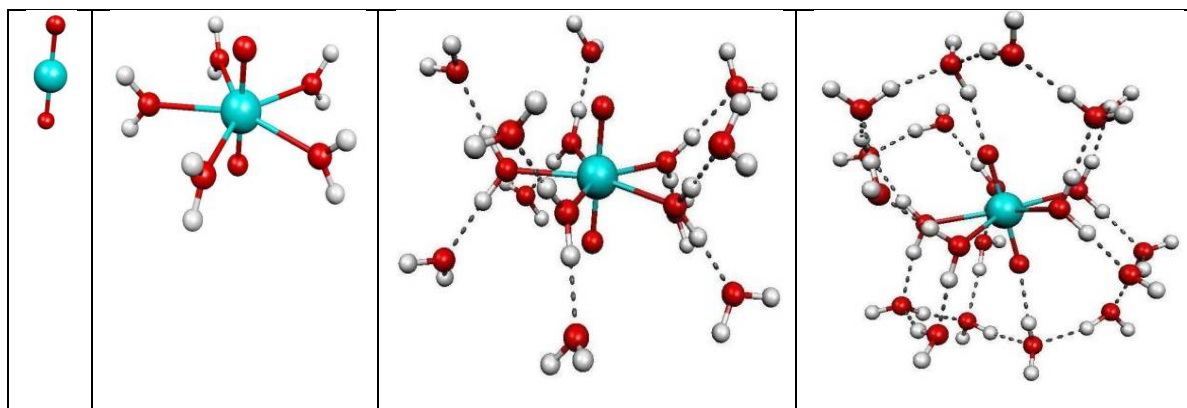


Figure 1.5: Geometrical models for the hydration of UO_2^{2+} .

(With 1 and 2 hydration layers, and with 2 hydration layers with apical H_2O water molecules (from left to right); U is blue, O red and H white [192]. The figure is drawn with MOLEKEL [206,207]).

The theoretical chemical calculations have been used to study the hydration of the UO_2^{2+} uranyl ion [190,191, 194-202]. Significant bond length improvement is obtained if the first hydration shell is treated explicitly by quantum mechanics, and using COSMO [203,204]. This confirms that the first hydration layer is essential to model aq. UO_2^{2+} as observed for the hydration of other cations. Besides the static optimizations of two hydration sphere clusters, Ikeda et al. 2008 [205] reported and concluded that their molecular dynamics simulations gave U- O_{eq} distances in agreement with EXAFS results, while it was not the case for their actually one hydration layer based on static DFT results.

Arnold and co-authors [208] have successfully synthesized the oxo group silylated uranyl(V) complex and have proved that the uranyl(VI) axial group can actively participate in chemical reactions. The work by Arnold et al. has a large impact on the uranium chemistry as discussed by Boncella [209]. There are also increasing interests in the catalytic behaviour of uranium [209 – 212]. The rate of oxygen exchange increases with increasing concentration of uranyl hydroxo dimer complex, $(\text{UO}_2)_2(\text{OH})_2^{2+}$ [213 - 216].

Many researchers have been utilising different sorbents to remove uranium(VI) from aqueous radioactive wastes for their wastewater treatment followed by final disposal. For disposable nuclear wastewaters, where stable cationic uranium complex is mainly present as mononuclear ($[\text{UO}_2(\text{OH})]^+$) hydrolysis product of U(VI) due to solution $\text{pH} > 7$, molecular modelling study literature for the case is scarce. For the purpose metal-ligand bonding plays a vital role. It is important to understand the uranium coordination chemistry related to metal-ligand bonding for specifically developed effective sorbent. Acidity of sorbent increases in aqueous solution when a hydroxyl group is attached to the nitrogen in a functional group of sorbent like, hydroxamic acid based sorbent. Here oxygen acts as donor atom. This enhances U(VI) sorption, particularly in alkaline solutions, forming rigid bonds. Along with establishing potential application for uranium sorption on hydroxamic acid based sorbent it is important to understand the mechanism of exhibiting superior uranium sequestering ability with its functional group to explore its wider and proper utilization. This can be carried out by molecular modelling with respect to the selective sorbent, PHOA. The study also aims to discuss the possible structural consequences observed when the hydroxamate anion binds UO_2^{2+} applying molecular modelling using DFT method. Possible geometries need to be evaluated under the prevailing conditions and relative stabilities of possible binding motifs. The theoretical model result is required to be supported by the instrumental measurement as well as experimental analysis.

1.8 Problem definition and scope of work

Recovery of uranium, a valuable material from a multi-component dilute feed, like wastewater of nuclear establishments is one of the techno-economical challenging problems that require considerations of chemical, kinematical and process design aspects. As listed in **Table 1.4**, calixarene and macrocyclic derivatives are highly selective towards UO_2^{2+} , but the major problem associated with these ligands is that their complexation with uranyl ion

under pH >7 condition is kinetically unfavourable. The poly (acrylhydroxamic acid) (PHOA) is found to be more suitable for uranium recovery from effluent of uranium processing plant in that condition due to: (i) selectivity, (ii) strong adsorption and desorption ability, (iii) high loading capacity, (iv) good mechanical and chemical strength, (v) safer in chemical handling during synthesis and (vi) ease with which hydroxylamine can be anchored to different polymer matrices of various shapes and sizes. The economic viability of recovery of uranium from the effluent still critically depends upon the kinetics of sorption of uranium in sorbents. It is desirable that the uranium species present in the effluent should be instantaneously sorbed when it comes in contact with the surface of sorbent in the local condition. Therefore, the major challenge for making uranium recovery viable is to develop a sorbent that has high uranium sorption rate and reasonable loading capacity. The major problems pertaining to the development of a suitable recovery system for uranium from nuclear wastewater are due to its very low concentration (<10 ppm), and chemical form $[\text{UO}_2(\text{CO}_3)_3]^{4-}$ might be and/ or hydroxyl complex, and large excess of competing ions. The diffusion mobility of U(VI), either in $[\text{UO}_2(\text{CO}_3)_3]^{4-}$ form or UO_2^{2+} form, in the sorbent would be dependent on the physical as well as chemical interactions (electrostatic and covalent) with the fixed-sites in matrix. These interactions retard the mobility of U(VI) species considerably in the matrix of sorbent. Sorption of U(VI) from its dilute solution has been found to be highly dependent on the physical parameters of the sorbent matrix (free volume, pore structure, tortuosity etc.) as well as its hydrophilicity. The chemical composition of the sorbent affects the de-complexation of $[\text{UO}_2(\text{CO}_3)_3]^{4-}$ to UO_2^{2+} if any, followed by complexation of UO_2^{2+} with functional groups (fixed-sites). Since de-complexation of $[\text{UO}_2(\text{CO}_3)_3]^{4-}$ can be catalyzed by H^+ -ions, the presence of acidic monomer or co-monomer with appropriate pK_a value may enhance the sorption kinetics of U(VI) in the sorbent from the wastewaters. Considering these parameters, a new sorbent **Poly (Acrylhydroxamic Acid), PHOA** has been evaluated for

uranium recovery from a nuclear wastewater; multi-component feed. As existing processes are economically prohibited, exploratory work, process methodology study and process development for recovery of uranium, a nuclear fuel, from unconventional source namely wastewater (effluent) generated in uranium purification process and also for polishing the wastewater for safer disposal has been carried out and reported in the thesis. Following several important characterisations and process developmental parameters have been carried out and described in the thesis:

1. Synthesis and physical characterisation of Sorbent and characterisation of wastewater
2. Instrumental characterisation of sorbent with respect to virgin sorbent and uranium loaded sorbent
3. Evaluation of sorption performance in batch experiments
4. Evaluation of elution performance in batch experiments
5. Evaluation of sorption and elution performance in continuous experiments
6. Geometrical analysis of uranium loaded sorbent using molecular modelling technique and validation with experimental results

CHAPTER – 2

SORBENT AND WASTEWATER

2.1 Introduction

Unlike organic pollutants, metals are non-biodegradable hence removal from their respective waste streams of heavy metal ions becomes essential. The removal of uranium ions is significant to many nuclear establishments/industries for environmental reasons, as well as for water reuse and the potential for metal recovery as the metal happens to be precious. In recent years, public awareness has increased with regard to the long term toxic effects of water containing dissolved uranium ions. Concentrations of these pollutants must be reduced in order to meet the stringent legislative standards and/or recover valuable metals from effluents. An adsorption system is frequently used in the final stage of a wastewater system to polish the effluent before discharging or recycling. Adsorbent performance is critical factor in the design and performance of an adsorption system. Commercial adsorbents though effective often turn out to be economically unviable. In addition, large quantities of adsorbents are often required making their final disposal an additional environmental concern since these adsorbents are non-biodegradable. In order to work out alternative to conventional polymeric cross linked adsorbents a novel sorbent **Poly (Acrylhydroxamic Acid), PHOA** has been studied for the removal of uranium from their aqueous solutions in this work. The novelty of the sorbent has been taken care during designing and planning stage of the sorbent preparation so as to perform in alkaline medium. Synthesis route of the sorbent has been chosen carefully to follow safe and economic process. Prepared sorbent's few physical characteristics like size distribution, density pattern with size, swelling nature in different condition, solubility or stability in different medium are need to evaluate for testing its suitability in treatment condition and hence, important. It is needed to understand the characteristic of the plant effluent to be treated. These characteristic studies were carried out in batch experiment with simulated solution as well as plant effluent and results have been

described in this chapter thoroughly. These parameters are found to be necessary to establish the achievement of sorbent design success and also to establish the suitability.

2.1.1 Novelty of the sorbent

The poly (acrylhydroxamic acid) (PHOA) is found to be more suitable for uranium recovery from effluent of uranium processing plant in that condition as it is generated ($\text{pH} > 7$) due to: (i) selectivity, (ii) strong adsorption and desorption ability, (iii) high loading capacity, (iv) good mechanical and chemical strength, (v) safer in chemical handling during synthesis and (vi) ease with which hydroxylamine can be anchored to different polymer matrices of various shapes and sizes. The economic viability of recovery of uranium from the effluent critically depends upon the kinetics of sorption of uranium in sorbents. It is desirable that the uranium species present in the effluent should be instantaneously sorbed when it comes in contact with the surface of sorbent in the local condition. Therefore, the major challenge for making uranium recovery viable is to develop a sorbent that has high uranium sorption rate and reasonable loading capacity. The major problems pertaining to the development of a suitable recovery system for uranium from nuclear wastewater are due to its very low concentration (<10 ppm), and chemical form $[\text{UO}_2(\text{CO}_3)_3]^{4-}$ might be and/ or hydroxyl complex, and large excess of competing ions. The diffusion mobility of U(VI), either in $[\text{UO}_2(\text{CO}_3)_3]^{4-}$ form or UO_2^{2+} form, in the sorbent would be dependent on the physical as well as chemical interactions (electrostatic and covalent) with the fixed-sites in matrix. These interactions retard the mobility of U(VI) species considerably in the matrix of sorbent. Sorption of U(VI) from its dilute solution has been found to be highly dependent on the physical parameters of the sorbent matrix (free volume, pore structure, tortuosity etc.) as well as its hydrophilicity. The chemical composition of the sorbent affects the de-complexation of $[\text{UO}_2(\text{CO}_3)_3]^{4-}$ to UO_2^{2+} if any, followed by complexation of UO_2^{2+} with functional groups (fixed-sites). Since de-complexation of $[\text{UO}_2(\text{CO}_3)_3]^{4-}$ can be catalyzed by H^+ -ions, the presence of acidic

monomer or co-monomer with appropriate pK_a value may enhance the sorption kinetics of U(VI) in the sorbent from the wastewaters. The PHOA sorbent has been designed purposely to catalyse the soluble carbonate and hydroxide complex of uranium in the wastewater by releasing hydrogen ion attached with hydroxamic acid group of PHOA sorbent.

2.1.2 Uranium processing plant effluent (wastewater)

Nuclear pure metal is produced in Uranium Metal Plant (UMP) by purifying crude uranyl nitrate solution via several processing steps like Solvent Extraction, ADU precipitation, Calcination, Reduction and Hydro-fluorination to obtain uranium tetra-fluoride (green salt). Finally this green salt is converted to metallic uranium with magnesium metal chips. **Figure 2.1** shows simplified flow sheet of the nuclear grade uranium metal production process. Uranium oxides, the starting materials are dissolved in nitric acid. The crude uranyl nitrate (CUN) solution, obtained after dissolution, is purified by solvent extraction using diluted Tri-Butyl Phosphate (TBP) as solvent. The pure uranyl nitrate solution (UNPS) is neutralized with ammonia gas to precipitate uranium as Ammonium Diuranate (ADU). The pure ADU is calcined to obtain uranium trioxide (UO_3) which is further processed through pyrometallurgical route to obtain finally uranium metal. The raffinate leaving from extraction unit contains different metal ions (impurity) along with uranium ions. The raffinate is treated with magnesia to recover active cake containing small amount of uranium after filtration. The treated raffinate filtrate, the wastewater / effluent having uranium (<10 ppm) and other metal ions along with NO_3^- ions is disposed after monitoring and following safe disposal procedure. The treated raffinate filtrate, wastewater was characterized and composition analysis is shown in **Table 2.1**. The composition shows that wastewater contents high concentration of Mg, Ca and nitrate ions (g/L level) along with low concentration of Fe, Cu, Mn and uranium (mg/L level) and the wastewater is alkaline in nature ($pH > 7$).

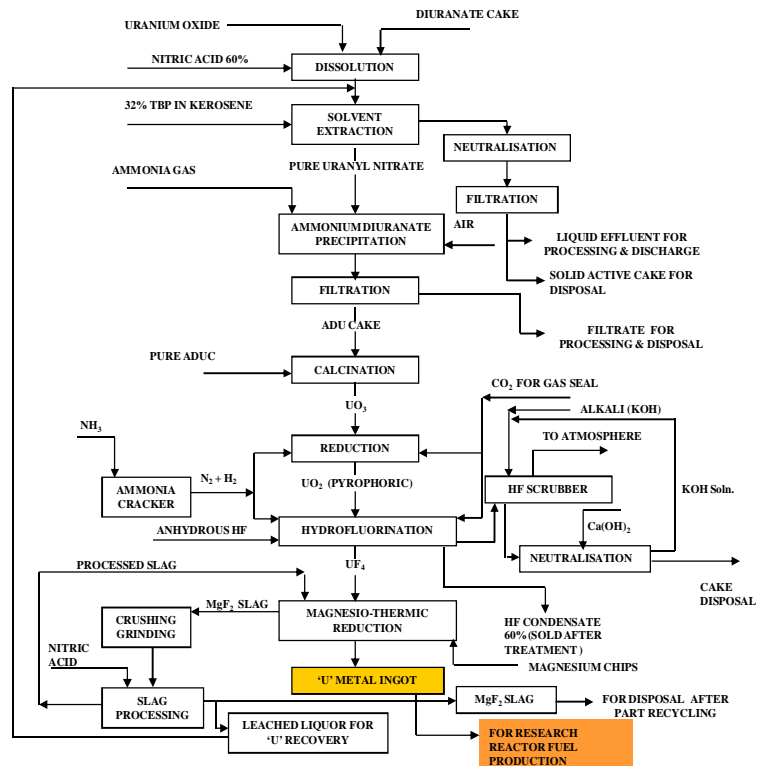


Figure 2.1: Process flow sheet of uranium production plant

Table 2.1: Composition of plant wastewater

Element	Concentration (mg/L)	Element	Concentration (mg/L)
Al	< 2.0	Ca	500 - 800
Cr	<2.0	Mg	5000 - 17000
Fe	2.0-5.0	Mn	1.0-5.0
Cu	2.0-5.0	Ni	<1.0
Cd	< 2.0	U	5.0-10.0
pH = 7.0 – 9.0			
Nitrate = 70000 – 90000 mg/L			

2.2 Sorbent synthesis and physical characterisation

2.2.1 Materials

Materials such as acrylamide (BDS, A.R.grade), N, N' methylene bis acrylamide (BDS, A.R. grade), hydroxyl amine hydrochloride (Loba Chemie, A.R. grade), methanol (E-mark, A.R. grade), acetone (E-mark, A.R. grade), sodium hydroxide (E-mark, A.R. grade) were procured

PAAM to Polyacrylhydroxamic Acid chelating Resin (PHOA), solution of a calculated amount of hydroxylamine hydrochloride and sodium hydroxide was added to a suspension of dry crosslinked PAAM. The resulting mixture was stirred for 5 min at room temperature. The reaction was continued for 6 h at 70°C. Ammonia was liberated during the reaction. The resulting polymer was washed with water followed by acidified with 3(N) HCl solution and then again washed with water to make it chlorine free.

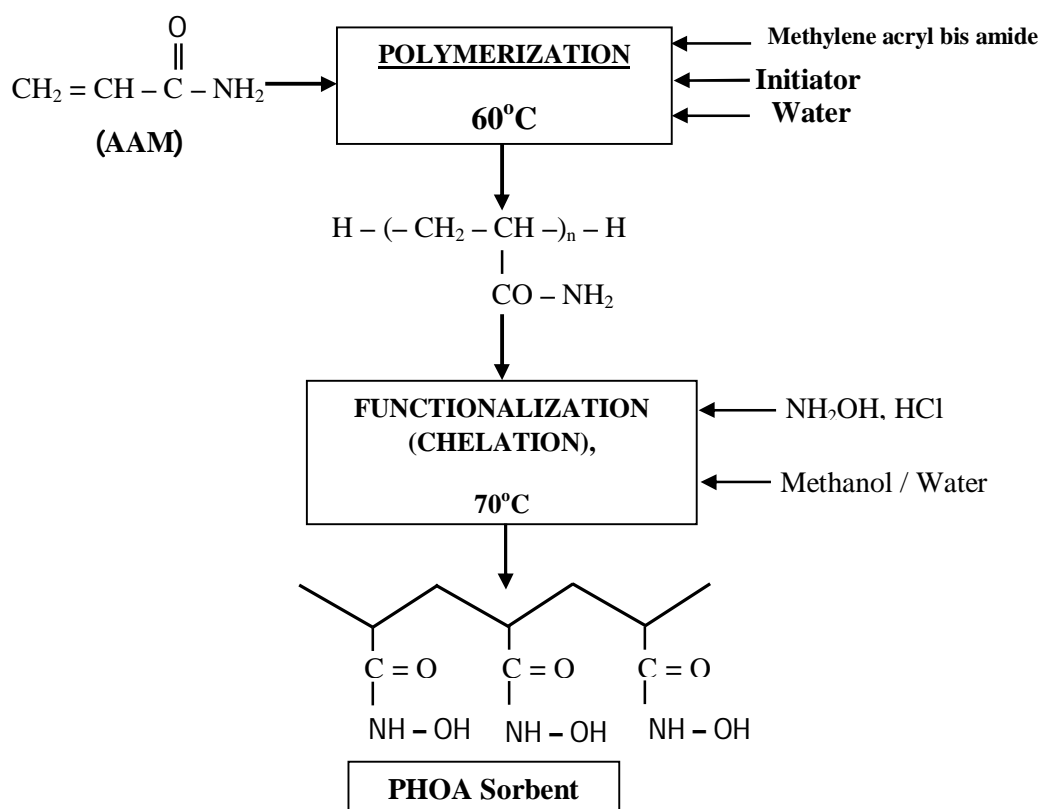




Figure 2.2: Preparation scheme of PHOA

The polymer was synthesized with acrylamide to N, N'-methylene bis acrylamide mole ratio 0.95/0.05 functionalization. The degree of crosslinking affects the moisture uptake of the polymer, as well as decreases the concentration of free amide groups available for conversion.

2.3 Physical characterisation of sorbent

The characterization data in terms of elemental composition is given in **Table 2.2** and results indicated that there was a good agreement between observed value and calculated value. The moisture uptake as a function of relative humidity has been noticed which shows that the moisture recovery is reduced with an increasing crosslinking. With the mentioned crosslinking PHOA picks up 29% moisture at 90% relative humidity (RH) and 5.3% moisture at 29% RH. Comparison of the un-reacted polyacrylamide with its hydroxamic acid derivative indicates that the un-reacted polymer picks up more moisture, probably due to increased intermolecular or intra molecular bonding in the case of the reacted derivative. This is also indicated in the TGA analysis of the sorbent. Higher moisture uptake may allow better interaction with metal ions.

Table 2.2: C, N, H, O analysis of novel sorbent, POHA; 5% POHA
Elemental Composition (wt. %)

	% C	% H	% N	%O
Observed value	44.12	6.41	17.69	31.78
Calculated value	44.93	6.42	17.20	31.45

2.3.1 Mesh size distribution of sorbent

The sorbent was dried in an oven at 100°C. An oven of Meta-Lab, model MSI-66 was used to dry the sorbent beads. PHOA sorbent is peach coloured irregular solid beads. Dried sorbent beads were crushed and sieved before used. Beads were sieved using different ASTM steel wire meshes (Jayant make) by normal shaking. The sorbent remained in each mesh container was collected and labelled for respective mesh size beads. The sorbent as prepared was taken for four size distribution measurement namely 10, 16, 18 and 30 meshes. Distribution pattern has been shown in **Figure 2.3**. The size distribution of sorbent consisted of: 10 mesh 21.66%, 16 mesh 59.96%, 18 mesh 8.31% and 25 mesh 10.07%.

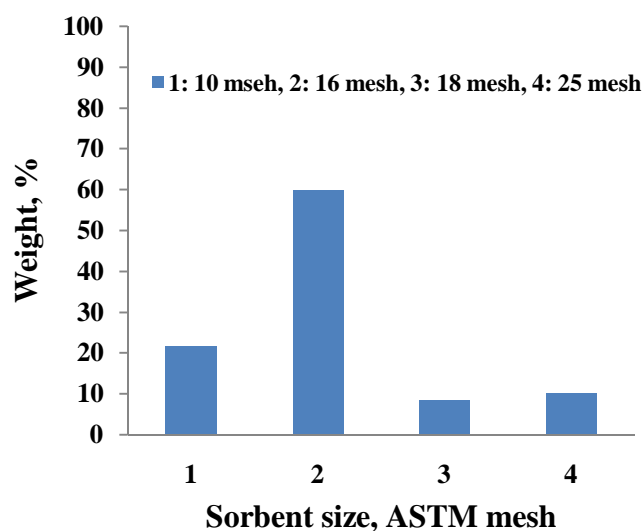


Figure 2.3: Mesh size distribution of sorbent

2.3.2 Effect of mesh size on density and swelling of sorbent

Individual mesh size sorbent bead was used for volume / density tests varying sorbent mesh size. 1g dry the sorbent was poured in 10 mL measuring cylinder and tap volume of compacted bead was evaluated as dry sorbent volume. All swelling / volume expansion tests were carried out in a 250 mL measuring cylinder having bottom drain out facility for medium removal. 1g dried sorbent and 100 mL swelling medium was used for the swelling tests. Swelling medium was poured in the cylinder having measured quantity dried sorbent.

Swelling time and medium draining time was 3h and 1h respectively for all the tests. Volume of swelled sorbent (after draining) was evaluated directly from the measuring cylinder. Whatman-42 grade filter paper was used for filtration.

In the study, intention was to evaluate the performance of different size sorbents. Density variation in term of volume with mesh size is shown in **Figure 2.4**. Swelling effect of the sorbent in distilled water with the mesh size variation has been shown in **Figure 2.4**. Swell volume was increased with increase of mesh size due to increase of total surface area. Sorbent's surface pores were getting opened up in the water because of hydrophilic nature of the sorbent, as designed for the purpose. Sorption characteristic varies proportionately with sorbent's swelled volume. Increase of swelled volume between 15 to 20 mesh sizes was sharp from 33 mL to 36 mL and thereafter volume gradient reduces, 37 mL for 25 mesh size, as volume effect was dominated by inter-bead voids. The result was confirmed by measuring volume of dry sorbent which has been shown in Fig. 3, secondary y-axis. Bulk density of dry sorbent was increased with decreasing of dry sorbent bead size.

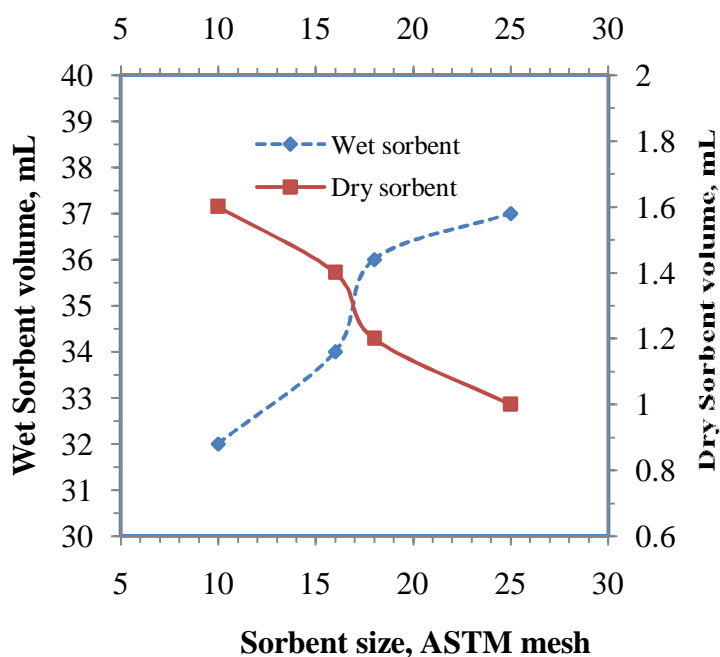


Figure 2.4: Volume of sorbent in dry and fully swelled in DW (room temperature)

2.3.3 Effect of competitive ions and its concentration on sorbent swelling with mesh size variation

For swelling tests, salt solutions were prepared by adding known quantity of chemical in laboratory prepared distilled water (DW). Five different swelling mediums, distilled water, effluent and solution of NaCl, CaCl₂ and MgCl₂ were used for the study. Na⁺ ion in low concentration is normally present in effluent. Ca²⁺ and Mg²⁺ ions in high concentration were present in the effluent (**Table 2.1**). Different cation concentration (mono- and di- valent), for Na⁺: 10 – 7012 mg/L, for Mg⁺⁺: 27 – 10021 mg/L and for Ca⁺⁺: 23 – 812 mg/L were used for evaluating effect of metal ion and its concentration on sorbent swelling. Solution pH was maintained at about 8 by adding 0.01(M) ammonium hydroxide solution as and when required, just before use.

Variation of swelling volume of the sorbent was evaluated in variable concentration of different metal ions like Na⁺, Ca⁺⁺ and Mg⁺⁺ ions present in the feed solutions. The effect of Na⁺ ion concentration on different mesh size sorbents has been shown in **Figure 2.5**.

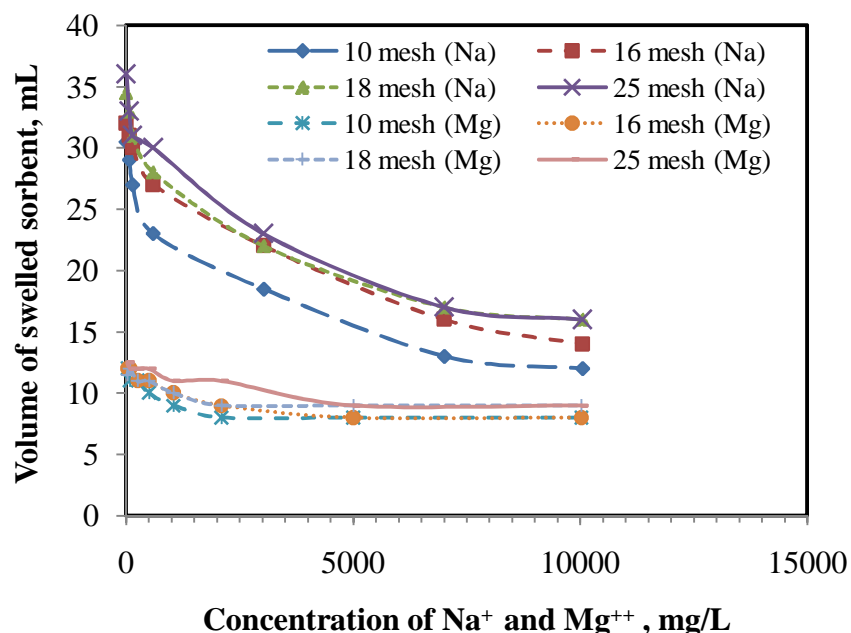


Figure 2.5: Effect of Na⁺ and Mg⁺⁺ concentration on swelling of sorbent (1g sorbent, RT, time 3h)

Swelled sorbent volume was decreased rapidly for all the sizes and was stabilised around at 7000 mg/L Na^+ ion concentration. At lower ion concentration of sodium ion (~ 10 mg/L) swelled sorbent volume was about 32-34 mL range and it was reduced to about 14-16 mL range at higher concentration (≥ 7000 mg/L). Mono-valent ion was used to analyse and compare the effect with the result of the divalent cations. Uranium processing plant effluents are treated and neutralised with magnesium oxide before regulated disposal. Calcium and magnesium ions in higher concentration were present in the effluent. Effects of different concentration of Mg^{++} ion and Ca^{++} ion on sorbent swelling have been shown in **Figure 2.5** and **Figure 2.6** respectively. Swelling volume was decreased sharply with concentration of both the ions. Presence of calcium ion was found to be more detrimental as swelling volume decreases to around 7-9 mL/g sorbent for Ca^{++} concentration about 500 mg/L, whereas similar effect was observed for Mg^{++} concentration at about 1000 mg/L. Thereafter further reduction of the volume was not noticed.

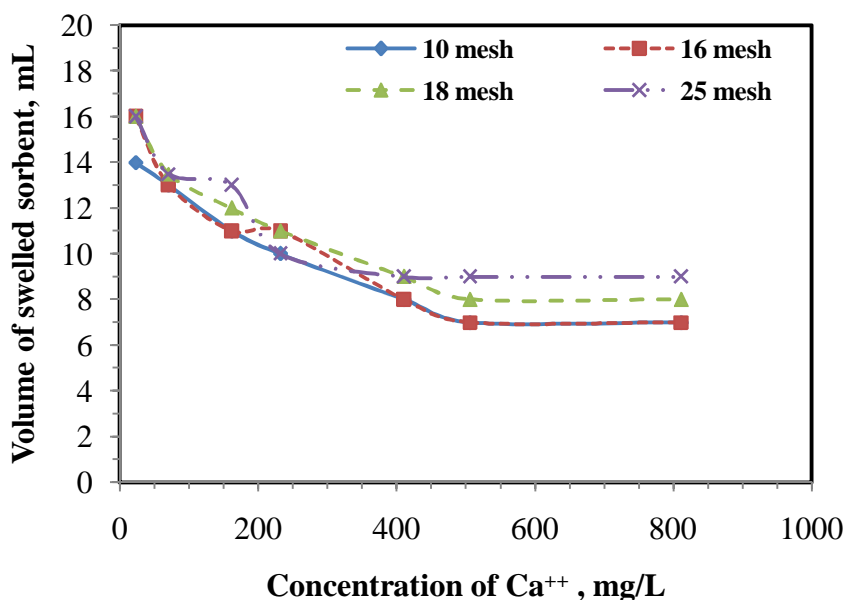


Figure 2.6: Effect of Ca^{++} concentration on swelling of sorbent (1g sorbent, RT, time 3h)

Though swelled volume was decreased all the cases, due to relative valency difference and atomic size variation, the negative slope rate was sharper for divalent ions compared to mono-valent ions. Comparing the figures it was noticed that sorbent swelled volume was 12-

16 mL/g sorbent for divalent ions concentration 20 – 30 mg/L which was equivalent to the mono-valent ion concentration > 10000 mg/L.

2.3.4 Swelling of sorbent in different medium

Experiments were carried out following similar procedure as discussed in 2.3.2 with different contacting medium such as acid (varying concentration), alkali (varying concentration) and organic; the swelling rates have been compared with the same in water medium. The swelling rate measured (with time variation) in different medium has been shown in **Figure 2.7**. From the figure it was understood that the sorbent swells better in aqueous medium than acid and alcohol mediums, and it further swells in alkaline medium. It indicates that the sorbent can better perform for the metal sorption in alkaline medium than neutral medium. The swelling test result also indicates that swelling of sorbent increases with increasing concentration of NaOH. This may be because of opening up of new sorbent surface due to repulsive forces of negatively charged sorbent surface after losing H^+ in alkaline medium. Hence, there is a possibility of U(VI) sorption in the newly generated surface of the sorbent and this is why total sorption capacity increases.

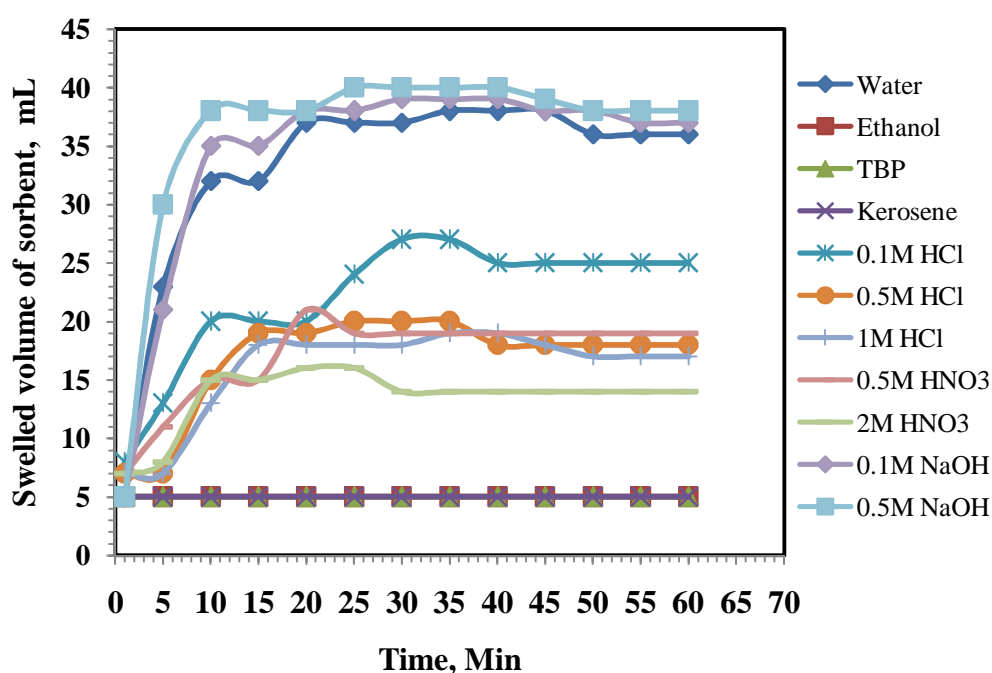


Figure 2.7: Swelling of PHOA (as prepared) with time in different medium

2.3.5 Solubility of sorbent in different media

The solubility of sorbent is an important parameter for showing the robustness of the sorbent against different acids, alkali and solvent treatment. The lesser the solubility of the sorbent, the greater will be its stability and reusability for recovery of metal ions from different aqueous media. The solubility test of the sorbent, POHA was carried out by taking 1 g sorbent in 10 mL of different chemical agents such as water, ethanol, TBP, kerosene, HCl, HNO₃, and NaOH for a period of 48 hours. The changes in different physical properties observed during the experiments were listed in **Table 2.3**.

Table 2.3: Solubility of sorbent, PHOA in different solvents

Sr. No.	Solvent	% Solubility	Remarks
1	Water	0.34	Whitish, dryable & soft
2	Ethanol	-	Whitish, non dryable & soft
3	TBP	-	Whitish, non dryable & soft
4	Kerosene	-	Whitish, non dryable & soft
5	0.5M HCl	0.65	Dark Brown; Filterable
6	0.5M HNO ₃	2.40	Whitish; Filterable
7	0.5M NaOH	0.40	Whitish; Filterable

The results indicate that the sorbent is soluble in organic solvent such as ethanol, TBP and kerosene and form non filterable, non dryable semisolid soft material where as treatment of sorbent with inorganic solvents such as water, HNO₃, NaOH showed that the sorbent is insoluble or sparingly soluble in such medium.

The organic solvents such as ethanol, TBP and kerosene react with sorbent, POHA and form gel. Further, the weight loss of the sorbent in such different medium follows the order: water < 0.5 M NaOH < 0.5 M HCl < 0.5 M HNO₃. The POHA is an acidic sorbent containing -OH as functional group. The larger solubility of the sorbent in HNO₃ medium is due to the oxidative degradation of sorbent, POHA. The results also indicate that the sorbent is suitable for alkaline medium for sorption process and elution process may be carried out in HCl medium (non-oxidative acid) to achieve reduced loss of the sorbent.

CHAPTER – 3

INSTRUMENTAL

CHARACTERISATION

3.1 Introduction

There are several reasons why it is necessary to characterise a polymeric material. Theoretical analysis, recycling and reclamation and failure analysis of a component are required for identification of the polymer type although they may not be concerned with the precise measurement of all of its physical properties. Design of polymers for its specific application will often also require knowledge of the physical properties of a material and the techniques used may also be those used for characterisation. A typical polymeric material is often not a single component and hence simple chemical analysis will rarely provide all the information required. Determining its stability in contacting medium is an important aspect. To analyse the availability and usefulness of attached functional group in chelating polymer and effect of improving its aspect, characterisation is needed to be carried out. When a chemist is asked to design a polymer for a particular application, a number of factors have to be considered and it is essential that a number of characteristics are determined. Some of the properties which are often required to characterise a chelating sorbent are:

- i. Surface analysis
- ii. Microstructure of the sorbent
- iii. Sorption ability
- iv. Presence of functional groups responsible for sorption
- v. Thermal stability of the sorbent

Characterisation of sorbent permits correlation to be made between feature of the molecular structures and macroscopic physical properties. Having established such correlation design of a molecule is confirmed with structure favouring a particular property or combination of properties. This will assist avoiding the failure or improving the properties of sorbent in future.

3.2 Instrument used for characterisation

Orion 720A+ model pH meter (Thermo Electron Corporation) was used for measuring pH of the solution. For sorbent drying an oven of Meta-Lab model MSI-66 was used and Whatman-42 grade filter paper was used for sorbent-solution filtration. Thermo-bath used for batch mode sorption experiments was obtained from Joshi Scientific Corporation. METTLER TOLEDO-DSC-822 model Differential Scanning Calorimetry (DSC) was used with 5°C/min heating rate for analysing thermal characteristics of sorbents. Porosity and specific surface area of the sorbent determined using Thermo-fisher SURFER model Brunauer-Emmett-Teller (BET) surface area analyser. Morphology of sorbent beads was examined by scanning electron microscope (SEM) using QUANTA 200 with ≥ 10 KV accelerated voltage. Infrared spectrum (FTIR) was examined using VERTEX 70 FTIR. Raman spectra of sorbent without uranium loading and with metal loading were recorded using JASCO make Raman Spectrophotometer. An inverted optical microscope (GX-51, Olympus) was used for observation of microstructures. 100 Watt halogen lights source was used in combinations with lights filters according to the requirement. Micrographs were captured using a digital camera (Olympus Colour View 1) attached to it.

3.3 Results and discussion

3.3.1 Brunauer–Emmett–Teller (BET) analysis

Determination of inner surface of the sorbent was carried out using BET analyser. Nitrogen gas was used as adsorbate and specific surface area was calculated by measuring the amount of physically adsorbed gas according to BET method. P/P^0 is the relative pressure which corresponds to the quantity of gas adsorbed. P is the actual gas pressure and P^0 is the saturated vapour pressure of the adsorbate. For sorption process, surface area of sorbent is an important factor. Result of the test is shown in **Table 3.1** and isotherm profile in **Figure 3.1**. It revealed that the sorbent has large surface area of 54.19 m²/g of sorbent which confirms its

porosity characteristics. Intra-surface pore size and its distribution were determined for the PHOA sorbent. Average pore diameter and monolayer volume was found to be 1.354 micron and 12.39 cm³/g of sorbent respectively. The sorbent is highly porous having smaller distributed pore inside the sorbent indicating possibility of application for efficient sorption operation.

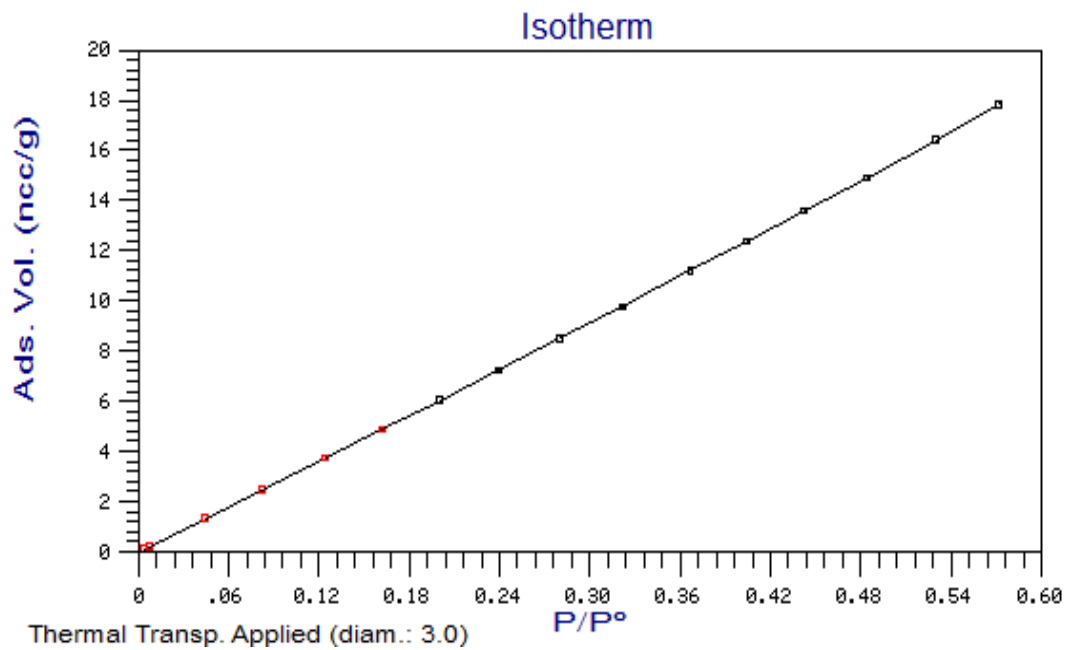


Figure 3.1: Isotherm profile of PHOA sorbent in BET

Table 3.1: BET results of the PHOA sorbent

Initial – final P/P ⁰	0.05 – 0.35
Specific surface area, m ² /g	54.19
C value for BET equation	2.4885
Correlation factor	0.996
Average pore diameter, micron	1.354
Monolayer volume, ncc/g	12.39

3.3.2 Optical microscopic view

From optical microscopic view as shown in **Figure 3.2**, it was observed that the PHOA sorbent is a porous material having smaller number of smaller pore on the surfaces leading to higher specific surface volume determined in BET analysis. It is also seen from the figure that the sorbent pores was filled up after sorption the uranium on to PHOA (loaded PHOA).

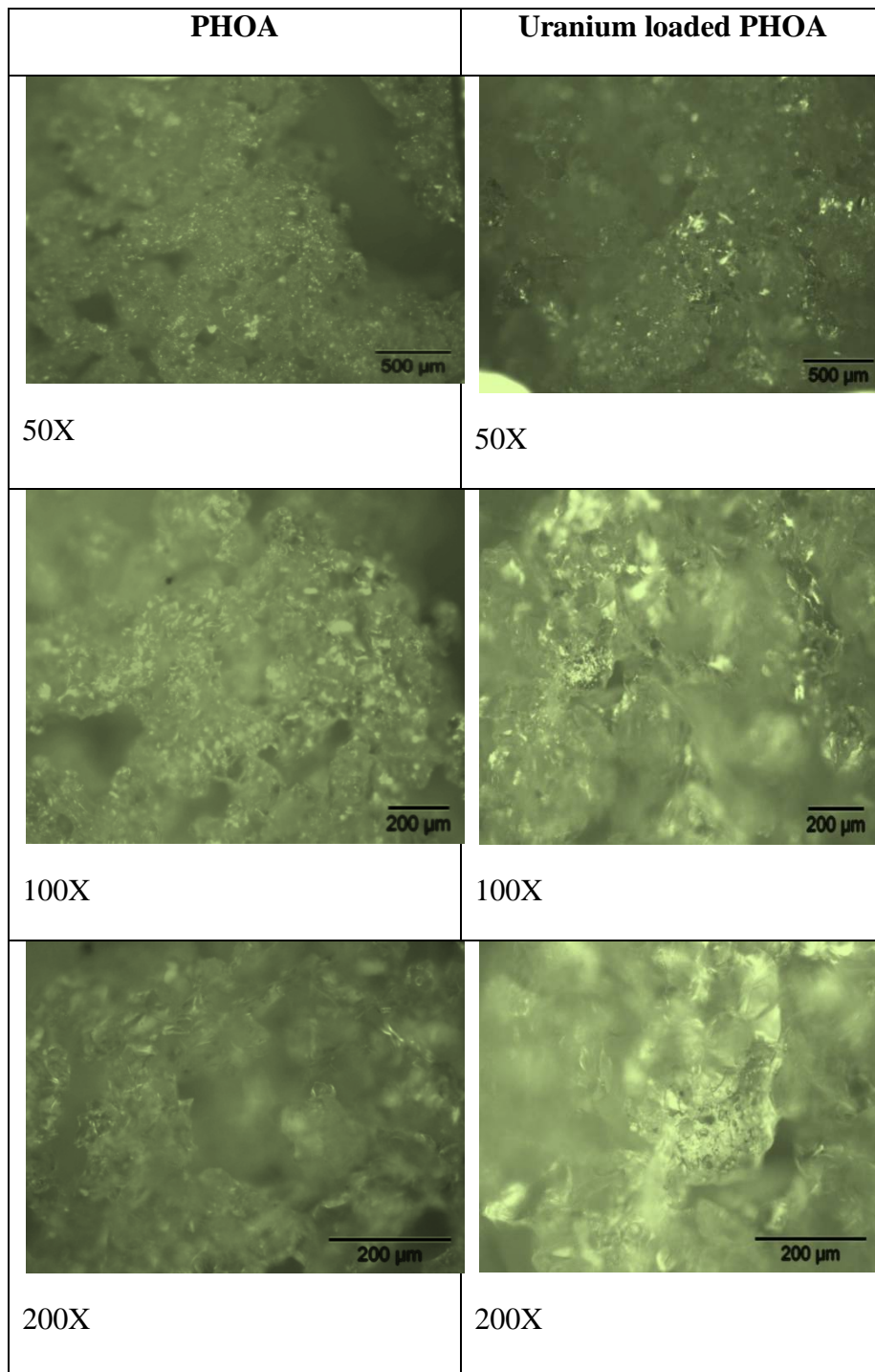
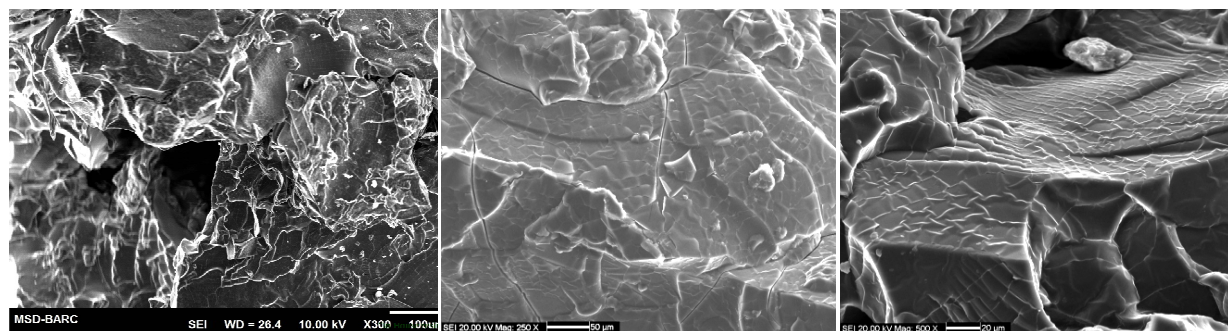


Figure 3.2: Microscopic view of PHOA and loaded PHOA

As the visibility of the pores was not clear it was felt that it is worth for microstructure / morphology analysis by scanning electron microscope which has been carried out further and has been shown below.

3.3.3 Scanning electron microscope (SEM) & energy dispersive X-ray spectroscopy (EDS) analysis

Scanning electron microscope (SEM) study is generally used as a diagnostic tool for morphology study. **Figure 3.3** shows SEM photographs of the PHOA surface cross section (a) before and after (b) sorption of uranium (VI) and (c) after elution of uranium by 1M HCl. As seen from the images PHOA has well-defined, interconnected, three dimensional porous structures with micro-pores of mean size 50 μ m. These pores having regular and thin wall before sorption of uranium (VI), suggested the orderly aggregate of polymer chains for enhancing the strength of sorbent. The stable chains were contributed to support the pore wall to encage and trap uranium (VI).



(a) PHOA

(b) U loaded PHOA

(c) Eluted PHOA

Figure 3.3: Morphology view of PHOA before and after uranium sorption and after uranium elution

The pore size were reduced and somewhere disappeared after encaging U(VI) (**Figure 3.3 b**) which indicates that the pore was filled by U(VI) due to intermolecular interaction. The porous PHOA matrix was suitable for the sorption of U(VI) and there was a stable bonding between the sorbent and sorbate. The pores were regenerated on the PHOA surface after elution (Figure 3.6 c) which confirmed the reusability of the sorbent. **Figure 3.4** shows

energy dispersive X-ray spectroscopy (EDS) spectrum of PHOA before (a) and after (b) uranium sorption and (c) after uranium elution. EDS was examined along with SEM. EDS characterisation based on elemental analysis of uranium confirmed the uranium(VI) sorption on the sorbent.

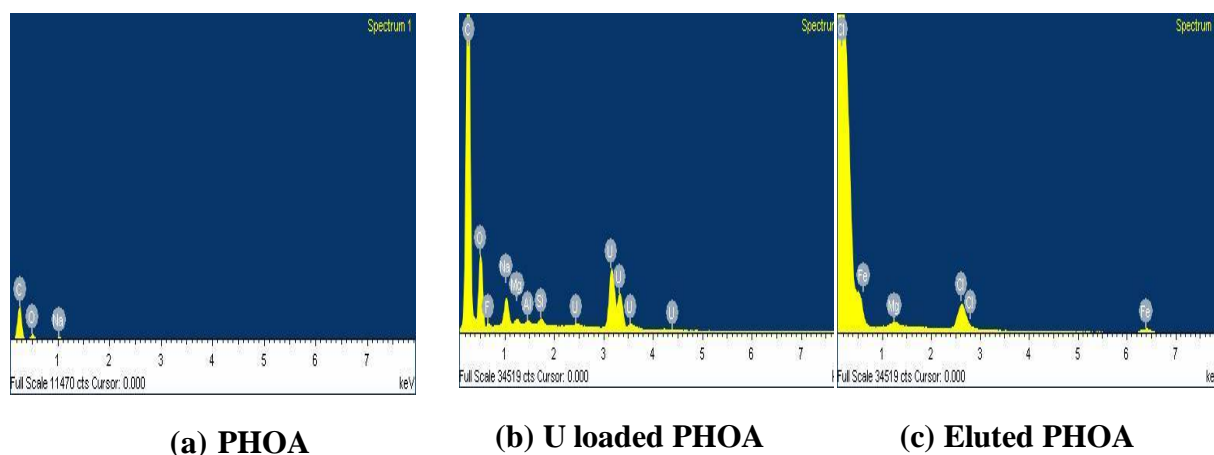


Figure 3.4: EDS analysis of PHOA before and after uranium sorption and after uranium elution

3.3.4 Differential Scanning Calorimetry (DSC), Thermogravimetric (TG) & differential Thermogravimetric (dTG) analysis

Differential Scanning Calorimetry is used for examining polymeric materials to determine their thermal transition, to confirm existence of bonded moisture and also to understand thermal stability of the materials. The experiments were carried out in Argon atmosphere with 5°C/min heating rate. **Figure 3.5** shows thermo-grams of PHOA sorbent for temperature range from room temperature to 350°C. Peak at 121°C was due to removal of moisture from the sorbent which was less in quantity. Existence of bonded water was evidenced from the peak at 155°C, which was not driven out at 121°C. Peaks at 227°C and 285°C correspond to condensation reaction of functional groups of the sorbent followed by intra-molecular arrangement. Further heating leads to decomposition of functional group of the sorbent and cyclization which was observed at temperature 322°C. The PHOA is thermally stable upto about 225°C with its functional group. Similar findings were obtained from the TG and dTG

studies of the uranium loaded resin which has been shown in **Figure 3.6 (a)**. From the figure it was confirmed that the PHOA retains its stability after elution (comparing **Figure 3.6 (a)**, (b) and (c)).

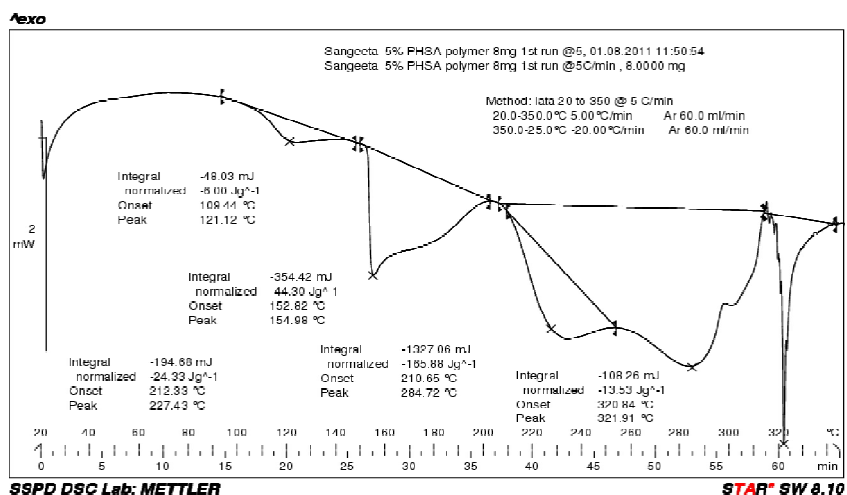
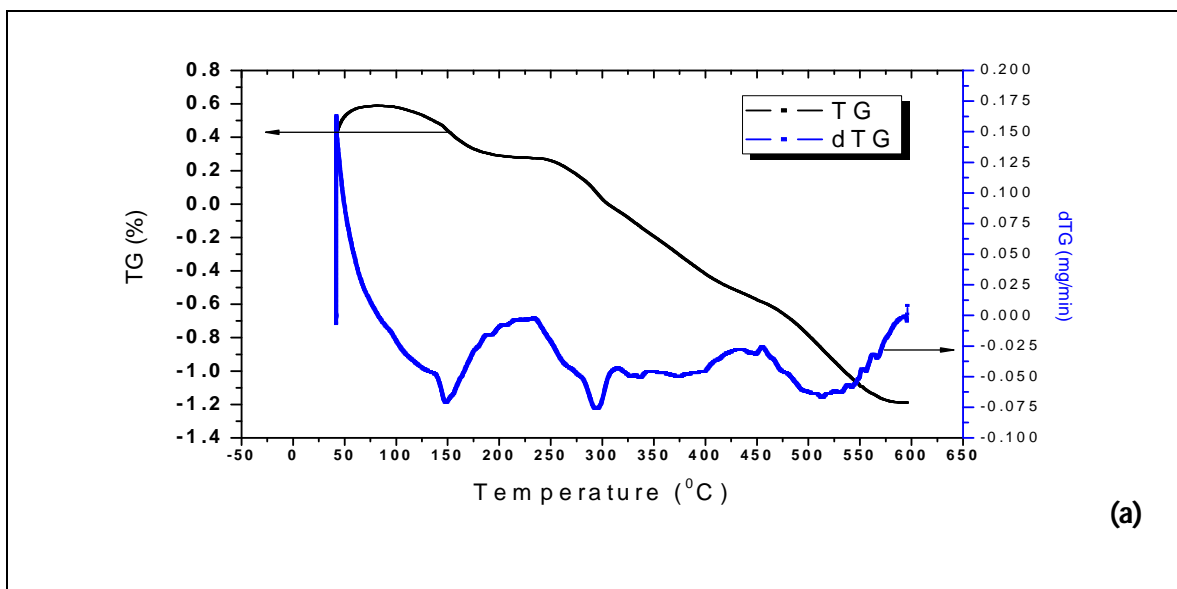


Figure 3.5: DSC thermo-grams of the uranium loaded PHOA sorbent



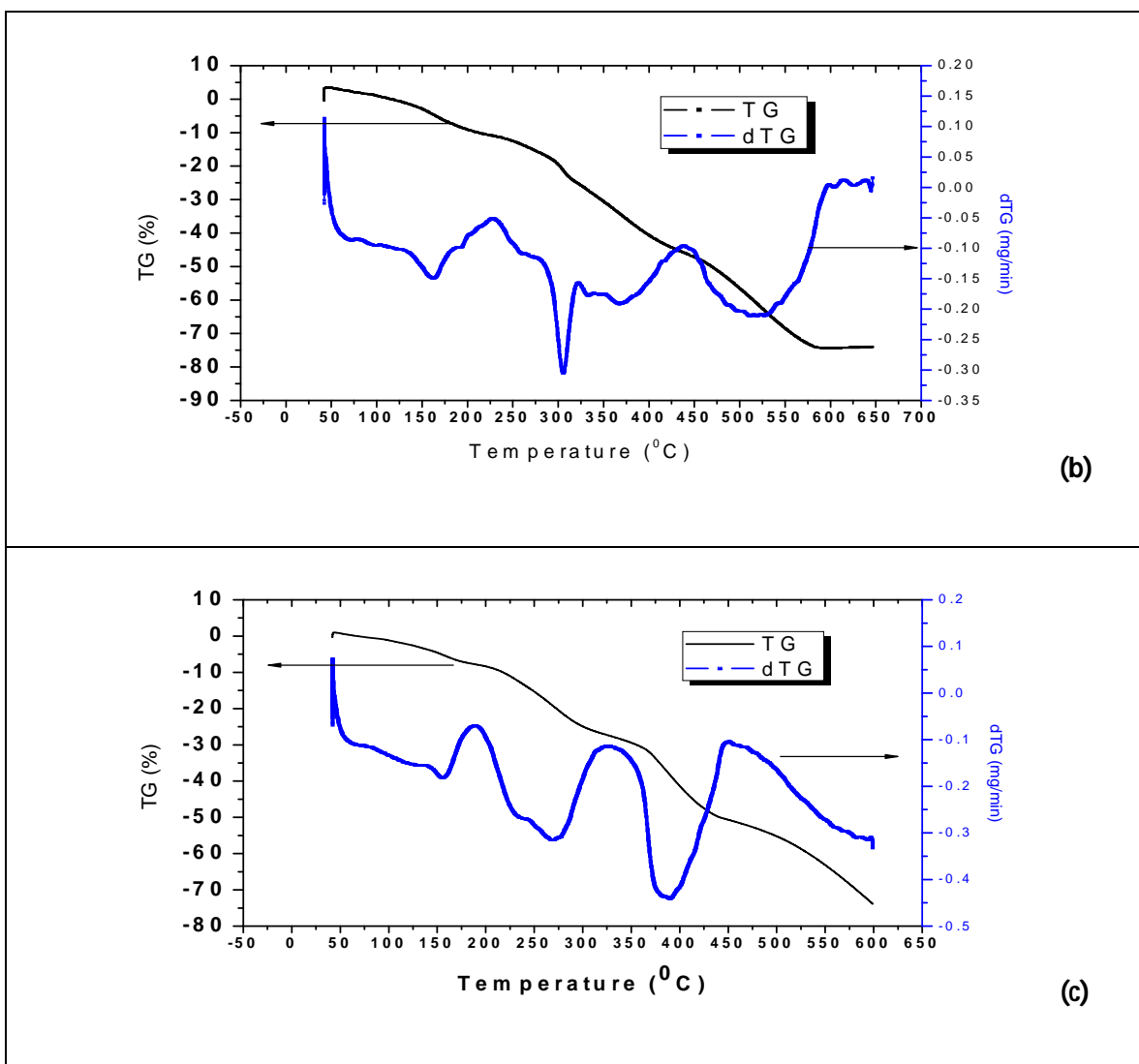


Figure 3.6: TG and dTG thermo-grams of the PHOA, (a) before, (b) after uranium sorption and (c) after uranium elution

3.3.5 Fourier transforms infrared (FTIR) study

FT-IR spectra of virgin PHOA sorbent and PHOA loaded with uranium were taken using KBr pelletization technique. N-O peak spectra of virgin and loaded PHOA were compared for understanding the interaction of uranium with the sorbent. The IR spectra recorded for (A) virgin PHOA, (B) uranium loaded PHOA and, (C) eluted PHOA samples have been shown in **Fig. 3.7**. Shift of characteristic sorption peaks for carbonyl stretching from 1689 cm^{-1} to 1640 cm^{-1} and for N-O stretching from 1321 cm^{-1} to 1384 cm^{-1} has indicated a strong interaction of hydroxamates with uranium. Uptake of uranium in the sorbent was attributed to

additional peaks at 934 cm^{-1} , 1098 cm^{-1} in loaded sorbent spectra (B), which are characteristics of O-U-O stretching vibrations and N-H bending vibrations respectively.

Uranium elution and sorbent reusability was indicated comparing spectra (A) and (C), which are similar in nature and peak for O-U-O stretching vibration was absent.

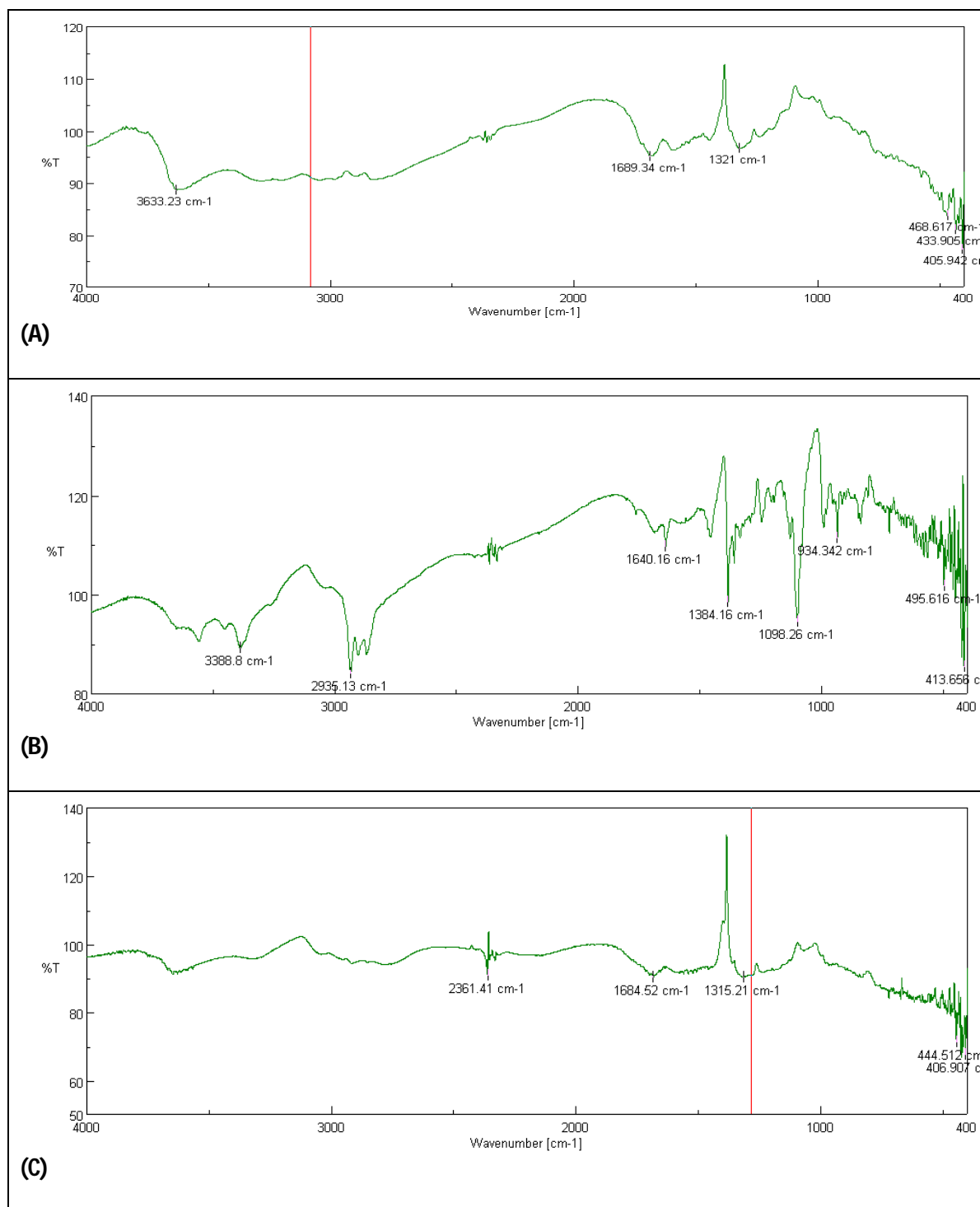


Figure 3.7: FTIR spectra of (A) PHOA, (B) loaded PHOA and (C) eluted PHOA

3.3.6 Characterization of sorbent using Raman Spectroscopy

The characterization of functional groups present in the sorbent, POHA were performed using Raman Spectroscopic technique where the spectra was collected in a wide range of wave number. **Figure 3.8 (a) & (b)** shows that the Raman spectra of freshly prepared sorbent and sorbent loaded with uranium. The Raman band at 3200 cm^{-1} is due to O-H stretch where as the bands at 2924 , 1725 cm^{-1} , 1662 cm^{-1} and 1319 cm^{-1} are due to C-H, C=O, N-H and C-N band. All the Raman spectral stretching frequencies of fresh and uranium loaded sorbent has been listed in **Table 3.2**.

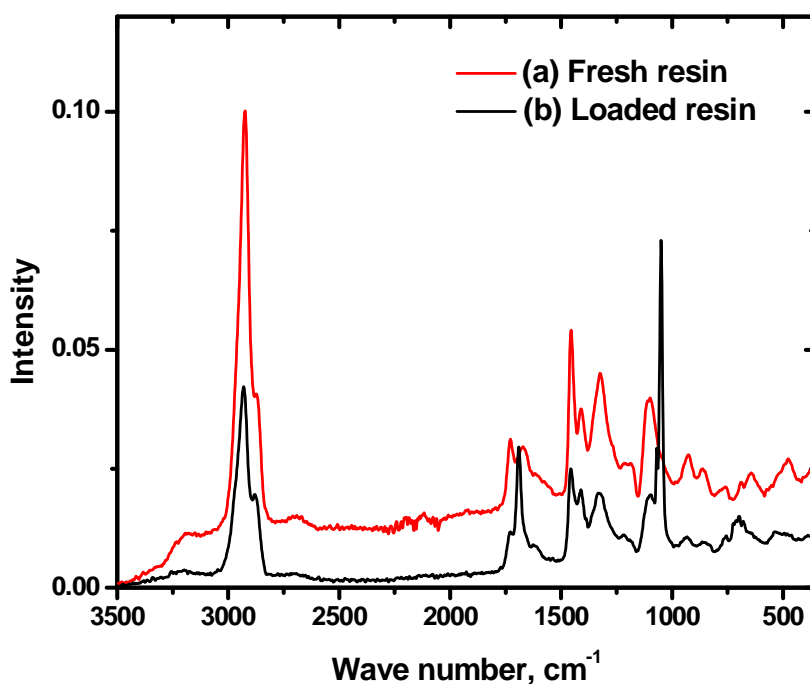


Figure 3.8: Raman spectra of (a) fresh sorbent and (b) uranium loaded sorbent

The C=O stretching frequency in uranium loaded sorbent was found at much lower range (1690 cm^{-1}) than the fresh one. Similarly the intensity of O-H band at 3200 cm^{-1} decrease for loaded sorbent compared to fresh one. Further, there is a new stretching band at 1047 cm^{-1} in loaded sorbent which indicate the presence of UO_2^{2+} ions in the sorbent. The difference in

Raman spectral frequencies in fresh as well as loaded sorbent indicate that the O-H and C=O groups take part in bond formation with UO_2^{2+} ions during uranium loading.

Table 3.2: Raman spectral data of fresh sorbent and uranium loaded sorbent

Fresh sorbent		Uranium loaded sorbent	
<u>Peak position (cm⁻¹)</u>	<u>Approximate description</u>	<u>Peak position (cm⁻¹)</u>	<u>Approximate description</u>
3200 (w)	O-H stretching	3224 (w)	O-H stretching
2924 (s)	C-H stretching	2924 (s)	C-H stretching
2677 (w)	C-H stretching	1733 (w)	-
2113 (w)	C-H stretching	1690 (s)	C=O stretching
1725 (s)	C=O stretching	1452 (m)	-
1662 (m, b)	N-H stretching	1319 (s)	C-N stretching
1452 (m)	-	1100 (w)	C-N stretching
1399 (m)	-	1046 (s)	O=U=O stretching
1319 (s)	C-N stretching	932 (w)	C-C stretching
1100 (w)	C-N stretching	862 (w)	C-C stretching
932 (m)	C-C stretching	765 (w)	C-C stretching
862 (m)	C-C stretching	694 (w)	-
765 (w)	C-C stretching	536 (w)	-
633(w)	-		
474 (w)	C-C stretching		

3.3.7 Uranium sorbed PHOA characterisation by EDXRF

Further, presence of uranium in loaded sorbent was confirmed using EDXRF technique.

Figure 3.9 shows the uranium determination plot from Energy Dispersive X-ray Fluorescence (EDXRF) Spectrophotometer, Jordon Valley (Model No Ex-3600M) and

Figure 3.10 shows the same using experimental set up shown in **Figure 3.10** where (a) reference plot and (b) elemental determination plot. The figures confirm the sorption of uranium on to the PHOA sorbent.

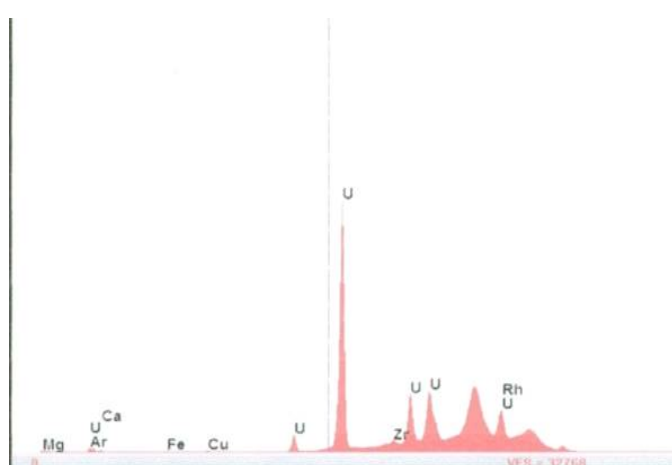


Figure 3.9: EDXRF spectra of PHOA sorbed with uranium

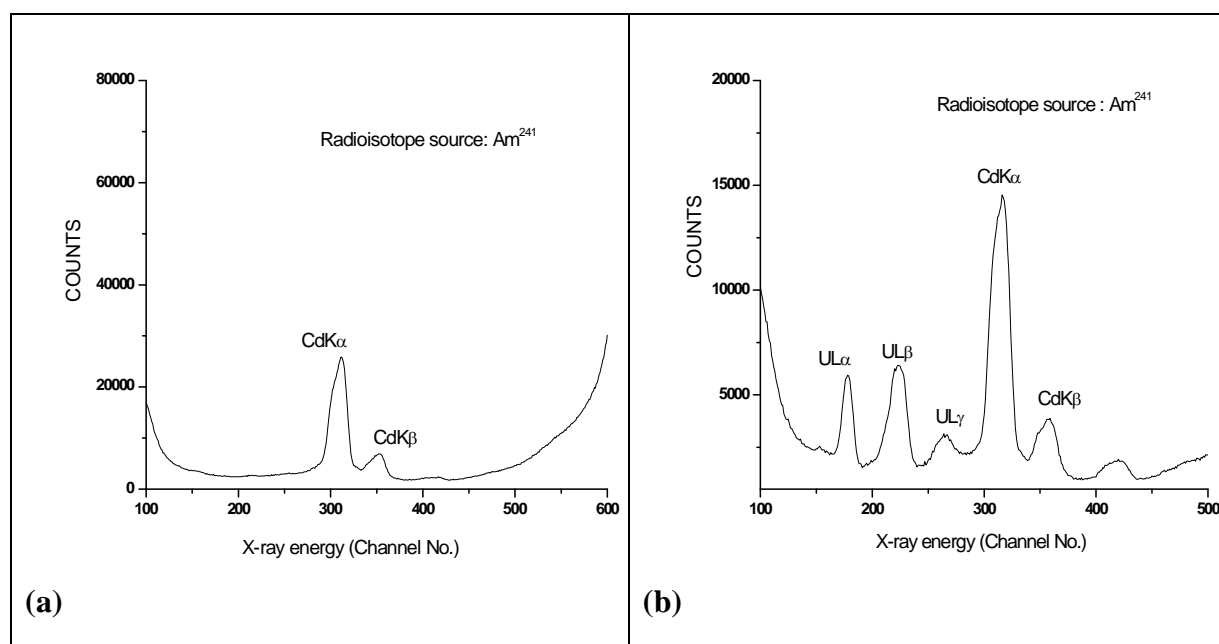


Figure 3.10: EDXRF of (a) reference and (b) uranium loaded PHOA sorbent

CHAPTER – 4

BATCH EXPERIMENT: SORPTION

4.1 Introduction

Sorption reaction may be defined as the reversible (for separation and pre-concentration / recovery) or irreversible (only separation) interchange of ions (like ion-exchange) between a solid phase (the sorbent) and a solution phase, the sorbent being insoluble in the medium in which exchange is carried out. If a sorbent (ion-exchanger) R^-A^+ , carrying cations A^+ as the exchanger ions, is placed in an aqueous solution phase containing B^+ cations; a sorption reaction takes place which may be represented by the following **Equation 4.1**.



An ion may be defined as an atom or combination of atoms (molecules) which carry a net positive (cation) electrical charge, in this case. As electro-neutrality is preserved at all times in both the sorbent and solution phases, counter-ions are exchanged in equivalent amounts.

The most important features characterising an ideal sorbent are:

1. A hydrophilic structure of regular and reproducible form (crosslinking)
2. Physical stability in terms of mechanical strength and resistant to attrition
3. Chemical stability with respect to application medium and condition (like acidic / alkaline, temperature, radiation etc)
4. Consistent particle size and effective surface area compatible with the hydraulic design requirements for large scale operation
5. Controlled & effective sorption capacity and Rapid rate of sorption

Developers of novel sorbent materials have progressed a long way towards meeting all these requirements and improve the sorbent characteristics. Sorption isotherms, kinetics, mechanism of sorption and thermodynamic analysis are important and need to study in detailed for evaluating the sorbent performance in application condition. The efficiency of the sorbents was investigated using batch sorption technique under different experimental conditions namely sorbent characteristics, pH, initial metal-ion concentration, contact time,

temperature using simulated as well as the plant effluent (nuclear wastewater) in this study. The experimental data were correlated to different equilibrium sorption and kinetic models and the corresponding parameters along with thermodynamic parameters have been determined and analyzed in the thesis. These parameters are considered fundamental for further studies involving the scale up of the process.

4.2 Materials and methods

4.2.1 Sorbent

Mixed size sorbent, PHOA as prepared was used having size distribution: 10 mesh 21.66%, 16 mesh 59.96%, 18 mesh 8.31% and 25 mesh 10.07% as detailed in **Chapter 2 (Para. 2.3.1)** for all experiments except those experiments carried out for performance evaluation of different mesh size sorbent. The PHOA was indigenously developed and prepared in Desalination Division, BARC. The sorbent was washed with distilled water (DW) before use to remove the soluble impurities if any. No pre-treatment was given to avoid extra expenditure. Preparation and characteristic details have been described in previous **Chapter 2** and **Chapter 3**.

4.2.2 Uranium solution

The hexa-hydrated uranyl nitrate standard solution was used as stock solution. Uranium metal used had natural isotopic abundance and which is not generally considered significant health hazardous. Safe procedure was followed in handling and disposing of uranium solution wherever carried out. The stock solution was diluted to demanded / required concentration and was adjusted to desired pH with sodium hydroxide solution at room temperature, $28\pm 2^\circ\text{C}$. The solution was used immediately after preparation.

4.2.3 Uranium and other metal ion determination

An Inductively Coupled Plasma Emission Spectrophotometer (ICPAES), Jobinyvon Emission, Model No. JY 328 was used to determine uranium and other metal ions'

concentrations in solutions. The detection limit (3σ) of the instrument for non-transition elements: > 0.2 ppb, transition elements: > 1 ppb and rear earths elements: > 3 ppb. Concentration of uranium and other metal ions in the solution before and after equilibrium and as required (for kinetic study) was estimated.

4.2.4 Reagents

The reagents used in the experiments were of analytical reagent (AR) grade. Sodium hydroxide, $\text{CaCl}_2 \cdot 2\text{H}_2\text{O}$, MgSO_4 , $\text{MnCl}_2 \cdot 4\text{H}_2\text{O}$, FeCl_3 , $\text{CuSO}_4 \cdot 5\text{H}_2\text{O}$, NaNO_3 (procured from S.D. fine chemicals) were used as received without purification and treatment. Distilled water of Millipore ultra pure water system was used in investigations (Millipore Q) whenever needed for dilution and washing / rinsing. Solutions containing metal ions were prepared by dissolving appropriate amount of salts of corresponding metals in uranyl nitrate solution.

4. 2.5 Apparatus

The sorption experiments were carried out using Borosil glass beaker and other glass items with which alkaline uranium solution does not get affected. PARAFILM PM-992 (laboratory film) was used as sealing material for glass apparatus wherever required. Thermo-bath used for batch mode sorption experiments was obtained from Joshi Scientific Corporation. Solution pH was measured using Orion 720 A+ model pH meter of Thermo Electron Corporation. Calibrated laboratory weighing scale was used for sorbent weight measurement. Whatman-42 grade filter paper was used for filtration.

4. 2.6 Sorption / uptake evaluation method

The amount of sorbed metal was calculated from the difference of metal ion concentration in aqueous solution before and after the sorption. The equilibrium sorption / uptake (Q_e , mg/g of sorbent), distribution constant (K_d , L/g), and sorption percentage (%) were calculated according to formulae in **Equation 4.2-4.4**.

$$Q_e = \frac{(C_i - C_e) \times V}{m} \quad 4.2$$

$$K_d = \frac{Q_e}{C_e} \quad 4.3$$

$$\% \text{ Sorption} = \frac{(C_i - C_e)}{C_i} \times 100 \quad 4.4$$

Where, C_i and C_e are the concentration of the metal ion (mg/L) in initial sample solution and final equilibrium solution respectively, V is the volume of the aqueous phase (mL) and m is the weight of the sorbent, PHOA beads (g).

4.2.7 Sorption isotherm models

An adsorption isotherm describes the equilibrium of the sorption of a material from an aqueous media onto a solid phase adsorbent surface at constant temperature [217]. The equilibrium represents the ratio of the amount of substance adsorbed to that in the aqueous medium. The adsorption mechanism and adsorbent's affinity for the metal ion can be determined by analysing the physicochemical parameters. Majorly four isotherm models are used as discussed below.

4.2.7.1 Langmuir isotherm model

Langmuir isotherm equation is derived from simple mass kinetics, considering chemisorption. The basic assumption of the Langmuir model is that the adsorption is monolayer without any interaction between the adsorbed molecules and all sites are identical [218]. Several adsorption processes for uranium recovery correlating well in the Langmuir isotherm have been analyzed to calculate the adsorption capacities with R^2 values ranging from 0.95 to 0.99. Langmuir isotherm is applicable to homogeneous sorption where the sorption of each sorbate molecule onto the surface has equal sorption activation energy. The Langmuir model can be represented as:

$$Q_e = \frac{X}{m} = \frac{Q_m b C_e}{(1 + b C_e)} \quad 4.5$$

A linear form the equation is

$$\frac{1}{Q_e} = \frac{1}{Q_m b C_e} + \frac{1}{Q_m} \quad 4.6$$

Where, X is the total amount of solute adsorbed in adsorbent at equilibrium (mg), C_e is the equilibrium concentration of metal in solution (mg/L), Q_e is the amount of metal ions sorbed onto sorbent in equilibrium (mg/g), and Q_m and b are Langmuir constants related to sorption capacity and sorption energy, respectively. Maximum sorption capacity (Q_m) represents monolayer coverage of sorbent with sorbate, and b represents enthalpy of sorption and should vary with temperature. The value of correlation coefficients of the linearized Langmuir equation should preferably be high, indicating that the model can explain metal ion adsorption by the adsorbents satisfactorily. The essential features of a Langmuir isotherm can be expressed in terms of a dimensionless equilibrium parameter, R_L which is defined as:

$$R_L = \frac{1}{1+bC_0} \quad 4.7$$

Where b (L/mg) is the Langmuir constant and C_0 (mg/L) is the initial concentration. The calculated values of the dimensionless factor R_L provides information as to whether the adsorption is irreversible ($R_L = 0$), favourable ($0 < R_L < 1$), linear favourable ($R_L = 1$) or unfavourable ($R_L > 1$).

4.2.7.2 Freundlich isotherm model

The Freundlich isotherm model gives an empirical expression expressing the isothermal variation of adsorbed quantity of gas by unit mass of solid adsorbent with pressure/concentration taking into account heterogeneous adsorption surfaces. The adsorption capacity is correlated to the concentration of metal ions at equilibrium. The adsorption pattern of uranium by *Citrobacter freundii* [219] was in accordance with the Freundlich isotherm with correlation factor up to 0.98. The Freundlich adsorption isotherm is mathematically expressed as

$$\frac{x}{m} = K C^n \quad 4.8$$

where, x/m is the adsorption amount per unit mass of adsorbent, c is the equilibrium concentration of adsorbate in solution and K and n are constants for a given adsorbate and adsorbent pair for a given temperature. In the linearized form:

$$\ln Q_e = \ln K_F + \frac{1}{n} \ln C_e \quad 4.9$$

The maximum sorption capacity can be determined by varying the sorbent dose while keeping the initial concentration constant. The extrapolated value of $\ln Q_e$ for $C_e = C_0$ gives the maximum adsorption capacity. The value of n and K_F can be determined by plotting a graph between $\ln Q_e$ and $\ln C_e$ and analysing the slope and intercept of the curve. When the value of $1/n$ ranges from 0.1 to 0.5, the sorption is highly favourable; from 0.5 to 1 the sorption is quite acceptable and for >1 the sorbent is not acceptable for the requirement.

4.2.7.3 Other isotherm models

i. Temkin isotherm model

The Temkin isotherm assumes uniform distribution of molecules on the adsorbent surface. The heat of adsorption of all the molecules in the layer decreases linearly with the coverage of molecules due to the adsorbate–adsorbate repulsions [220] and the fall in the heat of adsorption is linear rather than logarithmic as implied in the Freundlich equation. The Temkin isotherm equation is as follows:

$$Q_e = \frac{RT}{b_T} \times \ln(a_T) + \frac{RT}{b_T} \ln C_e \quad 4.10$$

Where R is gas constant, value is $8.314 \times 10^{-3} \text{ kJ mol}^{-1} \text{ K}^{-1}$. T is absolute temperature K , b_T is the Temkin constant related to the heat of adsorption (kJ mol^{-1}) and a_T is the equilibrium binding constant corresponding to the maximum binding energy (L/g). The linear plots of Q_e versus $\ln C_e$ enable to determine the constant a_T and b_T .

ii. Dubinin–Radushkevich (D-R) isotherm model

Dubinin proposed the isotherm to estimate the mean free energy of adsorption. The Dubinin–Radushkevich (D–R) isotherm describes the adsorption on a single type of uniform pores

and is applied to distinguish between physical and chemical adsorption. This isotherm does not assume a homogeneous surface or a constant adsorption potential [221]. The linear form of the equation:

$$\ln Q_e = \ln Q_{\max} - K^2 \quad 4.11$$

Where K ($\text{mol}^2 \text{kJ}^{-2}$) is a constant related to the mean adsorption energy, Q_e is the amount of solute adsorbed per unit weight of adsorbent (mol/g) at equilibrium, Q_{\max} is the adsorption capacity (mol/g) and ε is the Polanyi potential, which can be calculated from equation

$$= RT \ln\left(1 + \frac{1}{C_e}\right) \quad 4.12$$

The plot between $\ln Q_e$ and ε^2 at fixed temperature yields the constant K and Q_{\max} . The constant K provides the mean free energy sorption per molecule of the sorbate when it is transferred to the surface of the solid from infinity in the solution, represented as E , and can be computed using:

$$E = \frac{1}{\sqrt{2K}} \quad 4.13$$

The value of E is useful to estimate the type of adsorption process. Value of E in between 8 and 16 kJ/mol indicates towards an ion- exchange mechanism. A value lesser than 8 kJ/mol shows that the adsorption process is physical in nature [222].

4.2.8 Kinetic models

Kinetic models are studied to analyze the effect of several experimental conditions such as adsorbent weight, initial metal concentration, percentage additive used, pH, etc., on the rate of reactions and the yield. They are also used to determine the reaction mechanism and describe the characteristics of the reaction. The data on the kinetics of the reaction are finally used to optimize the conditions for the uranium ion uptake. The kinetic models addressed are pseudo-first-order, pseudo-second- order, Elovich and intra-particle diffusion and they have been applied to examine the rate controlling mechanism of the adsorption process.

4.2.8.1 Sorption mechanism analysis

Defining the sorption pathway related to isotherm studies, effort was put to understand the effect of initial concentration and time on the uranium uptake of PHOA in equilibrium. It was indicated as described above that U(VI) sorbed on PHOA as a monolayer sorption. If it is so, then the sorption rate of U(VI) can mainly be affected by the available concentration of U(VI), i.e., $(q_e - q_t)$ and the effect of time on the sorption process is negligible. The sorption equation can be expressed as **Equation 4.14** and followed by **Equation 4.15**.

$$\frac{dq_t}{dt} = K_s (q_e - q_t) \quad 4.14$$

$$-\ln(1 - F) = K_s t \quad 4.15$$

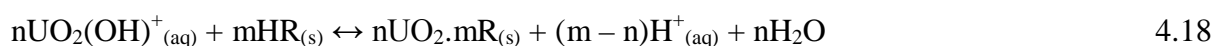
Where, K_s is the sorption constant and F is (q_t/q_e) . Following the hypothesis, a plot of $-\ln(1 - F)$ vs. t should be a straight line and the slope of the resultant straight line is K_s . Similarly, if the sorption of PHOA for U(VI) is the multilayer molecule sorption, the sorption rate of U(VI) onto PHOA usually increases with an increase of available concentration of U(VI) while with decrease of the contact time. The sorption rate equation can be described as **Equation 4.16** and followed by **Equation 4.17** after solving and simplification.

$$\frac{dq_t}{dt} = K_s \frac{q_e - q_t}{t} \quad 4.16$$

$$-\ln(1 - F) = K_s \ln t \quad 4.17$$

The plot of $-\ln(1 - F)$ vs. $\ln t$ also must be a straight line if the sorption process follow multilayer hypothesis.

To understand the sorption mechanism as well as composition of the complex between U(VI) and PHOA, the sorption behavior of U(VI) on PHOA was examined by the method of the slope, which is conventional measurement of the thermodynamics. Assuming the composition of the complex formed between U(VI) and PHOA is $n\text{UO}_2 \cdot m\text{R}$ i.e. n mole of UO_2^{++} is attached with m mole of sorbent (HR), the adsorption equilibrium equation can be expressed as Eq. (4).



Where, the subscripts (aq) and (s) represents the U(VI) solution in aqueous phase and PHOA sorbent in solid phase, respectively. The apparent equilibrium constant (K_a) and the distribution constant (K_d) of U(VI) can be expressed as **Equation 4.19 and 4.20** respectively.

$$K_a = \frac{[nUO_2.mR]_{(s)} [H^+]^{(m-n)}_{(aq)}}{[UO_2(OH)^+]^n_{(aq)} [HR]^m_{(s)}} \quad 4.19$$

$$K_d = \frac{[nUO_2.mR]_{(s)}}{[UO_2(OH)^+]_{(aq)}} \cdot \frac{V}{W} \quad 4.20$$

From above equations, K_a can be written as :

$$K_a = K_d \frac{W [H^+]^{(m-n)}_{(aq)}}{V [UO_2(OH)^+]^{(n-1)}_{(aq)} [HR]^m_{(s)}} \quad 4.21$$

The relationship between K_a and K_d can be expressed as:

$$\ln K_d = (n-1)\ln[U(VI)]_{(aq)} + m \ln[HR]_{(s)} + (m-n)\text{pH} + \ln K_a + \ln(V/W) \quad 4.22$$

By plotting $\ln K_d$ vs respective parameters from experimental data m , n and K_a can be evaluated which gives the probable composition of the U(VI) sorbed PHOA complex. The composition can also be confirmed by theoretical study namely molecular modeling study by geometrical stability analysis.

4.2.8.2 Pseudo first order kinetic model

To avoid complication and cost of a second order reaction, it is treated as a pseudo first order, wherein the concentration of one component is taken significantly higher than the other one, equation as:

$$R = k[A][B] \quad 4.23$$

Since the concentration of one of the components, say A, is very high in comparison to that of B, we can assume [A] to be constant. Hence, the equation reduces to,

$$R = k'[B] \quad 4.24$$

Where k' is $k[A]$. This kinetic was found to fit well with uranium adsorption using few sorbents as described by Lagergren in 1993 showed that the rate of adsorption of solute on

the adsorbent is based on the adsorption capacity and follow pseudo first order equation which is often used to estimate the k_{ad} , mass transfer coefficient in the design calculations.

The pseudo first-order rate equation is given as:

$$\frac{1}{q_t} = \left(\frac{K_1}{q_{e1}}\right) \left(\frac{1}{t}\right) + \frac{1}{q_{e1}} \quad 4.25$$

Where q_{e1} (mg/g) is the amount of metal ion sorbed at equilibrium, q_t (mg/g) is the amount of adsorbed metal ion adsorbed at time t where K_1 is the first-order adsorption rate constant (min^{-1}). For pseudo first order reaction the plot of $1/q_t$ versus $1/t$ gives a straight line and the pseudo first order rate constant can be calculate from the slope value [223].

4.2.8.3 Pseudo-second order kinetic model

In 1995, Ho described a kinetic process of the adsorption of divalent metal ions onto peat [224] which involved the assumption that the rate limiting step may be chemical adsorption involving covalent forces through sharing or the exchange of electrons between the adsorbent and divalent metal ions. In addition, the adsorption follows the Langmuir equation [225]. The pseudo-second order reaction is greatly influenced by the amount of metal on the adsorbent's surface and the amount of metal adsorbed at equilibrium. The rate is directly proportional to the number of active surface sites. This kinetic model for uranium adsorption was studied by many research workers. The pseudo second order equation is given as:

$$\frac{t}{q_t} = \frac{1}{K_2 q_{e2}^2} + \left(\frac{1}{q_{e2}}\right) t \quad 4.26$$

where K_2 is the second-order adsorption rate constant ($\text{g mg}^{-1} \text{min}^{-1}$) and q_{e2} is the adsorption capacity calculated by the pseudo-second-order kinetic model (mg/g).The constant K_2 is used to calculate the initial sorption rate 'h' ($\text{mg}/(\text{g min})$), at $t \rightarrow 0$ by using $h = K_2 q_{e2}$. The application of the pseudo second order kinetics by plotting t/q_t versus t yields the second order rate constant K_2 .

4.2.8.4 Elovich model

A kinetic equation of chemisorption was established by Zeldowitsch and was used to describe the rate of adsorption of carbon monoxide on manganese dioxide that decreases exponentially with an increase in the amount of gas adsorbed [226], which is the so-called Elovich equation. In reactions involving chemisorption of adsorbate on a solid surface without desorption of products, adsorption rate decreases with time due to an increased surface coverage. One of the most useful models for describing such ‘activated’ chemisorption is the Elovich equation [227]. Elovich equation is a rate equation based on the adsorption capacity describing the adsorption on highly heterogeneous adsorbent which is expressed as [228]

$$\frac{dq_t}{dt} = \alpha e^{-\beta q_t} \quad 4.27$$

Where, α ($\text{mg g}^{-1} \text{min}^{-1}$) is the initial adsorption rate and β (g/mg) is the desorption constant related to the extent of surface coverage and activation energy for chemisorption. The linearized form of Elovich kinetic equation is a plot of q_t versus $\ln t$ to obtain the kinetic constants. Elovich equation is applied to determine the kinetics of chemisorption of gases onto heterogeneous solids and very rarely used in solute sorption case from liquid to solid mass transfer, hence the model is not considered in this thesis for parametric evaluation.

4.2.8.5 Intra-particle diffusion

The prediction of the rate-limiting step is an important factor to be considered in the adsorption process. It is governed by the adsorption mechanism, which is generally required for design mechanism. For a solid–liquid sorption process, the solute transfer is usually characterized by external mass transfer (boundary layer diffusion), or intra-particle diffusion, or both. The most commonly used technique for identifying the mechanism involved in the sorption process is the fitting of intra-particle diffusion plot. According to Weber and Morris an intra-particle diffusion coefficient k_p is given by the equation:

$$q_t = k_p t^{0.5} + C \quad 4.28$$

Where, k_p is the intra-particle diffusion rate constant ($\text{mg g}^{-1}\text{min}^{-0.5}$) and C is a constant. According to the model q_t versus $t^{0.5}$ should be linear if intra-particle diffusion is only rate determining operation involved in the sorption process [229]. The plot of q_t versus $t^{0.5}$ at different initial solution concentrations gives the value of k_p and the plot may have multi-linearity which indicates two or more steps occurring in the sorption process. Generally the first sharper portion is the external surface adsorption or instantaneous adsorption stage. The second portion is the gradual adsorption stage where the intra-particle diffusion rate is controlled. The third is the final equilibrium stage where intra-particle diffusion starts to slow down due to extremely low solute concentration in the solution. The intra-particle diffusion rate is obtained from the slope of the gentle-sloped portion.

4.2.9 Thermodynamic properties

It is essential to examine the influence of the sorption on PHOA beads with the change of thermodynamic parameters. Both enthalpy and entropy are important properties for any process design. It is essential to clarify the change of thermodynamic parameters to evaluate the feasibility and also to explain temperature dependency of the sorption process. Gibbs energy change, ΔG^0 are estimated by applying following thermodynamic equations.

$$\Delta G^0 = -RT \ln K_d \quad 4.29$$

$$\Delta G^0 = \Delta H^0 + T\Delta S^0 \quad 4.30$$

The van't Hoff equation can be used to calculate the values of ΔH^0 and ΔS^0 ;

$$\ln K_d = \frac{\Delta S^0}{R} - \frac{\Delta H^0}{RT} \quad 4.31$$

Where, K_d is the equilibrium constant at temperature T , R is gas constant ($8.314 \text{ Jmol}^{-1}\text{K}^{-1}$) and T is absolute temperature (K).

The activation energy (E_a) can be calculated from Arrhenius equation, which is used to determine the type of sorption. Arrhenius equation is expressed as:

$$\ln K_2 = \ln A - \frac{E_a}{RT} \quad 4.32$$

Where, K_2 is the rate constant of pseudo-second order sorption ($\text{g mg}^{-1} \text{h}^{-1}$), A the Arrhenius factor, R gas constant ($8.314 \text{ J mol}^{-1} \text{K}^{-1}$), T absolute temperature (K). Generally, low activation energies ($5\text{-}40 \text{ KJ.mol}^{-1}$) are characteristic of physical adsorptions, while high ones ($40\text{-}800 \text{ KJ.mol}^{-1}$) suggest chemisorptions.

4.3 Experimental procedure for sorption parameters

Experiments were performed using desired quantity of PHOA beads added into a 100 mL Borosil glass beaker along with 50 mL of synthetic solution containing uranium ion /or multi-ion and of plant effluent at a selected pH. The sorption system was filtered using whatman-42 filter paper. In the beaker, the same amount 0.5 g (dry weight) of PHOA sorbent was added for all sorption experiment except for variation of sorbent amount. Representative uranium (VI) concentration of $<10 \text{ mg/L}$ was used in most of the experiments as the process methodology was planned to be used for nuclear effluent treatment. Effect of sorbent properties like sorbent size, sorbent quantity on uranium sorption uptake was evaluated treating with the uranium solution for 24h at $\text{pH}>7$. Effects of important process parameters like contact time, temperature, agitation speed, pH and uranium concentration of initial samples were investigated and optimum pH and contact time required for equilibrium was evaluated. Selectivity of the sorbent was evaluated by uranium uptake study in presence of different competitive metal ions in initial solution. Sorption isotherms were measured in batch equilibrium mode. Sorption experiments were carried out with uranium solution of different concentrations ranging from 1.51 to 25.11 mg/L for sorption time 24h. In order to obtain thermodynamic parameters, the same procedures were also performed at the solution temperatures of 301K, 323K and 353K. To study the pH effect on uranium sorption onto the PHOA, the experiments were carried out at different pH ranging from 1 to 10 for sorption time 24 h. Kinetic experiments were performed over time intervals from 30 to 300 minutes.

Different amounts (0.1 – 3.0 g) of PHOA were used to conduct the batch sorption varying sorbent amount.

A typical plant effluent having 9.81 mg U /L, 576 mg Ca /L, 15121 mg Mg /L, 74211 mg NO₃ /L at pH 9.1 was used to carry out all experiments except mentioned separately. pH of the solution was adjusted adding dilute sodium hydroxide or dilute nitric acid wherever required. Volume reduction after each sampling was incorporated in resultant's uranium concentration calculation. All experiments were performed in duplicates. The total (experimental and analytical) relative standard deviation (RSD) was calculated and found maximum $\pm 5\%$.

4.4 Results and discussion

4.4.1 Sorbent performance with plant effluent

In the study, intention was to evaluate the performance of mixed sorbent, as prepared in first hand for plant effluent application. Separation and recovery characteristics of the sorbent for uranium, magnesium and calcium using plant effluent (batch experiment) have been listed in **Table 4.1**. Distribution coefficient (K_d) of uranium was substantially higher, about 100 times than that of calcium and magnesium. Percent sorption of uranium was about 93% whereas, for calcium and magnesium it was about 10% and 15% respectively. The sorbent is found to be highly selective to uranium. Recovery characteristic will be discussed separately in the elution chapter.

Table 4.1: Sorption characteristics of uranium, magnesium and calcium using plant effluent in batch experiment

Parameters studied (Element)	Uranium processing plant effluent		
	(U)	(Mg)	(Ca)
Sorption % (24h)	92.59 \pm 1.8	9.67 \pm 0.2	14.92 \pm 0.3
$K_d = (C_0 - C_e)/C_e$. V/m (mL of effluent/g of dry sorbent)	1250 \pm 14.5	10.71 \pm 0.3	17.64 \pm 0.4
Elution % (24h)	97.22 \pm 1.9	96.53 \pm 1.9	85.52 \pm 1.6
Immobilization factor	0.028	0.035	0.145

4.4.2 Effect of sorbent size on uranium uptake

Individual mesh size sorbent bead was used in tests for uranium uptake varying sorbent mesh size in plant effluent. Four numbers of each effluent was contacted with dry sorbent of different mesh size 10, 16, 18 and 25 separately for 24h. Next day, the resultant solutions were filtered and filtrates were analyzed for uranium ion. Uranium uptake profile varying sorbent mesh size has been shown in **Figure 4.1**.

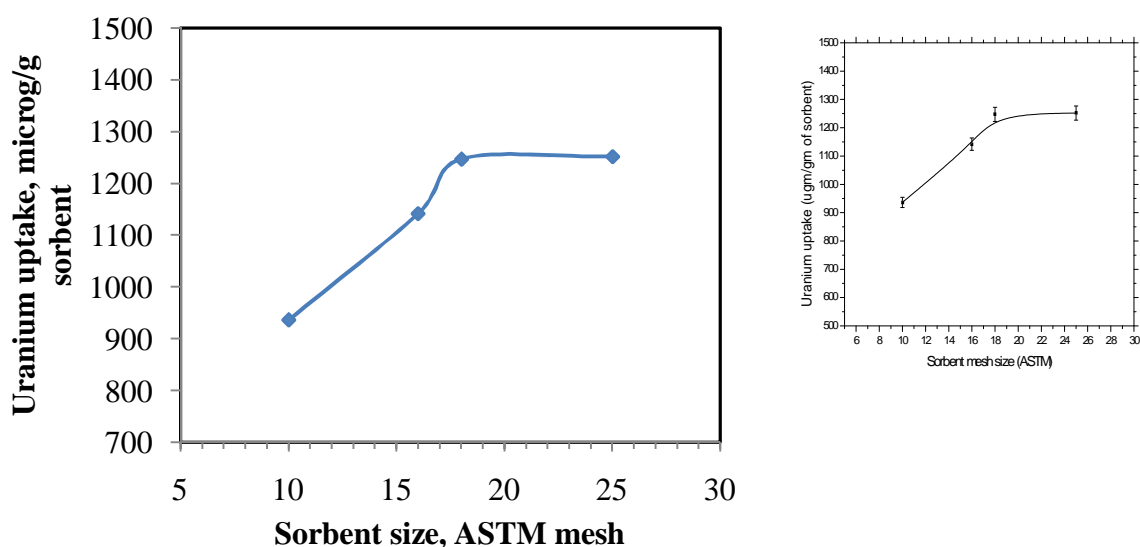


Figure 4.1: Uranium uptake with mesh size variation (effluent pH 8.1, RT, time 24h, sorbent 0.5g)

Uranium uptake was increased sharply up to 18 mesh size as swelling volume increased (**Figure 4.1**) and thereafter the increase was not prominent. Maximum uptake 1142 $\mu\text{g-U/g}$, 1247 $\mu\text{g-U/g}$ and 1252 $\mu\text{g-U/g}$ sorbent were observed with 16, 18 and 25 mesh size beads respectively. Effective uptake was lowered (slop) with increasing mesh size may be because of hindrance of sorbent swelling due to compactness of lower size beads (density increased).

4.4.3 Effect of sorbent quantity on uranium uptake

Different amounts (0.1 – 3.0 g) of PHOA were used to conduct the batch sorption for the purpose. U(VI) sorption profile against PHOA dosage has been shown in **Figure 4.2**.

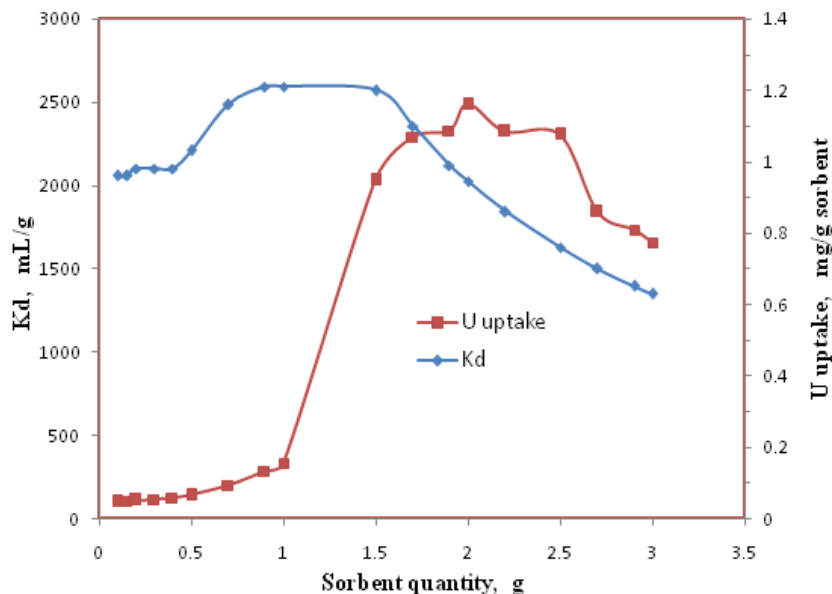


Figure 4.2: Variation of K_d and uranium uptake vs. Sorbent dosage (synthetic solution U: 9.37 mg/L, V: 50 mL, pH: 9, t: 240 min, T: 301K)

The result shows that the sorption efficiency is strongly dependent on the PHOA dosage. Initially Q_e of U(VI) is increased with increasing sorbent amount up to 0.4 g and thereafter, the uptake is reduced. This may be due to non-availability of uranium in the solution for sorption. Sorption capacity of about 1.2 mg of uranium / g of PHOA was found for all the dosage variation cases up to 0.4 g sorbent. PHOA could remove about 97% of the total uranium present in the solution with increase of sorbent dosage. Value of K_d was increased up to 0.5 g sorbent dosage due to further removal of uranium from the solution and thereafter, it was decreased as availability of uranium reduced with respect to sorbent amount available. Therefore, the optimum PHOA sorbent dosage was selected as 0.5 g sorbent for the prevailed condition under study.

4.4.4 Effect of solution pH on uranium uptake

Uranium sorption on a specific sorbent is strongly dependent on pH of sorption medium [230,231]. Change in pH influences the ionization of surface functional group which in turn affects the sorption process. The sorption of U(VI) on the investigated sorbent as a function of pH has been shown in **Figure 4.3**, a) with synthetic solution and b) with plant effluent.

Similar trend was noticed in both the figures. There was very low uptake up to pH 6 and then U(VI) uptake was increased with increasing pH of the reaction medium. Higher uptake was observed at pH 9 and more. The maximum sorption of PHOA sorbent was found to be 97.5% at > pH 9.

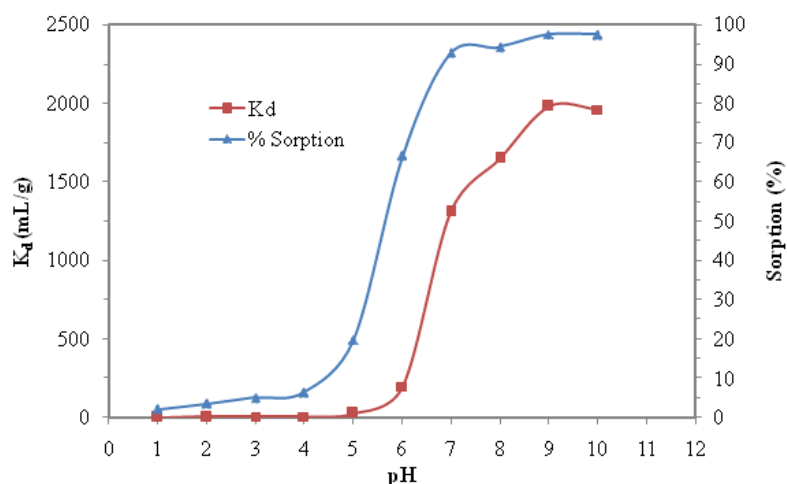


Figure 4.3 a): Effect of pH on K_d of U(VI) ions on the PHOA beads (U: 8.87 mg/L, m:0.5 g, V: 50 mL, t: 24 h, T: 301K)

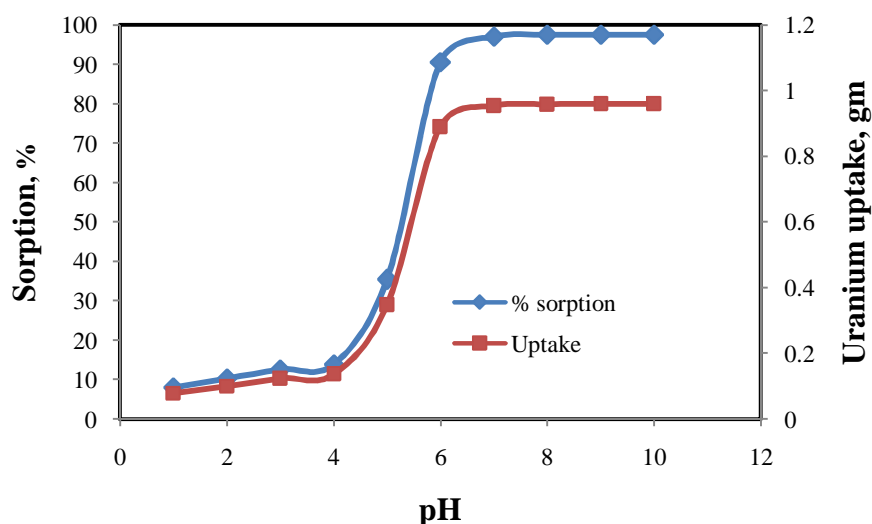


Figure 4.3 b): Effect of pH on K_d of U(VI) ions on the PHOA beads (plant effluent, m:0.5 g, V: 50 mL, t: 24 h, T: 301K)

Lower sorption value below pH 6 is attributed to the increased extend of protonation of hydroxamic acid group at lower pH value. In alkaline pH, at >pH 7, various oligomeric and monomeric hydrolysed species of UO_2^{2+} has been reported namely $[UO_2OH]^+$, $[(UO_2)_3(OH)_4]^{2+}$, $[(UO_2)_2OH]^{3+}$, $[(UO_2)_2(OH)_2]^{2+}$, $[(UO_2)_3(OH)_5]^+$ etc. Under standard

environmental conditions, uranium typically occurs in natural aquatic systems as a mobile hexa-valent uranyl ion (UO_2^{2+}) [232]. It is reasonable to accept that chemical species of uranium in alkaline aqueous medium is UO_2^{2+} as prominent species even in nitrate medium [230]. Different coordination of UO_2^{2+} ion has been reported ranging from four to six donor atoms depending on interaction medium and nature of ligand associated [233,234]. The stable complex of uranyl cation with functional groups and water molecules in aqueous medium leading to a coordination number of 8 for central uranium atom has been reported by molecular modelling studies. The mechanism of interaction between hydroxamic active sites and positively charged species of uranyl ion is of coordination type and an envisaged schematic representation of hexa-coordinated uranyl complex has been shown in **Figure 4.4**.

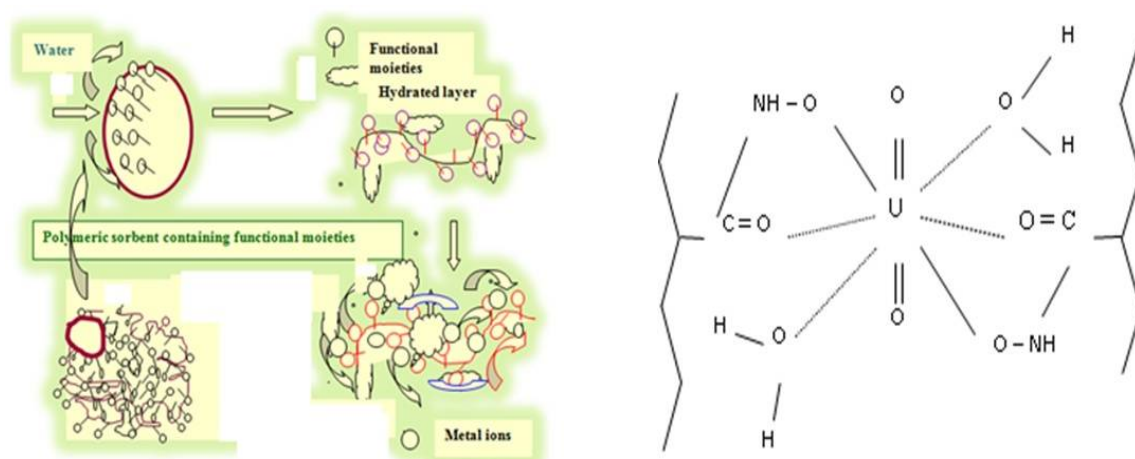


Figure 4.4: Probable (envisaged) structure of hydrated complex: $[\text{UO}_2(\text{R})_2(\text{H}_2\text{O})_2]$

Among the different mechanisms for metal ion binding in sorption process such as ion-exchange, complexation, electrostatic attraction etc. the electrostatic attraction was considered as the main mechanism responsible for metal sequestering. Sorption tendency of hydrolysed species of uranyl ions is better than the free hydrated ions because they could replace easily the protons of binding sites in the sorbent. The observed increased sorption of UO_2^{2+} at alkaline pH can be explained on the basis of these species for their sorption affinities. As seen in **Fig. 4.3**, the sorption of uranium was increased from 19.8% to 97.5%

with an increase of pH of the solution from 5 to 9 and then sorption was remained almost constant. The uranium uptake was reached a maximum at $\text{pH} \geq 9$ and therefore, $\text{pH} \geq 9$ was selected for further experiments. The result obtained confirms the functional ability of the sorbent as designed to perform in alkaline medium for removing uranium from wastewater.

4.4.5 Effect of agitation on uranium uptake

Sorption is a multistep process where external film diffusion plays an important role and this may affect the mass transfer of U(VI) from aqueous phase to the sorbent surface. Boundary layer effect, which is controlled providing mechanical agitation of the reaction mixture, may affect the external mass transfer of sorbate in the sorption operation. The uptake study was carried out for understanding the effect of mechanical agitation of sorbent-solution mixture. The mixture was agitated in different stirrer speed ranging from 50 to 300 rpm. The sorption profile has been shown in **Figure 4.5**.

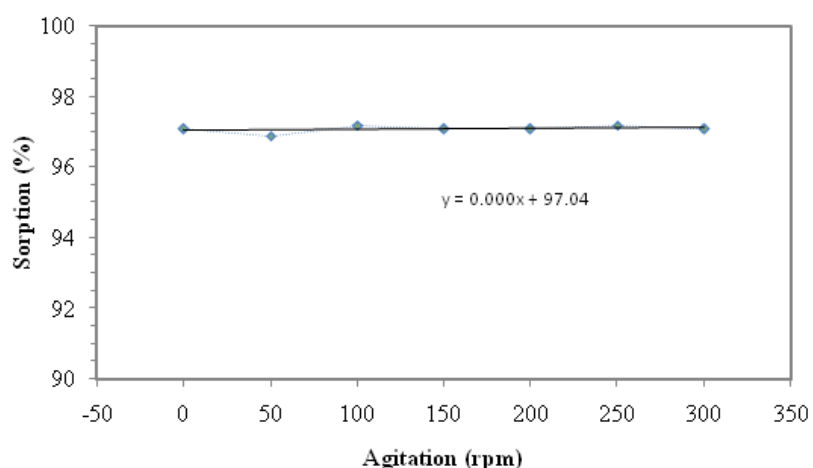


Figure 4.5: Effect of agitation of solution-sorbent mixture on sorption of uranium on PHOA sorbent beads (U: 8.87 mg/L, m: 0.5 g, V: 50 mL, pH: 9, T: 301K)

For all the experiments, sorption was about 97% and mass transfer of U(VI) from solution to sorbent was not influenced by the mechanical agitation. The result shows that uranium uptake of the sorbent was unaffected by the mechanical agitation of the sorbent-solution mixture. This indicates that transport of U(VI) molecules from the aqueous phase to the surface of solid PHOA sorbent is unaffected / not influenced by boundary layer effect and overall

sorption rate controlling process may be either intra-sorbent diffusion or sorption reaction inside the sorbent. Based on the result, further uptake experiments were conducted without agitation/shaking.

4.4.6 Uranium sorption in presence of competitive ions (cations and anion)

4.4.6.1 Combined effect of competitive ions on sorption of uranium

A typical ion composition of an effluent from uranium refining plant of India as shown in **Table 2.1** in previous Chapter was encountered for study. Industrial application of a sorption process must deal with the fact that waste streams often contain other ions along with uranium metal ion which may interfere with the uranium uptake in sorbent. Synthetic solution containing different concentrations of multiple ions such as U(VI), Mg(II), Ca(II), Cu(II), Fe(III), Mn(II) and nitrate ions was prepared for this purpose. The experiment was conducted to evaluate the effect of all associated ions on the sorption of uranium by PHOA beads. A mixed ionic solution: concentration of U(VI) was 9.37 mg/L, while the concentration of the other ions were Mg²⁺: 5.86 g/L, Ca²⁺: 600 mg/L, Mn²⁺: 5.5 mg/L, Fe³⁺: 5.6 mg/L Cu²⁺: 6.4 mg/L, NO₃⁻: 87 g/L was taken for the experiment. The experiment was carried out in duplicate and the mean value was noted. **Figure 4.6** shows comparative result of uranium sorption on the PHOA beads in presence of referred metal ions and nitrate anion. It is evident that the uranium uptake by the sorbent was affected by the metal ions as mentioned. Sorption of uranium was recorded as 87%, whereas of iron and copper ions was about 100% and of manganese ion was about 91%. Uptake of magnesium, calcium and nitrate ions was very less compared to the others. As a result, it can be stated that uptake of uranium in PHOA sorbent is strongly affected by Fe(III), Cu(II) and Mn(II) ions. However, the uptake of uranium was adequately good in presence of those competitive ions. Effect of the presence of calcium, magnesium and nitrate ions on the uranium sorption was found to be insignificant though these were present in much higher concentration (g/L).

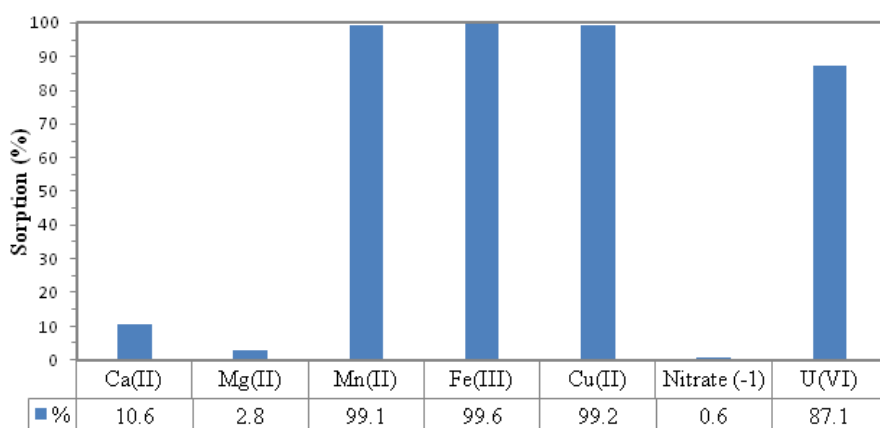


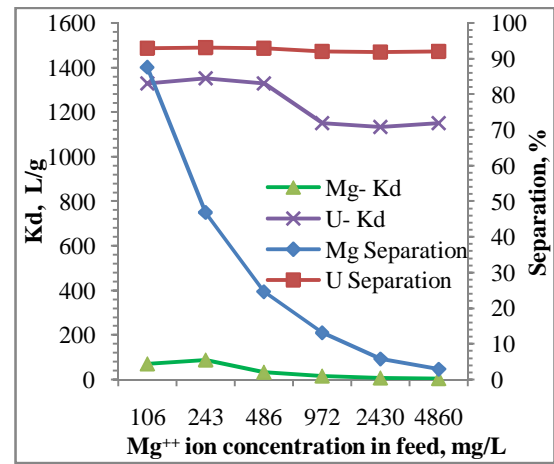
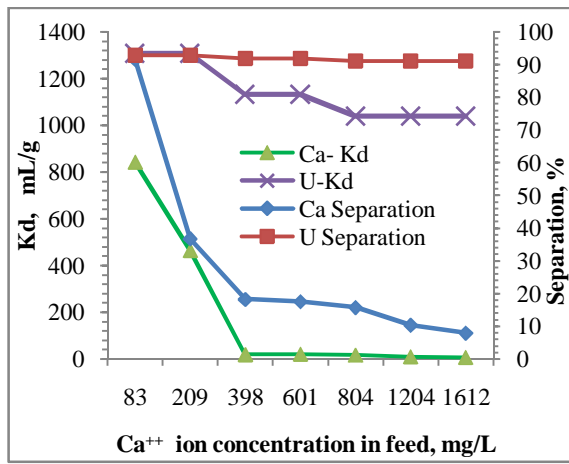
Figure 4.6: Combine effect of competitive ions on uranium sorption on the PHOA (U: 9.37 mg/L, Mg^{+2} : 4.86 g/L, Ca^{+2} : 600 mg/L, Mn^{+2} : 5.5 mg/L, Fe^{+3} : 5.6 mg/L Cu^{+2} : 6.4 mg/L, NO_3^- : 87 g/L, pH: 9, m: 0.5 g, V: 50 mL, t: 240 min, T: 301K)

4.4.6.2 Effect of individual Ca^{2+} , Mg^{2+} , Mn^{2+} , Cu^{2+} , Fe^{3+} and NO_3^- ion on sorption of uranium

To understand the effect of individual competitive ion on the uranium sorption to PHOA separate studies were conducted. A wide range and higher concentration of individual ions was used to evaluate the possible worst effect of the ions on uranium sorption. For sorption studies synthetic solution of pH ~9 containing Ca^{2+} (7 samples: 83, 209, 398, 601, 804, 1204, 1612 mg/L); Mg^{2+} (6 samples: 106, 243, 486, 972, 2430, 4860 mg/L); Mn^{2+} (6 samples: 2.8, 5.5, 11, 16.5, 22, 27.5 mg/L); Cu^{2+} (6 samples: 3.2, 6.4, 12.7, 19.1, 25.4, 31.8 mg/L); Fe^{3+} (5 samples: 5.6, 11.2, 22.4, 44.8, 56 mg/L); NO_3^- (7 samples: 50 g/L, 62 g/L, 74 g/L, 87g/L, 99 g/L, 112 g/L, 124 g/L) and U(VI) (9.6 mg/L in all individual solution) were equilibrated separately (with respect to individual ion and individual concentration) with dry sorbent. The K_d values of respective metal ions at different feed concentrations were calculated and plotted (**Figure 4.7 a) to f)** with respect to concentration of individual ion (signifying better distribution of uranium throughout the matrix in details).

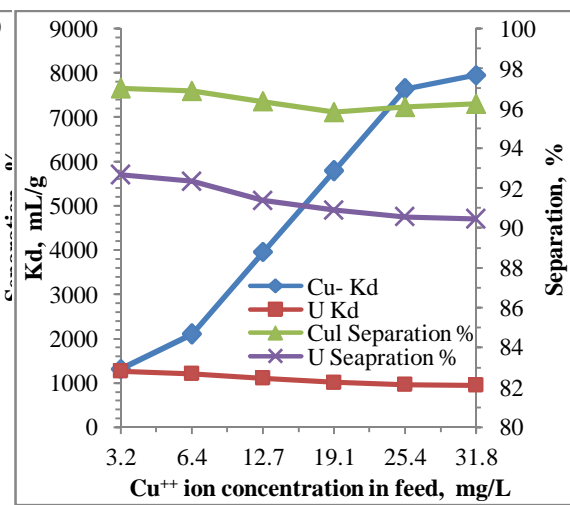
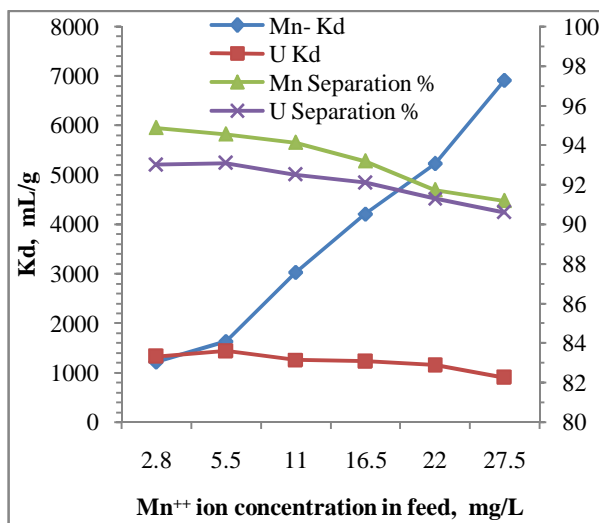
As Ca^{2+} and Mg^{2+} present in solution is in much higher concentration compared to other multivalent elements, it was wise to study the effect of Ca^{2+} and Mg^{2+} on uranium sorption. Although initial K_d values of uranium (1300 mL/g to 1350 mL/g) are significantly high

compared to Ca^{2+} and Mg^{2+} but it is decreased with both the ion concentrations and it becomes constant at about 800-900 mg/L metal ion concentration (**Figure 4.7 a) & b)**). It was observed that the K_d values of Mg^{2+} is very low at low concentration of Mg^{2+} and it decreases with increasing Mg^{2+} concentration. However, there is very little effect of Mg^{2+} concentration on U(VI) separation. But K_d value of calcium ion at lower concentration is significant and it decreases sharply as calcium ion concentration increases. This may be indicating that a certain quantity of calcium ion co-extracted along with the uranium and saturated. This implies that calcium ion is more detrimental than magnesium ion in the influent for uranium sorption. When distribution co-efficient of Mn^{2+} , Cu^{2+} and Fe^{3+} plotted with their concentration, a reverse trend was found compared to Ca^{2+} and Mg^{2+} , where distribution coefficient of Mn^{2+} , Cu^{2+} and Fe^{3+} are several (5 to 28) times higher than that of uranium indicates that the sorbent is extremely aggressive for Mn^{2+} , Cu^{2+} and Fe^{3+} (**Figure 4.7 c), d) & e)**) but at lower concentration of each ion the uranium sorption is reasonably acceptable. When separation was compared, Mn^{2+} showed ~94% with respect to U(VI) ~93%, Cu^{2+} showed ~97% with respect to U(VI) ~92% and Fe^{3+} showed ~98% with respect to U(VI) ~89% at lower concentrations of the metal ions. The plant effluent contains large amount of NO_3^- anions (70-90 g/L) as impurities which may influence the sorption of uranium and may affect the matrix. To study the effect of anions on uranium sorption onto sorbent a high concentration range of 50 g/L-124 g/L NO_3^- was considered. The separation of uranium was not significantly affected by NO_3^- with respect to the sorbent and when distribution ratio plotted with respect to various feed concentration uranium of 1200 mL/g K_d , almost 90% separation was achieved (**Figure 4.7 f)**). The results indicate that uranium sorption in sorbent is not affected by presence of NO_3^- ions in the effluent.



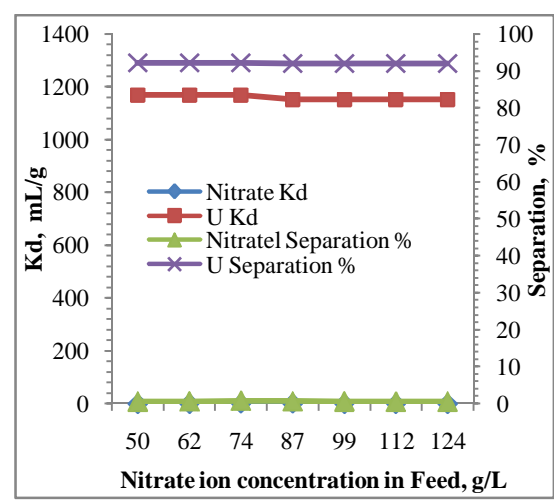
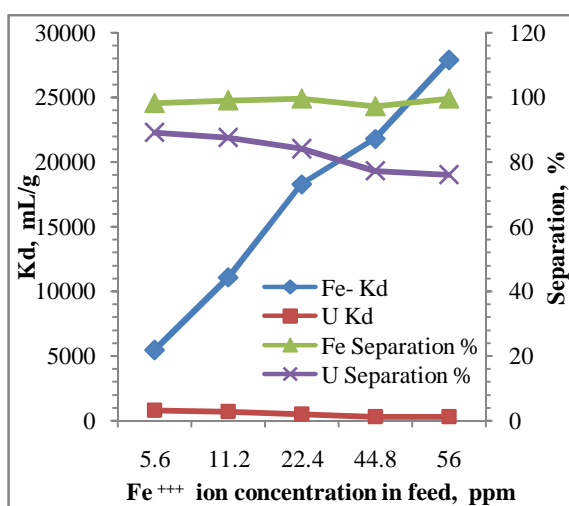
a)

b)



c)

d)



e)

f)

Figure 4.7: Effect of individual competitive ion on uranium sorption in PHOA

4.4.7 Sorption isotherm

4.4.7.1 Langmuir isotherm

The equilibrium data for U(VI) over the concentration range from 2.82 to 25.11 mg/L with 0.5g PHOA for 24h at 301K has been correlated and uptake and distribution coefficient values are shown in **Figure 4.8 a) & b)** respectively and with the Langmuir isotherm (Equation 4.6) are shown in **Figure 4.9**.

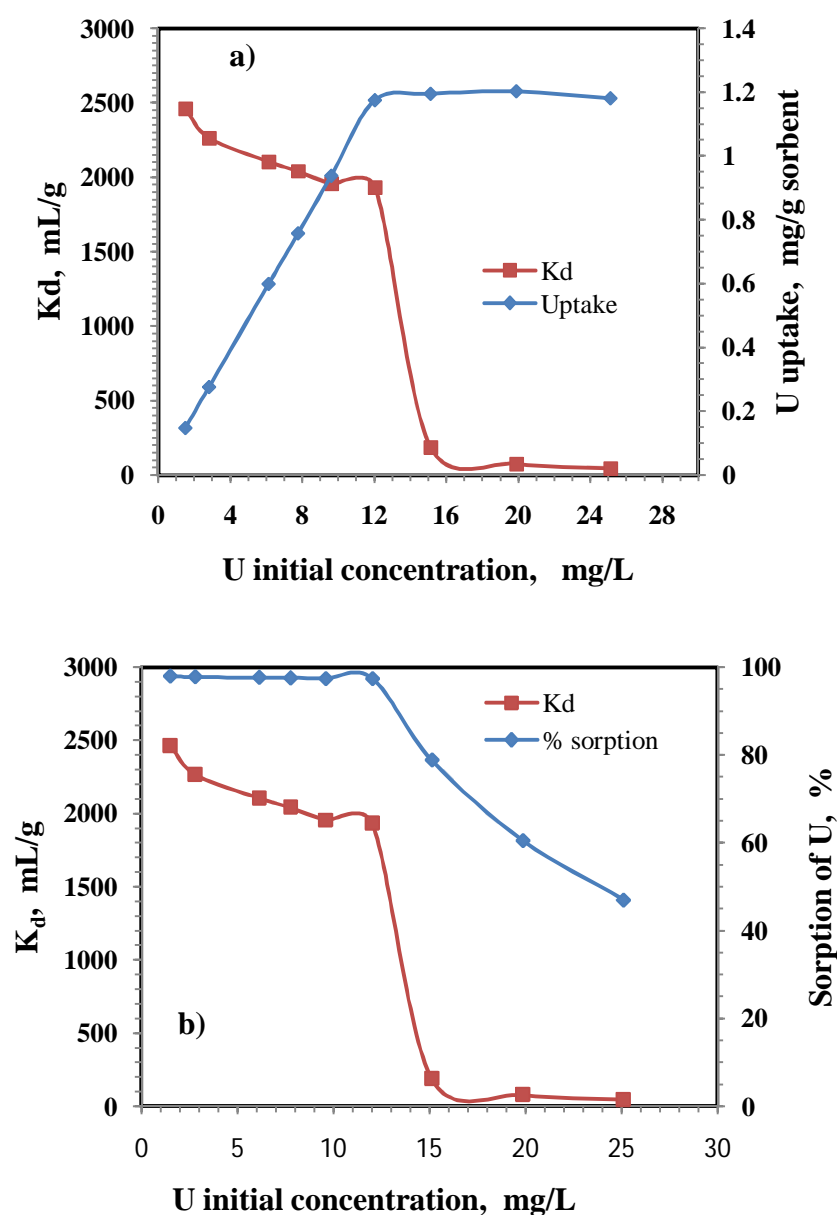


Figure 4.8: Variation in K_d , uptake and % sorption on PHOA beads as a function of initial uranium concentration (m: 0.5 g, V: 50 mL, pH: 9, t: 24 h, T: 301K)

A linear plot is obtained when $1/Q_e$ is plotted against C_e over the entire concentration range of metal ions investigated. The Langmuir model parameters and the statistical fits of the sorption data to this equation are given in **Table 4.2**. The Langmuir model effectively described the sorption data with R^2 values > 0.99 (**Table 1**) with lower uranium concentrations.

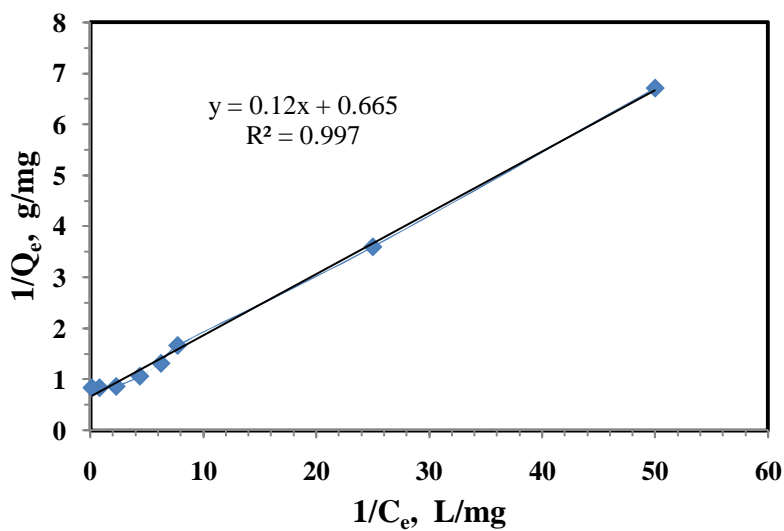


Figure 4.9: Langmuir sorption isotherm of uranium ion on PHOA beads

As seen from the figure, uranium uptake was increased with increasing uranium initial concentration. This may be due the increased availability of uranium ions for sorption to reach the equilibrium values. Nature of uptake profile confirms that the sorption process was favourable. The adsorption isotherms of UO_2^{2+} exhibit Langmuir behaviour, which indicates a monolayer adsorption. The maximum monomolecular capacity is found to be 1.504 mg/g for U(VI) at 301K and maximum distribution constant about 2500 mL/g was achieved. Distribution constant profile also indicates that the sorption is more efficient in diluted uranium solution. At higher uranium concentration uptake by the PHOA is found constant in **Figure 4.8 a)** because of non availability of sorption site (maximum sorption achieved) in PHOA as the quantity of PHOA was fixed and uptake is defined per g basis. Figure 4.8 b) shows that distribution coefficient decreases with increasing initial uranium concentration

after achieving maximum sorption due to increase of uranium concentration in filtrate (ref, **Equation (4.3 b)**) which is as expected.

The values of R_L are calculated (**Equation 4.7**) for different initial concentration which is found to be between 0.01 and 0.1 indicating suitability of the sorbent for U(VI) sorption in the alkaline aqueous solution i.e. the sorption process with PHOA is favourable with respect to the wastewater. It also indicates that U(VI) sorbed on PHOA as a monolayer sorption.

4.4.7.2 Freundlich isotherm

From the slope and intercept of straight portion of the plot using **Equation 4.9** the values of Freundlich parameters were calculated and results are represented in **Figure 4.10**. It is found that though the sorption data did not follow this isotherm but it was also somewhat obeyed the Freundlich isotherm ($R^2=0.893$). The parameters of the equation are shown in **Table 4.2**. Value $1/n$ is usually dependent on the nature and strength of the sorption as well as the distribution of active sites. The Freundlich sorption isotherm gives an expression encompassing the surface heterogeneity and the exponential distribution of active sites and their energies.

Table 4.2: Isotherm parameters of sorption of uranium ion on PHOA sorbent beads

Langmuir parameters			Freundlich parameters		
Q_m (mg/g)	b (L/mg)	R^2	K_F (mg/g)	$1/n$	R^2
1.504	5.542	0.997	1.592	0.532	0.893

This isotherm does not predict any saturation of the sorbent by the sorbate thus infinite surface coverage is predicted mathematically, indicating a multilayer sorption of the surface. The magnitude of the $1/n$ gives an indication of favourability of the sorbate system. As shown in **Table 4.2**, the $1/n$ is 0.532 at 301K indicating that U(VI) could be easily sorbed on

the PHOA sorbent but, indication is clear that U(VI) sorbed on PHOA predominantly as a monolayer sorption.

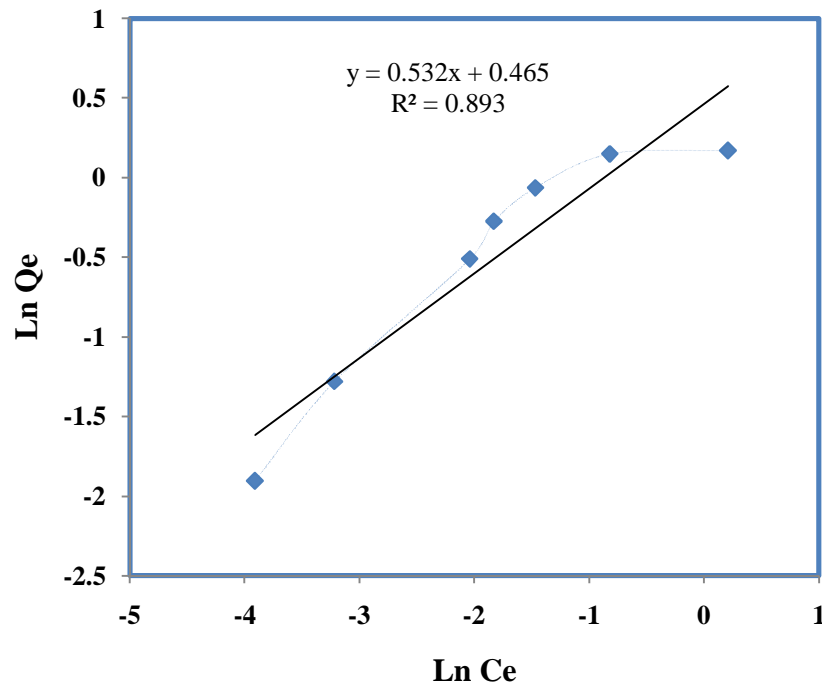


Figure 4.10: Freundlich sorption isotherm of uranium ion on PHOA beads

4.4.7.3 Other isotherms

The linear plots of q_e versus $\log C_e$ enable to determine the constant K_T and b_T from Temkin isotherm model (**Equation 4.10**). The values obtained for K_T and b_T from the plot **Figure 4.11** are 1.003 Lmg^{-1} and 5.829 KJg^{-1} .

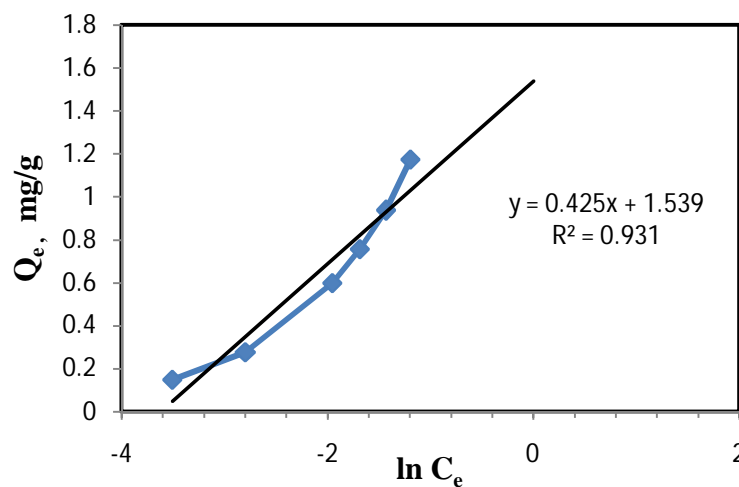


Figure 4.11: Temkin sorption isotherm of uranium ion on PHOA beads

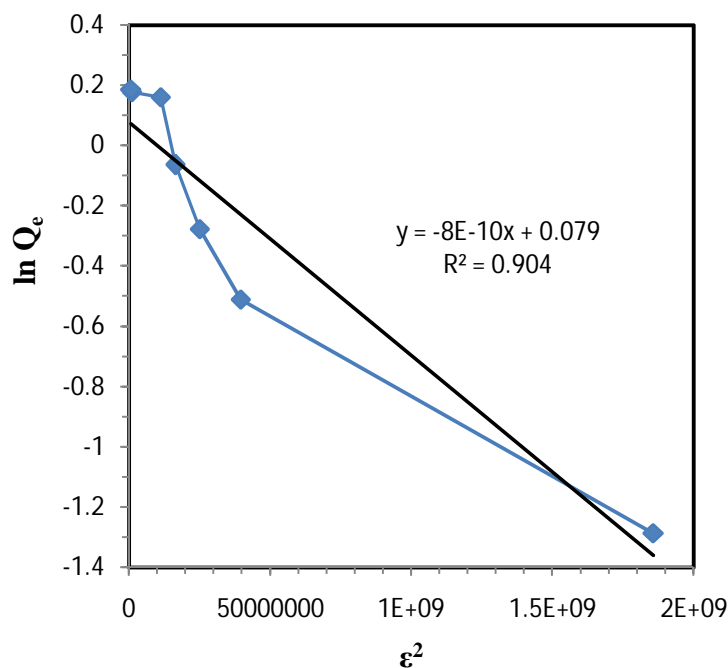


Figure 4.12: Dubinin–Radushkevich sorption isotherm of uranium ion on PHOA beads

The plot of $\ln Q_e$ versus ϵ^2 from Dubinin–Radushkevich (D-R) isotherm model (**Equation 4.11**) gives the values of K and Q_{\max} as 8×10^{-10} and 5.77 mg/g respectively from **Figure 4.12**. E has been calculated by using **Equation 4.13** and found it is 25 kJ/g (<8 kJ/mol). The positive value of E indicates that the adsorption process is the endothermic and hence, it is expected that a higher solution temperature would favour the sorption process. Lesser E value indicates that physical mode of sorption may be the prominent pathway for the sorption process. It is essential to establish the inference thermodynamically evaluating activation energy.

4.4.8 Sorption kinetic study

4.4.8.1 Sorption mechanism analysis and kinetic

The sorption reaction between PHOA and U(VI) was investigated under pH value, the PHOA quantity and the U(VI) concentration of 9.0, 0.5g and 9.11 mg/L respectively for the sorption time of 10 min to 300 min. The results are shown in **Figure 4.13** for monolayer sorption and

Figure 4.14 for multilayer sorption. As shown in **Figure 4.13**, the linearity of plot of $-\ln(1 - F)$ versus t (using **Equation 4.15**) follows the monolayer hypothesis.

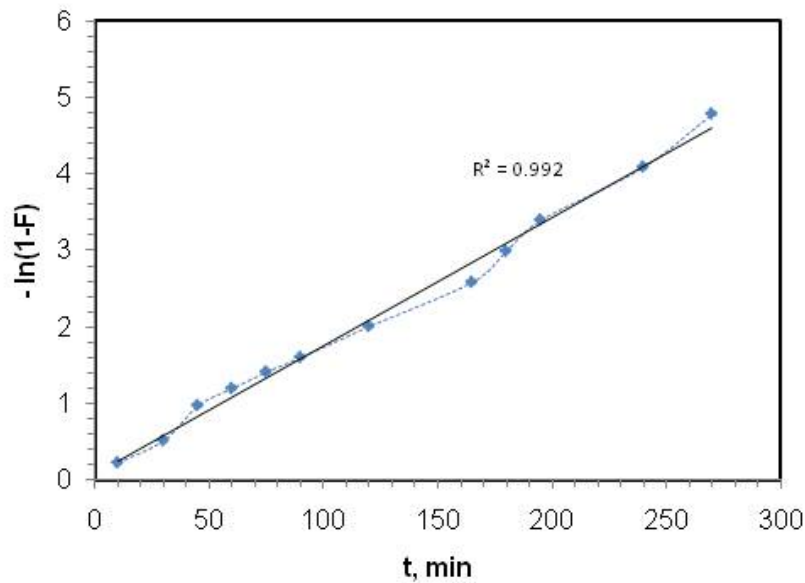


Figure 4.13: Plot for prediction of monolayer sorption of U(VI) with respect to contact time (PHOA:0.5g, U(VI):9.11 mg/L, pH:9, Temperature: 301K).

Figure 4.14 shows that the multilayer molecule sorption mechanism is unacceptable because of the non-linearity of plots of $-\ln(1 - F)$ versus $\ln t$ (**Equation 4.17**). Hence, the sorption mechanism of U(VI) onto PHOA is demonstrated to be mainly the monolayer molecule sorption procedure. It also reflects that chemical process is also in the sorption process and for the chelating reaction between U(VI) and PHOA chemical sorption may be the pathway.

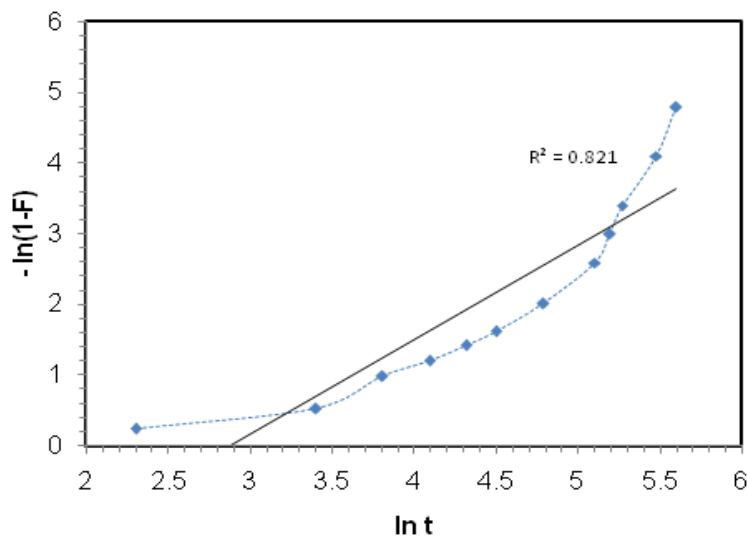


Figure 4.14: Plot for prediction of multilayer sorption of U(VI) with respect to contact time (PHOA:0.5g, U(VI):9.11 mg/L, pH:9, Temperature: 301K).

According to **Equation 4.22**, the influence of the U(VI) concentration on the sorption reaction was studied at the constant pH value of 9 and the PHOA concentration of 9.11 g/L. The linearity of a graph of $\ln K_d$ versus $\ln[U(VI)]_{(aq)}$ is shown in **Figure 4.15**.

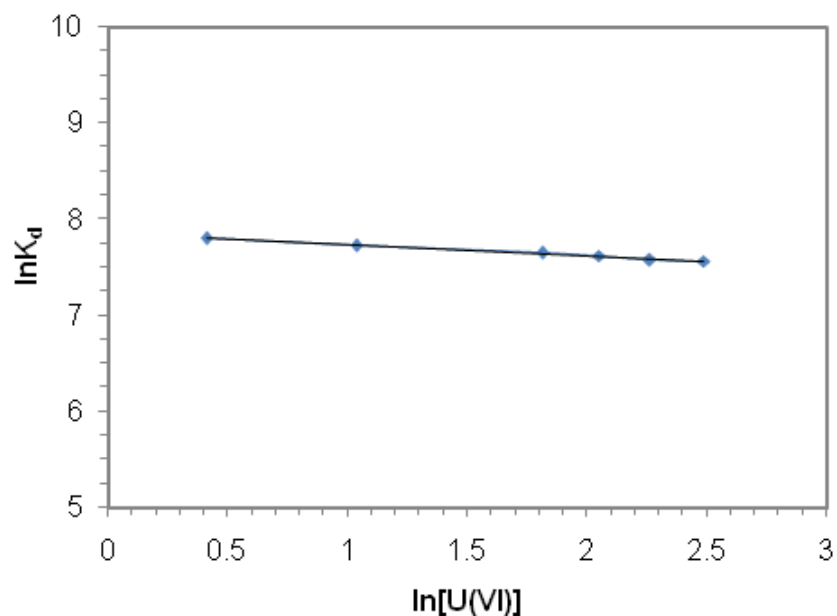


Figure 4.15: Effect of U(VI) concentration on the sorption of PHOA at pH value 9, the PHOA concentration of 9.11 g/L, residence time 24h and temperature 301K.

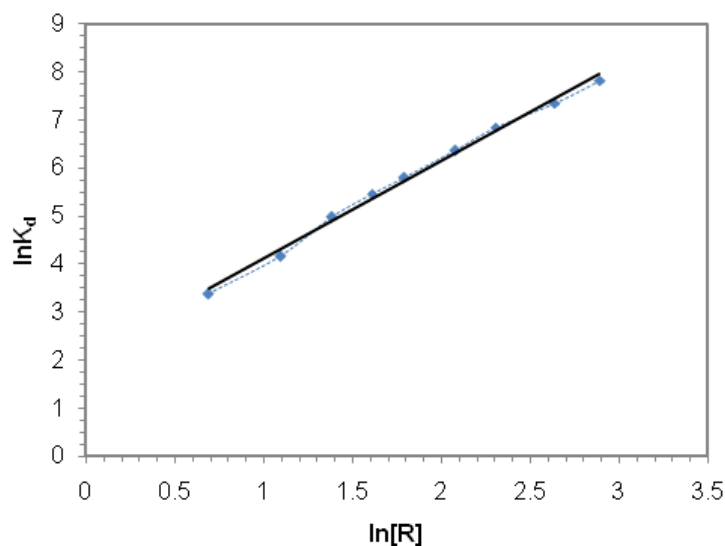


Figure 4.16: Effect of PHOA concentration on the adsorption of U(VI) at U(VI) concentration of 9.11 mg/L, pH value of 9, residence time 24h and temperature 301K.

The slope of the resultant straight line is -0.1 with a correlation coefficient of 0.994, i.e., n is approximately 1. The figure shows that the formation of U(VI) and PHOA is the

mononuclear complex. Similarly, the influence of the PHOA concentration (quantity/volume) on the adsorption reaction was examined at the fixed U(VI) concentration of 9.11 mg/L and pH value of 9. The result is shown in **Figure 4.16**. The slope of resulting straight line is 2.04 with a correlation coefficient of 0.994, i.e., $m = 2$. It indicates that 1 mole $\text{UO}_2(\text{OH})^+$ ion is attached with 2 mole PHOA and it forms 1:2 type of complex.

To evaluate the behavior of H^+ , the effect of H^+ concentration from pH 1.0 to pH 10 on the sorption reaction was investigated at the fixed PHOA concentration of 10 g/L, and U(VI) concentration of 9.11 mg/L. The results are illustrated in **Figure 4.17**. At pH 1.0, experiment found that U(VI) was not adsorbed traceably by PHOA sorbent. When pH exceeds this value, the sorption of U(VI) onto the sorbent increases with increasing pH value from pH 2.0 to pH 10. Such a change shows that increasing pH value of the aqueous phase is beneficial to the sorption of PHOA for U(VI). However, in this wide pH value region increase of $\ln K_d$ follows two different slopes. The adsorption of U(VI) on PHOA increases sharply at the pH range of 2.0-7.0. The resultant slope of the straight line is 1.05 with correlation coefficient of >0.99 , hence, $m - n = 1$ approximately.

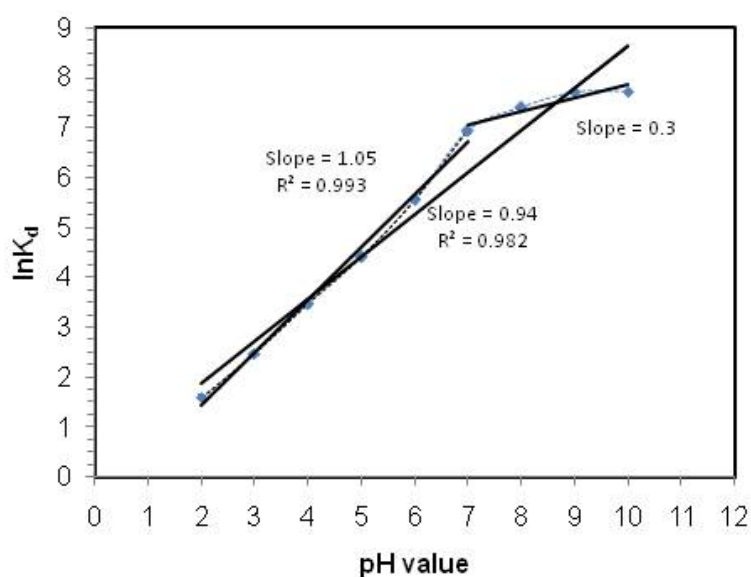


Figure 4.17: Effect of pH on the sorption of U(VI) (PHOA:10 g/L, U(VI):9.11 mg/L, Temperature: 301K, Residence time: 24h).

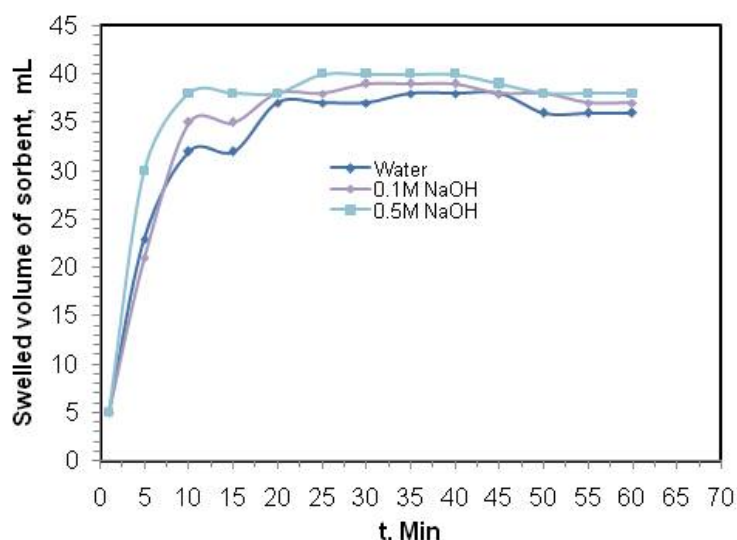
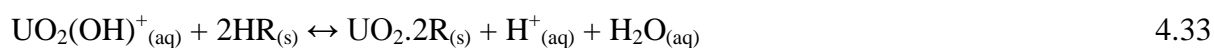


Figure 4.18: Swelling effect of PHOA in NaOH solution at temperature 301K.

This slope indicates that 1 mol H^+ ion is released out in the sorption reaction of 1 mol U(VI) with 2 mol PHOA sorbent. In the range of pH 7.0 to 10, the increase of $\ln K_d$ is slower than that in pH 2.0-7.0 and the slope of the resultant straight line is 0.3. This shows that at higher pH value the sorption is less pH dependent. But in excess of pH 7.0, the adsorption of U(VI) on PHOA evidently increases with an increase in pH value. The result was analyzed correlating with swelling test of the sorbent in alkaline medium, namely NaOH solution in different concentration. The swelling test result (**Figure 4.18**) shows that swelling of sorbent increases with increase in concentration of NaOH. This may be because of opening up of sorbent surface due to repulsive forces of negatively charged sorbent surface after losing H^+ in alkaline medium. Hence, there is a increase of U(VI) sorption in the newly generated surface of the sorbent with increase of pH.

Therefore, the sorption process of U(VI) onto PHOA sorbent in neutral to alkaline solution especially in $pH \geq 7.0$ can be expressed as shown as



This shows that the adsorption mechanism of PHOA for U(VI) belongs to the neutral complex phenomena. The apparent equilibrium constant is calculated to be $K_a = 1.21 \times 10^{-2} g^{-1}$.

Sorption kinetic of synthetic uranium (only) solution and plant effluent was evaluated for comparison study and also to understand any effect of the presence of competitive ions on uranium sorption kinetics onto PHOA sorbent. The sorption kinetics is shown in **Figure 4.19**

a) for synthetic solution and b) for the plant effluent.

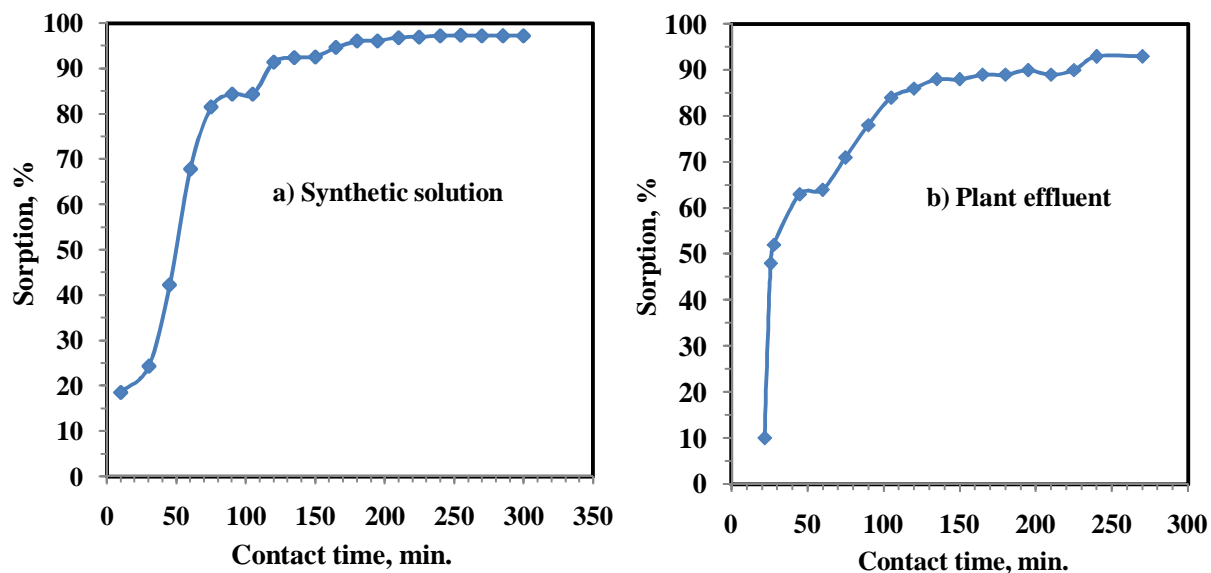


Figure 4.19: Kinetics of uranium sorption onto PHOA (PHOA: 0.5g, synthetic U(VI): 9.11 mg/L, T: 301K, pH: ~9).

For both the cases the sorption pattern is similar and it is reached to almost its maximum level within 4 h and thereafter changes are not appreciable. Comparing the figures it is found that the equilibrium time was not affected by the presence of competitive ions (plant effluent). But for synthetic uranium solution possible sorption is about 98% and for the plant solution it is about 93% due to presence of competitive ions in the effluent. Based on the observation 4h equilibrium time has been considered for further experiments.

4.4.8.2 Pseudo first order kinetic

The kinetic parameters using pseudo-first order model (**Equation 4.25**) are determined from the linear plots of $(1/q_t)$ vs. $1/t$. **Figure 4.20** shows the plot of the pseudo-first order model from where first order rate constant and other parameters are calculated and listed in **Table 4.3**.

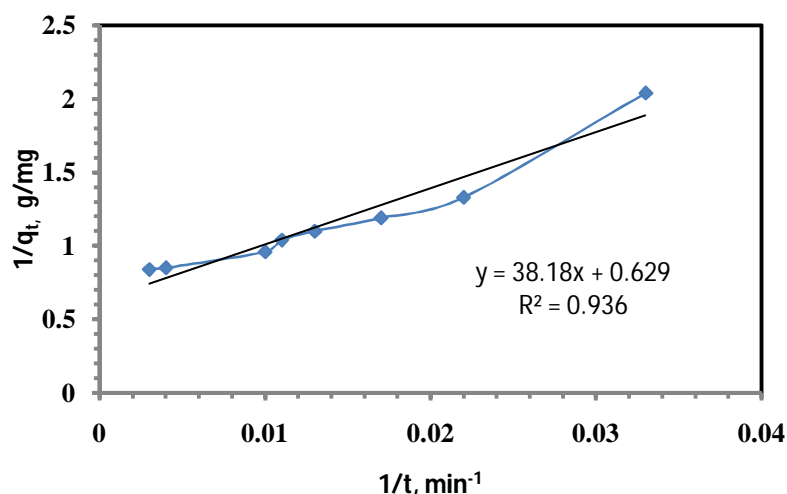


Figure 4.20: Pseudo-first order plot for sorption of U(VI) (PHOA:0.5g, U(VI):9.11 mg/L, pH:9, Temperature: 301K).

Table 4.3: Kinetic parameters for U(VI) sorption into PHOA at 301 K

q_e (mg/g)	The pseudo-first order			The pseudo-second order		
	K_1 ($h^{-1} \text{ min}^{-1}$)	q_{e1} (mg g^{-1})	R_1^2	K_2 ($\text{g mg}^{-1} \text{ min}^{-1}$)	q_{e2} ($\text{g mg}^{-1} \text{ min}^{-1}$)	R_2^2
1.19	57.41	1.53	0.942	0.017	1.36	0.999

As the plot is not straight line the uranium sorption onto the PHOA sorbent does not follow the pseudo first order kinetic reaction.

4.4.8.3 Pseudo-second order kinetic

The kinetic parameters for pseudo-second order models (**Equation 4.26**) are determined from the linear plots of (t/q_t) vs. t as shown **Figure 4.21** and listed in **Table 4.3**. The plot follows the straight line against the experimental results; hence follow the pseudo second order kinetic reaction.

The validity of each model could be checked by the fitness of the straight lines (R^2 values). The K_1 , K_2 , q_{e1} , q_{e2} and correlation coefficients R_1^2 and R_2^2 of U(VI) under different conditions were calculated from these plots, and are given in **Table 4.3**. Accordingly the sorption of U(VI) on the PHOA is more accurately fitted to pseudo-second order model ($R^2 = 0.999$) rather than pseudo-first order ($R^2 = 0.936$). In addition, the experimental and

theoretical values of q_{e2} (obtained from pseudo-second order model) are closer, confirming the validity of the pseudo-second order kinetic model to the sorption system under consideration. From these results, the sorption system obeys the pseudo-second order kinetic model. This implies that the sorption reaction rate mainly depends on two parameters or steps.

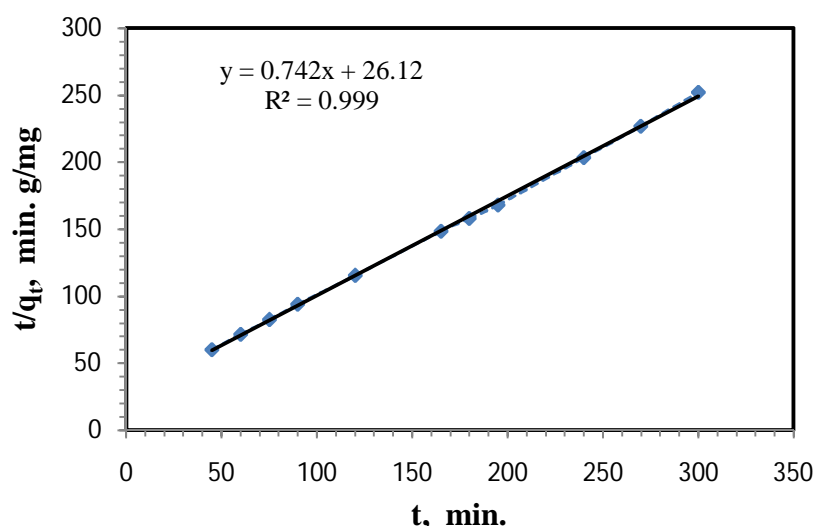


Figure 4.21: Pseudo-second order plot for sorption of U(VI) (PHOA:0.5g, U(VI):9.11 mg/L, pH:9, Temperature: 301K).

Sorption is a multi-step process involving transport of solute molecules from the aqueous phase to the surface of the solid sorbent, then diffusion of the solute molecules into the interior of pores of sorbent, and interaction between the solute molecules and active sites of sorbent for sorption process. The rate determining step of the sorption reaction may be one of above three steps. The external film diffusion can be eliminated by stirring solid-liquid mixture during sorption reaction. In the study, it was evidently noticed that the stirring does not have effect on the sorption operation. In support of the observation, the phenomena could be corroborated by the analysis of data from Boyd's model [235]. The model of Boyd is expressed as

$$F = 1 - \frac{6}{\pi^2} \exp(-B_t) \quad 4.34$$

Where B_t is a function of F. **Equation 4.34** can be rearranged to

$$B_t = -0.4977 - \ln(1 - F) \quad 4.35$$

The values of B_t were calculated using **Equation 4.35** and plotted against time t which is shown in **Figure 4.22**. The linearity of this plot can provide available information to distinguish intra-particle diffusion and boundary layer effect (film diffusion) rates of sorption.

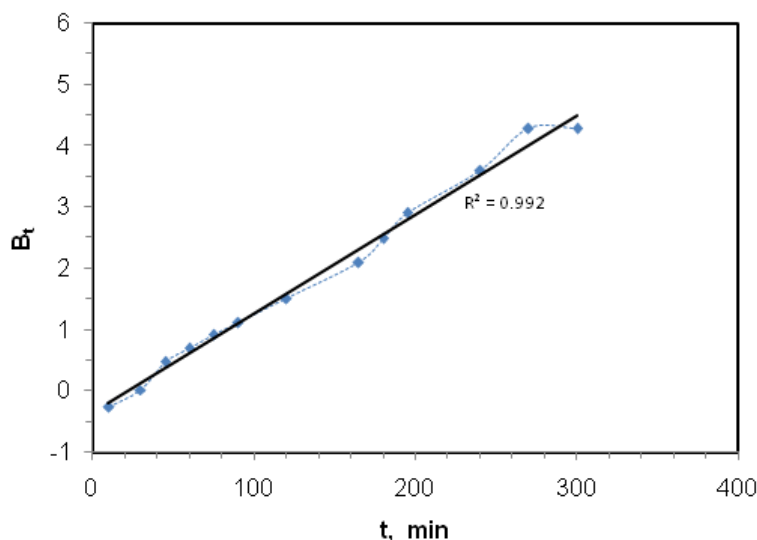


Figure 4.22: Boyd plot for U(VI) sorption onto PHOA (PHOA:0.5g, U(VI):9.11 mg/L, pH:9, Temperature: 301K).

If a plot of B_t versus t is a straight line passing through the origin, then adsorption will fit to boundary layer effect. The plot does not pass through the origin indicating that external mass transfer is not the rate limiting process. So, the sorption rate may be controlled by intra-particle diffusion or metal-ligands interaction step.

4.4.8.4 Intra-particle diffusion

According to the model q_t versus $t^{0.5}$ (**Equation 4.28**) should be linear if intra-particle diffusion is only rate determining operation involved in the sorption process. The overall correlation coefficient (R_p^2) for the intra-particle diffusion model was 0.876 (**Figure 4.23**), indicating that the intra-particle diffusion was not the only rate controlling step throughout the process, other mechanism could also control the rate of sorption. From the Figure, the plot of q_t against $t^{0.5}$ may present a multi-linearity correlation, which indicates that three steps occur during the diffusion process itself. In first step, the sorption process is controlled by

intra-particle diffusion of U(VI) onto the pores of the sorbent and unaffected by chemisorption as the fitted line is linear and it passes near through the origin with R^2 value 0.977.

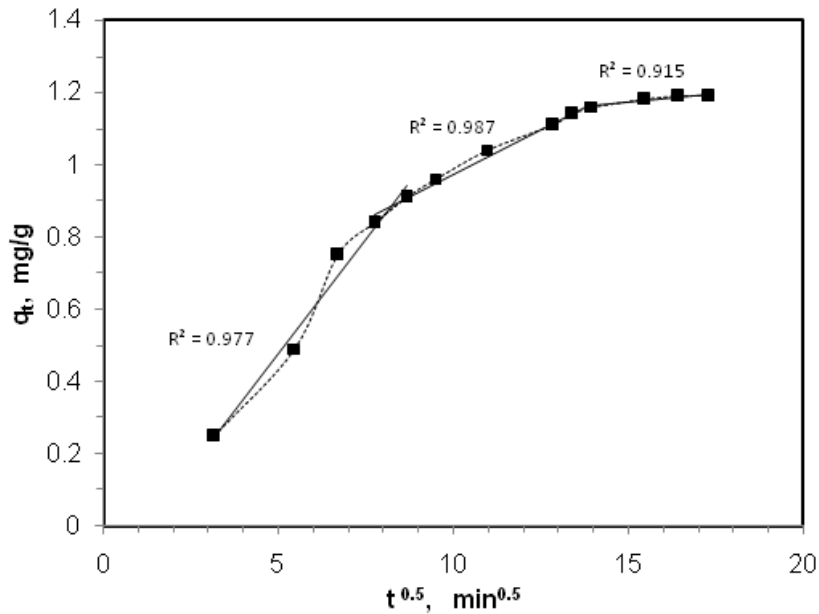


Figure 4.23: Intra-particle diffusion model plot for sorption of U(VI) (PHOA:0.5g, U(VI):9.03 mg/L, pH:9, Temperature: 301K).

In the second portion, the diffusion is minor affected (slow down) by the chemisorption at reactive site of PHOA. The third portion is the final equilibrium stage, where the intra-particle diffusion process is strongly affected by the chemisorption. In this stage, the uranium molecules were sorbed on the active sites of the internal pore surface of the sorbent. The intra-particle diffusion starts to slow down due to the solute concentration getting lower and lower in solution and also due to lesser availability (because of partial saturation) of sorbent active site. This implies that the rate determining step of the sorption reaction of the system under discussion depends on both, the textural properties as well as the total content of the PHOA active sites.

4.4.9 Uranium uptake with temperature variation

The thermodynamic parameters of the adsorption process were obtained from sorption experiments at various temperatures. The influence of temperature variation on the sorption

of U(VI) ions on PHOA beads from aqueous solution was examined using 0.5 g PHOA beads in 50 mL of 9.37 mg/L solution from 298 to 353 K at pH 9.1. The values of the thermodynamic parameters for the sorption of U(VI) on PHOA beads are given in **Table 4.4**. ΔH° and ΔS° were calculated from the slope and intercept of vant's Hoff plots on $\ln K_d$ versus $1/T$ (using **Equation 4.31**), as shown in **Figure 4.24**.

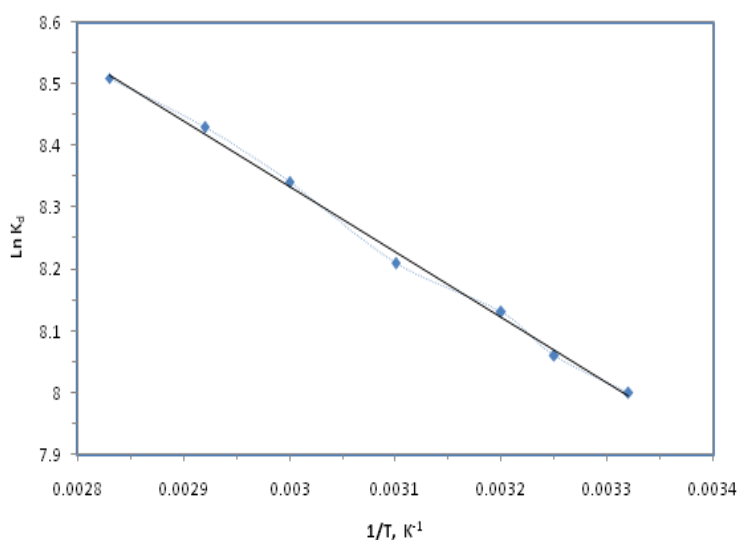


Figure 4.24: Influence of temperature on the thermodynamic properties of uranium sorption process on PHOA beads (U: 9.37 mg/L, m: 0.5 g, V: 50 mL, pH: 9.1, t: 240 min)

The ΔH° and ΔS° values were 8.85 KJ/mol and 0.096 KJ/mol respectively. The positive value of ΔH° suggested the endothermic nature of the sorption process. The positive value of enthalpy change (ΔH°) shows that the sorption of uranium (VI) ions was an endothermic in nature, which favours the sorption process at higher temperature. Further, the positive value of entropy indicates stability of sorption system [236,237]. The positive value of ΔS° suggested good affinity of U(VI) towards the PHOA and increased randomness at the solid-solution interface. The resultant effect of complex bonding and steric hindrance of the sorbed species in the system might be the reason for positive values of entropy and enthalpy. The numerical value of ΔG° decreased with increasing temperature as shown in **Table 4.4**, which indicates that the sorption process was spontaneous and more favourable at higher

temperatures. An attempt was taken to check whether the sorption process kinetic can follow pseudo second order at different temperature. From **Figure 4.25** it is evident that uranium sorption onto PHOA follows pseudo second order kinetic at three different temperatures namely 301K, 323K and 353K.

Table 4.4: Thermodynamic parameters of sorption of uranium ion on PHOA sorbent beads

ΔH^0 (KJ/mol)	ΔS^0 (KJ/mol. K)	ΔG^0 (KJ/mol)						
		301K	308K	313K	323K	333K	343K	353K
8.85	0.096	-19.98	-20.65	-21.13	-22.09	-22.05	-24.00	-24.96

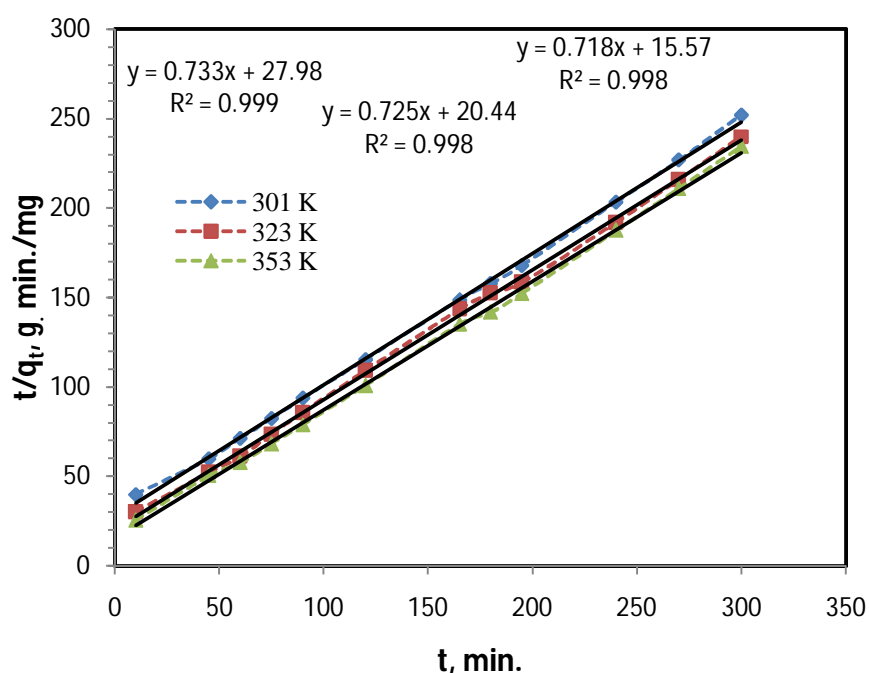


Figure 4.25: Influence of temperature on kinetic property of uranium sorption process on PHOA beads (U: 9.37 mg/L, m: 0.5 g, V: 50 mL, pH: 9.1, t: 240 min)

As shown in **Figure 4.26** the E_a , the activation energy for U(VI) sorption on PHOA is evaluated and found to be 9.137 KJ.mol⁻¹. From the E_a value it can be confirmed that the sorption process is associated with a physical sorption (8-40 KJ.mol⁻¹) mechanism [238], and there was a lower energy barrier in the sorption process, which was also inferred in kinetic studies in this Chapter.

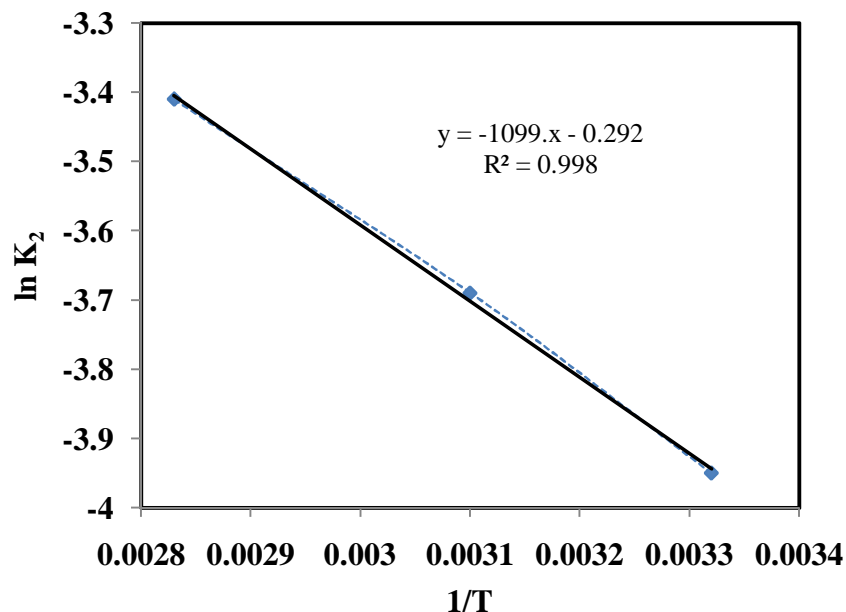


Figure 4.26: The Arrhenius plot for U(VI) sorption on PHOA.

4.4.10 Reusability of sorbent

The same sorbent beads were used for a number of cycle for U(VI) sorption after every desorption process to ensure reusability of the sorbent under the present experimental conditions. The sorption of U(VI) was carried out from the solution containing 9.37 mg/L U(VI) synthetic solution at pH 9.1. **Figure 4.27** has shown the plot of % U(VI) sorption vs. number of sorption cycle.

It was observed that the sorption is not 100 % efficient even in 1st cycle and for the 1st sorption cycle about 98 % sorption was observed. With increase in number of sorption cycle from 1-6 sorption efficiency has been decrease from 98 % to 95 %. The experimental data on recycle of sorbent for sorption for a number of times (up to 6 cycle) showed that the sorbent can be reused for U(VI) sorption from alkaline solution for several times.

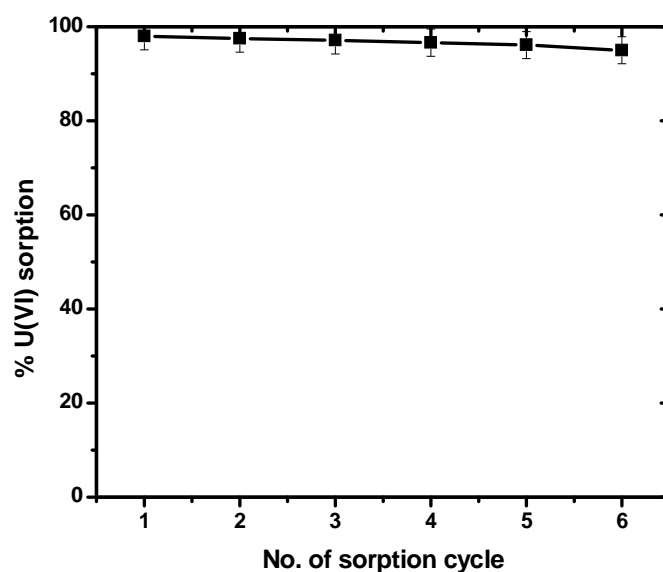


Figure 4.27: Stability of PHOA with respect to sorption of uranium

4.5 Conclusion

Uranium from the plant effluent in its condition can efficiently be removed / separated using the promising sorbent PHOA. The uranium separation was found to 93% from the plant effluent due to presence of competitive ions (mainly iron, copper and manganese) whereas from the pure synthetic solution was about 98%. Among the competitive ions iron was the most detrimental for and it affects the separation of uranium. The sorption process follows the Langmuir isotherm mainly and pseudo-second order kinetic and it is more favourable with increasing of temperature. External mass transfer does not affect the uranium sorption on to the PHOA and the process follows a physical sorption process indicating low mass transfer resistant process. The PHOA can be recycled / reused several times (six times at least) which is an essential condition for industrial application.

CHAPTER – 5

BATCH EXPERIMENT: ELUTION

5.1 Introduction

The principle of displacement of selectively binding ions by less selective binding ions is the basis for each regeneration process. Most ion sorbents can be regenerated by acids (excess of H^+ -ions), salt-brines (excess of sodium or chloride ions) or by alkali (excess of OH^- - ions). During regeneration the sorbed metal ions are removed and replaced by the ions named above. The regeneration process is called elution and the chemical used for the purpose is called eluent. The spent eluent solution contains the formerly sorbed metal ions /pollutants as it was in sorbed form. Generally the eluent solutions must be treated for recovery and disposal, or reuse. The treated wastewater solutions can be re-used in the production process where it was generated.

For effective elution, the stronger an ion binds on the sorbent, the more eluent solution must be typically be applied. Thus a sorbent /resin with high selectivity may have advantages regarding the efficiency of removal from the wastewater, but the elution efficiency must also be taken into account to judge the overall value of the process. Hence, sorption study can be complemented with desorption ones that recover the metal retained and reuse the sorbent in subsequent loading and unloading cycles.

The sorbent regeneration may be crucially important to keep low processing costs and open the possibility to recover the extracted metals from the liquid phase. The desorption process, elution give up metals in a concentrated form, which facilitates disposal and restores sorbent for effective reuse [239,240]. The desorption mechanism is similar to ion exchange, where metals are eluted from the sorbent by an appropriate solution to give a small, concentrated volume of metal containing solution. The sorbent stripping can be achieved with a relatively inexpensive acid such as HCl, HNO_3 and H_2SO_4 [241–244]. In an attempt to determine the suitable eluent and optimum concentration of the eluent for recovering uranium from PHOA sorbent systematic studies were carried out which have been described in this thesis. The

thesis also elaborates the kinetic and thermodynamic parameters of desorption process along with effect of agitation in desorption medium and effect of presence of competitive ions with its different concentrations.

5.2 Materials and methods

5.2.1 Sorbent

Mixed size sorbent, PHOA used for sorption experiments, discussed in Chapter 5, the same after filtration (called loaded) was taken for desorption experiments. No washing or pre-treatment was given to the loaded sorbent. After filtration minimum one hour time was given for dripping out the adhered water from the loaded PHOA before use for desorption experiments. The sorbent loss due to handling and attrition was found to be about 2% on average which was considered during recovery calculation.

5.2.2 Elute solution preparation

The prepared standard eluent chemical solutions were used as stocks elute solution. Safe procedure was followed in handling and disposing of uranium solution and chemicals wherever carried out. The stock solutions was diluted to demanded / required concentration and was adjusted to desired concentration with distilled water at room temperature, $28\pm 2^\circ\text{C}$.

5.2.3 Metal ion determination

Inductively Coupled Plasma Emission Spectrophotometer (ICPAES), Jobinyvon Emission, Model No. JY 328 was used to determine uranium and other metal ions' concentrations in elute solutions. Concentration of uranium and other metal ions in the solution before (when reused) and after equilibrium and as required (for kinetic study) was estimated elution performance evaluation.

5.2.4 Reagents

The reagents used in the experiments were of analytical reagent (AR) grade. HCl, HNO₃, H₂SO₄, Malic acid, Oxalic acid, Acetic acid procured from S.D. fine chemicals, were used as

received without purification and treatment. Distilled water of Millipore ultra pure water system was used in investigations (Millipore Q) whenever needed for elute solution preparation, dilution and washing / rinsing.

5.2.5 Apparatus

Desorption / elution experiments were carried out using Borosil glass beaker and other glass items with which elute solutions do not get affected. PARAFILM PM-992 (laboratory film) was used as sealing material for glass apparatus wherever required. Thermo-bath used for batch mode elution experiments was obtained from Joshi Scientific Corporation. Concentration of elute solution was measured by standard acid-base titration. Calibrated laboratory weighing scale was used for sorbent weight measurement. Whatman-42 grade filter paper was used for filtering medium.

5.2.6 Desorption / recovery evaluation method

The amount of eluted metal was calculated from the difference of metal ion concentration in elute solution before (for reuse) and after desorption. The equilibrium desorption / recovery (%) and immobilization were calculated according to formulae:

$$\mathbf{Elution\ factor} = \frac{\mathbf{Total\ amount\ of\ metal\ ion\ in\ elute\ solution}}{\mathbf{Total\ amount\ of\ metal\ ion\ sorbed\ by\ the\ sorbent}} \quad 5.1$$

$$\mathbf{Recovery, \%} = \mathbf{Elution\ factor} \times \mathbf{100} \quad 5.2$$

$$\mathbf{Immobilization\ factor} = \mathbf{(1 - Elution\ factor)} \quad 5.3$$

$$\mathbf{Total\ recovery} = \frac{\mathbf{Total\ amount\ of\ metal\ ion\ in\ elute\ solution}}{\mathbf{Total\ amount\ of\ metal\ ion\ in\ initial\ solution}} \quad 5.4$$

5.3 Experimental procedure for sorption parameters

Experiments were performed using 0.5g PHOA beads added into a 100 mL beaker along with 50 mL of synthetic solution either uranium (< 10 mg/L U) or multi-ion with uranium at about pH 9 and of plant effluent for loading the metal ion onto sorbent, as it was carried out for sorption experiments. A typical plant effluent having 9.81 mg U/L, 576 mg Ca/L, 15121

mg Mg/L, 74211 mg NO₃/L at pH 8.1 was used to carry out all experiments except mentioned separately. The sorption system was filtered and allowed the water dripped out for one hour. The dewatered loaded sorbent was used for elution experiment at room temperature except temperature variation study. For elution study the loaded sorbent was taken in a 100 mL beaker with 50 mL desired concentration of selected eluent without agitation (except effect of agitation) for required time to attend equilibrium and the equilibrated solution was filtered.

Effect of concentration of eluent was studied for eluent concentration range 0.1 – 4.0 M. In order to obtain thermodynamic parameters, the same procedures were also performed at the solution temperatures of 28 – 80°C range. Effect of elution properties like performance in different elutes, elute concentration on uranium recovery and sorbent reusability was evaluated for 24h. Effects of important process parameters like contact time, temperature, agitation speed, fractional recovery performance were investigated and optimum contact time for equilibrium was evaluated. Recovery of the uranium ion was evaluated in presence of different competitive metal ions in initial solution. All experiments were performed in duplicates. The total (experimental and analytical) relative standard deviation (RSD) was calculated and found maximum $\pm 5\%$.

5.4 Results and discussion

5.4.1 Selection of effective eluent

The results of efficiency of different chemical agents, eluents are shown in **Figure 5.1**. The result indicates that the desorption performance of U(VI) from loaded sorbent was varied with the nature of eluents as H₂SO₄ > HCl > HNO₃ > Organic acids. The desorption efficiency of U(VI) from loaded sorbent is related to the complexing properties of anion present in chemical agents with UO₂²⁺ ion. The complexing ability of various anion with

UO_2^{2+} ion follows the order $\text{H}_2\text{SO}_4 > \text{HCl} > \text{HNO}_3 > \text{Organic acids}$ and hence the efficiencies of elution follow the same order.

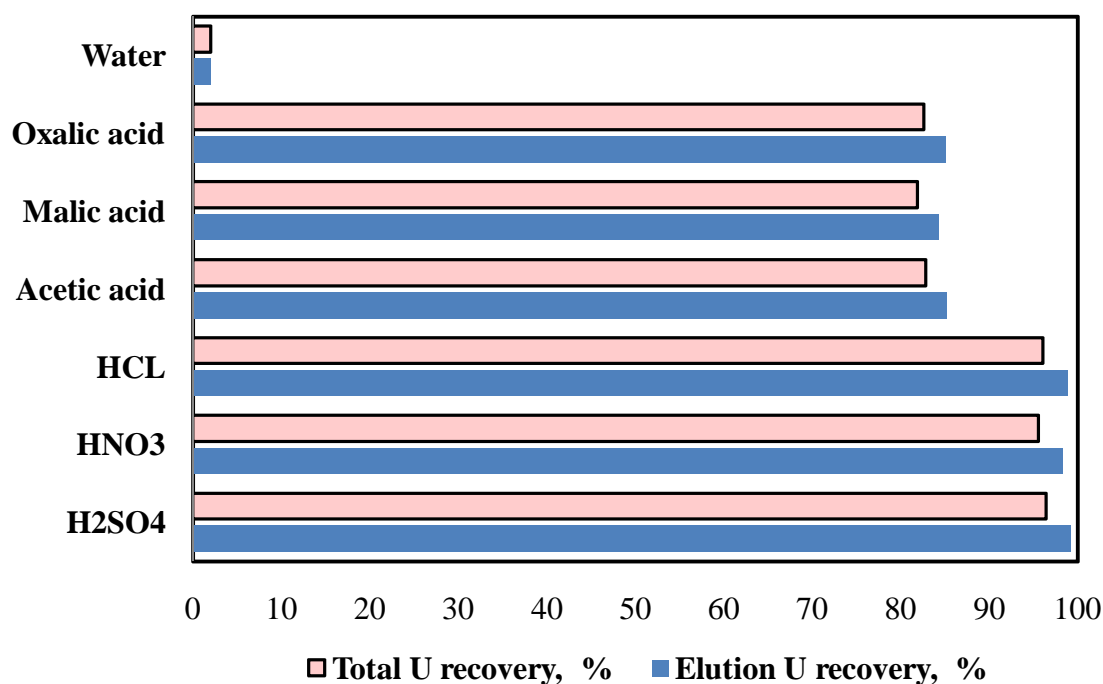


Figure 5.1: Desorption performance of uranium from loaded PHOA with various eluent.

Elution efficiency of inorganic acids is better than that of organic acids and the difference is adequate. H_2SO_4 is found to be the better eluent among the inorganic acids because of its higher complexing ability may be due to presence of more $-\text{OH}$. But the difference is $< 0.5\%$ w.r.t. HCl and about 1% w.r.t. HNO_3 . However, for further studies HCl was chosen as chemical agent / suitable eluent because the HCl is not an oxidising acid like H_2SO_4 and HNO_3 which may damage the cross linked polymeric structure of sorbent and hence to avoid degradation of the sorbent. In addition the HCl can elute Fe^{3+} from sorbent phase, if any present which can decrease the sorption efficiency of the sorbent.

5.4.2 Effect of concentration of eluent on recovery

The elution performance of different concentration of HCl is shown in **Figure 5.2**. From 0.1M to 0.5M HCl the recovery increased from about 70% to 98.7% and there after recovery increase is not adequate with increase of eluent concentration (maximum obtained 99.5%).

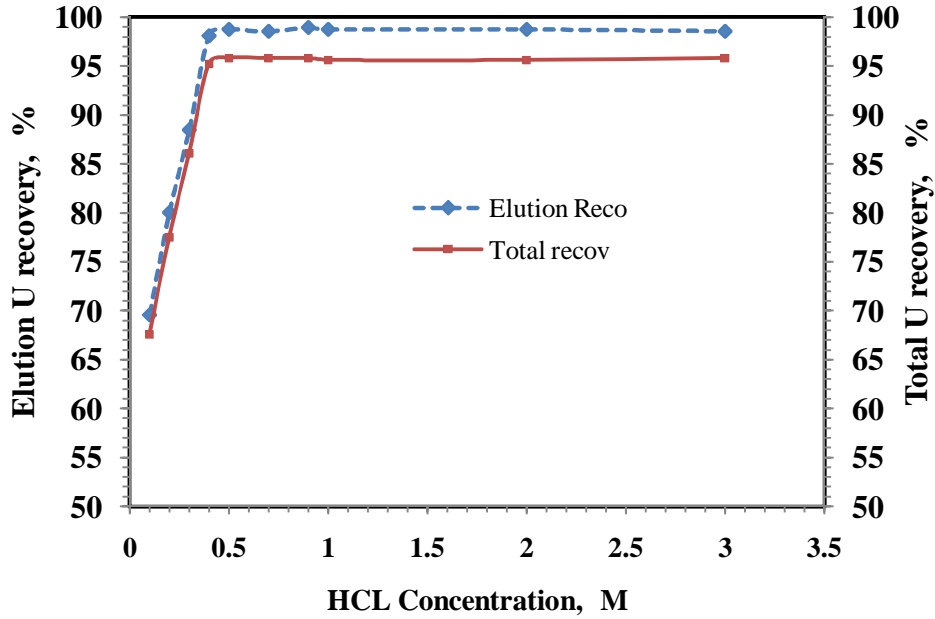


Figure 5.2: Elution performance of uranium from loaded PHOA with different HCl concentration (synthetic solution, U: 9.11 mg/L)

The total recovery is about 96%. The initial increase in recovery due to availability of hydrogen ion for replacing the uranium ion from sorbent ligand and further increase might be due to increase of hydrogen concentration. Similar trend in elution performance was observed with sorbent loaded with uranium from plant effluent as shown in **Figure 5.3**.

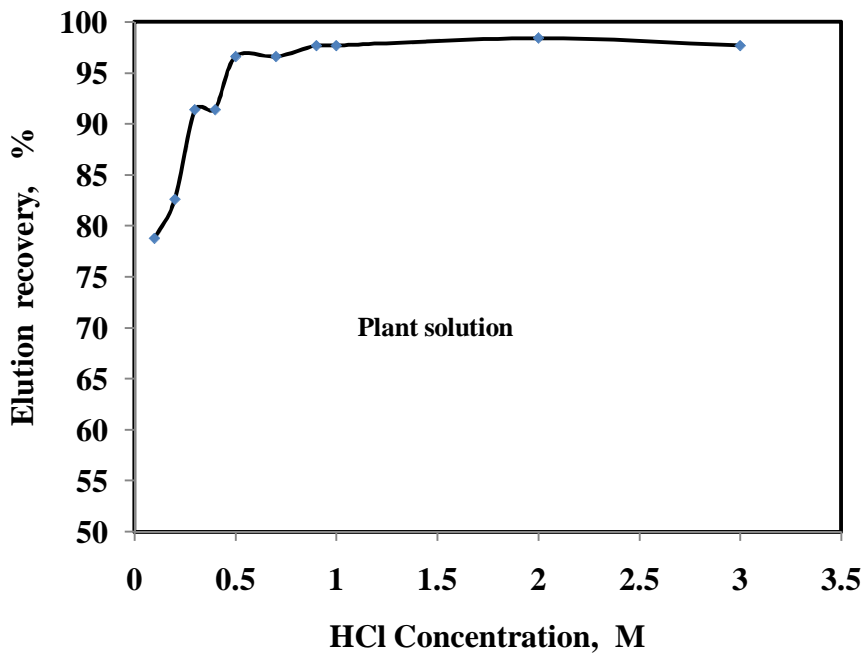


Figure 5.3: Elution performance of uranium from loaded PHOA with different HCl concentration (Plant effluent)

For this case elution recovery was found to be about 98% even after increasing the HCl concentration (total recovery 93%) which may be due to hindrances of competitive ions present in the loaded sorbent. The effect of presence of competitive ions in loaded sorbent on elution performance is found to be necessary. For further study 1M HCl was chosen as eluent.

5.4.3 Effect of agitation on uranium recovery

Boundary layer effect, which is controlled providing mechanical agitation of the elution mixture, may affect the external mass transfer of sorbate in the elution process. The elution study was carried out for understanding the effect of mechanical agitation of sorbent-elute mixture. The mixture was agitated in different stirrer speed ranging from 50 to 300 rpm. Sorption profile is shown in **Figure 5.4 a) and b)**. For all the experiments, recovery was about 99% and total recovery was 96% for loaded sorbent with synthetic solution (**Figure 5.4 a)**) and mass transfer of U(VI) from sorbent to eluent was not influenced by the mechanical agitation.

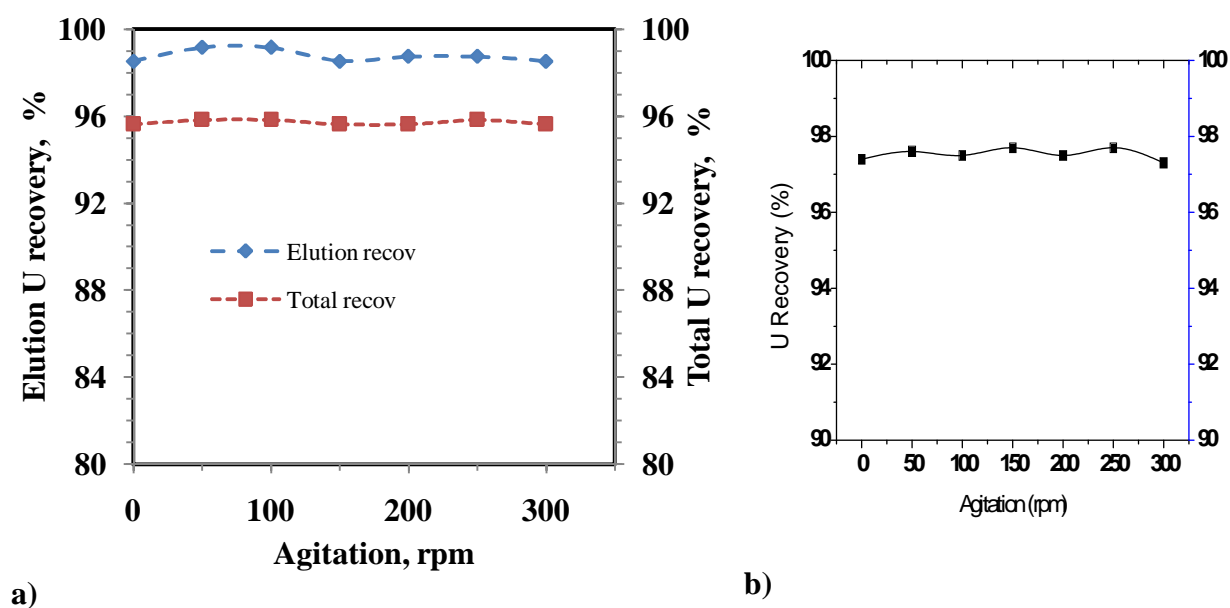


Figure 5.4: Elution performance of uranium from loaded PHOA with variation of agitation, a) loaded sorbent with synthetic uranium solution, b) loaded sorbent with plant effluent

The result showed that uranium uptake of the sorbent remains unaffected by the mechanical agitation of the sorbent-eluent mixture. Similar result was noticed for the loaded sorbent with plant effluent as shown in **Figure 5.4 b)**. Based on the result, further uptake experiments were conducted without agitation/shaking.

5.4.4 Recovery of uranium from plant effluent

In plant effluent, Magnesium and Calcium ions are present in high concentration (g/L) as main competitive ions along with the uranium ion (<10 mg/L). Recovery of the competitive ions were evaluated along with the uranium and shown in **Table 5.1**.

Table 5.1: Elution characteristics of uranium, magnesium and calcium in plant effluent in batch experiment

Parameters studied (Element)	Uranium processing plant effluent		
	(U)	(Mg)	(Ca)
Elution recovery % (24h)	97.22 ± 1.9	96.53 ± 1.9	85.52 ± 1.6
Immobilization factor	0.028	0.035	0.145

About 97% recovery was achieved in the plant effluent with PHOA and recovery of magnesium and calcium was found to be 96.5% and 86.5% respectively. Immobilization factor for uranium and magnesium is quite appreciable which is 0.028 and 0.035 and the same for calcium is 0.145. Calcium ion was not getting removed completely from the PHOA in the elution medium. The calcium ion is more detrimental than magnesium ion for reusing the PHOA. Effect of fractional elution in different concentration of eluent may be needed to study for removing the calcium ions along with other possible competitive ions, which has been carried out and discussed subsequently.

5.4.5 Kinetic study of uranium desorption process

Elution kinetics of PHOA sorbent with respect to uranium recovery using synthetic uranium solution and the plant effluent in batch experiments has been shown in **Figure 5.5 a) & b)**.

Within 1h time uranium recovery of about 92.5% from synthetic solution and 89% from the effluent was observed.

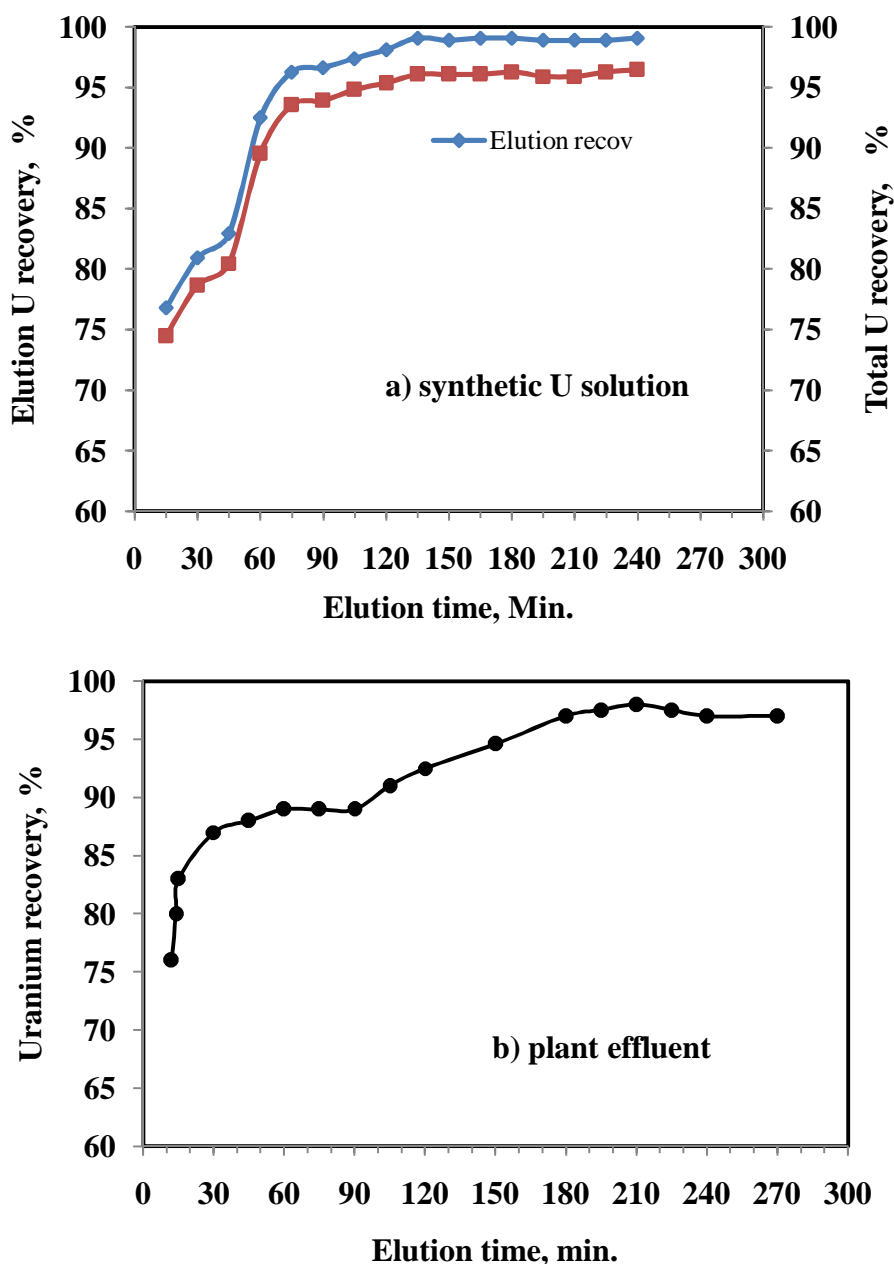


Figure 5.5: Elution performance with time (1M HCl, RT) with a) synthetic U solution and b) plant effluent.

A substantial amount, about 75% of uranium elution within 10 min and 97% elution was observed in 3h with the 1M HCl eluent and loaded PHOA from the plant effluent. The elution kinetics was found to be faster than the sorption kinetics and presence of competitive ions does not affect the elution kinetic. There was about 2% weight loss of the sorbent in the

laboratory scale batch experiment. Degradation of the sorbent is envisaged to be appeared in sorbent reuse due to presence of high concentration of nitrate in the effluent (oxidising medium) and also because of sorbent attrition.

5.4.6 Effect of temperature on uranium desorption process

It is essential to examine the influence of thermodynamic parameters on the uranium elution from the PHOA beads. The influence of temperature variation on the elution of U(VI) ions from PHOA beads in 1M HCl was examined in a range of temperature 28 – 80°C and the result has been shown in **Figure 5.6**. Uranium elution from the loaded PHOA is found to be independent of temperature variation. Average elution recovery and total recovery was about 99% and 96% respectively within the temperature range studied.

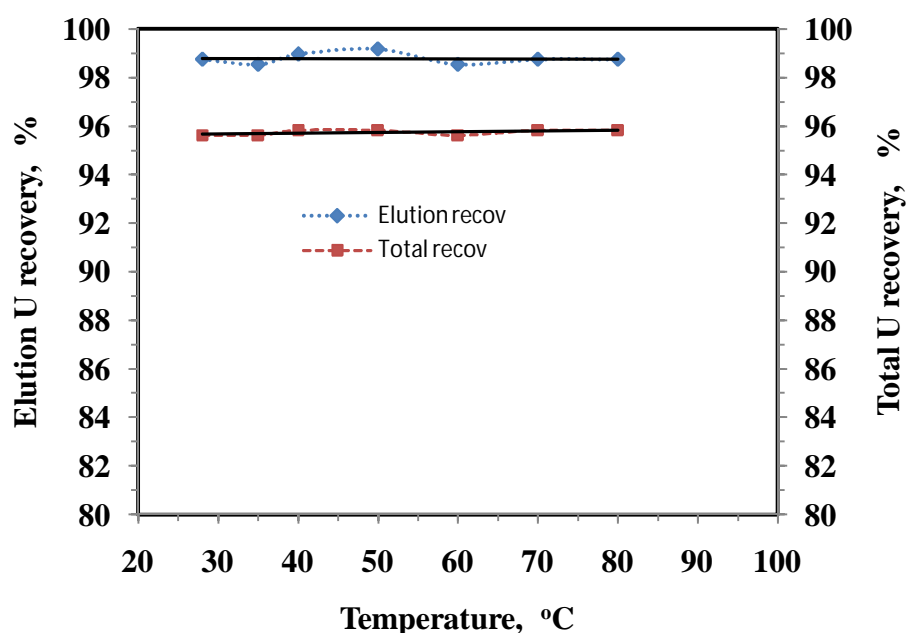


Figure 5.6: Elution performance with temperature

5.4.7 Effect of presence of competitive ions on the uranium elution process

To understand the effect of competitive ions present in the plant effluent on the uranium elution process with variation of their individual concentration separate experiments were carried out. One set of experiment was conducted with higher concentration of individual metal ion along with uranium ion (synthetic solution). Ca^{++} 804 mg/L, Mg^{++} 4860 mg/L,

Mn^{++} 11 mg/L, Cu^{++} 19.1 mg/L, Fe^{+++} 22.4 mg/L and anion NO_3^- 124 g/L individual ion concentration were taken along with uranium ion to evaluate the effect of metal ion on elution process and whether metal ions can be recovered from the PHOA. Appearance of the individual competitive ion (higher concentration, as sample) with uranium loaded PHOA is shown in **Figure 5.7** which were taken for elution in 0.5M HCl solution. Sorption of Cu^{++} and Fe^{+++} can be easily identified from the colour of loaded PHOA (**a**) and (**c**) respectively).

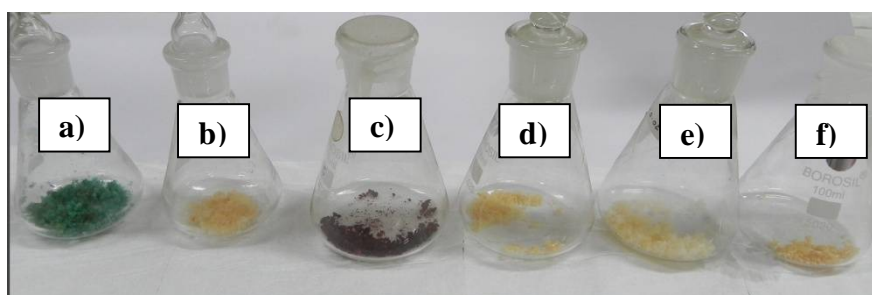


Figure 5.7: Metals ions loaded PHOA: a) Cu^{++} , b) NO_3^- , c) Fe^{+++} , d) Ca^{++} , e) Mg^{++} and f) Mn^{++}

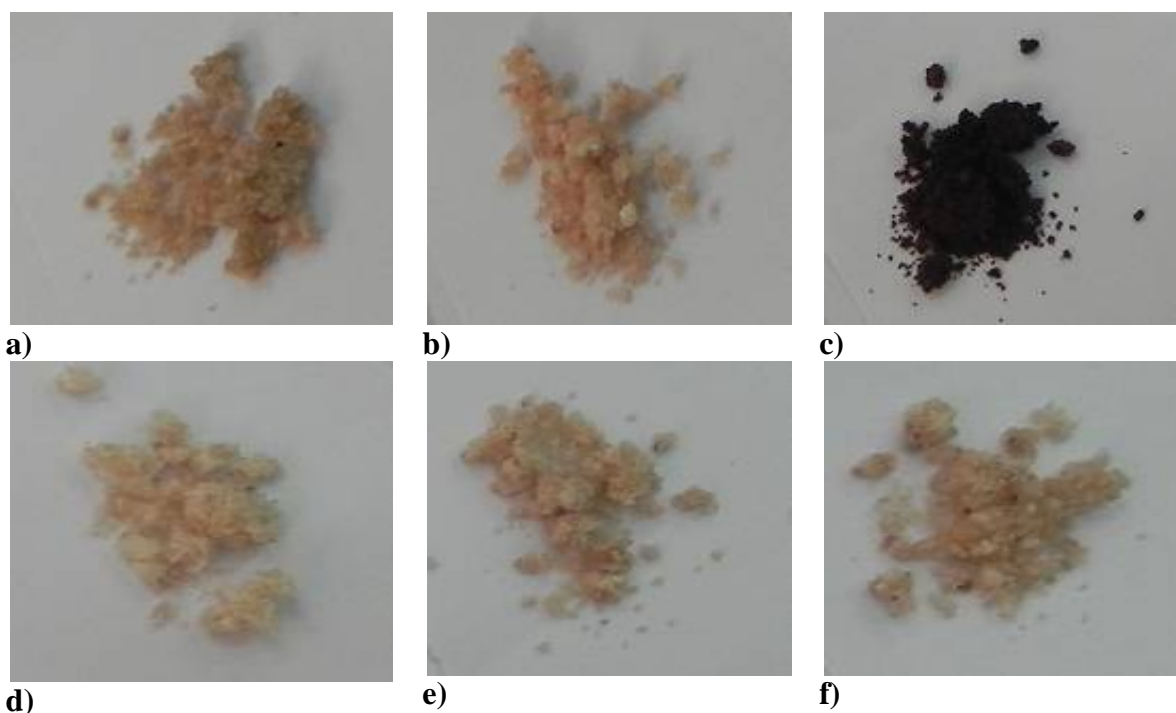
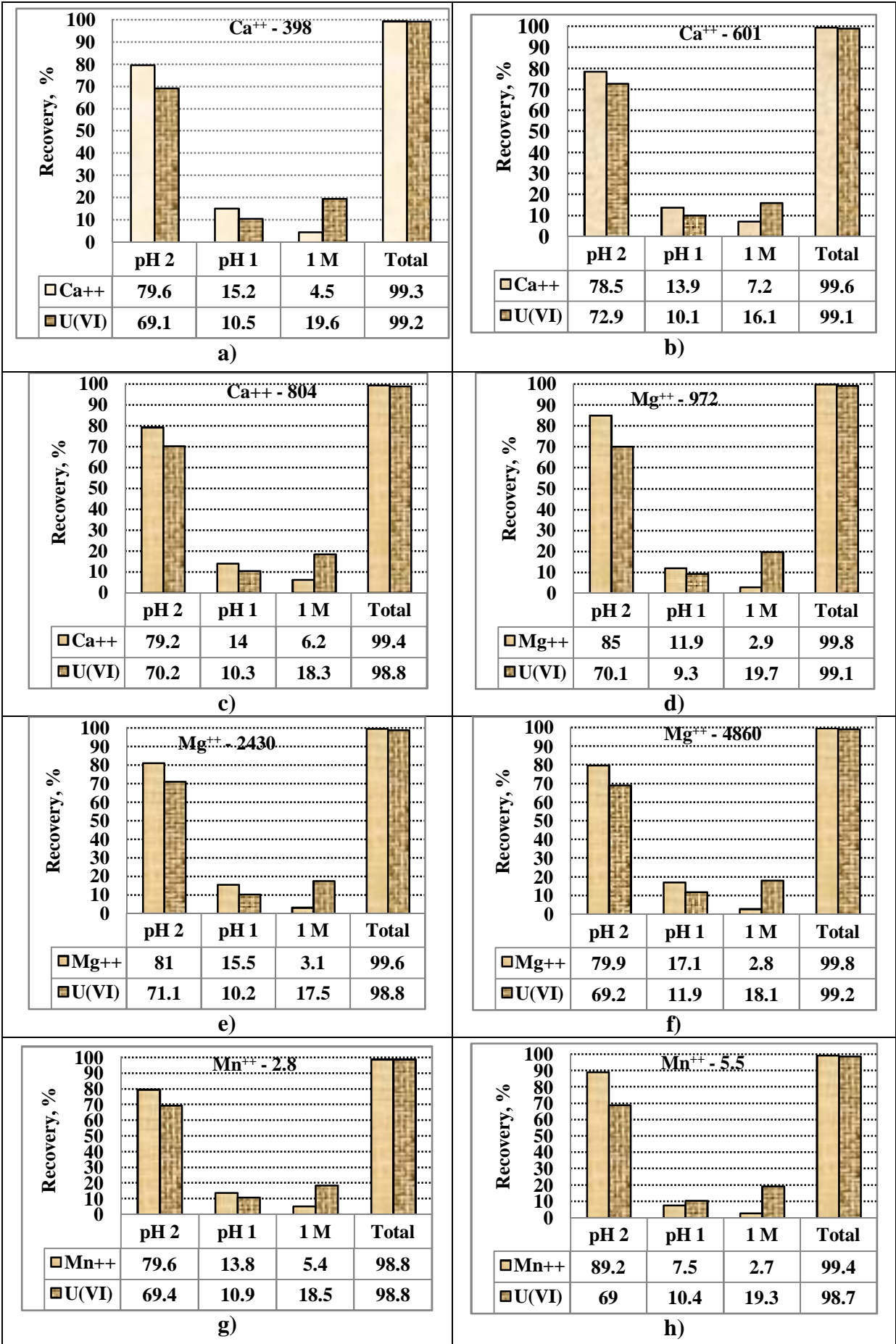
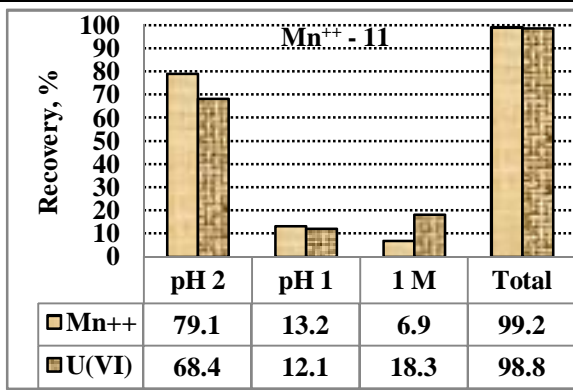


Figure 5.8: Eluted PHOA: a) Cu^{++} , b) NO_3^- , c) Fe^{+++} , d) Ca^{++} , e) Mg^{++} , f) Mn^{++}

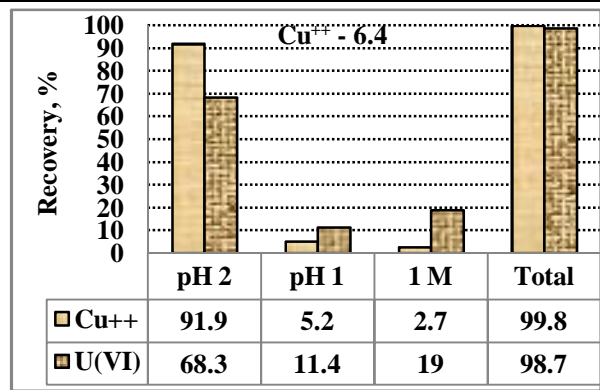
Appearance of the PHOA after elution of metal ions is shown in **Figure 5.8** where it is understood that only Fe^{+++} does not get removed completely from the PHOA after elution in 0.5M HCl. This is because of greater affinity of Fe^{+++} ion towards PHOA functional group which may lead to decrease in efficiency of PHOA to reuse. To understand the recovery of individual metal ions along with uranium ion and also to decide the requirement of elute concentration fractional elution experiment was planned.

As concentration of the competitive ions may vary in the plant effluent there are three different higher side concentrations of individual metal ions like Ca^{++} (398, 601, 804 mg/L), Mg^{++} (972, 2430, 4860 mg/L), Mn^{++} (2.8, 5.5, 11 mg/L), Cu^{++} (6.4, 12.7, 19.1 mg/L), Fe^{+++} (5.6, 11.2, 22.4 mg/L) and anion NO_3^- (99, 112, 124 g/L) ions were considered along with uranium ion for elution performance evaluation. The metals ion loaded PHOA were taken for elution in three different concentration of HCl namely pH = 2, pH=1, 1M for fractional separation to understand whether all metal ions can be removed from the PHOA in a fixed elute concentration. The result of the studies has been shown in **Figure 5.9**. From the figure it is understood that except Fe^{+++} ion all other metal ions get separated from the PHOA at lower HCl concentration. Fe^{+++} ion gets separated in higher concentration i.e. 1M HCl solution (**Figure 5.9 m)-o**) may be due to increase of concentration gradient of H^+ in the elute solution. Concentration of nitrate ion does not have notable affect on the uranium elution (**Figure 5.9 p)-r**). As nitrate ions were not sorbed in the PHOA recovery of nitrate ions were almost nil. Based on the studies it is decided to use elute solution of 1M HCl for recycle the PHOA sorbent.

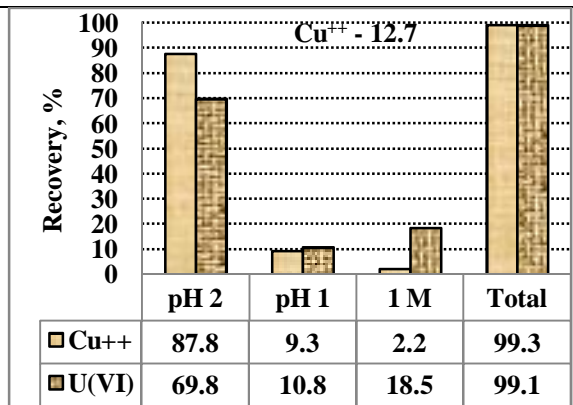




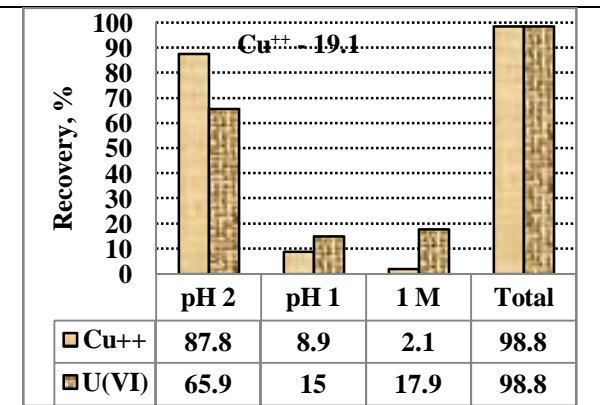
i)



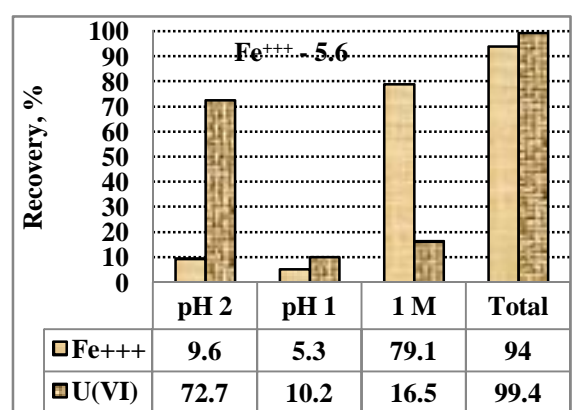
j)



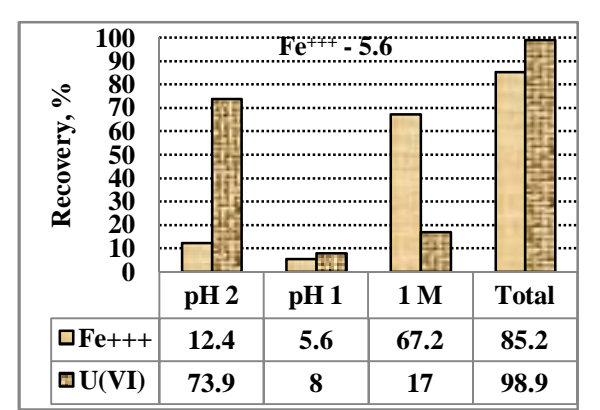
k)



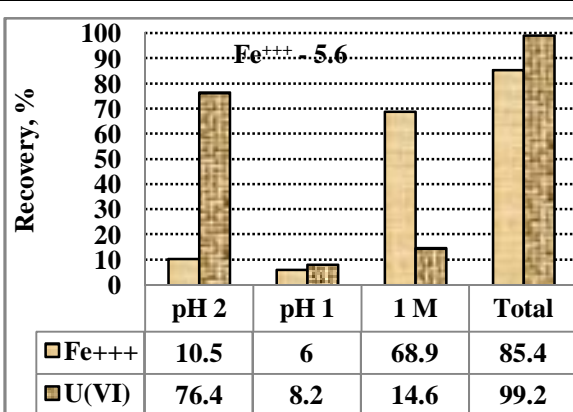
l)



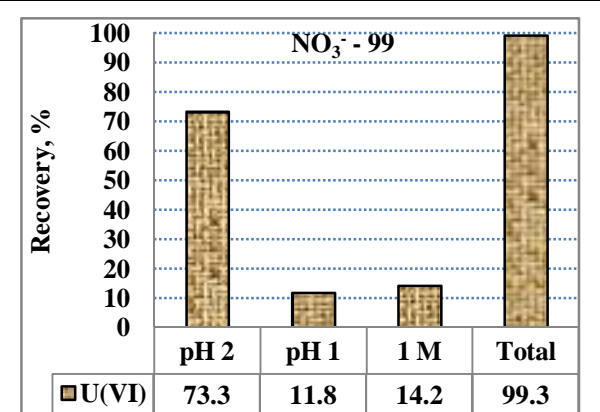
m)



n)



o)



p)

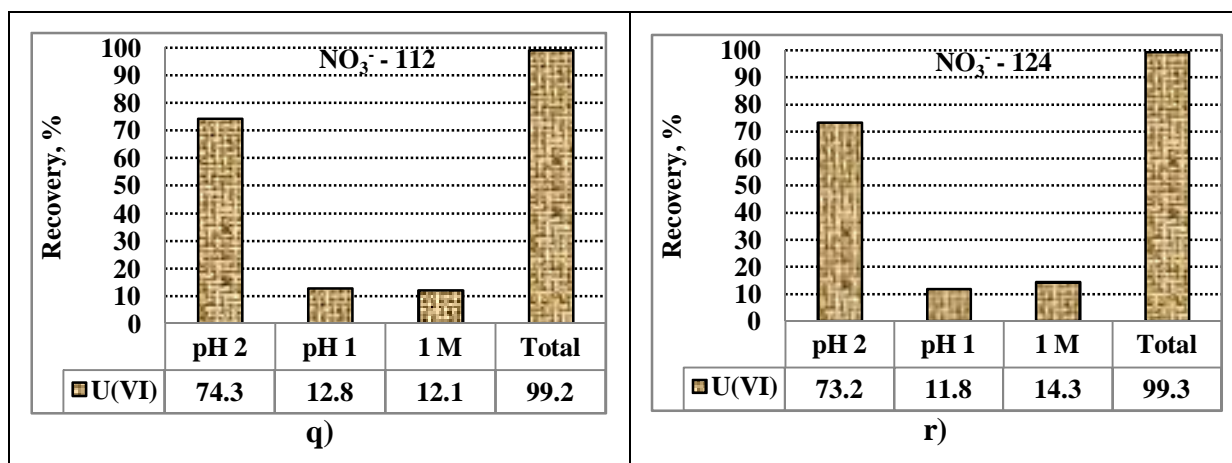


Figure 5.9: Effect of presence of competitive on elution performance a)-c): Ca⁺⁺, d)-f): Mg⁺⁺, g)-i): Mn⁺⁺, j)-l): Cu⁺⁺, m)-o): Fe⁺⁺⁺, p)-r): NO₃⁻

5.4.8 Recycle of the PHOA sorbent

The sorbent has been recycled for a number of cycle for U(VI) sorption as well as desorption to ensure the reusability of the sorbent under the present experimental conditions, sorption at pH 9 and desorption at 1M HCl. **Figure 5.10** showed the plot of % U(VI) desorption vs no. of elution cycle.

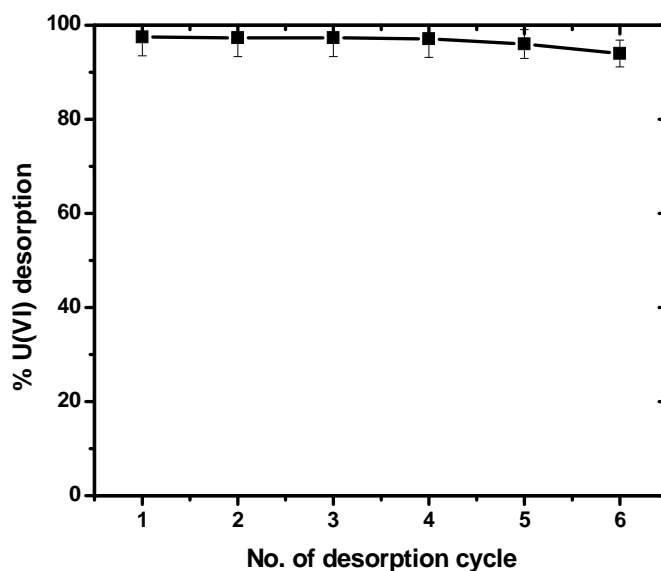


Figure 5.10: Reusability of PHOA with respect to desorption of uranium

The elution studies indicate that there is no significant decrease in desorption of U(VI) up to 6th elution cycle. The minor decrease in % desorption of uranium, as indicated in the figure is

due to decrease of uranium sorption on to PHOA. This may also be anticipated if dilute eluent is used due to non-availability of required hydrogen ion for protonation. This can be prevented maintaining HCl concentration. The experimental data on recycle of sorbent for sorption (as described in previous chapter) as well as desorption for a number of times (up to 6 cycle) showed that the sorbent can be reused for U(VI) sorption from alkaline solution for several times.

5.5 Conclusion

Regeneration of sorbent is an important cost effective parameter for developing industrial wastewater treatment process. PHOA sorbent is efficiently re-generable after uranium sorption from the plant effluent by 1M HCl as most suitable eluent amongst inorganic and organic acids. The elution process is faster in kinetics and the process does not get affected by agitation and temperature of process solution as well as in presence of competitive ions in sorbate. About 1000 times uranium pre-concentration is viable by maintaining suitable eluent concentration. The PHOA can be successfully recycled / reused for minimum 6 times with its full efficiency of uranium sorption-desorption application from nuclear wastewater.

CHAPTER – 6

COLUMN EXPERIMENT: SORPTION AND ELUTION

6.1 Introduction

Experimental sorption processes can be performed in batch and continuous mode. Batch mode experiments are usually done to measure the capability and effectiveness of sorption processes of a specific sorbent and to determine the maximum sorption capacity. For industrial purposes the continuous sorption in fixed-bed column is often desired [245]. However, determining the design parameters is important in the continuous removal of U(VI) from waste water.

Design of a sorption column starts with laboratory testing to establish the breakthrough curve. At time intervals, the effluent from a column is sampled. Time zero is when the solution is applied to the column. At first, the sorbent is fresh with all its adsorption sites. Essentially none of the metal ion to be removed escapes from the column. As time passes, some of the sorption sites are used up, and concentration of metal ion in the effluent / outlet of the column rises. If all the sites were occupied, it is expected that the inlet concentration and the outlet concentrations to become the same. The breakthrough concentration is determined by the process specifications. This is the allowable concentration. If a pollutant is being removed, the breakthrough concentration might be as per regulation for the plant. For a commercial product, the breakthrough concentration is determined by specification for product quality. Breakthrough concentration is not some fundamental number but depends on how operator decides to operate the process. A practical way to design a sorption column is to experiment with a laboratory column and scale up is a matter of increasing the area to match the volume to be treated. A major source of error is the effect of flow rate because this determines contact time, and the approach towards equilibrium residential time. Successful design of a column sorption process requires prediction of the breakthrough curve for the effluent [246]. Over the years, several mathematical models have also been developed for describing and analyzing

the lab-scale column studies for the purpose of industrial applications [247,248] and up-gradation.

The performance of the sorbent was investigated using continuous sorption technique named as column experiment varying different important parameters namely i) flow rate of nuclear wastewater, ii) sorbent mass / sorbent volume and iii) diameter of the column in this thesis. The experimental data were used for breakthrough analysis and mathematical curve modeling which are found to be useful for scale up of the process. These models have been discussed in the thesis and suitable model has been selected based on applicability. In this study, Adams–Bohart and Thomas models were used as identified the suitable model for predicting the dynamic behaviour of the column for breakthrough model analysis.

6.2 Materials and methods

6.2.1 Sorbent

Mixed size sorbent, PHOA as prepared was used having size distribution: 10 mesh 21.66%, 16 mesh 59.96%, 18 mesh 8.31% and 25 mesh 10.07% as detailed in **Chapter 2 (Para. 2.3.1)** for all the experiments. The sorbent was washed and swelled for 30 min. with distilled water (DW) before use. No pre-treatment was given to avoid extra expenditure and for simplicity. Preparation and characteristic details have been described in previous Chapters.

6.2.2 Uranium solution

A typical plant effluent having 9.81 mg U /L, 576 mg Ca /L, 15121 mg Mg /L, 74211 mg NO₃/L at pH 9.1 was used to carry out all experiments except concentration variation tests. All experiments were conducted at room temperature, 28±2°C.

6.2.3 Uranium and other metal ion determination

Inductively Coupled Plasma Atomic Emission Spectrophotometer (ICPAES), Jobinyvon France, Model No. JY 328 was used to determine uranium concentrations in solutions. The detection limit (3σ) of the instrument for non-transition elements: > 0.2 ppb, transition

elements: > 1 ppb and rear earths elements: > 3 ppb. Concentration of uranium in the solutions collected in required time interval was analyzed.

6.2.4 Reagents

The prepared standard 1M HCl was used to elute uranium laden PHOA. Distilled water of Millipore ultra pure water system was used in investigations (Millipore Q) for washing / rinsing off.

6. 2.5 Apparatus

All column studies were accomplished in a glass column of 3 – 5 mm thick with varying internal diameter. A sintered glass filter was placed in the bottom of column to maintain the PHOA sorbent beads. The samples were collected at different time intervals in the bottom of column and analyzed for U(VI). Solution pH was measured using Orion 720 A+ model pH meter of Thermo Electron Corporation. Calibrated laboratory weighing scale from Kern, Germany was used for sorbent weight measurement.

6.3 Column model evaluation

6.3.1 Column model

The loading behaviour of U(VI) to be removed from solution in a fixed bed has been usually expressed in term of C_t/C_0 where (C_t = effluent U(VI) ion concentration and C_0 = influent U(VI) ion concentration in mg/L). The maximum column capacity, q_{total} (mg), for a given feed concentration and flow rate is equal to the area under the plot of the sorbed U(VI) concentration, C_{ad} ($C_{ad} = C_0 - C_t$) (mg/L) versus effluent time (t , min) and is calculated from

Equation 6.1:

$$q_{total} = \frac{QA}{1000} = \frac{Q}{1000} \int_{t=0}^{t-t_{total}} C_{ad} dt \quad 6.1$$

Where t_{total} , Q and A are the total flow time (min), volumetric flow rate (ml/min) and the area under the breakthrough curve, respectively. The equilibrium uptake ($q_{eq(exp)}$) is calculated as follows :

$$q_{eq}(exp) = \frac{q_{total}}{m} \quad 6.2$$

Where, m is the total dry weight of PHOA in column (g). The total amount of U(VI) sent to the column (W_{total}) is calculated from equation below:

$$W_{total} = \frac{C_0 Q_{total}}{1000} \quad 6.3$$

Total removal percent (Y , %) of U(VI) is the ratio of the maximum capacity of the column (q_{total}) to the total amount of U(VI) sent to column (W_{total}).

$$Y = \left(\frac{q_{total}}{W_{total}} \right) \times 100 \quad 6.4$$

For the successful design of a column sorption process, it is important to predict the breakthrough curve for effluent parameters. Various kinetic models have been developed to predict the dynamic behaviour of the column.

The sorption column does not show a clear separation between treated and un-treated water but a sorption zone occurs. The position of sorption zone is not fixed and moves down through the sorbent bed until it reaches the sorber end, where the effluent concentration begins to rise in the aqueous phase [249]. The typical breakthrough curve is usually expressed by plotting C_t or C_t/C_0 versus treated volume V or service time t . The concentration at breakthrough point is chosen arbitrarily at some low value. In this study, the point where the effluent concentration (C_t) reached 10% of its influent value (C_0) is called the breakthrough point. When the effluent concentration C_t is approaching to 90% of C_0 the sorbent is generally considered to be exhausted [250].

6.3.2 Kinetic models

Amongst the several kinetic models for column sorption study, three models are used anonymously which are Thomas model, Yoon-Nelson model and Adam- Bohart model. Since the appropriate design of column needs a good prediction of breakthrough curve for the

effluent, two well-known models were applied for the prediction of breakthrough curves. These models will be described below.

6.3.2.1 Yoon–Nelson model

Yoon and Nelson (Yoon and Nelson, 1984) developed a model to investigate the breakthrough behaviour of adsorbate gases on activated charcoal. The Yoon–Nelson model is based on the assumption that the rate of decrease in the probability of adsorption for each adsorbate molecule is proportional to the probability of adsorbate adsorption and the probability of adsorbate breakthrough on the adsorbent [251]. The linearized Yoon–Nelson model for a single component system can be expressed as:

$$\ln\left(\frac{C_t}{C_0 - C_t}\right) = k_{YN}t - \tau k_{YN} \quad 6.5$$

Where k_{YN} (1/min) is the rate velocity constant, τ (min) is the time required for 50% adsorbate breakthrough. From a linear plot of $\ln[C_t/(C_0 - C_t)]$ against sampling time (t), values of k_{YN} and τ were determined from the intercept and slope of the plot.

Assumptions of this model are preferentially applicable for gas-solid adsorption processes. Hence, the model has not been considered and applied in this study of liquid-solid sorption process and is not included in the thesis.

6.3.2.2 The Thomas model

Thomas equation is one of the most general models often used to interpret column data. This model supposes that sorption process follows Langmuir isotherm for equilibrium and also obeys second-order reversible reaction kinetics. Especially in the absence of internal and external diffusion limitation, this model can be used well. The linearized form of Thomas model is given by [251]:

$$\ln\left(\frac{C_0}{C_t} - 1\right) = \frac{K_{Th}q_0m}{Q} - K_{Th}C_0t \quad 6.6$$

where C_0 (mg/L) is the inlet concentration of adsorbate, C_t (mg/L) is the outlet concentration at time t (min), K_{Th} (L/min mg) is the Thomas rate constant, q_0 is the maximum solid phase

concentration (mg/g), m is the mass of adsorbent (g) and Q is the flow rate of solution (mL/min). Hence, K_{Th} and q_0 can be obtained by the slope and intercept from a plot of $\ln(C_0/C_t - 1)$ versus t .

Findings of the studies carried out in batch sorption processes (Langmuir isotherm for equilibrium and obeys second-order reversible reaction kinetics) support utilisation of this model and hence, this model is found to be suitable for this studies.

6.3.2.3 Adam-Bohart model

The Adams–Bohart adsorption model is often applied to experimental data for the description of the initial part of the breakthrough curve. The main assumption behind this model is that the sorption rate is proportional to the residual capacity of the adsorbent and the concentration of the sorbate and also equilibrium does not take place instantaneous. The mathematical equation of the model can be written as [252]:

$$\ln\left(\frac{C_t}{C_0}\right) = k_a C_0 t - k_a N_0 \left(\frac{Z}{U_0}\right) \quad 6.7$$

where C_t (mg/L) is the outlet concentration at time t (min), C_0 (mg/L) is the inlet concentration of adsorbate, k_a is the kinetic constant (L/mg min), N_0 is the saturation concentration (mg/L), Z is the bed depth of column (cm) and U_0 is the linear velocity (cm/min) which can be calculated by dividing the volumetric flow rate to the column cross sectional area. The values of k_a and N_0 can be obtained from a plot of $\ln(C_t/C_0)$ versus t .

As the model is general in nature and also is common for sorption processes, thorough analysis of column experimental data has been carried out using this model.

6.3.2.4 Bed Depth Service Time (BDST)

BDST model is used to predict the bed capacity by utilizing the different breakthrough values [246]. The modified version of the equation used in this evaluation is given as follows:

$$t = \frac{N_0}{C_0 F} Z + \frac{1}{k_a C_0} \ln \left[\frac{C_0}{C_t} - 1 \right] \quad 6.8$$

where t is the time (min.), N_0 is the adsorption capacity (mg/L), C_0 is the inlet concentration of U(VI) ions (mg/L), F is the linear velocity of U(VI) ions across the column (cm/min), Z is the bed depth (cm), k_a is the rate constant in BDST model (L/mg min), and C_t is the effluent concentration of the U(VI) ions (mg/L). A plot of t versus Z is expected to yield a linear curve in which N_0 and k_a could be evaluated, from the slope and y-axis intersection point, respectively.

The breakthrough profile can then be evaluated [253] from the original equation re-casted in form:

$$\frac{C_t}{C_0} = \frac{e^{k_a C_0 t}}{e^{k_a C_0 t} + e^{k_a W/F} - 1} \quad 6.9$$

Where W is the bed capacity (total weight of sorbate adsorbed). The profile can be constructed from knowledge of two experimentally determined values: k_a and W . W is the capacity under dynamic conditions and becomes equal to the static capacity when capacity becomes invariant with bed depth. The critical bed depth, Z_0 is obtained for $t = 0$ and for fixed outlet concentration $C_t = C_b$ where C_b is the concentration at the breakthrough defined as a limit concentration or a fixed percent of initial concentration

$$Z_0 = \frac{V}{k_a N_0} \ln \left[\frac{C_0}{C_b} - 1 \right] \quad 6.10$$

6.3.2.5 Mass transfer coefficient

Mass transfer analysis for the removal of uranium was carried out using the following equation [253]:

$$\ln \left[\frac{C_t}{C_0} - \frac{1}{1+MK} \right] = \ln \left[\frac{MK}{1+MK} \right] - \left[\frac{1+MK}{MK} \right] \beta S_s t \quad 6.11$$

Where K is the constant obtained by multiplying q_m and b (L/g), M is the mass of the sorbent per unit volume of particle free adsorbate solution (g/l). S_s is the outer surface of sorbent per unit volume of particle free slurry (1/cm) and β is the mass transfer coefficient (cm/min).

6.4 Experimental procedure for column parameters

All experiments were performed using desired quantity of PHOA beads added into different diameters Borosil glass column with required volume of the plant effluent at a fixed alkaline pH. 1", 2", 2.4" and 3.5" ID glass columns were fabricated having each height 750 mm and PP made bottom filter. Schematic experimental set up has been shown in **Figure 6.1**. In this study, (i) effect of variation of concentration of uranium in effluent (sorption), (ii) column diameter, (iii) sorbent quantity (bed height) and (iv) flow rate of the effluent / eluent were evaluated.

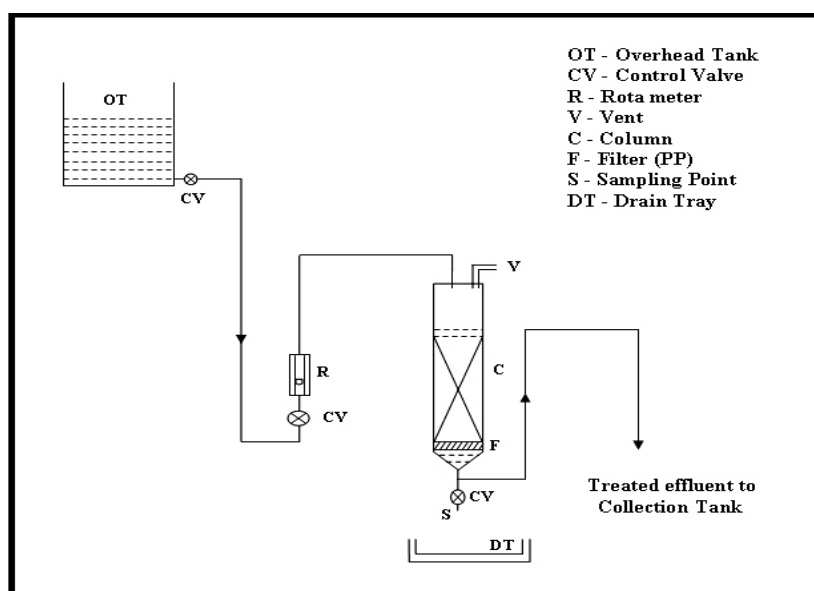


Figure 6.1: Experimental set up for column study

Experiments have been conducted with the columns as per details below:

- i. 1" column: 5g sorbent with 2mL/min – with three different concentration of uranium in the effluent 8.37, 9.81 and 14.1 mg/L (other metal ion concentration and pH within a narrow range).
- ii. 2" column: 10g resin with flow rate 2, 5, 7 and 15 mL/min.; keeping flow rate 15 mL/min sorbent quantity varied as 20g and 30g.
- iii. 2.5" column: 20g, 30g and 40g sorbent with flow rate 15 mL/h.
- iv. 3.5" column: 40g and 60g resin with 15 mL/h.

The loaded sorbents after sorption experiments were eluted with 1M HCl with flow rate as sorption experiments were carried out for with the effluent following similar procedure putting the eluent in overhead tank and collecting in different collection pot. After every experiment the full system was washed / rinsed with distilled water followed by one day natural drying. The samples collected from sample point in different time for sorption as well as elution experiments were analysed for uranium concentration. The total (experimental and analytical) relative standard deviation (RSD) was evaluated and found maximum $\pm 5\%$.

6.5 Results and discussion

6.5.1 Column performance – sorption and elution

Break through results for sorption profile as well as elution profile in column experiments with column diameter 1” ID, uranium concentration 9.81 mg/L, 5 g PHOA and flow rate 2 mL/min have been shown in **Figure 6.2**.

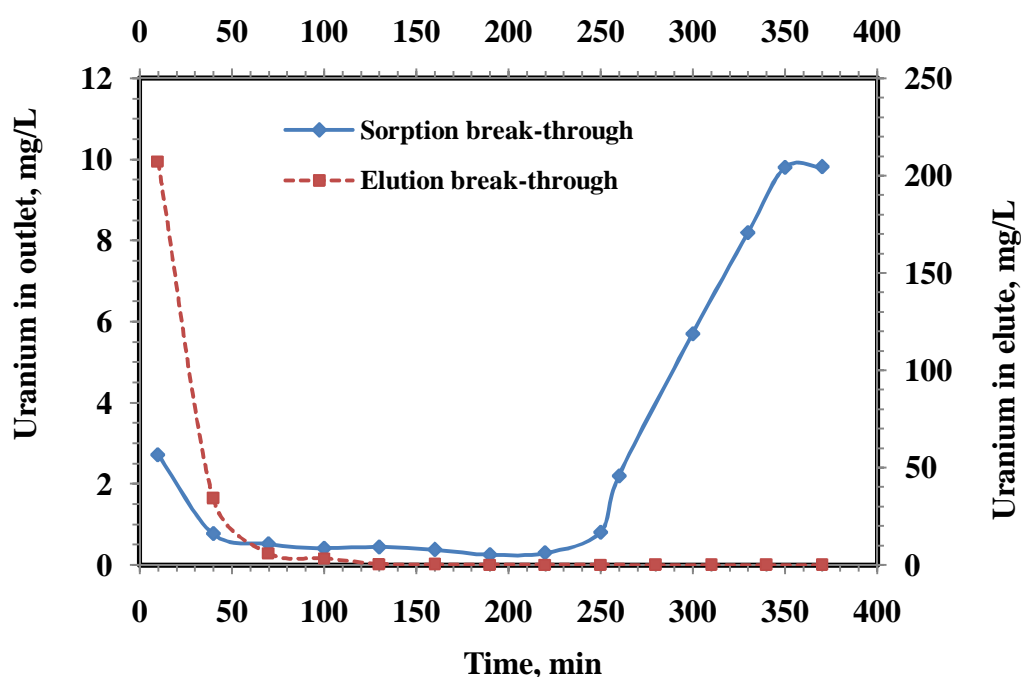


Figure 6.2: Breakthrough of sorption and elution in 1” ID column using plant effluent, PHOA: 5g, flow rate: 2 mL/min, U: 9.81 mg/L.

In the column sorption operation, initial concentration of 2.6 mg/L uranium was obtained in first 10 min which may be due to channelling of flow, and outlet concentration came down to

below 0.7 ppm within next 30 min. About 5% sorption break-through was achieved within 250 min and bed was used up within one hour in the elution break through because of faster kinetics of elution process with respect to actual plant effluent.

6.5.2 Column performance at various operating conditions

6.5.2.1 Effect of inlet U(VI) concentration

To determine the effect of metal concentration on the breakthrough curve three different inlet initial concentrations of U(VI) was investigated with the same flow rate of 2 mL/min and bed height of 5g PHOA sorbent. The results have been shown in **Figure 6.3**.

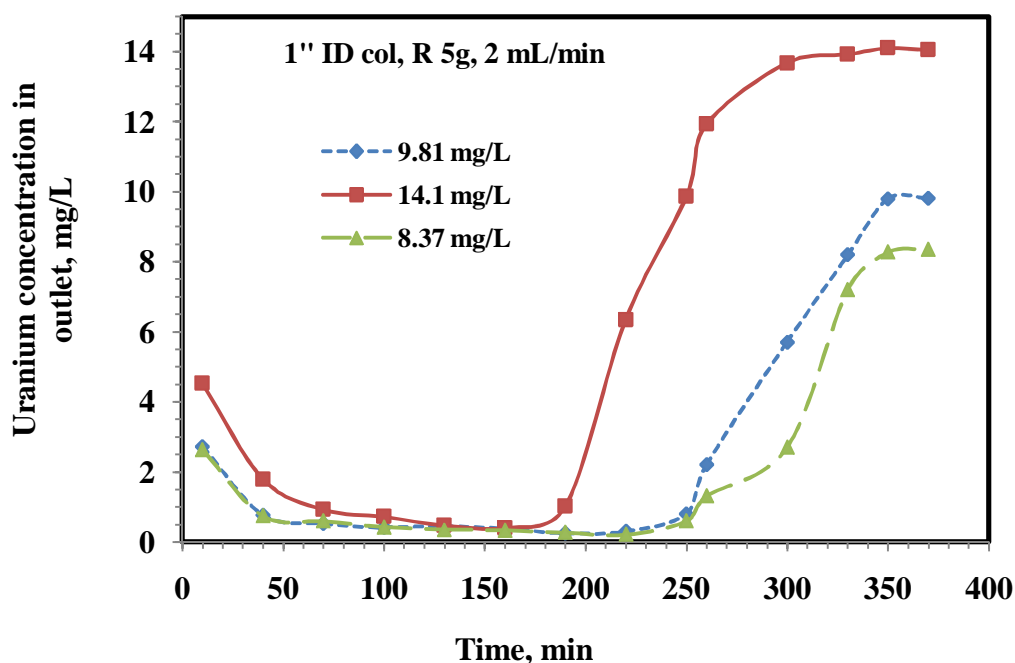


Figure 6.3: Effects of inlet uranium concentrations on sorption breakthrough.

As observed in the figure, a decreased inlet uranium concentration gave a later breakthrough curve and the breakthrough time increased with decreasing initial uranium concentration. This may be explained by the fact that a lower concentration gradient caused a slower transport due to a decreased diffusion coefficient or decreased mass transfer coefficient [254]. As the influent concentration increased, uranium loading rate also increased as the driving force increased for mass transfer. Similar results were obtained in some literatures [255,256].

Thus, the better column performance can be achieved with the higher concentration of solution.

6.5.2.2 Effect of U(VI) solution flow rate

The effect of flow rate on performance of the column was studied at four different flow rates of 2, 5, 7 and 15 mL/min with 2" ID column. During the experiments the bed height and initial concentration of feed was maintained in constant values of 10g PHOA and 9.81 mg/L respectively. The breakthrough curves are depicted in **Figure 6.4**. It was observed that breakthrough time occurred faster with higher flow rate.

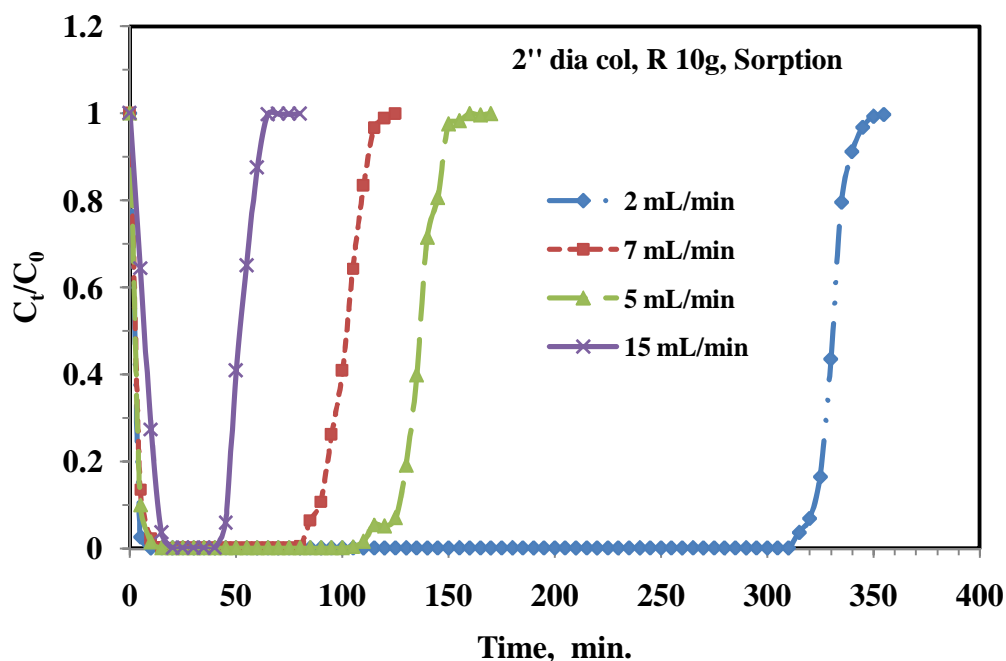


Figure 6.4: Sorption breakthroughs for different flow rates of effluent solution.

The breakthrough time decreases from 315 to 45 min for the flow rates ranging between 2 and 15 mL/min respectively. Also from the experimental data it was observed that the sorption capacity increases with increasing of flow rate. The sorption capacity was increased from 0.91 to 0.95 mg/g PHOA when the volumetric flow rate of uranium solution was changed from 2 to 15 mL/min. The effects of flow rate on adsorption results can be illustrated according to mass transfer concept. With increasing flow rate the concentration gradient on the surface of the PHOA sorbent begins to increase and this leads to increase of mass transfer

on the surface of sorbent beads. Therefore, increase of rate of metal transferring to sorbent surface leads to fast saturation and earlier breakthrough time in higher flow rates. Moreover retention time of metal ions in the column depends on flow rate and with increasing flow rate the contact time of sorbent – metal ions decreases. Hence, the required amount of uranium ions does not have enough time for sorption onto the PHOA surfaces. Therefore, there is a lower uranium removal possibility in lower bed depth in higher flow rate of solution probably due to non-achievement of required residence time. Hence, further study is needed to understand the performance of the column in higher bed depth i.e., with more quantity of sorbent for increasing residence time. However, the overall processing time increases at lower flow rates which is not favourable in industrial applications where large volumes of metal wastewater must be treated [255]. Higher flow rate 15 mL/min was chosen to correlate with sorption study of varying bed depth and column diameter.

6.5.2.3 Effect of sorbent bed height

The other factor that has the great effect on metal uptake capacity in a packed bed column is the height of adsorbent inside the column. To produce different bed heights, 10, 20, 30 and 40 g of the PHOA were added to 2'' ID column. During the experiments the flow rate and uranium solution concentration were maintained in constant values of 15 mL/min and 9.81 mg/L respectively. The obtained breakthrough curves for the different bed heights are shown in **Figure 6.5**. As can be seen from the plots, the breakthrough time was increased with increasing bed height (mass of the sorbent) and reached from about 45 min to 175 min when the PHOA mass changed from 10 to 40 g. It was noticed that the uranium uptake capacity of the PHOA increased with increasing the bed height. The sorption capacity of column changed as 0.95, 0.98, 1.05 and 1.06 mg/g of PHOA for sorbent mass 10, 20, 30 and 40 g respectively. Thus for better performance of packed bed column and higher uranium ion removal capacity of PHOA the higher bed depth of PHOA should be desirable. It is obvious that with higher

quantity of sorbent, more binding sites for sorption are available for sorbate ions. Therefore, higher breakthrough time is expected with increasing bed height in the column. Moreover, with increasing bed depth the residence time of metal ions increases and sorbate ions are getting longer contact time in the process that results higher uptake and removal efficiency [255,256]. Column bed depth should be decided based on the flow rate of the effluent to be treated for which adequate residence time to be assured. To understand the performance it is necessary to carry out the experiment with different column diameter with same flow rate where effect of residence time can be rechecked.

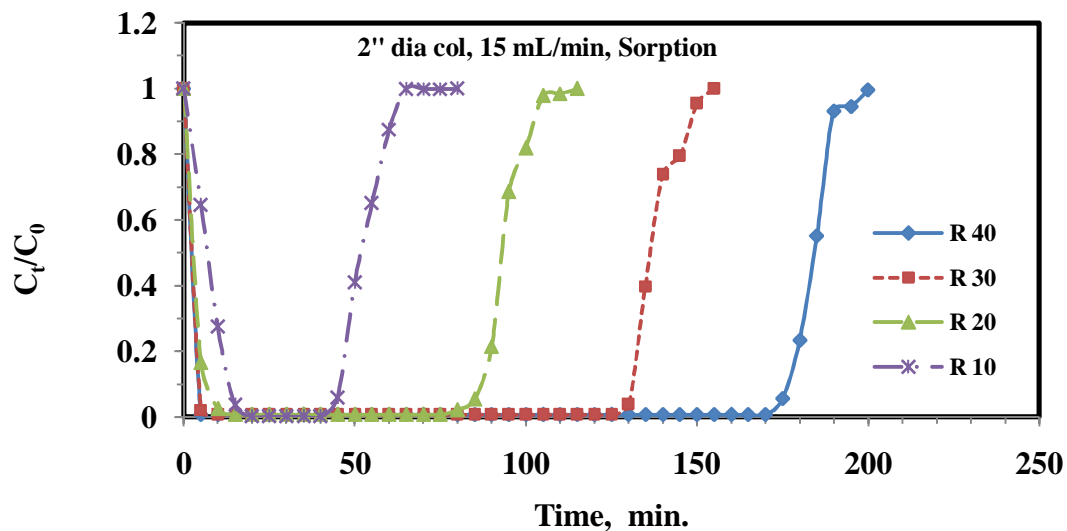


Figure 6.5: Sorption breakthroughs for different masses of sorbent, PHOA loaded in a column (bed height).

6.5.2.4 Effect of column diameter

The effect of column diameter on performance of the column was studied with two more different diameter 2.5” and 3.5” ID. During the experiments the effluent flow rate and initial concentration of feed was maintained in constant values of 15 mL/min and 9.81 mg/L respectively. The breakthrough curves are depicted in **Figure 6.6** and **Figure 6.7**. It was observed that breakthrough time occurred faster with lower bed depth for both the cases of column diameters similar to 2” ID column due to lesser contact time. It was noticed that the

uranium uptake capacity of the PHOA increased with increasing the bed height because higher contact time.

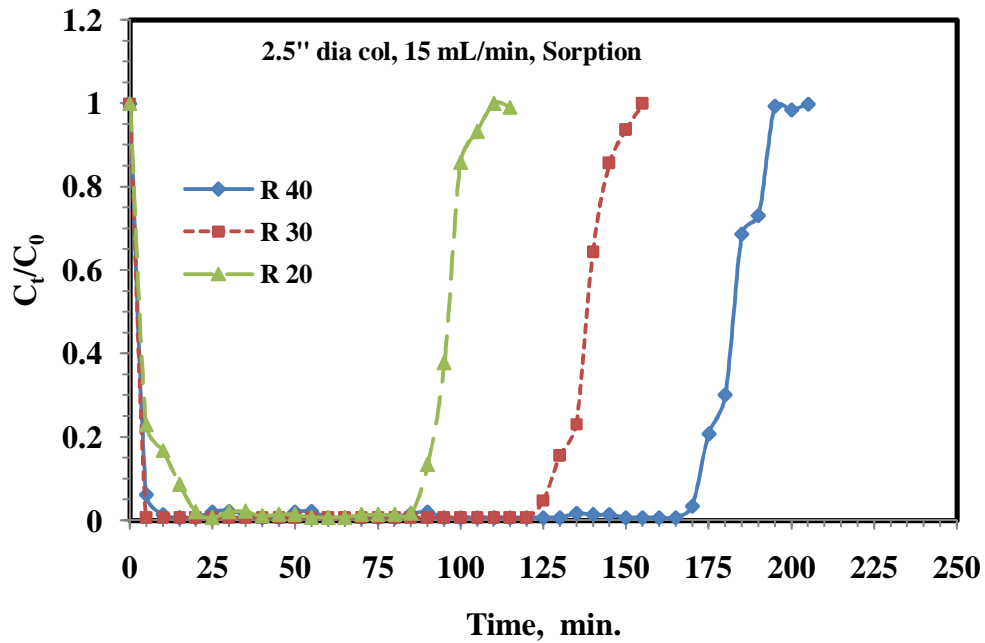


Figure 6.6: Effects of 2.5” ID column diameter on sorption breakthrough.

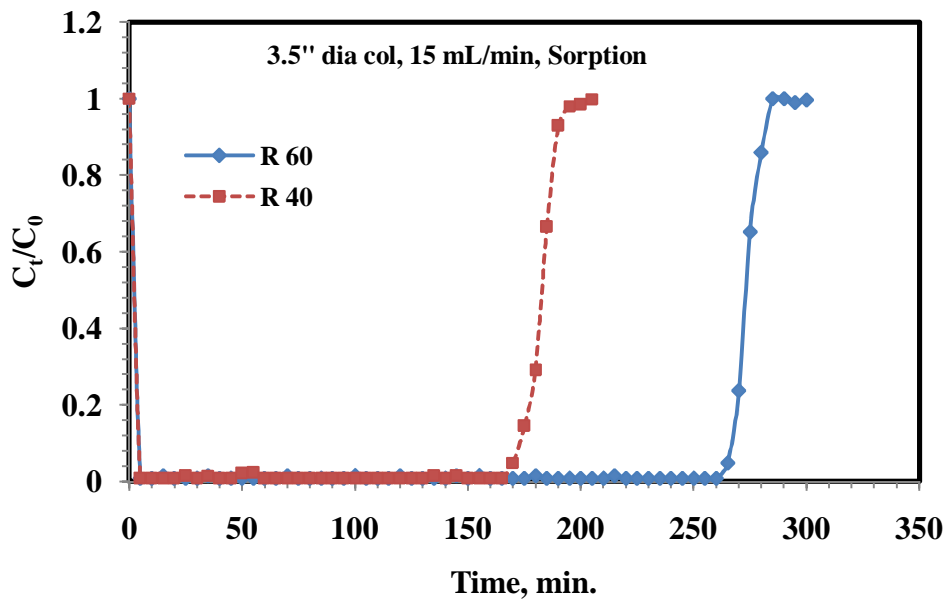


Figure 6.7: Effects of 3.5” ID column diameter on sorption breakthrough.

The sorption capacity of 2.5” ID column changed as 0.89, 0.94, and 1.02 mg/g of PHOA for sorbent mass 20, 30 and 40 g respectively and of 3.5” ID column changed as 0.92 and 0.98 mg/g of PHOA for sorbent mass 40 and 60 g respectively. The results higher sorption

capacity of PHOA with increasing bed height confirms the role of residence time in performance of the column.

6.5.3 Breakthrough curve modelling

6.5.3.1 Application of Thomas model

The Thomas model is suitable for adsorption processes where the external and internal diffusions will not be the limiting step. The column data were fitted to the Thomas model to determine the Thomas rate constant (K_{TH}) and maximum solid-phase concentration (q_0). The determined coefficients and relative constants were obtained using linear regression analysis according to **Equation 6.6** and the results have been shown in **Figure 6.8** for 2" ID column and **Figure 6.9** for 2.5" column and parameters were evaluated and shown in **Table 6.1**. The table shows that the value of q_0 increased and K_{TH} decreased with increasing bed height. The R^2 values range from 0.95 to 0.99.

Table 6.1: Thomas model parameters for 2" ID and 2.5" ID column with different bed height.

PHOA quantity	2" ID column		2.5" ID column	
	K_{th} (mL/min mg)	q_0 (mg/g)	K_{th} (mL/min mg)	q_0 (mg/g)
20	0.029	0.96	0.029	0.96
30	0.022	0.97	0.024	0.97
40	0.018	1.01	0.022	0.98

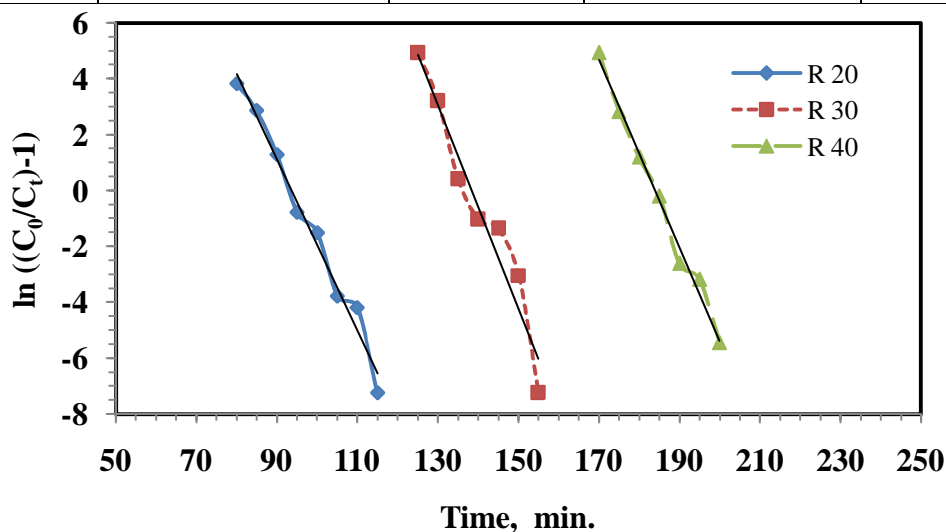


Figure 6.8: Thomas model plot for column 2" ID with different bed height.

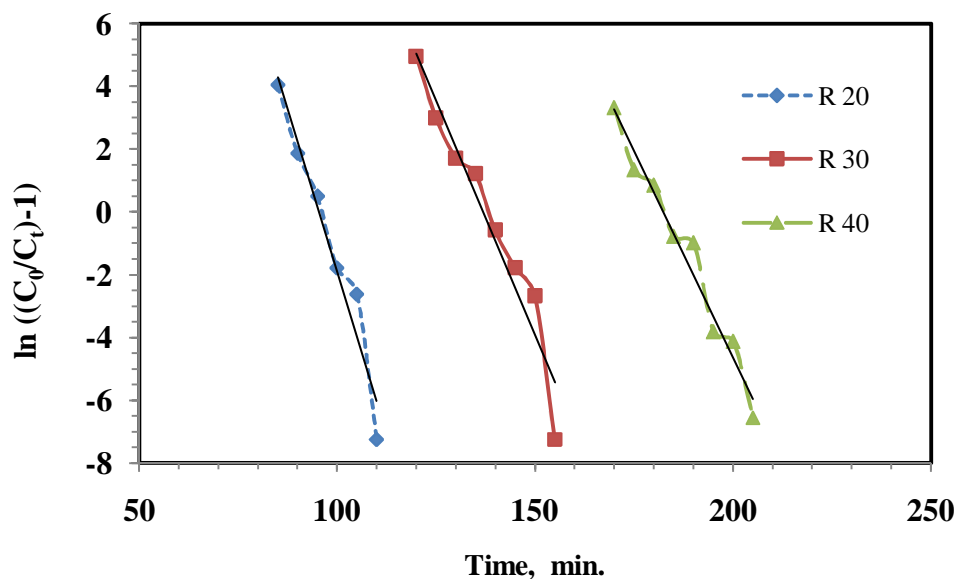


Figure 6.9: Thomas model plot for column 2.5" ID with different bed height.

6.5.3.2 Application of the Adams–Bohart model

For finding the Adams–Bohart parameters a linear relationship between $\ln(C_t/C_0)$ and time (Equation 6.7) was applied for the relative concentration up to about $C_t/C_0 = 0.5$ for breakthrough curves and then the values of saturation concentration (N_0) and kinetics constant (k_a) were calculated through the intercept and slope of the plots. As can be seen from the Figure 6.10 for 2" ID column and Figure 6.11 for 2.5" ID column, this model has a good agreement with the experimental data especially for initial part of breakthrough curves, suggesting that Adams–Bohart model may be valid for the sorption processes where relative concentration region was approximately 0.5 at operating conditions. The k_a , kinetic constant values are found to be in the range of 0.0183 and 0.023 mL/mg.min those are comparable with the pseudo second order kinetic constant value evaluated in batch sorption experimental study (Chapter 4). Additionally the value of N_0 (mg sorbed / L of effluent passed) increases with the increasing of bed depth. Although the Adams–Bohart model provides a simple and comprehensive approach to evaluate sorption column test, its validity is limited in the range of conditions used [257].

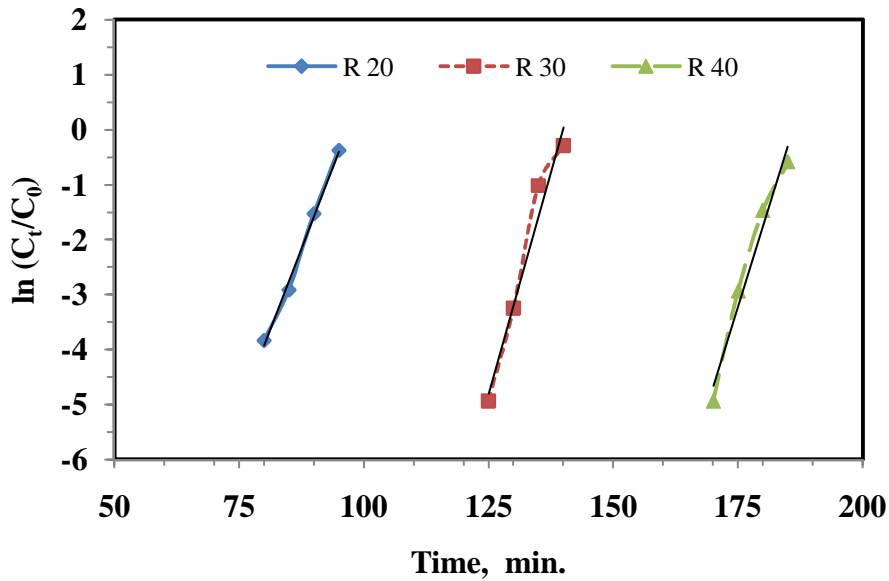


Figure 6.10: Adam-Bohart model plot for column 2'' ID with different bed height.

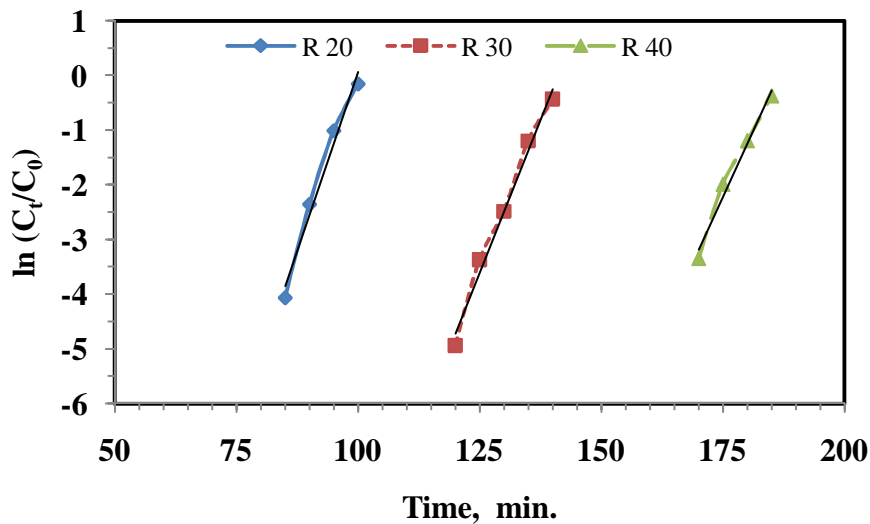


Figure 6.11: Adam-Bohart model plot for column 2.5'' ID with different bed height.

6.5.3.3 Bed Depth Service Time (BDST)

BDST model is used to predict the bed capacity by utilizing the different breakthrough values. The **Equation 6.8** was used for the modelling. A plot of t versus Z is expected to yield a linear curve in which N_0 and k_a could be evaluated, from the slope and y -axis intersection point, respectively. BDST analysis was done, and the linear plot of this model is given in **Figure 6.12**. From the figure, the values of N_0 and k_a were determined to be 0.048 mg/L and 0.047 mL/mg.min, respectively. Besides that, the correlation coefficient value (R^2)

= 1.000) shows that this model is applicable. The constants obtained from this model could be utilized to scaling up the process of this fixed bed column.

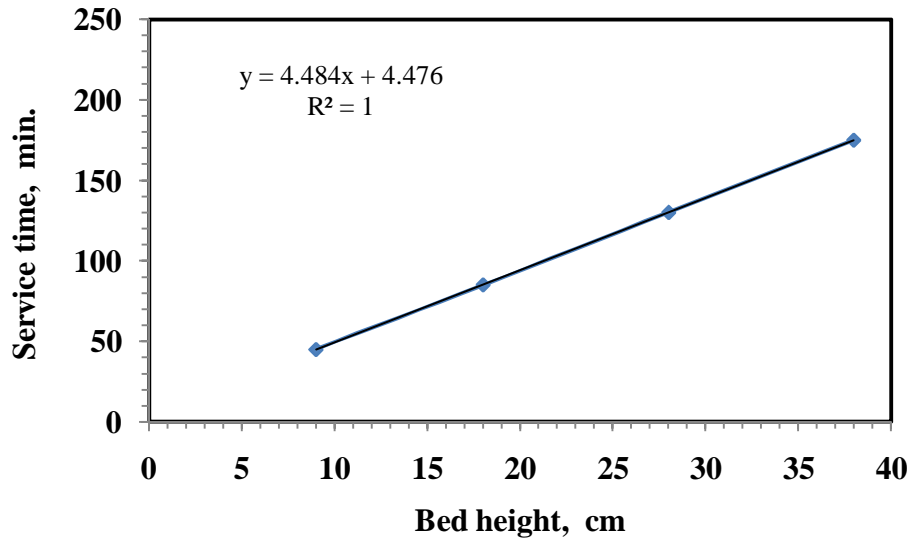


Figure 6.12: Bed depth service time of column at different bed height: $C_0=9.81$ mg/L and flow rate = 15 mL/min.

6.5.3.4 Effect of kinetic constant on breakthrough

The effects of varying k_a at fixed capacity for the sorbate/sorbent combination are shown in **Figure 6.13** based on results derived from **Equation 6.9**. The lower the value of k_a , the greater is the likelihood of an early breakthrough.

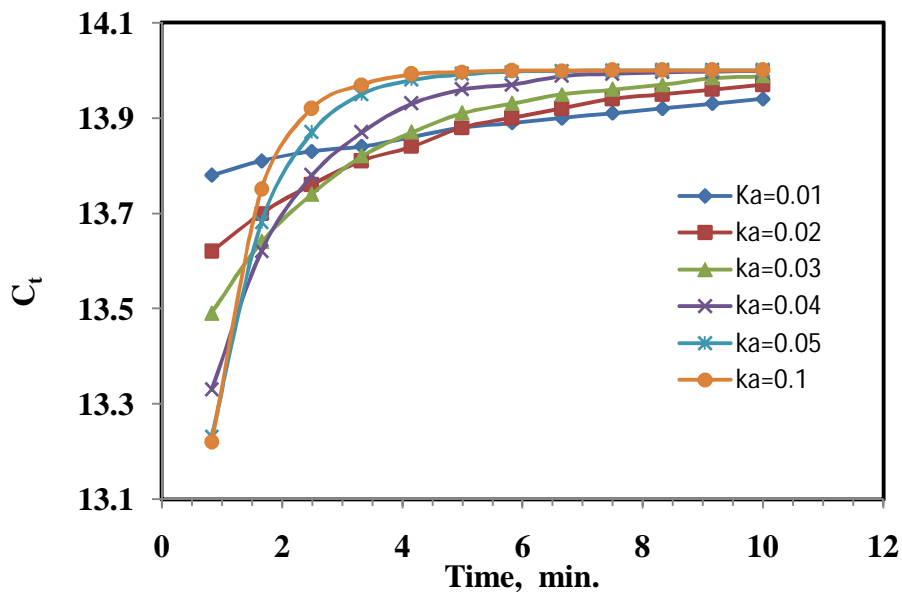


Figure 6.13: Effect of variation of k_a at fixed capacity: $C_0=9.81$ mg/L, flow rate = 15 mL/min.

6.5.4 Evaluation of mass transfer coefficient

Mass transfer coefficient was evaluated using **Equation 6.11** and $\ln ((C_t/C_0)-1/(1 +MK))$ versus t for the initial uranium concentration of 9.81 mg/L gave the straight line of slope $((1 +MK)/MK)\beta S_s$. The value of mass transfer coefficient β was calculated from the slope of the plots and was found to be as 0.54 cm/min (**Figure 6.14**). The β obtained in this study is comparable to the values reported for removal studies of different pollutants.

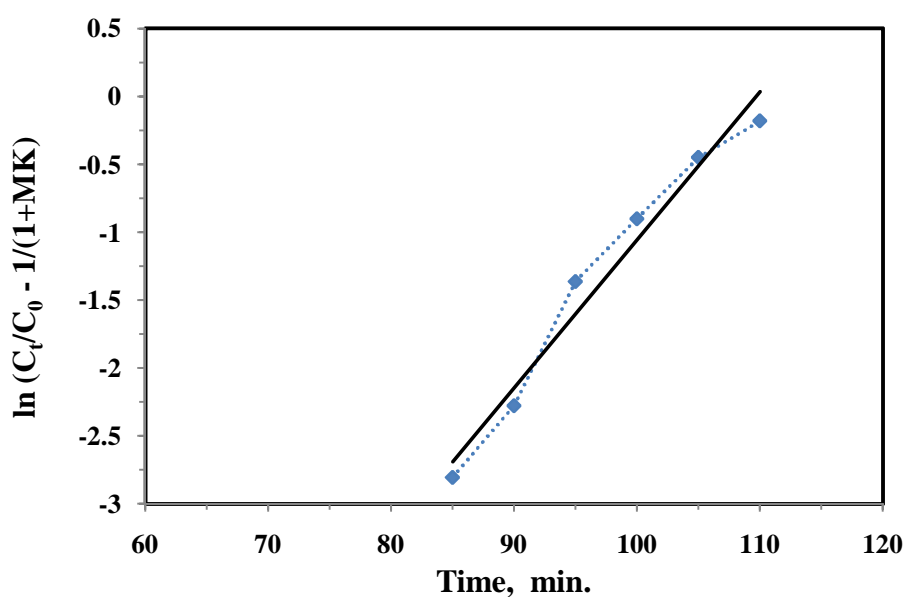


Figure 6.14: Estimation of mass transfer coefficient for sorption of U(VI) on PHOA at pH 9.

6.5.5 Elution performance of column

6.5.5.1 Effect of wastewater flow rate

Experiments were carried out with four different flow rates in 2" ID column and results have been shown in **Figure 6.15**. Breakthrough time (regeneration time) increases with increasing flow rate as expected due to low elution residence time. Breakthrough time (for outlet uranium concentration < 1 mg/L) with flow rate 15 mL/min is 75 min whereas the same with 2 mL/min is 45 min. The effect is reverse as seen in the effect of column sorption process. For all the cases sharp decrease of outlet uranium concentration in initial periods indicates faster elution kinetics and higher uranium concentration gradient between the sorbent surface

and eluent and lower concentration gradient in latter stage is may be due to lower concentration gradient.

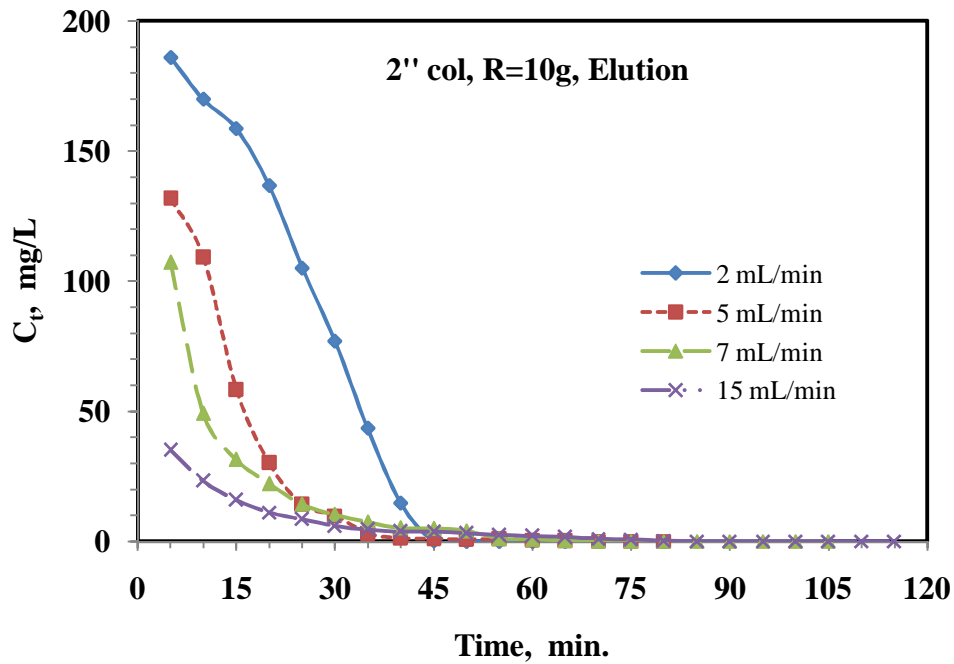


Figure 6.15: Effect of flow rate on elution breakthrough: 1M HCl

6.5.5.2 Effect of PHOA bed depth

Effect of sorbent bed depth (mass of PHOA) on elution performance was evaluated in 2" ID column and results are shown in Figure 6.16.

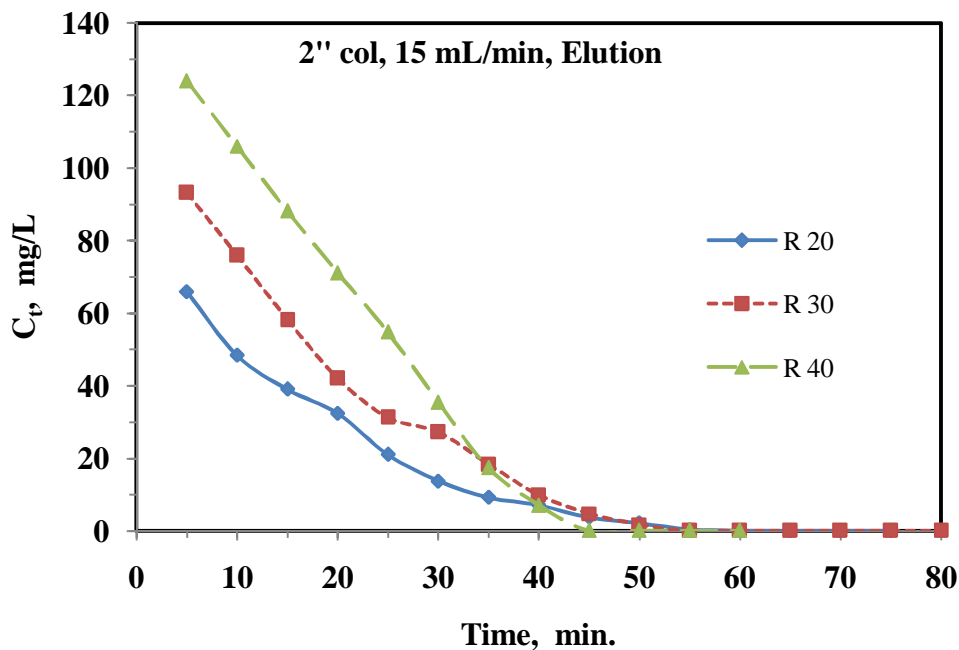


Figure 6.16: Effect of PHOA bed depth on elution breakthrough in 2" column: 1M HCl

The regeneration times (outlet uranium concentration < 1 mg/L) for 20, 30 and 40 g PHOA were found to be 60, 55 and 45 min respectively. Lower regeneration time with increasing sorbent mass in a fixed diameter column is due to higher residence time of the eluent leading to higher mass transfer interaction of eluent and sorbent surface. For confirming the cause of residence time the experiments were conducted in varying elution column diameter which has been shown in next study.

6.5.5.3 Effect of elution column diameter

To confirm the cause of contact time on regeneration time additional two different diameter 2.5" and 3.5" ID columns were used with variation of sorbent. Results have been shown in **Figure 6.17** and **Figure 6.18** for 2.5" and 3.5" ID column respectively. From **Figure 6.17** the regeneration time for 20, 30 and 40 g sorbent were found to be 50, 45 and 40 min respectively, which confirm the similar trend for 2" ID column. For further confirmation in higher diameter column (3.5" ID), 40 min regeneration time was obtained with 60 g sorbent and 45 min with 40 g sorbent (**Figure 6.18**).

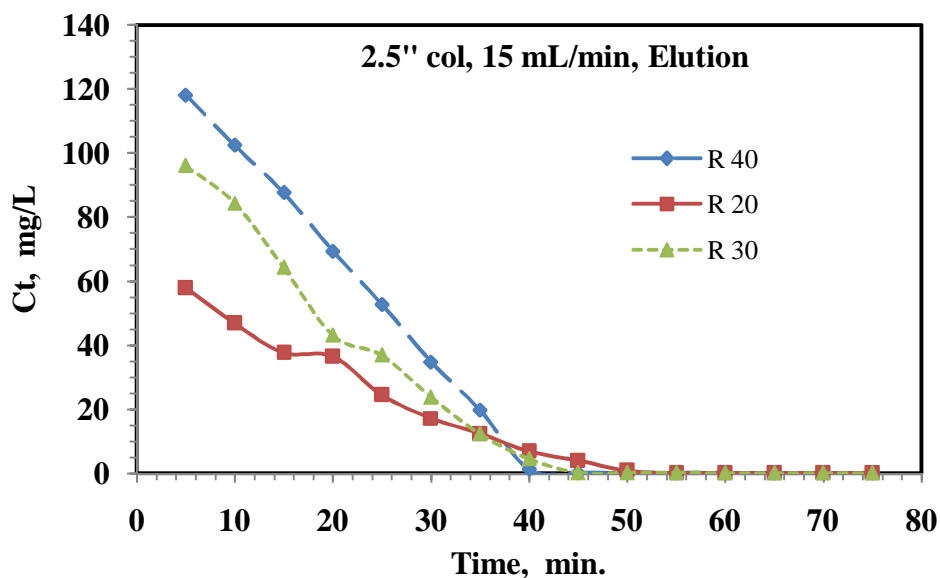


Figure 6.17: Effect of PHOA bed depth on elution breakthrough in 2.5" column: 1M HCl

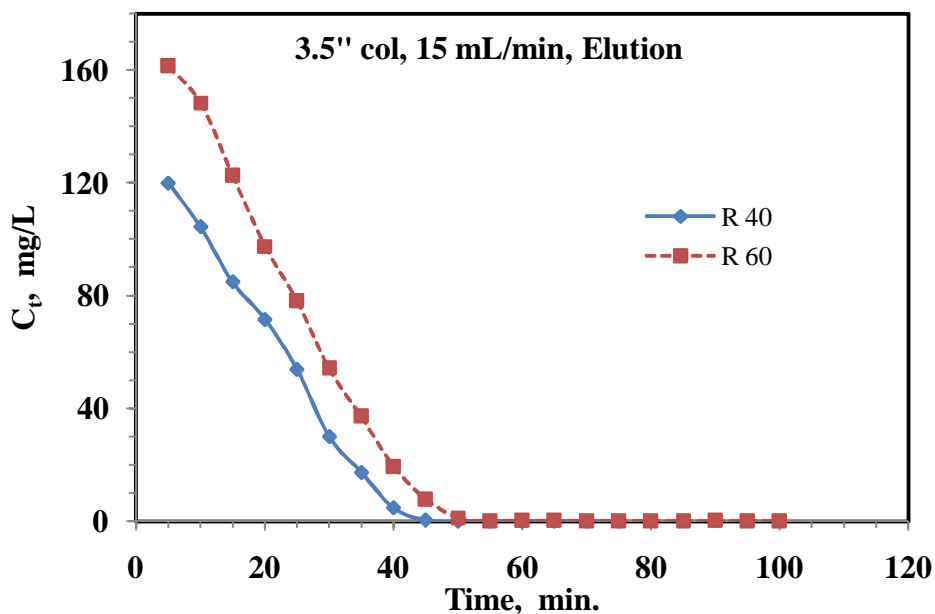


Figure 6.18: Effect of PHOA bed depth on elution breakthrough in 3.5” column: 1M HCl

6.6 Conclusion

Column study for continuous sorption and elution process is important for industrial application to treat wastewater for removal and recovery of uranium. Based on the capacity required for the wastewater treatment process flow rate is decided which is generally in higher side. Sorption and elution performance of PHOA sorbent has been evaluated for treating effluent of uranium processing plant in four different diameters column namely 1”, 2”, 2.5” and 3.5” ID. In sorption operation uranium uptake is reduced and breakthrough time is increased with increasing flow rate which is reverse in trend with increasing sorbent quantity (bed depth) due to effect of residence time of sorbate with sorbent. Overall uptake in the range of 0.9 – 1.0 mg/g of sorbent was obtained with flow rate 15 mL/min for 2” – 3.5” ID columns having 20 – 40 g sorbent. Sorption process follows the Adam-Bohart model and kinetic rate constant and mass transfer coefficient were found to be 0.047 g/mg.min and 0.54 cm/min respectively. Elution process is kinetically faster than the sorption process. Regeneration time is reduced with increasing bed height due to more contact between sorbent and sorbate.

CHAPTER – 7

MOLECULAR MODELING FOR URANIUM SORPTION ONTO PHOA

7.1 Introduction

In manufacturing processes the chemical industry faces considerable economic, environmental and social challenges in 21st century and the aspect of computational technology is most critical to the chemical industry for material development. The main goal of computational materials science is the rapid and accurate prediction of properties of new materials before after their development and production. In order to explore the utilisation of the newly developed material it is essential to predict and characterise these properties. This is of particular importance in the field of polymeric sorbent, where the properties of the material depend on the molecular structure. Molecular mechanics is a faster and more approximate method for computing the structure and behaviour of molecules or materials and useful for studying the behaviour of the polymer. Application of computational chemistry in chemical processing are widely practiced specially in product development. Computational molecular science so called molecular modelling involves model of chemical system at the molecular or atomistic level as well as predictions of quantum effects. In basic molecular level this involves the solution of Schrodinger equation for electronic motion [258]. The molecular modelling provides quantitative estimation of engineering parameters like heat of formation, entropies, total energy, transport properties etc. And it gives valuable insight into the properties of new materials so necessary for efficient process development. By reliably predicting thermo chemistry, it is possible to examine the possibility of reaction pathways to determine whether the product or produced complex (for polymer sorption) is thermodynamically stable.

The fundamental starting point of the scheme is the quantum chemistry and quantum mechanics ab-initio calculation to obtain a solution of the Schrodinger equation and for ultimately defining interaction potential and force fields resulting from hydrogen-bonding and van der Waals interactions. Thereafter with the obtained results geometrical structure of

the resultant stable product/complex material can be evaluated using suitable macroscopic model (**Figure 7.1**). Structures and properties of materials are used for developing the methods as well as for validation of the obtained force fields. Structure and properties may directly also be used for defining reaction mechanism which is key input to any process development [259].

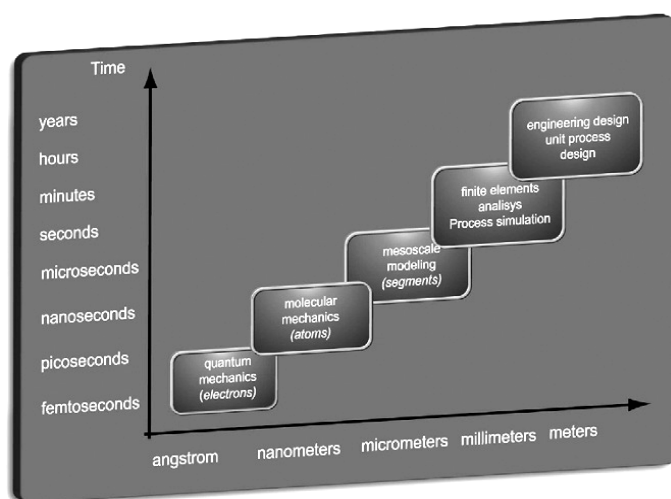


Figure 7.1: Multi scale molecular modelling scheme

In this direction molecular modelling study was carried out for understanding the mechanism of uranium sorption onto the PHOA and for evaluating minimum energy structure of possible binding geometry.

7.2 Materials and methods

For experiment same materials and method as discussed in **Chapter 3** and **Chapter 4** for sorbent, synthetic uranium solution, reagents, apparatus and sorption/ uptake evaluation procedures was followed and results of the Chapters were used for analysis.

7.3 Computational Methods

Minimum energy structures for resin unit and its complexes with UO_2^{2+} are obtained applying a popular non-local correlated hybrid density functional, namely, B3LYP. Gaussian type atomic basis functions, 6-31+G(d) are adopted for H, C, N and O atoms and for U atom a very recently suggested basis set, SARC-ZORA [260] are considered for all the

calculations. SARC-ZORA basis sets are segmented all-electron scalar relativistic basis sets in which the coefficients of contracted GTOs are optimized for use with the ZORA scalar relativistic Hamiltonian. This particular basis sets for U are obtained from Extensible Computational Chemistry Environment Basis Set Database, Pacific Northwest National Laboratory [261]. The quasi-Newton-Raphson based algorithm is applied to carry out geometry optimization to locate the minimum energy structure in each case. Macroscopic solvation effect of solvent water is incorporated in energy calculation through polarizable continuum model (PCM). All these calculations are carried out with the GAMESS suite of ab-initio programs on a LINUX cluster platform [262]. Visualization of molecular systems has been carried out by MOLDEN program.

7.4 Results and discussion

7.4.1 Computational studies of complexes

To examine the modes of binding of uranyl ion with the sorbent PHOA, quantum chemical calculations are carried out on monomer unit of the sorbent as well as many possible complexes between resin units and uranyl ion in absence and presence of a few water molecules. Full geometry optimization of possible complexes is performed in the gas phase as well as in water medium following a macroscopic solvation model.

7.4.1.1 Uranyl ion with two monomer functional groups from different sorbent chain

The minimum energy structures predicted are presented in Figures below. **Figure 7.2** depicts the optimized structure of a complex between two monomer units of the sorbent (different chain) and UO_2^{2+} in gas phase where two monomer units approach in anti fashion, $-\text{NHO}^-$ as well as $\text{C}=\text{O}$ groups of two monomer units are in trans position. In the minimum energy structure of the complexes (**Figure 7.2** and **7.3**), the calculated $\text{U}=\text{O}$ and $\text{U}-\text{ON}$ bond distances are 1.72, 2.43 Å. Bond distance between U and carbonyl O ($>\text{C}=\text{O}$) is predicted as 2.85 Å in this hexa-coordinated complex.

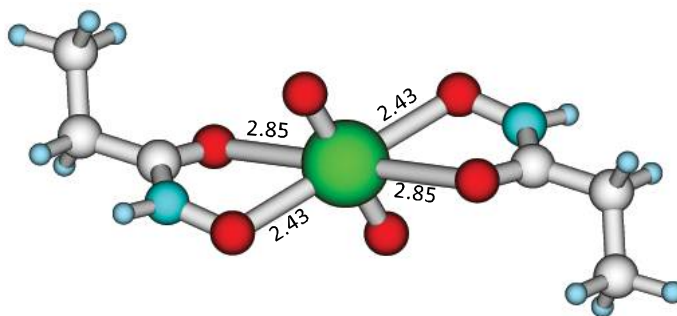


Figure 7.2: Optimised structure of complex containing two functional groups (from different sorbent chain) and one uranyl ion in gas phase, without water, anti position.

When the two monomer units are in syn fashion in the complex (**Figure 7.3**) keeping -NHO^- as well as C=O groups of two monomer units in syn position, the calculated U-O(=C) and U-O(-N) bond distances are 2.79, 2.48 Å respectively.

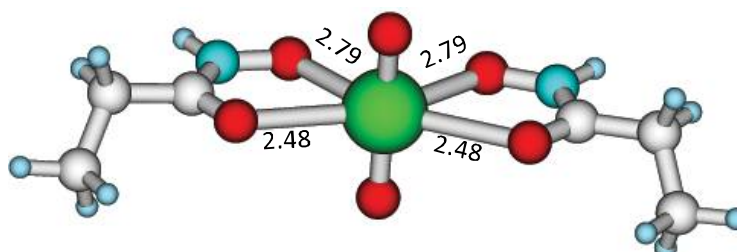


Figure 7.3: Optimised structure of complex containing two functional groups (from different sorbent chain) and one uranyl ion in gas phase, without water, syn position.

This syn complex is also hexa-coordinated and predicted to be more stable than anti complex by 0.2 kcal/mol energy. When these structures are re-optimized in presence of water medium following PCM continuum solvation model, structures are predicted to be tetra coordinated with equal stability in both the cases. Based on predicted bond angles of these complexes, it is noted that the complex can accommodate one or two water molecules to form hepta or octa coordinated complexes.

7.4.1.2 Uranyl ion with two monomer functional groups from different sorbent chain and water

To examine the feasibility, complexes are first designed with one water molecule based the predicted structures without any water molecule as discussed above and optimized in gas

Figure 7.6 and the corresponding minimum energy structure with syn configuration is displayed in **Figure 7.7**.

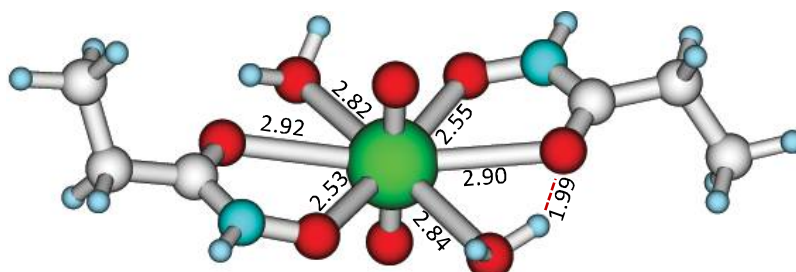


Figure 7.6: Optimised structure of complex containing two functional groups (from different sorbent chain) and one uranyl ion in liquid phase with two waters, anti position.

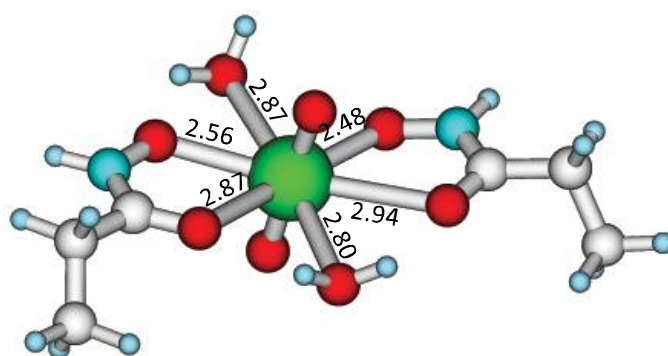


Figure 7.7: Optimised structure of complex containing two functional groups (from different sorbent chain) and one uranyl ion in liquid phase with two waters, syn position.

It is clearly seen that in both the cases the complexes are octa coordinated and both the water molecules are coordinated to U. Calculated energy suggests that syn configuration is more stable than the trans / anti one by 0.5 kcal/mol. Attempts are made to obtain structures of these complexes adding three water molecules. However, the third water molecule is observed to be not bonded with U and residing in the second hydration shell.

7.4.1.3 Two uranyl ion with four functional group and water

To mimic the experimental situation of sorbent laden with UO_2^{2+} , calculations are extended to system with four monomer units of sorbent and two UO_2^{2+} ions. Optimized most stable

minimum energy structure is displayed in **Figure 7.8 (a)** where U are hexa coordinated. Then a molecule of water is added to the complex and it is re-optimized. The predicted complex is shown in **Figure 7.8 (b)** in which coordination by one C=O group is displaced by the water molecule keeping central metal ion to be hexa coordinated.

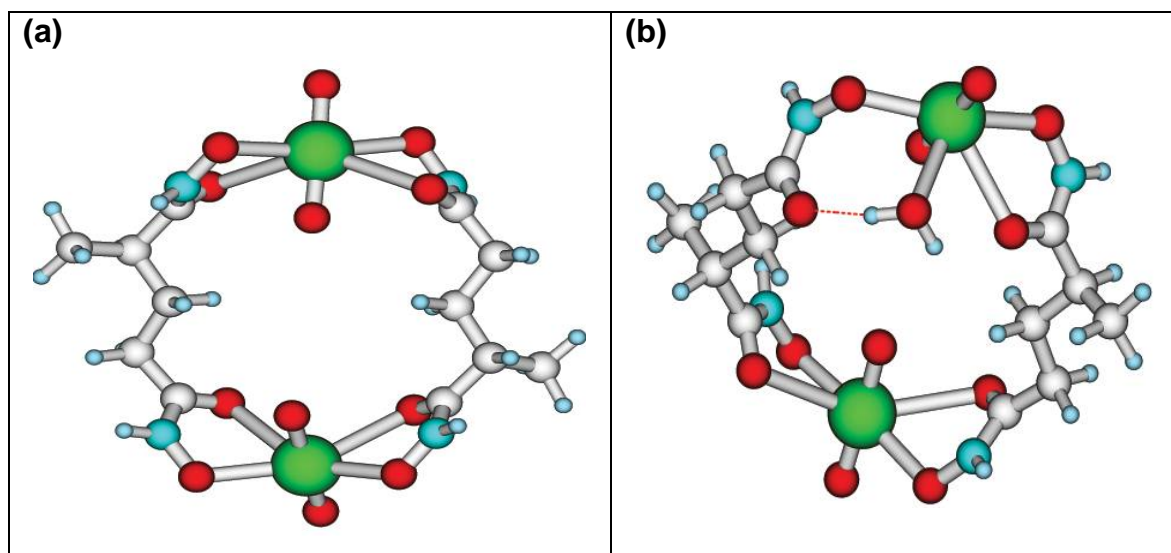


Figure 7.8: Optimised structure of complex containing four functional groups and two uranyl ions (a) without water, (b) with one water

When second water molecule is added into the system keeping it inside the cavity of the complex and allowed to relax, a C=O group from the second metal centre is displaced by the second water molecule. The minimum energy structure is shown in **Figure 7.9**.

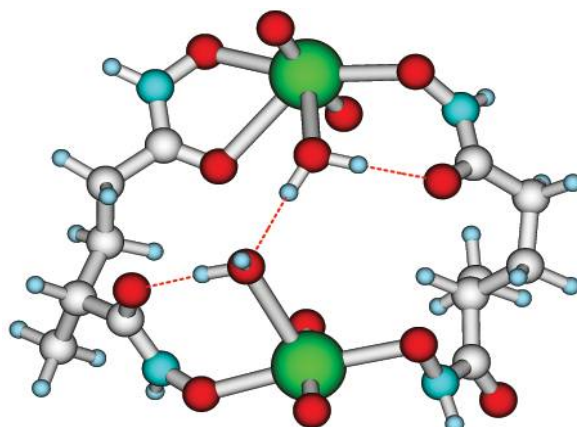


Figure 7.9: Optimised structure of complex containing four functional groups and two uranyl ions with two waters

To examine how much water can be accommodated in the cavity of the complex and the status of these water molecules in the system, third water molecule is also added to the cavity of the complex followed by geometry optimization. It is observed that the third water remains in the cavity and forms H-bonding with other two water molecules (as shown in **Figure 7.10**).

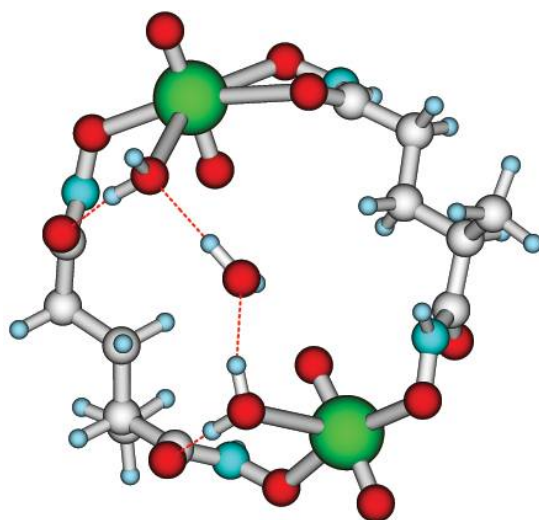


Figure 7.10: Optimised structure of complex containing four functional groups and two uranyl ions with three waters

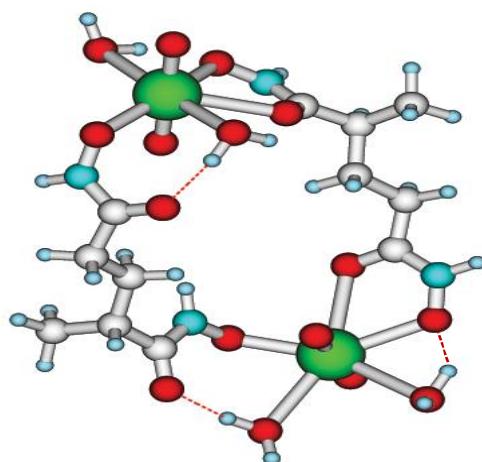


Figure 7.11: Optimised structure of complex containing four functional groups and two uranyl ions with four waters

However, it is not directly bonded to either of the metal ions. **Figure 7.11** is obtained on geometry optimization of the complex in which four water molecules are added to the

system. Only one water molecule remains in the cavity in case of the most stable structure. It is clear from these calculations that in the part of the sorbent having two monomer units in each of the parallel layers, two units of UO_2^{2+} can be absorbed and three molecules of water can reside in the cavity.

7.4.2 Validation of the modelling results

From the molecular modelling study for uranium sorption onto PHOA it is clearly understood that hydroxamic acid ($-\text{CO} - \text{NHOH}$) functional group is participating in the complex formation with $-\text{NH} - \text{O} -$ and with $-\text{CO} -$ bonding with U for all combinations which was determined and confirmed by FTIR and Raman spectra studies in **Figure 3.10 (Para 3.4.5)** and **Figure 3.11, Table 3.2 (Para 3.4.6)** respectively with shifting of peaks. Modelling analysis using solvation method predicted involvement of water molecules in the stable complex formation with direct bonding with U as well as with hydrogen bonding. Similar inference was drawn in **Chapter 3, Para 4.3.4** with DSC and TG & dTG studies (refer **Figure 3.8 and Figure 3.9 (b)** respectively) where removal of hydrogen bonded water was confirmed at temperature 121°C and removal of bonded water was confirmed at temperature 155°C . Stable $\text{UO}_2^{2+} - \text{PHOA}$ complex of two functional groups and one UO_2^{2+} ion (all figures of this chapter) has been predicted in the molecular modelling study. Similar observation was obtained in batch mode sorption experimental studies (**Chapter 4, Para 4.4.8.1**) where 1:2 U:PHOA type complex was predicted using slope analysis method of complex reaction.

Conclusion and Recommendation

Synthesis of a new novel sorbent, Poly-acryl Hydroxamic Acid (PHOA) has been carried out and characterised by evaluating different physical parameters and using different instrumental techniques. Various sorption as well as elution parameters have been evaluated in batch and in column experiments which are useful for industrial application. It was observed that the sorbent, PHOA can be selectively used for recovery of U(VI) from nuclear wastewater containing a number of other metal ions and anions. The sorption – desorption cycle performance test shows that the sorbent can be recycled without any significant loss. Molecular modelling study helped to understand the mechanism of U-PHOA complex formation and to confirm the stability of the complex. The important outcomes indicated potential application of the in-house prepared novel PHOA beads for removal of hazardous uranium ions from nuclear industrial effluents without pre-treatment. Complete flow sheet of the uranium separation and recovery process has been established and demonstrated with scientific and technological analysis for nuclear effluent treatment using the novel sorbent, PHOA.

The sorbent has been synthesized using readily available non-toxic chemicals and following simple methods. Synthesis cost of PHOA is comparable and lesser than the cost of sorbents commercially available in market for the purpose. No pre-treatment or pre-conditioning is required for treatment of nuclear wastewater and the sorbent can be directly used as prepared. This assures techno-economical viability of the developed process. It is also to be noted that the unconventional sources of uranium should not be seen to be competing with primary resources. They should be recognized as supplementing and augmenting the uranium supply. Only the incremental cost of uranium recovery against the main processing cost to be considered in addition to the betterment of environmental aspect.

References:

- [1] T.K. Mukherjee, H. Singh, 14th Indian Nuclear Society Annual Conference (INSAC), 2003, IT-7, 1-9.
- [2] Integrated Energy Policy: Report of the Expert Committee. Planning Commission Document, Government of India, (2006) 1-147.
- [3] B. Bhattacharjee, An overview of R&D in fuel cycle activities of AHWR, 4th Indian Nuclear Society Annual Conference (INSAC), IT-1 (2003) 1-27.
- [4] A. Krestou, A. Xenidis, D. Panias, Mechanism of aqueous uranium (VI) uptake by 1011 natural zeolitic tuff, *Miner. Eng.* 16 (2003) 1363–1370.
- [5] Department of Atomic Energy, Annual Report 4 (2011) 1211-12.
- [6] C.K. Gupta and H. Hingh, “Uranium Resource Processing: Secondary Resources”, Springer, Germany, 2003
- [7] A. Suresh, T. G. Srinivasan, and P. R. Vasudeva Rao, , Extraction of U(VI), Pu(IV) and Th(IV) by some trialkyl phosphates, *Solvent Extr. Ion Exch.* 12 (4) (1994) 727-744.
- [8] IUPAC SC-Database: A comprehensive database of published data on equilibrium constants of metal complexes and ligands.
- [9] N. N. Greenwood, A. Earnshaw, *Chemistry of the Elements* (2nd ed.). Butterworth-Heinemann. (1997) 1273–1274 ISBN 0080379419.
- [10] A.N. Holden, *Physical Metallurgy of Uranium*, Addison-Wesley, London (1958).
- [11] R.J. Finch and T. Murakami, *Rev. Miner.*, 38 (1999) 91-180.
- [12] J. Plant, P. R. Simpson, B. Smith and B.F. Windley, *Rev. Miner.*, 38 (1999) 255-319.
- [13] P.C. Burns and R.J. Finch, *Am. Miner.*, 84 (1999) 1456-1460.
- [14] L.H. Fuchs, and E. Gebert, *Am. Miner.*, 43 (1958) 243- 248.

- [15] Gmelin Hand Book of Inorganic Chemistry, Suppl. Ser., Uranium, C14 Springer-Verlag, Berlin, Heidelberg, and New York (1981).
- [16] C. D. Harrington, A. E. Ruehle, (Ed.) Uranium Production Technology, D.Van Nostrand Company Inc., New Jersey (1959).
- [17] S. Pal, S. Prabhakar, K.L. Thalor, and P.K. Tewari, "In-house Sorbents for Water Treatment and Value Recovery", Indian Nuclear Society News, 6 (3) (2009) 39-40.
- [18] C.R. Hammond, The elements, in: Handbook of Chemistry and Physics, 81st ed., CRC Press, ISBN: 0-8493-0481-4 (2000).
- [19] B.S. Hopkins, Chemistry of the Rarer Elements, D.C. Heath and Company, (1923).
- [20] WHO, Guidelines for Drinking Water Quality, 2nd edition, Addendum to vol. 2. Health Criteria and Other Supporting Information, WHO/EOS/98.1, Geneva, (1998) 283.
- [21] WHO, Guidelines for Drinking Water Quality, 3rd edition, (2003).
- [22] D.M. Taylor, S.K. Taylor, Environmental uranium and human health, Rev. Environ. Health 12 (1997) 147–157.
- [23] D.K. Craig, Chemical and Radiological Toxicity of Uranium and its Compounds, Westinghouse Savannah River Company, U.S.A, (2001).
- [24] H. Coetze, F. Winde, P.W. Wade, An assessment of sources, pathways, mechanisms and risks of current and potential future pollution of water and sediments in gold-mining areas of the Wonderfonteinspruit catchment Report to the Water Research Commission, Research Report No.1214/1/06 (2006).
- [25] A.D. Rollett, Applications of Texture Analysis, John Wiley and Sons, 108 ISBN: 0-470-40835-9 (2008).

- [26] N.H. Harley, E.C. Foulkes, L.H. Hilborne, A. Hudson, C.R. Anthony, A review of the scientific Literature as it pertains to gulf war illness, National Defense Research Institute, Rand. 7 (1999).
- [27] C.C. Choy, G.P. Korfiatis, X. Meng, Removal of depleted uranium from contaminated soils, *J. Hazard. Mater.* 136 (2006) 53–60.
- [28] M. Alrakabi, G. Singh, A. Bhalla, S. Kumar, A. Srivastava, B. Rai, N. Singh, J.S. Shahi, D. Mehta, Study of uranium contamination of ground water in Punjab state in India using X-ray fluorescence technique, *J. Radioanal. Nucl. Chem.* 294 (2012) 221–227.
- [29] H.A. Saleem, *Mining, the Environment, and Indigenous Development Conflicts*, The University of Arizona Press, ISBN: 0-8165-2312-6 (2009).
- [30] J. Pasternak, *Yellow Dirt: A Poisoned Land and a People Betrayed*, Free Press, ISBN: 1416594825, 149 (2010).
- [31] C. Shuey, *Uranium Exposure and Public Health in New Mexico and the Navajo Nation: A Literature Summary*, Southwest Research and Information Centre, Occupational Exposures and Health Effects, (2000).
- [32] R. Pinderhughes, The impact of race on environmental quality: an empirical and theoretical discussion, *Soc. Perspect.* 39 (1996) 231–248.
- [33] A. Krestou, A. Xenidis, D. Panias, Mechanism of aqueous uranium (VI) uptake by natural zeolitic tuff, *Miner. Eng.* 16 (2003) 1363–1370.
- [34] A. Meinrath, P. Schneider, G. Meinrath, Uranium ores and depleted uranium in the environment, with a reference to uranium in the biosphere from the Erzgebirge/Sachsen, Germany, *J. Environ. Radioact.* 64 (2003) 175–193.
- [35] C. Mitsakou, K. Eleftheriadis, C. Housiadas, M. Lazaridis, Modeling of the dispersion of depleted uranium aerosol, *Health Phys.* 84 (2003) 538–544.

- [36] P.X. Sheng, Y.P. Ting, J.P. Chen, L. Hong, *J. Colloid Interface Sci.* 275 (2004) 131.
- [37] M. Sprynskyya, I. Kovalchuk, B. Buszewski, *J. Hazard. Mater.* 181 (2010) 700.
- [38] A. Mellah, S. Chegrouche, M. Barkat, The removal of uranium(VI) from aqueous solutions onto activated carbon: kinetic and thermodynamic investigations, *J. Colloid Interface Sci.* 296 (2006) 434–441.
- [39] V.K. Gupta, Alok Mittal, Jyoti Mittal, *J. Colloid Interface Sci.* 343 (2010) 463.
- [40] S. Karthikeyan, V.K. Gupta, R. Boopathy, A. Titus, G. Sekaran, *J. Mol. Liq.* 173 (2012) 153.
- [41] V.K. Gupta, I. Ali, T.A. Saleh, A. Nayak, S.H. Agarwal, *RSC Adv.* 2 (2012) 6380.
- [42] A. Mellah, S. Chegrouche, M. Barkat, *Hydrometallurgy* 85 (2007) 163.
- [43] B. Yu Kornilovich, I.A. Kovalchuk, G.N. Pshinko, E.A. Tsapyuk, A.P. Krivoruchko, *J. Water Chem. Technol.* 22 (2000) 43.
- [44] V.K. Gupta, R.N. Goyal, R.A. Sharma, *Anal. Chim. Acta* 647 (2009) 66.
- [45] H. Singh, S.L. Mishra, R. Vijayalakshmi, *Hydrometallurgy* 73 (2004) 63.
- [46] A.M. Shoushtari, M. Zargaran, M. Abdouss, *J. Appl. Polym. Sci.* 101 (2006) 2202.
- [47] T.R. Prasadao, P. Metilda, J.M. Gladis, *Talanta* 68 (2006) 1047.
- [48] V.V. Goncharuk, B.Yu. Kornilovich, V.M. Pavlenko, M.I. Babak, G.N. Pshinko, B.V. Pysmennyi, I.A. Kovalchuk, V.G. Safronova, *J. Water Chem. Technol.* 23 (2001) 44.
- [49] S. Abbasizadeh, A.R. Keshtkar, M.A. Mousavian, *Chem. Eng. J.* 220 (2013) 161.
- [50] V.K. Gupta, B. Gupta, A. Rastogi, Shilpi Agarwal, A. Nayak, *J. Hazard. Mater.* 186 (2011) 891.
- [51] V.K. Gupta, A. Mittal, A. Malviya, J. Mittal, *J. Colloid Interface Sci.* 355 (2009) 24.
- [52] V.K. Gupta, A. Rastogi, *J. Hazard. Mater.* 163 (2009) 396.

- [53] X. Ren, S. Wang, S. Yang, J. Li, Influence of contact time, pH, soil humic/fulvic acids, ionic strength and temperature on sorption of U(VI) onto MX-80 bentonite, *J. Radioanal. Nucl. Chem.* 283 (2009) 253–259.
- [54] X. Song, Y. Wang, J. Cai, S. Lu, Y. Chen, Interaction of U(VI) with Na-attapulgite in the presence and absence of humic acid as a function of pH, ionic strength and temperature, *J. Radioanal. Nucl. Chem.* 295 (2012) 685–695.
- [55] G. Zhao, T. Wen, X. Yang, S. Yang, J. Liao, J. Hu, et al., Preconcentration of U(VI) ions on few-layered graphene oxide nanosheets from aqueous solutions, *Dalton Trans.* 41 (2012) 6182–6188.
- [56] Y. Zhao, J. Li, L. Zhao, S. Zhang, Y. Huang, X. Wu, et al., Synthesis of amidoxime-functionalized Fe₃O₄@SiO₂ core-shell magnetic microspheres for highly efficient sorption of U(VI), *Chem. Eng. J.* 235 (2014) 275–283.
- [57] X.K. Wang, C.L. Chen, X. Zhou, X.L. Tan, W.P. Hu, Diffusion and sorption of U(VI) in compacted bentonite studied by a capillary method, *Radiochim. Acta* 93 (2005) 273–278.
- [58] S.H. Ahmed, E.M. El Sheikh, A.M.A. Morsy, Potentiality of uranium biosorption from nitric acid solutions using shrimp shells, *J. Environ. Radioact.* 134C (2014) 120–127.
- [59] J. Wei, X. Zhang, Q. Liu, Z. Li, L. Liu, J. Wang, Magnetic separation of uranium by CoFe₂O₄ hollow spheres, *Chem. Eng. J.* 241 (2014) 228–234.
- [60] M. Zeng, Y. Huang, S. Zhang, S. Qin, J. Li, J. Xu, Removal of uranium(vi) from aqueous solution by magnetic yolk-shell iron oxide @ magnesium silicate microspheres, *RSC Adv.* 4 (5021) (2014).

- [61] B. Van der Bruggen, C. Vandecasteele, Removal of pollutants from surface water and groundwater by nanofiltration: overview of possible applications in the drinking water industry, *Environ. Pollut.* 122 (2003) 435–445.
- [62] P. Bacchin, D. Si-Hassen, V. Starov, M. Clifton, P. Aimar, A unifying model for concentration polarization, gel-layer formation and particle deposition in cross-flow membrane filtration of colloidal suspensions, *Chem. Eng. Sci.* 57 (2002) 77–91.
- [63] A. Favre-Reguillon, G. Lebizit, J. Foos, A. Guy, M. Draye, M. Lemaire, Selective concentration of uranium from seawater by nanofiltration, *Ind. Eng. Chem. Res.* 42 (2003) 5900–5904.
- [64] C. Bellona, J.E. Drewes, P. Xu, G. Amy, Factors affecting the rejection of organic solutes during NF/RO treatment—a literature review, *Water Res.* 38 (2004) 2795–2809.
- [65] O. Raff, R.D. Wilken, Removal of dissolved uranium by nanofiltration, *Desalination* 122 (1999) 147–150.
- [66] N. Hilal, H. Al-Zoubi, N.A. Darwish, A.W. Mohamma, M. Abu Arabi, A comprehensive review of nanofiltration membranes: treatment, pretreatment, modeling, and atomic force microscopy, *Desalination* 170 (2004) 281–308.
- [67] T. Matsuura, Progress in membrane science and technology for seawater desalination—a review, *Desalination* 134 (2001) 47–54.
- [68] R. Semiat, Present and future, *Water Int.* 25 (2000) 54–65.
- [69] J.C. Crittenden, R.R. Trussell, D.W. Hand, K.J. Howe, G. Tchobanoglous, *MWH's Water Treatment: Principles and Design*, Wiley, (2012).
- [70] B. Gu, L. Liang, M.J. Dickey, X. Yin, S. Dai, Reductive precipitation of uranium(VI) by zero-valent iron, *Environ. Sci. Technol.* 32 (1998) 3366–3373.

- [71] R. Ganesh, Reductive precipitation of uranium by *Desulfovibrio desulfuricans*: evaluation of co-contaminant effects and selective removal, *Water Res.* 33 (1999) 3447–3458.
- [72] A. Tapia-Rodriguez, A. Luna-Velasco, J.A. Field, R. Sierra-Alvarez, Anaerobic bioremediation of hexavalent uranium in groundwater by reductive precipitation with methanogenic granular sludge, *Water Res.* 44 (2010) 2153–2162.
- [73] F. Jroundi, M.L. Merroun, J.M. Arias, A. Rossberg, S. Selenska-Pobell, M.T. González Lez Muñoz, Spectroscopic and microscopic characterization of uranium biomineralization in *Myxococcus xanthus*, *Geomicrobiol. J.* 24 (2007) 441–449.
- [74] M. Nedelkova, M.L. Merroun, A. Rossberg, C. Hennig, S. Selenska-Pobell, Microbacterium isolates from the vicinity of a radioactive waste depository and their interactions with uranium, *FEMS Microbiol. Ecol.* 59 (2007) 694–705.
- [75] M. Merroun, C. Hennig, A. Rossberg, T. Reich, S. Selenska-Pobell, Characterization of U(VI)—*Acidithiobacillus ferrooxidans* complexes using EXAFS, transmission electron microscopy, and energy-dispersive X-ray analysis, *Radiochim. Acta* 91 (2003) 583–592.
- [76] M.L. Merroun, J. Raff, A. Rossberg, C. Hennig, T. Reich, S. Selenska-Pobell, Complexation of uranium by cells and S-layer sheets of *Bacillus sphaericus* JG- A12, *Appl. Environ. Microbiol.* 71 (2005) 5532–5543.
- [77] M.L. Merroun, M. Nedelkova, J.J. Ojeda, T. Reitz, M.L. Fernández, J.M. Arias, M. Romero-González, S. Selenska-Pobell, Bio-precipitation of uranium by two bacterial isolates recovered from extreme environments as estimated by potentiometric titration, TEM and X-ray absorption spectroscopic analyses, *J. Hazard. Mater.* 197 (2011) 1–10.

- [78] S. Mishra, V. Chakravorty, Extraction of uranium(VI) by the binary mixture of Aliquat 336 and PC88A from aqueous H_3PO_4 medium, *Hydrometallurgy*, 44 (1997) 371-376.
- [79] D. D. Sood, and S. K. Patil, Chemistry of nuclear fuel reprocessing: Current status, *J. Radioanal. Nucl. Chem. Articles*, 203 (2) (1996) 547-573.
- [80] A. Suresh, S. Subramaniam, T. G. Srinivasan, and P. R. Vasudeva Rao, , Studies on U/Th separation using tri-sec butyl phosphate, *Solvent Extr. Ion Exch.* 13 (3) (1995) 415-430.
- [81] Harvinderpal Singh, S. L. Mishra and, R. Vijayalakshmi, Uranium recovery from phosphoric acid by solvent extraction using a synergistic mixture of di-nonyl phenyl phosphoric acid and tri-n-butyl phosphate. *Hydrometallurgy*, 73 (2004) 63-70.
- [82] A. Suresh; T. G. Srinivasan; P. R. Vasudeva Rao, Parameters Influencing Third-Phase Formation in the Extraction of $Th(NO_3)_4$ by some Trialkyl Phosphates, *Solvent Extr. Ion Exch.*, 27 (2) (2009) 132 – 158.
- [83] Bruce J. Mincher; Giuseppe Modolo, Stephen P. Mezyk, The Effects of Radiation Chemistry on Solvent Extraction: 1. Conditions in Acidic Solution and a Review of TBP Radiolysis, *Solvent Extr. Ion Exch.*, 27, (1) (2009) 1 – 25.
- [84] IUPAC Technical Report Series No. 431, Application of Membrane Technologies for Liquid Waste Processing. IAEA, Vienna, (2004).
- [85] P.K. Mohapatra, V.K. Manchanda, Handbook of Membrane Separations: Chemical, Pharmaceuticals, Food and Biological Applications, Anil Kumar Pabby, S.S.H. Rizvi, Ana Maria Sastre (Eds.), Chapter-31, Liquid membrane-based separations of actinides. CRC Press, Taylor & Francis Group, (2009) 883-910.

- [86] S. Shailesh, P.N. Pathak, P.K. Mohapatra, V.K. Manchanda, Role of diluents in uranium transport across a supported liquid membrane using di(2-ethylhexyl)isobutyramide as the carrier, *Desalination*. 232 (1-3) (2008) 281-290.
- [87] S. Panja, P.K. Mohapatra, S.C. Tripathi, V.K. Manchanda, Studies on uranium(VI) pertraction across a N,N,N',N'-tetraoctyldiglycolamide (TODGA) supported liquid membrane, *J. Memb. Sci.*, 337 (2009) 274-281.
- [88] S.K. Singh, S.K. Misra, M. Sudersanan, A. Dakshinamoorthy, Studies on the recovery of uranium from phosphoric acid medium by D2EHPA/n-dodecane supported liquid membrane, *Sep. Sci. Technol.*, 44 (2009) 169-189.
- [89] J.M. Joshi, P.N. Pathak, A.K. Pandey, V.K. Manchanda, , Study on synergistic carriers facilitated transport of uranium(VI) and europium(III) across supported liquid membrane from phosphoric acid media, *Hydrometallurgy* 96 (2009) 117-122.
- [90] S.K. Singh, S.K. Misra, M. Sudersanan, A. Dakshinamoorthy, S.K. Munshi, P.K. Dey, Carrier-mediated transport of uranium from phosphoric acid medium across TOPO/n-dodecane-supported liquid membrane, *Hydrometallurgy* 87 (2007) 190-196.
- [91] S. D. Dogmane, R. K. Singh, D. D. Bajpai and J. N. Mathur, Extraction of U(VI) by cyanex-272, *J. Radioanal. Nucl. Chem.*, 253 (3) (2002) 477- 482.
- [92] S.R. Sawant, J.V. Sonawane, A.K. Venugopalan, P.K. Dey, Kumar Anil, J.N. Mathur, Membrane based U(VI) transport across supported liquid membrane from aqueous acidic media, *Ind. J. of Chemical technology*, 10 (2003) 531- 538.
- [93] S. A. El-Reefy, Y. T. Selim and Y. F. Aly, "Equilibrium and kinetic studies on the separation of uranium and thorium from nitric acid medium by liquid emulsion membrane based on TOPO extractant", *Analytical Sci.*, 13 (1997) 333.

- [94] S. A. El-Reefy, Y. T. Selim and H. F. Aly, "Recovery of Uranium from thorium in hydrochloric acid medium by liquid emulsion membranes containing tri-octylphosphine oxide", *J. Radioanal. and Nucl. Chem.*, 228(1-2) (1998) 21.
- [95] P. S. Kulkarni, S. Mukhopadhyay, M. P. Bellary and S. K. Ghosh, "Studies on membrane stability and recovery of uranium (VI) from aqueous solutions using liquid emulsion membrane process", *Hydrometallurgy*, 64 (2002) 49.
- [96] C. S. Kedari, S. S. Pandit, S. K. Mishra and A. Ramanujan, "Mass transfer mechanism of the carrier facilitated transport of uranium(VI) 2-ethylhexyl phosphoric acid mono 2-ethylhexyl ester immobilised liquid membrane", *Hydrometallurgy*, 62 (2001) 47.
- [97] M. Sprynskyy, I. Kovalchuk, B. Buszewski, The separation of uranium ions by natural and modified diatomite from aqueous solution, *J. Hazard. Mater.* 181 (2010) 700–707.
- [98] M.S. Hosseini, A. Hosseini-Bandegharai, Comparison of sorption behaviour of Th(IV) and U(VI) on modified impregnated resin containing quinizarin with that conventional prepared impregnated resin, *J. Hazard. Mater.* 190 (2011) 755–765.
- [99] A.R. Qaiser, M. Saleemi, M. Ahmad, Heavy metal uptake by agro based waste materials, *Environ. Biotechnol.* 10 (2007) 409–416.
- [100] S. Aytas, S. Akyil, M.A.A. Aslani, U. Aytekin, Removal of uranium from aqueous solutions by diatomite (Kieselguhr), *J. Radioanal. Nucl. Chem.* 240 (1999) 973–976.
- [101] M. Sprynskyy, I. Kovalchuk, B. Buszewski, The separation of uranium ions by natural and modified diatomite from aqueous solution, *Journal of Hazardous Materials*, 181 (2010) 700–707.
- [102] J. Tashkhourian, L. Moradi Abdoluofofi, M. Pakniat, M. Montazerozohori, Sodium dodecyl sulfate coated alumina modified with a new Schiff's base as a uranyl ion selective adsorbent, *Journal of Hazardous Materials*, 187 (2011) 75–81.

- [103] R. Donat, The removal of uranium (VI) from aqueous solutions onto natural sepiolite. *J. Chem. Thermodynamics* 41 (2009) 829–835.
- [104] F. Fan, H. Ding, J. Bai, X. Wu, F. Lei, W. Tian, Y. Wang, Z. Qin, Sorption of uranium(VI) from aqueous solution onto magnesium silicate hollow spheres, *J. Radioanal. Nucl. Chem.* 289 (2011) 367–375.
- [105] W. Guanghui, W. Xuegang, Xinjun, L. Jinsheng, D. Nansheng, Adsorption of uranium (VI) from aqueous solution on calcined and acid-activated kaolin. *Appl. Clay Sci.* 47 (2010) 448–451.
- [106] S. Xie, C. Zhang, X. Zhou, J. Yang., X. Zhang, J. Wang, Removal of uranium (VI) from aqueous solution by adsorption of hematite. *J. Environ. Radioact.* 100 (2009) 162–166.
- [107] C. Charnay, S. Lagerge, S. Partyka, Assessment of the surface heterogeneity of talc materials, *J. Colloid Interface Sci.* 233 (2001) 250–258.
- [108] J.H. Meldon, M. Sprynskyy, T. Kowalkowski, H. Tutu, E.M. Cukrowska, B. Buszewski, Adsorption performance of talc for uranium removal from aqueous solution, *Chem. Eng. J.* 171 (2011) 1185–1193.
- [109] A. Nilchi, T. Shariati Dehaghan, S. Rasouli Garmarodi, Kinetics, isotherm and thermodynamics for uranium and thorium ions adsorption from aqueous solutions by crystalline tin oxide nanoparticles, *Desalination* 321 (2013) 67–71
- [110] R.A. Crane, M. Dickinson, I.C. Popescu, T.B. Scott, Magnetite and zero-valent iron nanoparticles for the remediation of uranium contaminated environmental water, *water research* 45 (2011) 2931-942.
- [111] M. Dickinson, T.B. Scott, The application of zero-valent iron nanoparticles for the remediation of a uranium contaminated waste effluent. *Journal of Hazardous Materials* 178 (1e3) (2010) 171-179.

- [112] O. Riba, T.B. Scott, K. Vala Ragnarsdottir, G.C. Allen, Reaction mechanism of uranyl in the presence of zero-valent iron nanoparticles. *Geochimica et Cosmochimica Acta* 72 (16) (2008) 4047-4057.
- [113] Y. Zhao, J. Li, L. Zhao, S. Zhang, Y. Huang, X. Wu, et al., Synthesis of amidoxime-functionalized Fe₃O₄@SiO₂ core-shell magnetic microspheres for highly efficient sorption of U(VI), *Chem. Eng. J.* 235 (2014) 275–283.
- [114] M. Zeng, Y. Huang, S. Zhang, S. Qin, J. Li, J. Xu, Removal of uranium(vi) from aqueous solution by magnetic yolk-shell iron oxide@magnesium silicate microspheres, *RSC Adv.* 4 (5021) (2014).
- [115] G. Jing, Z. Zhou, L. Song, M. Dong, *Desalination* 279 (2011) 423–427
- [116] R.S. Praveen, P. Metilda, S. Daniel, T.P. Rao, *Talanta* 67 (2005) 960–967.
- [117] Y. Zhao, C. Liu, M. Feng, Z. Chen, S. Li, G. Tian, L. Wang, J. Huang, S. Li, J. Hazard. Mater. 176 (2010) 119–124.
- [118] G. Tian, J. Geng, Y. Jin, C. Wang, S. Li, Z. Chen, H. Wang, Y. Zhao, S. Li, J. Hazard. Mater. 190 (2011) 442–450.
- [119] C. Kutahyah, M. Eral, Y. Altas, Adsorption of uranium from aqueous solutions using activated carbon prepared from olive stones, *Nucl. Sci. ITS Appl.* (2004) 110.
- [120] Q. Li, D. Wang, Y. Wu, W. Li, Y. Zhang, J. Xing, Z. Su, One step recovery of succinic acid from fermentation broths by crystallization, *Sep. Purif. Technol.* 72 (2010) 294–300.
- [121] C. Zhang, R. Zhang, B. Xing, G. Cheng, Y. Xie, W. Qiao, L. Zhan, X. Liang, L. Ling, Effect of pore structure on the electrochemical performance of coal-based activated carbons in non-aqueous electrolyte, *New Carbon Mater.* 25 (2010) 129–133.

- [122] A. Mellah, S. Chegrouche, M. Barkat, The removal of uranium(VI) from aqueous solutions onto activated carbon: kinetic and thermodynamic investigations, *J. Colloid Interface Sci.* 296 (2006) 434–441.
- [123] M. Merdivan, M.Z. Du" z, C. Hamamci, Sorption behaviour of uranium(VI) with N,N-dibutyl-N0-benzoylthiourea Impregnated in Amberlite XAD-16, *Talanta* 55 (2001) 639–645.
- [124] M. Merdivan, S. Seyhan, C. Gok, Use of benzoylthiourea immobilized on silica gel for separation and preconcentration of uranium(VI), *Microchim. Acta* 154 (2006) 109–114.
- [125] K.Y. Foo, B.H. Hameed, Potential of activated carbon adsorption processes for the remediation of nuclear effluents: a recent literature, *Desalin. Water Treat.* 41 (2012) 72–78.
- [126] Y. Jung, S. Kim, S.-J. Park, J.M. Kim, Preparation of functionalized nanoporous carbons for uranium loading, *Colloids Surf. A: Physicochem. Eng. Asp.* 313–314 (2008) 292–295.
- [127] M. Sevilla, A.B. Fuertes, Chemical and structural properties of carbonaceous products obtained by hydrothermal carbonization of saccharides, *Chem. Eur. J.* 15 (2009) 4195–4203.
- [128] B. Hu, K. Wang, L. Wu, S.-H. Yu, M. Antonietti, M. M. Titirici, Engineering carbon materials from the hydrothermal carbonization process of biomass, *Adv. Mater.* 22 (2010) 813–828.
- [129] Z.C. Yang, X. Li, J. Wang, Intrinsically fluorescent nitrogen-containing carbon nanoparticles synthesized by a hydrothermal process, *Carbon, N.Y.* 49 (2011) 5207–5212.

- [130] Z. Kolarik, Complexation and separation of lanthanides(III) and actinides(III) by heterocyclic N-donors in solutions, *Chem. Rev.* 108 (2008) 4208–4252.
- [131] F. Lewis, M. Hudson, L. Harwood, Development of highly selective ligands for separations of actinides from lanthanides in the nuclear fuel cycle, *Synlett* (2011).
- [132] Q. Song, L. Q. Song, L. Ma, J. Liu, C. Bai, J. Geng, H. Wang, B. Li, L. Wang, S. Li, Preparation and adsorption performance of 5-azacytosine-functionalized hydrothermal carbon for selective solid-phase extraction of uranium, *J. Colloid Interface Sci.* 386 (2012) 291–299.
- [133] X.M. Ren, C.L. Chen, M. Nagatsu, X.K. Wang, Carbon nanotubes as adsorbents in environmental pollution management: a review. *Chem Eng J* 170(2–3) (2011) 395–410.
- [134] F. Belloni, C. Kütahyalı, V.V. Rondinella, A. Mangione, Can carbon nanotubes play a role in the field of nuclear waste management? *Environ. Sci. Technol.* 43 (2009) 1250-1255.
- [135] L. Qin, X. Zhao, K. Hirahara, Y. Miyamoto, Y. Ando, S. Iijima, *Nature* 408 (2000) 50.
- [136] P.J.F. Harris, *Carbon* 45 (2007) 229–239.
- [137] D.D. Shao, Z.Q. Jiang, X.K. Wang, J.X. Li, Y.D. Meng, Plasma induced drafting carboxymethyl cellulose on multiwalled carbon nanotubes for the removal of UO_2^{2+} from aqueous solution, *J. Phys. Chem. B* 113 (2009) 860–864.
- [138] P. Lian, X. Zhu, S. Liang, Z. Li, W. Yang, H. Wang, Large reversible capacity of high quality graphene sheets as an anode material for lithium-ion batteries, *Electrochim. Acta* 55 (2010) 3909–3914.

- [139] Z. Li, F. Chen, L. Yuan, Y. Liu, Y. Zhao, Z. Chai, W. Shi, Uranium(VI) adsorption on graphene oxide nanosheets from aqueous solutions, *Chem. Eng. J.* 210 (2012) 539–546.
- [140] Chen Shuiping, Hongb Jianxun, Yanga Hongxiao, Yang Jizhen, Adsorption of uranium (VI) from aqueous solution using a novel graphene oxide-activated carbon felt composite, *Journal of Environmental Radioactivity* 126 (2013) 253-258
- [141] G. Zhao, T. Wen, X. Yang, S. Yang, J. Liao, J. Hu, et al., Preconcentration of U(VI) ions on few-layered graphene oxide nanosheets from aqueous solutions, *Dalton Trans.* 41 (2012) 6182–6188.
- [142] M. Anbia, N. Mohammadi, K. Mohammadi, Fast and efficient mesoporous adsorbents for the separation of toxic compounds from aqueous media, *J. Hazard. Mater.* 176 (2010) 965–972.
- [143] G. Tian, J. Geng, Y. Jin, C. Wang, S. Li, Z. Chen, H. Wang, Y. Zhao, S. Li, Sorption of uranium(VI) using oxime-grafted ordered mesoporous carbon CMK-5, *Journal of Hazardous Materials*, 190 (2011) 442–450.
- [144] K.C. Bhainsa, S.F. D'Souza. Uranium(VI) biosorption by dried roots of *Eichhornia crassipes* (water hyacinth). *Journal of Environmental Science & Health, Part A: Toxic/Hazardous Substances and Environmental Engineering*, 36 (2001) 1621–31.
- [145] P. Sar, S.K. Kazy, S.F. D'Souza, Radionuclide remediation using a bacterial biosorbent, *International Biodeterioration and Biodegradation*, 54 (2004) 193–202.
- [146] M. Kalin, W.N. Wheeler, G. Meinrath. The removal of uranium from mining waste water using algal/microbial biomass, *Journal of Environment Radioactivity*, 78 (2005) 151–77.

- [147] R. Tykva, J. Novák, E. Podracká, K. Popa. Bioaccumulation of uranium from waste water using different strains of *Saccharomyces cerevisiae*, *Nukleonika*, 54 |(2009) 143-8.
- [148] J. Bai, H.J. Yao, F.L. Fan, M.S. Lin, L.N. Zhang, H.J. Ding, Biosorption of uranium by chemically modified *Rhodotorula glutinis*, *Journal of Environment Radioactivity*, 101 (2010) 969–73.
- [149] C.S.Kedari, Biosorption of long lived radionuclides using immobilized cells of *Saccharomyces cerevisiae*, *World J. Microb. Biot.* 17 (2001) 789-793.
- [150] R. Tykva, Bio-accumulation of uranium from wastewater using different strains of *Saccharomyces cerevisiae*, *Nukleonika* 54 (2009) 143-148.
- [151] J. Bai, H. Yao, F. Fan, M. Lin, L. Zhang, H. Ding, F. Lei, X. Wu, X.i Li, J. Guo, Z. Qin, Biosorption of uranium by chemically modified *Rhodotorula glutinis*, *Journal of Environmental Radioactivity* 101 (2010) 969-973.
- [152] C. Jeon, I.W. Nah, K.Y. Hwang. Adsorption of heavy metals using magnetically modified alginic acid, *Hydrometallurgy*, 86 (2007)140–6.
- [153] J. Bai, X. Wu, F. Fan, W. Tiana, X. Yin, L. Zhaoa, F. Fana, Z. Li, L. Tiana, Z. Qina, J. Guo, Biosorption of uranium by magnetically modified *Rhodotorula glutinis*, *Enzyme and Microbial Technology*, 51 (2012) 382– 387.
- [154] K. Akhtar, A.M. Khalid, M.W. Akhtar, M.A. Ghauri, Removal and recovery of uranium from aqueous solution by ca-alginate immobilized *Trichoderma harzianum*, *Bioresour. Technol.* 100 (2009) 4551–4558.
- [155] C. Gok, S. Aytas, Biosorption of uranium (VI) from aqueous solution using calcium alginate beads, *J. Hazard. Mater.* 168 (2009) 369–375.
- [156] Z. Portakal, C. Gok, S. Aytas, Separation of uranium by an extractant encapsulated magnetic alginate gels, in: A. Vaseashta, E. Braman, P. Susmann (Eds.),

- Technological Innovations in Sensing and Detection of Chemical, Biological, Radiological, Nuclear Threats and Ecological Terrorism, Springer Science, (2012) 357–360 (Chapter 38).
- [157] K. Kim, A.A. Keller, J. Yang, Removal of heavy metals from aqueous solution using a novel composite of recycled materials, *Colloids and Surfaces A: Physicochem. Eng. Aspects*, 425 (2013) 6– 14.
- [158] A. Tripathi, J.S. Melo, S.F. D’Souza, Uranium (VI) recovery from aqueous medium using novel floating macroporous alginate-agarose-magnetite cryobeads, *Journal of Hazardous Materials* 246– 247 (2013) 87– 95.
- [159] T.S. Anirudhan, S. Rijith, Synthesis and characterization of carboxyl terminated poly(methacrylic acid) grafted chitosan/bentonite composite and its application for the recovery of uranium(VI) from aqueous media, *Journal of Environmental Radioactivity*, 106 (2012) 8-19.
- [160] S.E. Bailey, T.J. Olin, R.M. Bricka, D.D. Adrian, A review of potentially low-cost sorbents for heavy metals, *Water Res.* 33 (1999) 2469–2479.
- [161] I. Shtangeeva, Uptake of uranium and thorium by native and cultivated plants, *J. Environ. Radioact.* 101 (2010) 458–463.
- [162] A.F. Bishay, Environmental application of rice straw in energy production and potential adsorption of uranium and heavy metals, *J. Radioanal. Nucl. Chem.* 286 (2010) 81–89.
- [163] Shilpi Kushwaha, Padmaja P. Sudhakar, Sorption of uranium from aqueous solutions using palm-shell-based adsorbents: a kinetic and equilibrium study, *Journal of Environmental Radioactivity*, 126 (2013) 115-124.

- [164] W. Zou, L. Zhao, R. Han, Removal of uranium (VI) by fixed bed ion-exchange column using natural zeolite coated with manganese oxide. *Chin. J. Chem. Eng.* 17 (2009) 585–593.
- [165] Hamed Tavakoli, Hamid Sepehrian, Fatemeh Semnani, Mohammad Samadfam, Recovery of uranium from UCF liquid waste by anion exchange resin CG-400: Breakthrough curves, elution behaviour and modelling studies, *Annals of Nuclear Energy*, 54 (2013) 149–153.
- [166] N.A. Peppas, P. Bures, W. Leobandung, H. Ichikawa, Hydrogels in pharmaceutical formulations, *Eur. J. Pharm. Biopharm.* 50 (2000) 27–46.
- [167] D. Myung, D. Waters, M. Wiseman, P.E. Duhamel, J. Noolandi, C.N. Ta, C.W. Frank, Progress in the development of interpenetrating polymer network hydrogels, *Polym. Adv. Technol.* 19 (2008) 647–657.
- [168] J.F. Bessbousse, L. Verchere, Lebrun, characterization of metal-complexing membranes prepared by the semi-interpenetrating polymer networks technique. Application to the removal of heavy metal ions from aqueous solutions, *Chem. Eng. J.* 187 (2012) 16–28.
- [169] J. Wang, F. Liu, Thermoresponsive – ion imprinted hydrogels with interpenetrating network structure for removal of heavy metal ions, *Adv. Mater. Res.* 643 (2013) 83–86.
- [170] Y. Liu, X. Cao, R. Hua, Y. Wang, Y. Liu, C. Pang, Y. Wang, Selective adsorption of uranyl ion on ion-imprinted chitosan/PVA cross-linked hydrogel, *Hydrometallurgy*, 104 (2010) 150–155.
- [171] E. Guibal, C. Milot, J.M. Tobin, Metal-anion sorption by chitosan beads: equilibrium and kinetic studies, *Ind. Eng. Chem. Res.* 37 (1998) 1454–1463.

- [172] W. Wan Ngah, Kamari, A.Y. Koay, Equilibrium and kinetics studies of adsorption of copper (II) on chitosan and chitosan/PVA beads, *Int. J. Biol. Macromol.* 34 (2004) 155–161.
- [173] W. Wan Ngah, C. Endud, R. Mayanar, Removal of copper(II) ions from aqueous solution onto chitosan and cross-linked chitosan beads, *React. Funct. Polym.* 50 (2002) 181–190.
- [174] S.H. Lee, S.Y. Park, J.H. Choi, Fiber formation and physical properties of chitosan fiber crosslinked by epichlorohydrin in a wet spinning system: the effect of the concentration of the crosslinking agent epichlorohydrin, *J. Appl. Polym. Sci.* 92 (2004) 2054–2062.
- [175] G. Wang, J. Liu, X. Wang, Z. Xie, N. Deng, Adsorption of uranium (VI) from aqueous solution onto cross-linked chitosan, *J. Hazard. Mater.* 168 (2009) 10 53–1058.
- [176] I. Akin, G. Arslan, A. Tor, M. Ersoz, Y. Cengelglu, Arsenic(V) removal from underground water by magnetic nanoparticles synthesized from waste red mud, *J. Hazard. Mater.* 235–236 (2012) 62–68.
- [177] J. Li, Z. Guo, S. Zhang, X. Wang, Enrich and seal radionuclides in magnetic agarose microspheres, *Chem. Eng. J.* 172 (2011) 892–897.
- [178] P. Ilaiyaraja, A.K.S. Deb, K. Sivasubramanian, D. Ponraju, B. Venkatraman, Adsorption of uranium from aqueous solution by PAMAM dendron functionalized styrene divinylbenzene, *J. Hazard. Mater.* 250–251 (2013) 155–166.
- [179] (a) S. Pal, V. Ramachandran, S. Prabhakar, P.K. Tewari; “Recovery of valuables from sea water, Trombay”, *Symp. On Desal. And water Reuse*, Feb. (2007) 7-9.
- [180] B.B. Jang, K. Lee, W.J. Kwon, J. Suh, *J. Poly. Sci.: Part A: Poly. Chem.*, 37 (1999) 3169.

- [181] K. Saito, K. Sugita, A. Katakai, N. Seko, T. Sugo, J. Kanno, T. Kawakami, *Ind. Engg. Chem. Res.* 39 (2000) 2910.
- [182] B.B. Jang, K. Lee, W.J. Kwon, J. Suh, *J. Poly. Sci.: Part A: Poly. Chem.* 37 (1999) 3169.
- [183] A. Hinchcliffe, *Modelling Molecular Structure*, Wiley, 1996; D. Young, *Computational Chemistry*, Wiley-Inter-science, (2001).
- [184] (a) C. J. Cramer, *Modelling. Principles and Applications*, Longman, (2001), (b) T. Schlick, *Molecular Modeling and Simulation*, Springer, (2002).
- [185] C. Hennig, T. Reich, R. Da'hn, A.M. Scheidegger, *Structure of uranium sorption complexes at montmorillonite edge sites*, *Radiochim. Acta*, 90 (2002) 653–657.
- [186] R. Kannappan, S. Tanase, D.M. Tooke, A.L. Spek, I. Mutikainen, U. Turpeinen, J. Reedijk, *Separation of actinides and lanthanides: crystal and molecular structures of N,N'-bis(3,5-dit-butylsalicylidene)-4,5-dimethyl-1,2-phenylenediamine and its uranium complex*. *Poyhedron*, 23 (2004) 2285–2291.
- [187] G. Lefe`vre, S. Noinville, M. Fe´doroff, *Study of uranyl sorption onto hematite by in situ attenuated total reflection – infrared spectroscopy*. *J. Colloid Interface Sci.* 296 (2006) 608–613.
- [188] C. Hennig, K. Schmeide, V. Brendler, H. Moll,; S. Tsushima,; A. C. Scheinost, *Inorg. Chem.* 46 (2007) 5882–5892.
- [189] W. Humphrey, A. Dalke, K. J. Schulten, *Molec. Graphics*, 14.1 (1996) 33-38.
- [190] M. Bühl,; R. Diss, G. J. Wipff, *Am. Chem. Soc.* 127 (2005) 13506-13507.
- [191] C. Clavaguéira-Sarrio, V. Brenner, S. Hoyau, C. J. Marsden, P. Millié, J.P. Dognon, *J. Phys. Chem. B.* 107 (2003) 3051-3060.
- [192] B. Siboulet, C.J. Marsden, P. Vitorge, *Chem. Phys.* 326 (2006) 289-296.
- [193] B. Siboulet, C.J. Marsden, P. Vitorge, *New J. Chem.* 32 (2008) 2080-2094.

- [194] M. Bühl, K. Hendrik, *ChemPhysChem*. 7 (2006) 2290-2293.
- [195] Z. Cao, K. Balasubramanian, *J. Chem. Phys.* 123 (2005) 1143-9.
- [196] Clavaguéra-Sarrio, C.; Brenner, V.; Hoyau, S.; Marsden, C. J.; Millié, P.; Dognon, J.-P. *J. Phys. Chem. B*. 107 (2003) 3051-3060.
- [197] K. E. Gutowski, D.A. Dixon, *J. Phys. Chem. A*, 110 (2006) 8840-8856.
- [198] P. J. Hay, R. L. Martin, G. Schreckenbach, *J. Phys. Chem. A*, 104 (2000) 6259-6270.
- [199] F. P. Rotzinger, *Chem.sEur. J.* 13 (2007) 800-811.
- [200] Shamov, G. A.; Schreckenbach, G. *J. Phys. Chem. A.*, 109 (2005) 10961-10974.
- [201] S. Spencer, L. Gagliardi, N. C. Handy, A. G. Ioannou, C.-K. Skylaris,; A. Willets, A. M. Simper, *J. Phys. Chem. A*, 103 (1999) 1831-1837.
- [202] V. Vallet, U. Wahlgren, B. Schimmelpfennig, Z. Szabó , I. Grenthe, *J. Am. Chem. Soc.* 123 (2001) 11999-12008.
- [203] M. S. K. Fuchs, A. M. Shor, N. Rosch, *International J. Quant. Chem.* 2002, 86, 487-501.
- [204] L. V. Moskaleva, S. Kruger, A. Sporl, N. Rosch, *Inorg. Chem.* 43 (2004) 4080-89
- [205] A. Ikeda, C. Hennig, A. Rossberg, S. Tsushima, A. C. Scheinost, G. Bernhard, *Anal. Chem.* 80 (2008) 1102-1110.
- [206] S. Portmann, H. P. Lüthi, *Chimia*, 54 (2000) 766-770
- [207] Flükiger, H. P. Lüthi, S. Portmann,; S. J. Weber, *MOLEKEL 4.2 P.*, Swiss Center for Scientific Computing, Manno (Switzerland) (2002).
- [208] P. L. Arnold, D. Patel, C. Wilson, J. B. Love, *Nature (London)*, 451 (2008) 315–318.
- [209] J. M. Boncella, *Nature (London)*, 451 (2008) 250–251.
- [210] A. R. Fox, S. C. Bart, K. Meyer, C. C. Cummins, *Nature (London)*, 455 (2008) 341–349.

- [211] J. C. Renshaw, L. J. C. Butchins, F. R. Livens, I. May, J. M. Charnock,; J. R. Lloyd, *Environ. Sci. Technol.* 39 (2005) 5657–5660.
- [212] E. S. Ilton, A. Haiduc, C. L. Cahil, A. R. Felmy, *Inorg. Chem.* 44 (2005) 2986–2988.
- [213] Z. Szabo, I. Grenthe, *Inorg. Chem.* 46 (2007) 9372–9378.
- [214] D. L. Clark, S. D. Conradson, R. J. Donohoe, D. W. Keogh, D. E. Morris, P. D. Palmer, R. D. Rogers, C. D. Tait, *Inorg. Chem.* 38 (1999) 1456–1466.
- [215] G. A. Shamov, G. Schreckenbach, *J. Am. Chem. Soc.* 130 (2008) 13735–13744.
- [216] H. P. Hratchian, J. L. Sonnenberg, P. J. Hay, R. L. Martin, B. E. Bursten, H. B. Schlegel, *J. Phys. Chem. A*, 109 (2005), 8579–8586.
- [217] R. Gonte, K. Balasubramanian, Heavy and toxic metal uptake by mesoporous hypercrosslinked SMA beads: isotherms and kinetics, *J. Saudi Chem. Soc.* (2013).
- [218] Y. Zhang, Y. Li, X. Li, L. Yang, X. Bai, Z. Ye, L. Zhou, L. Wang, Selective removal for Pb²⁺ in aqueous environment by using novel macroreticular PVA beads, *J. Hazard. Mater.* 181 (2010) 898–907.
- [219] S. Xie, J. Yang, C. Chen, X. Zhang, Q. Wang, C. Zhang, Study on biosorption kinetics and thermodynamics of uranium by *Citrobacter freudii*, *J. Environ. Radioact.* 99 (2008) 126–133.
- [220] N. Dhavale, G. Shelar, R.R. Gonte, K. Balasubramanian, Cellulosic Composite for Effluent Waste Water Treatment, *Applications of Nano Materials, Electronics, Energy and Environment*, (2012) ISBN: 978-93-982563-35-8.
- [221] S. Rengaraj, Y. Kim, C.K. Joo, K. Choi, J. Yi, Batch adsorptive removal of copper ions in aqueous solutions by ion exchange resins: 1200H and IRN97H, *Korean J. Chem. Eng.* 21 (2004) 187–194.
- [222] Z. Talip, M. Eral, U. Hicsonmez, Adsorption of thorium from aqueous solutions by perlite, *J. Environ. Radioact.* 100 (2009) 139–143.

- [223] Y. Sag, Y. Aktay, Kinetic studies on sorption of Cr(VI) and Cu(II) ions by chitin, chitosan and *Rhizopus arrhizus*, *Biochem. Eng. J.* 12 (2002) 143–153.
- [224] R.R. Gonte, G. Shelar, K. Balasubramanian, Polymer–agro-waste composites for removal of Congo red dye from wastewater: adsorption isotherms and kinetics, *Desalin. Water Treat.* (2013) 1–15.
- [225] R.R. Gonte, K. Balasubramanian, J.D. Mumbreakar, Porous and cross-linked cellulose beads for toxic metal ion removal: Hg(II) Ions, *J. Polym.* 2013 (2013) 1–9.
- [226] M.A. Farajzadeh, M.R. Fallahi, Study of phenolic compounds removal from aqueous solution by polymeric sorbent, *J. Chin. Chem. Soc.* 52 (2005) 295–301.
- [227] S. Rengaraj, J.W. Yeon, Y. Kim, Y. Jung, Y.K. Ha, W.H. Kim, Adsorption characteristics of Cu(II) onto ion exchange resins 252H and 1500H: kinetics, isotherms and error analysis, *J. Hazard. Mater.* 143 (2007) 469–477.
- [228] T.J. Sahetya, F. Dixit, K. Balasubramanian, Waste citrus fruit peels for removal of Hg(II) ions, *Desalin. Water Treat.* (2013) 1–13
- [229] M. Sarkar, P.K. Acharya, B. Bhattacharya, Modeling the adsorption kinetics of 1551 some priority organic pollutants in water from diffusion and activation energy 1552 parameters, *J. Colloid Interface Sci.* 266 (2003) 28–32.
- [230] D. Humelnicu, E. Popovici, E. K. Dvininov, C. Mita, Study on retention of uranyl ions on modified clays with titanium oxide, *J. Radioanal. Nuc. Chem.* 271 (1) (2009) 131.
- [231] J.M. Duran-Blanco, B. E. Lopez-Munoz, M. T. Olguin, Influence of pH on U(VI) adsorption using a thermally-treated Mg-Al hydrotaccite and a natural zeolite in a batch system, *Sepn. Sci. And Technol.* 48 (2013) 797 – 804.
- [232] P. N. Pathak, G. R. Choppin, Kinetics and thermodynamics of uranium (VI) sorption on hydrous silica, *Radiochim. Acta*, 95 (9) (2007) 507-512.

- [233] J. D. Van Horn, H. Huang, Uranium (VI) bio-coordination chemistry from biochemical, solution and protein structural data, *Coord. Chem.* 250 (7-8) (2006) 765-775.
- [234] J. L. Sessler, P. J. Melfi, G. Dan Pantos, Uranium complexes of multidentate N-donor ligands, *Coord. Chem. Rev.* 250(7-8) (2006) 816-843.
- [235] Y. Liu, Z. Liu, J. Gao, J. Dai, J. Han, Y. Wang, J. Xie, Y. Yan, Selective adsorption behaviour of Pb(II) by mesoporous silica SBA-15-supported Pb(II)-imprinted polymer based on surface molecularly imprinting technique, *J. Hazard. Mater.* 186 (2011) 197-205.
- [236] C. Ijagbemi, M. Baek, D. Kim, Montmorillonite surface properties and sorption characteristics for heavy metal removal from aqueous solutions, *J. Hazard. Mater.* 166 (2009) 538-546.
- [237] H. Tang, W. Zhou, L. Zhang, Adsorption isotherms and kinetics studies of malachite green on chitin hydrogels, *J. Hazard. Mater.* 209-210 (2012) 218-225.
- [238] X. Sun, S. Wang, X. Liu, W. Gong, N. Bao, B. Gao, H. Zhang, Biosorption of malachite green from aqueous solutions onto aerobic granules: kinetic and equilibrium studies, *Bioresour. Technol.* 99 (2008) 3475-3483.
- [239] J. Wase, C. Forster, *Biosorbents for Metal Ions*, Taylor & Francis, London, (1997).
- [240] B. Volesky, *Sorption and Biosorption*, 1st ed., BV Sorbex Inc., Quebec, (2003).
- [241] R. Gong, Y. Ding, H. Lui, Q. Chem, L. Z. iu, Lead biosorption and desorption by intact and pretreated spirula maxima biomass. *Chemosphere*, 58 (2005) 125–130.
- [242] M.A. Hashim, H.N. Tan, K.H. Chu, Immobilized marine algal biomass for multiple cycles of copper adsorption and desorption. *Separation and Purification Technology*, 19 (2000) 39–42.

- [243] F. Hammami, A. Gonzalez, M.L. Ballester, J.A. M. Blazquez, Biosorption of heavy metals by activated sludge and their desorption characteristics, *Journal of Environmental Management*, 84 (2007) 419–426.
- [244] V.K. Gupta, A. Rastogi, Sorption and desorption studies of chromium(VI) from nonviable cyanobacterium *Nostoc muscorum* biomass, *Journal of Hazardous Materials*, 154 (2008) 347–354.
- [245] J.M. Chern, Y.W. Chien, Adsorption of nitrophenol onto activated carbon: isotherms and breakthrough curves, *Water Res.* 36 (2002) 647–655.
- [246] R.P. Han, L.N. Zou, X. Zhao, Y.F. Xu, F. Xu, Y.L. Li, Y. Wang, Characterization and properties of iron oxide-coated zeolite as adsorbent for removal of copper(II) from solution in fixed bed column, *Chem. Eng. J.* 149 (2009) 123–131.
- [247] P.A. Kumar, S. Chakraborty, Fixed-bed column study for hexavalent chromium removal and recovery by short-chain polyaniline synthesized on jute fiber, *J. Hazard. Mater.* 162 (2009) 1086–1098.
- [248] V. Vinodhini, N. Das, Packed bed column studies on Cr (VI) removal from tannery wastewater by neem sawdust, *Desalination*, 264 (2010) 9–14.
- [249] Y.S. Al-Degs, M.A.M. Khraisheh, S.J. Allen, M.N. Ahmad, Adsorption characteristics of reactive dyes in columns of activated carbon, *J. Hazard. Mater.* 165 (2009) 944–949.
- [250] P. Suksabye, P. Thiravetyan, W. Nakbanpote, Column study of chromium (VI) adsorption from electroplating industry by coconut coir pith, *J. Hazard. Mater.* 160 (2008) 56–62.
- [251] A. Ahmad, B. Hameed, Fixed-bed adsorption of reactive azo dye onto granular activated carbon prepared from waste, *J. Hazard. Mater.* 175 (2010) 298–303.

- [252] M. Karimi, A. Shojaei, A. Nematollahzadeh, M. J. Abdekhodaie, Column study of Cr (VI) adsorption onto modified silica–polyacrylamide microspheres composite, *Chemical Engineering Journal*, 210 (2012) 280–288
- [253] S. Ghorai, K.K. Pant, Equilibrium, kinetics and breakthrough studies for adsorption of fluoride on activated alumina, *Separation and Purification Technology*, 42 (2005) 265–271.
- [254] S. Chen, Q. Yue, B. Gao, Q. Li, X. Xu, K. Fu, Adsorption of hexavalent chromium from aqueous solution by modified corn stalk: A fixed-bed column study, *Bioresource Technology*, 113 (2012) 114–120.
- [255] S. Sugashini and K. M. Meera Sheriffa Begum, Column Adsorption Studies for the Removal of Cr(VI) Ions by ethylamine Modified Chitosan Carbonized Rice husk Composite, Beads with Modelling and Optimization, *Journal of Chemistry*, (2013)
- [256] M. Karimi, A. Shojaei, A. Nematollahzadeh, M. J. Abdekhodaie, Column study of Cr (VI) adsorption onto modified silica–polyacrylamide microspheres composite, *Chemical Engineering Journal*, 210 (2012) 280–288.
- [257] S. Baral, N. Das, T. Ramulu, S. Sahoo, S. Das, G.R. Chaudhury, Removal of Cr (VI) by thermally activated weed *Salvinia cucullata* in a fixed-bed column, *J. Hazard. Mater.* 161 (2009) 1427–1435.
- [258] M. Fermeiglia, S. Priel, G. Longo, Molecular modelling and process simulation: real possibilities and challenges, *Chem. Biochem. Eng. Q.* 17(1) (2003) 19-29.
- [259] A.K. Sun, S.I. Sandler, *Fluid phase Equilibria*, 158 (1999) 158-160.
- [260] A. P. Dimitrios, N. Frank, *J. Chem. Theory Comput.* 7 (2011) 677- 684.
- [261] K. L. Schuchardt, B. T. Didier, T. Elsethagen, L. Sun, V. Gurumoorthi, J. Chase, J. Li, T. L. Windus, *J. Chem. Inf. Model.* 47 (2007) 1045-1052.

[262] Dilip K. Maity, How Much Water Is Needed To Ionize Formic Acid? *J. Phys. Chem. A*, 117 (2013) 8660–8670.